ANNUAL REPORT
2024-25

WADIA INSTITUTE OF HIMALAYAN GEOLOGY
DEHRADUN

(An Autonomous Institute of Dept. of Science & Technology, Govt. of India)

Cover Photo: The picture shows the impact of the 5 August 2025 debris flow triggered by intense rainfall above Dharali village (Uttarakhand). The Catastrophe event washed off a part of Dharali village and caused severe damage to the Bhagirathi valley.

(**Courtesy:** Amit Kumar & Manish Mehta)

ANNUAL REPORT
2024-25

WADIA INSTITUTE OF HIMALAYAN GEOLOGY

CONTENTS

WIHG ORGANISATIONAL SET-UP

GOVERNING BODY

(upto Feb. 17, 2025)
Talat Ahmad
Secretary, DST
Financial Adviser, DST
O.P. Mishra
M. Jayananda
Pulak Sengupta
N.V. Chalapathi Rao
Anupam Chattopadhyay
Saibal Gupta
S.C. Patel
Shakil Romshoo
Director, WIHG
Registrar, WIHG

(w.e.f. Feb. 18, 2025)
Shailesh Nayak
Secretary, DST
Financial Adviser, DST
Talat Ahmad
A.P. Dimri
Sunil Kumar Singh
O.P. Mishra
Prakash Chauhan
N.V. Chalapathi Rao
Kusala Rajendran
Prakash Kumar
Director, WIHG
Registrar, WIHG

RESEARCH ADVISORY COMMITTEE

Shailesh Nayak
T.N. Singh
D.C. Srivastava
Rajesh Kumar Srivastava
Rasik Ravindra
Rajesh K. Srivastava
Binita Phartiyal
Prakash Chauhan
O.P. Mishra
Prasun Jana
Kusala Rajendran
L.S. Chamyal
Santanu Banerjee
V. Balaram
Devesh K. Sinha
Saibal Gupta
Director, WIHG
R.J. Perumal

FINANCE COMMITTEE

Financial Adviser, DST
Anupam Chattopadhyay
Director, WIHG
Registrar, WIHG
AF&AO, WIHG

BUILDING COMMITTEE

Director, WIHG
Financial Adviser, DST
Representative of Surveyor of India
(Hathibarkala, Dehradun)
Chief Engineer, CPWD, Dehradun
Ashish Kumar Singh
(Representative of ONGC, Dehradun)
R.J. Perumal
Rajesh Kumar
(Representative of IIP, Dehradun)
Registrar, WIHG
Executive Engineer, WIHG

DIRECTOR

RESEARCH ACTIVITIES

Research Groups

- Structure & Tectonics
- Petrology & Geochemistry
- Biostratigraphy
- Geomorphology, Env. & Eng. Geology
- Sedimentology & Quaternary Geology
- Geophysics
- Glaciology & Hydrology

UNITS ANCILLARY TO RESEARCH

- TCPME
- Publication & Documentation
- Library
- Museum
- Analytical Services
- Sample Preparation
- Consultancy

ADMINISTRATION

Registrar's Office

- Finance & Accounts
- Establishment
- Stores & Purchase
- Computer and Networking
- Works, Building & Maintenance
- Transport
- Guest House

EXECUTIVE SUMMARY

The Wadia Institute of Himalayan Geology (WIHG), Dehradun, is an autonomous research Institute of the Department of Science & Technology, Govt. of India, established in 1968. The Institute is devoted to unravel various scientific aspects of the Himalaya, including geodynamic evolution, surface and subsurface structures, seismogenesis, climate-tectonic interaction, biotic evolution, ores and minerals- forming processes, glacial dynamics, fluvial system, geo-hazards (landslides, flash floods, avalanches, earthquakes), geo-resources (minerals, ore bodies, hydrocarbons, cold/hot springs), anthropogenic impact, etc. towards the well-being of the population and safeguarding the properties and structures in the Himalaya and adjoining areas. The Institute undertakes research work on the above themes based not only on field observations, but also on analysis of data using sophisticated instruments and modeling of different sets of data on structural geology, petrology, geochemistry, paleontology, biostratigraphy, sedimentology, glaciology, hydrology, geomorphology, engineering geology, seismology, gravity & magnetic, seismic, well logs, environment & engineering geology, quaternary geology, and remote sensing.

The institute has advanced analytical facilities, including Laser Ablation Multi-Collector Inductively Coupled Plasma Mass Spectrometry (LA-MC-ICP-MS), Inductively Coupled Plasma Mass Spectrometry (ICP-MS), Stable Isotope Mass Spectrometer, X-Ray Fluoresnece Spectrometer (XRF), X-ray Diffraction (XRD), Raman Spectrometer, Thermoluminescence/ Optically Stimulated Luminescence (TL/OSL), and a Magnetic Susceptibility meter, all managed by competent scientists and technicians. It also houses state-of-the-art laboratories for geophysical data acquisition, processing, modeling, and interpretation. These facilities serve WIHG scientists as well as researchers from universities, institutes, and organizations. The institute operates a seismological network comprising 80 Broad Band Seismographs and 15 Accelerographs across Himachal Pradesh, Uttarakhand, Punjab, Haryana, Arunachal Pradesh, Jammu & Kashmir, and Ladakh. Additionally, about 14 GPS instruments are installed in Himachal Pradesh, Uttarakhand, Jammu & Kashmir, and Ladakh. The institute also runs a 'Multi-Parametric Geophysical Observatory (MPGO)' in Ghuttu, Uttarakhand, to study earthquake precursors in the Himalayan region. Further,

the institute offers consultancy services for geo-engineering projects, groundwater surveys, natural hazards, and road/rail alignments in the Himalaya and neighboring areas. The institute is also monitoring 13 Himalayan glaciers.

The Institute is a national center of excellence for Himalayan geoscience education and research. It emphasizes nurturing young and dynamic talents to achieve a high level of competency through its Ph.D. programs. The Institute also provides training in different fields of Earth sciences to students of colleges/Institutes/Universities. The institute maintains a modern geological museum that showcases rocks, minerals, and fossils across various regions of the Himalaya. It conducts outreach programs for science education and geo-hazards awareness and organizes popular lectures and National/International seminars. Additionally, the institute engages in collaborative research with various universities, industries, and other institutes focused on Himalayan geosciences.

Ongoing research activities are focused on "Characterization and Assessment of Surface and Subsurface Processes in the Himalaya (CAP-Himalaya): Implications on Geodynamics, Seismogenesis, Bioevents, Paleo-climates, Natural Hazards, and Natural Resources for Sustainable Development". The research program planned for the year 2024-2025 has been grouped into 11 programs or activities. The themes and significant outcomes from each activity are summarized below.

Activity 1A: Geodynamics of Indo-Eurasian collisional zone and crystalline thrust sheets: crustal evolution, carbon sequestration and economic mineralization

The India-Eurasia collision zone is a key geological feature that help us understand the timing, geometry, and tectonic processes involved in the formation of the Himalaya and the broader collision system. It marked, by the presence of deep earth chemical foot print, forearc setting and indicates non-uniform tectonic uplift. The idea about the early subduction accretion, study the remains of plume lithosphere interaction and knowing the behaviour of ancient crust has added the extra impetus on the global scale collisional event.

Activity 1B: Mantle upwelling, fluid circulation, metasomatic processes-Implications on fluid-rock interaction

The Higher Himalayan Crystalline Sequence (HHCS) in the Dhauliganga Valley, Garhwal Himalaya, experienced at least 15% partial melting during the

Cenozoic Himalayan metamorphism. There are evidence supporting the existence of a metamorphic sole within the Spontong ophiolitic mélange. The exhumation of the Himalayan metamorphic core is interpreted to have been accommodated by simple shear along the Jhala Normal Fault and Main Central Thrust zone. Water chemistry of the Ganga, Alaknanda and Bhagirathi rivers indicate continuous weathering of the surrounding lithology of dolomitic limestone, metabasaltic rocks, slates, phyllites and clay minerals in the sediments and contribute the water chemical compositions. We could develop LA-ICPMS and LA-MC-ICPMS enabled zircon geochronology with 20- to 60-μm laser spot sizes.

Activity 2A: Development of Machine Learning approach to geoscientific data from Himalaya and adjoining region

Under this activity, the group developed and computed tectonic subsidence curves using borehole stratigraphic data from the Upper Assam Basin to investigate its tectonic evolution. This modelling approach allowed quantification of the total subsidence experienced by the basin over time. The seismic attribute-assisted machine learning workflows have been designed and implemented utilizing high-quality seismic data to interpret the subsurface sedimentary environments effectively. The group interpreted the geometry and disposition of basement structures using advanced seismic attributes and ML-assisted workflows. These methods, applied across the upper shelf regions of NE India, can be adapted for seismic interpretation in other global onshore and offshore sedimentary basins. The group also conducted geological fieldwork to validate subsurface interpretations through correlation with surface exposures and outcrops.

Activity 2B: Geometry and rheological assessment of the MHT, lithospheric flexuring - Implications toward seismogenesis, deep earth processes

The stress patterns elucidated within the western part of the India-Eurasia collision through stress tensor inversion of focal mechanism reveal underthrusting of the Indian plate through complex tectonics by dominant compression stresses with evidences of normal, strike-slip, and oblique fault mechanisms. We detected Hales discontinuity at a depth range of ~54-78 km in northeast India. Receiver function study reveals an increase in crustal thickness from ~29 km in the IGP to ~58 km in the Higher Himalaya, with a sharp change (~47–53 km) near the Jwalamukhi Thrust. High Vp/Vs in the IGP is due to the presence of mafic crust and surface sediments, while high Vp/Vs beneath the Higher Himalaya indicates the effect of volcanic rocks and partial melt zones. Magnetotelluric investigations along the Nahan-Kaurik-Chango transect indicate a flat-ramp-flat geometry of the Main Himalayan Thrust beneath the higher Himalaya. Seismic and radon anomalous signatures are utilized to monitor surface dynamics of the hazardous 2021 rock-ice avalanche in Chamoli, Uttarakhand. The multiparametric observation results suggest a gradual progression of rock/joints, subsequent material creep and slip advancement acceleration preceding the final failure. The earthquake scaling relations obtained through waveform inversion for the Garhwal Himalaya, are useful for earthquake hazard modelling. A seismic attenuation model has been developed for the NW Himalaya using 2,716 earthquakes (Mw 2.5–5.0) for seismic hazard assessment; estimated Q_c, Q_α, and Q_β to assess structural heterogeneity and depth-dependent attenuation.

Activity 2C: Seismicity and Seismic Hazard Assessment in the Himalaya

The group analysed the crustal state of the Uttarakhand Himalaya using three-dimensional attenuation tomography, which identifies a highly attenuated layer in the upper crust that varies from ~ 10 km depth in the Garhwal and ~ 5 km in the Kumaun region. Significantly variable sedimentary layer thickness was delineated beneath the Chandigarh–Ambala region in IGP, with thickness changes from 2.0 to 3.0 km. The shear-wave velocity contrast across Moho ($\delta\beta M$) varies from 0.7 km/s to 1.0 km/s across the Himalayan region. The scaling relation between $\delta\beta M$ and H is positive, which indicates the thick crust associated with a high $\delta\beta M$ meaning that the presence of a low-velocity material may be fluid at the lower crust beneath the Himalayan region. Unlike Northwest Himalaya, where the dominance of seismicity is up to the depth of decolloment and upper crust (25-30km), in the Eastern Himalayan sector, it is deeper, up to 60 km.

Activity 3: Biotic evolution with reference to Indo-Eurasian collision, evidences for global events

The absence of modified radial enamel in the incisors of cf. *Progonomys*, cf. *Democricetodon* and cf. *Sayimys* suggests that these rodents plausibly consumed a soft diet comprising leaves, flowers, seeds, fleshy roots, and insects, while the presence of specialized three-layered Schmelzmuster in the incisors of cf. *Tamias* suggests that the rodents may have preferred a diet composed of relatively harder parts such as acorns, walnuts and hazelnuts. The group quantitatively reconstructed the climate of the Laisong Formation using fossil leaf morphological traits deposited during the late Eocene–early Oligocene. The reconstruction suggests a mean annual temperature (MAT) of 25.3 ± 2.3 °C and a

cold month mean temperature (CMMT) of 19.2 ± 3.5 °C. Nannofossils from the Upper Bhubhan Formation of the Surma Group suggest middle Miocene.

Activity 4: Climate variability and landscape responses in selected transects in the NW and NE Himalaya

Sedimentological analysis from the Meso-to Neoproterozoic Rautgara Formation, Lesser Himalaya, identified products of six different palaeoenvironments, probably deposited in a barrier to back-barrier nearshore setting. Highly regular transition between the adjacent environments supports a stable barrier system that does not back-step significantly in the back barrier area. Millennial-scale changes of the Indian monsoon are primarily driven by solar insolation and the North Atlantic Oscillation. However, this relationship is non-linear. The deltaic sequence in the Pangong Tso exhibits characteristics of Gilbert-type deltas, reflects the history of lake-level fluctuations, and shows strong source-to-sink connectivity, which responds rapidly to changes in sediment supply and accommodation space. Multi-proxy data of the SS Tso Lake sediments from the Spiti reveal the Late Holocene climate variations and their linkage with solar forcing, which impacts the regional environment. Centennial-millennial scale Late Quaternary climate and environmental changes are revealed by multi-proxy data from the Lahaul-Spiti Himalaya, showing warmer and more humid conditions in the older period. The first micro-spectroscopic study of aerosols from the Gangotri Glacier Valley reveals a complex mix of carbonaceous aerosol, oxidised organics, and transported dust, which is critical for understanding their role in glacial melting and regional climate change. A 185-year-long tree ring-width chronology of *Picea smithiana* from the Lahaul region, Himachal Pradesh, reflecting February-March precipitation, captured the highest indices during 1951-1961CE and the lowest in 1858-1868CE, showing wettest and driest periods respectively, in the entire series.

Activity 5: Geological and geomorphic controls on landslide for risk assessment and zonation in the Himalaya

Fault trace along the Main Boundary Fault is mapped in the Giri River Valley that stretches about 25 km in length and trends almost east-west. Fault scarps, linear valleys, and sag ponds are associated with the fault trace. The fault scarps dip south and slickensides are observed in the fault plane. In the Sataun area, the Main Boundary Thrust, Main Boundary Fault and splay faults are closely spaced within 1km. This zone is severely affected by landslides, and the main factor for slope instability is structural and geological conditions, supplemented by toe erosion. Advanced deep learning techniques for landslide detection, utilizing attention-enhanced YOLO and GELAN models, combined with geospatial mapping of landslide susceptibility via AHP and Frequency Ratio methods in the Tehri region, provide a comprehensive tool for hazard assessment and risk mitigation in the Himalaya.

Activity 6A: Glacial dynamics, glacier hydrology, mountain meteorology and related hazard

Pensilungpa Glacier showed a net mass loss of $\sim 6.32 \times 10^6 m^3$ w.e. with an ELA at 5251m asl between 2023 and 2024. Maximum ablation occurred between 4800–5000 m under thin debris (~ 10 cm); thicker debris (4600–4800 m) reduced melt. Parkachik River discharge rose consistently, peaking at $23.67 \times 10^6 m^3$ in 2023. Periglacial lakes near the Pensila Pass grew by $\sim 6.5\%$ (area) and $\sim 7\%$ (volume), and Proglacial Lake near the Durung-Drung Glacier expanded by $\sim 177\%$ in area and 195% in volume (2004–2023). Durung-Drung Glacier retreated $\sim 165 \pm 95$ m (-21 ± 12 m/yr); Pensilungpa Glacier retreated $\sim 80 \pm 35$ m (-10 ± 4 m/yr) from 2015 to 2023. The number of lakes rose by 1.9%, and the area by 8.1% in Uttarakhand between 2013 and 2023. Lakes are concentrated above 4500 m; Chamoli and Uttarkashi hold most lakes. First evidence of geothermal melting at the Changmolung Glacier; localised melt reached ~ 390 cm/year near geothermal springs. SCA increased from 461.17 km^2 (2008–09) to 601.01 km^2 (2021–22) in the Kumaon Himalaya. Seasonal shifts indicate changing snowmelt dynamics and water availability risks. Panchachuli Glaciers reveal three significant advances (mid-MIS 3, ~ 20 ka, ~ 5–8 ka) via OSL dating, tied to global/regional climate shifts. Upper Bhagirathi and Alaknanda Rivers emit high CO_2 fluxes (88 and 175 $gCO_2 m^{-2} d^{-1}$); upstream turbulence significantly enhances degassing.

Activity 6B: Hydrogeology-Himalayan Fluvial System & Groundwaters

The group provided first insights into the geohydrology, modelled subsurface hydrogeological features, and determined elemental sources and quality characteristics of groundwater in tribal parts of the Dehradun district. In addition, Tectonics and its major control on the sedimentary budget of the Himalayan River basins were also evaluated in terms of the Teesta River Basin, a unique Himalayan River basin with sedimentary provenance in the Lesser Himalaya. The records of Holocene erosion as obtained from a sedimentary core from the Teesta basin suggest an increase in the Lesser Himalaya sediment contribution.

EXECUTIVE SUMMARY

Activity 7: Quantification of strain accumulation/release rate along Main Himalayan Thrust (MHT) at different time scales

Paleoseismological evidence for segmentation of the Main Himalayan Thrust in the Darjeeling-Sikkim Himalaya (DSH): The DSH is a 150 km-long independent segment bounded by a transverse ridge and fault and has a recurrence interval of ~ 949–1963 years, which is significantly larger than Nepal (~ 700–900 years) and Bhutan Himalaya (~ 339–761 years). A new zircon and apatite fission-track (ZFT-AFT) thermochronological study has been carried out along the Karakoram Fault (KF) zone in the Nubra Valley, SE Karakoram, India. The ZFT ages range from 8.7 ± 0.7 to 11.3 ± 0.6 Ma, and the AFT ages range from 3.8 ± 0.5 to 6.9 ± 1.1 Ma, respectively. The calculated exhumation rates using ZFT ages vary from $\sim0.54\pm0.04$ to 0.66 ± 0.04 mm yr -1 since ~9.87 Ma and for AFT ages from $\sim0.58\pm0.1$ to 0.68 ± 0.11 mm yr -1 since ~4.8 Ma. Five significant geological heritage sites were identified for conservation: Five geoheritage sites located in five different geological terrains in the Indian states of Odisha, Rajasthan, Uttar Pradesh and Uttarakhand, which are significant for geoscience education, and have scope for the development of "geotourism", were suggested for conservation for the forthcoming generations of geoscientists, researchers, students and science enthusiasts, in addition to growth and development of the local tourism. The Himalayan Metamorphic Core (HMC) extruded by simultaneous Mid-crustal channel flow and in-sequence thrusting from the Oligocene to early Miocene implying strain partitioning within the mid-crustal channel. From the Miocene onwards, SSW-ward extrusion of the HMC occurred as a tectonic wedge.

Academic Pursuit

The Institute researchers published 117 research papers in peer-reviewed SCI journals, 5 book chapters, 1 field excursion guide, and 5 technical reports in 2024-2025. The Academy of Scientific and Innovation Research (AcSIR) at WIHG takes the initiative in educating Ph.D. scholars through experienced scientists of the Institute. A total of 10 research scholars were awarded the Ph.D. degree, and 4 theses were submitted by the scholars for the award of the Ph.D. degree. The Institute had the privilege to organize (i) A one-day workshop on "Climate change, Natural Disasters, and Eco-System of Himalaya" during the Himalaya Diwas on September 9, 2024, which was attended by over 200 participants from different research/academic institutes, state disaster management departments, universities/colleges of Dehradun, army personals, engineers, research scholars and students, (ii) Industry Immersion Programme under Capacity Building Commission, Government of India was organized on September 17-18, 2024 at Wadia Institute of Himalayan Geology, Dehradun to provide exposure to Department of Science & Technology (DST) officials on WIHG schemes, functioning and laboratories, and (iii) 8th National Geo-Research Scholar's Meet at Shree Mata Vaishno Devi University (SMVDU) in Katra, Jammu & Kashmir, during November 22-25, 2024 which was attended by about 60 research scholars from different organizations across India.

The scientists of the Institute were recognized by awards and felicitations on various platforms. Dr. Som Dutt received the Dr. J.G. Negi Young Scientist Award 2024 at I.G.U., and Dr. Pankaj Chauhan was jointly awarded CDRI (Coalition for Disaster Resilient Infrastructure) Fellowship for the year 2024-25, funded by national governments and UN agencies.

Other Highlights

The institute participated and displayed its scientific exhibits at various forums in different parts of India. The Institute participated in the India International Science Festival (IISF) 2024 held at IIT Guwahati, Assam during November 30 – December 3, 2024. The Institute organized several awareness programs related to earthquakes and other geohazards for school children and the common people. The Institute strictly followed the Rajbhasha guideline and took various steps to promote the use of Hindi in routine office work as well as in Scientific Research publications. The Hindi Pakhwara was celebrated during September 14-30, 2024. The Annual Report of the Institute for the year 2023-24 was published in bilingual form (Hindi and English), along with the in-house Hindi magazine Ashmika. The Institute has its biannual (January and July) flagship scholarly journal 'Himalayan Geology', which publishes original research contributions on several aspects of earth science about the Himalaya and other regions.

Vineet Kumar Gahalaut
Director

RESEARCH ACTIVITIES

Activity: 1A
Geodynamics of Indo-Eurasian collisional zone and crystalline thrust sheets: crustal evolution, carbon sequestration, and economic mineralization
(Barun K. Mukherjee, Paramjeet Singh, Pratap Chandra Sethy, Hiredya Chauhan, M. Rajanikanta Singh and Kunda Badhe)

Reverse Zoning in Spinel from Kurzok Chromitite

In the ophiolite section, spinel in chromitites is the most stable and highly resistant mineral. They are therefore usually identified as the best container to retain the past chemical entity which bears the signature of deep Earth histories. In the mantle section of the Kurzok ophiolite, NW Himalaya, a small chromitite body of a~ 10 m long pod hosted by peridotite rocks, is studied. Petrological investigation of the chromitites manifests an asymmetrical texture that comprises occasional well-developed octahedral crystals of spinels. The spinels show both the homogeneous and patchy zoning, that characterised by Cr # varies from 0.78 to 0.91 in the cores and rims. It displays Al and Mg content high at the cores, accompanied by Cr and Fe high at the rims. The Raman shifts have measured on the spinels, show the CrO stretching region at $691 cm^{-1}$ to $708 cm^{-1}$. The most intense peak at $698 cm^{-1}$ is identified as the symmetric stretching vibrational mode of $(Mg, Fe) Cr_2O_4$. The broadening of the peak of A1g mode and shifting of the peak to higher wavenumber at $748 cm^{-1}$ observed as a result of increasing the proportion of Al in response to increasing pressure, have identified the formation of $FeAl_2O_4$. The observed reverse zoning in the spinels with the characteristic Raman shift at $1061 cm^{-1}$ and $3681 cm^{-1}$, register the appearance of nominally anhydrous mantle mineral. The study provides important lead to the spinel formation, which likely coexist with the garnet phase at very high pressure.

New U-Pb age from Bandal Granitoid

To understand the Paleoproterozoic magmatism and tectonic setting of the northern margin of the Indian block, and their possible connection with the Archean-Paleoproterozoic Aravali-Delhi-Bundelkhand (ADB) craton of NW India, U-Pb zircon geochronological studies from the Bandal Granitoids Complex (BGC) in the Himachal region of the northwest Himalaya has been carried out (Fig. 1). The U-Pb zircon age obtained from the three granitic gneisses samples of the BGC granitoids ranges from ~1.92−1.88 Ga and ~1.86−1.85 Ga with a few inherited older ages of ~2.45−2.33 Ga. Zircon grains are relatively small (50–200 μm), euhedral, and zoned with inclusions (CL images in figures 2e, g). The Pb/U ratio is > 0.1, which suggests an igneous origin (Hoskin & Ireland, 2000; Rubatto, 2002; Kirkland et al., 2015). A total of 109 spots have been identified in the zircon cores and rims for U-Pb ages. Sample BD-2/2 yields the age range of 1377.6 ± 21.0 and 3070.0 ± 70.0 Ma. BD-9/2 yields the age range of 1787.0 ± 19.5 Ma and 2780.0 ± 95.0 Ma, and BD-9A yields the age range of 1817.0 ± 18.5 and 3230.0 ± 12.5 Ma (Fig. 2). All the concordant to discordant ages are filtered up to 20% and overlapped with each other. The older component represents the protolith age of zircons of the BGC granites of the northwestern Himalaya. Whereas, the younger age component of ~1860 Ma is mostly present in the zircon rims. Based on the U-Pb age results, it is inferred that the Paleoproterozoic magmatism occurred along the north margin of the Indian continental block and experienced subduction-accretion between ~1.92−1.85 Ga, followed by the crustal extension around 1.80 Ga. Moreover, the zircon age data compared with the ADB craton suggest that it was a continuous magmatic event that occurred between ~2.10-1.85 Ga along the northern margin of the Indian block and related to the assembly of the Columbia supercontinent.

Remains of plume-lithosphere interaction in the mafic rock of the Himachal Himalaya

The Northwest Himalayan region has a record of several phases of mafic magmatic activity spanning from Precambrian to Cenozoic in a dynamic tectonic setting. Here, we studied detailed petrography and new whole-rock geochemistry of mafic volcanic and dykes from the Nagrota-Kathindi Section (NKS), Himachal region of the NW Himalaya, to understand the petrogenesis and possible tectonic setting. Both rock types have comparable mineralogical compositions (clinopyroxene + plagioclase + actinolite-tremolite + chlorite + iron oxides ± hornblende ± epidote ± quartz ± carbonates) overprinted by greenschist to lower amphibolite facies metamorphism. The mafic volcanic and dykes of NKS exhibit sub-alkaline basalts to basaltic andesites and a typical tholeiite compositional character. The chondrite-normalized rare earth element pattern exhibits similar LREE enrichment and strong HREE fractionation, whereas Primitive mantle
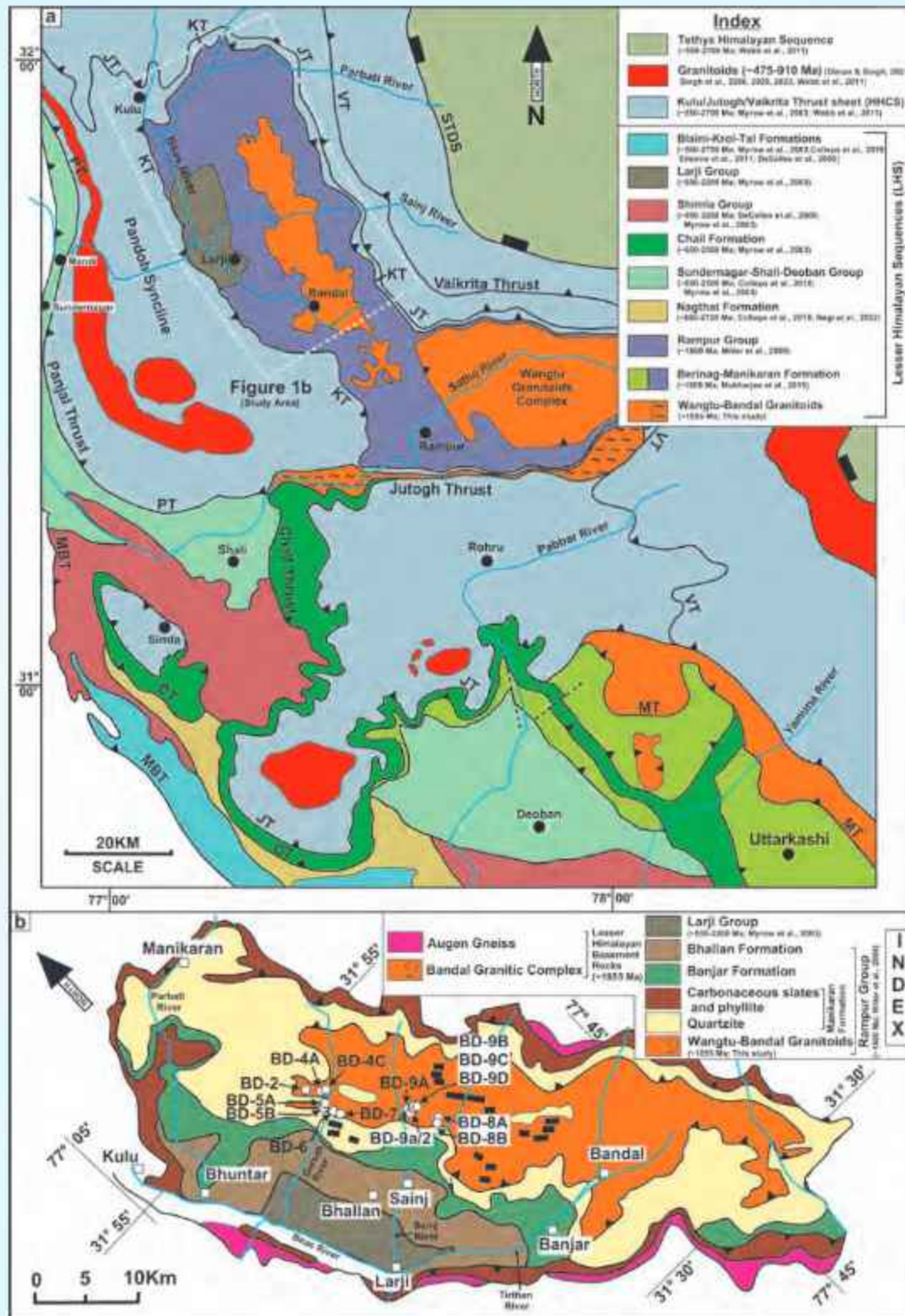
RESEARCH ACTIVITIES

Fig. 1: (a) Geological map of Himachal Pradesh, NW-Himalaya showing the tectonic setting of the present study areas (Modified after Thakur, 1992; Bhargava & Bassi, 1994; Singh et al., 2021; Valdiya, 1980), the rectangular box indicates the present study area. (b). Detailed geological and tectonic setting of Kulu-Larji-Rampur window and locations of collected samples from the Bandal Granitoids Complex (BGC) region of Himachal Himalaya (modified after Sharma, 1977; Sharma & Rashid, 2001; Rashid & Sharma, 2001). Black colour circle shows the sample locations.
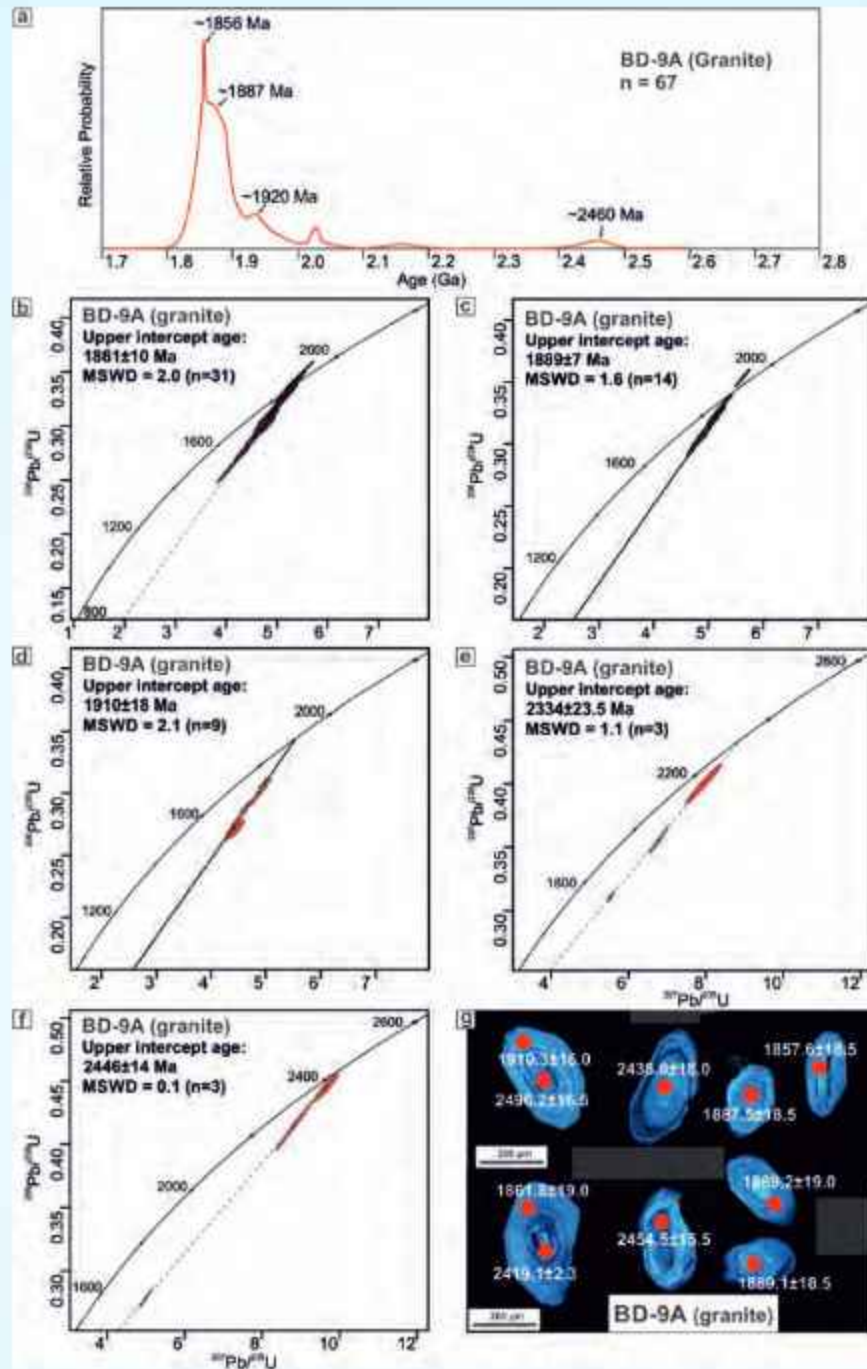
Fig. 2: (a) Probability density plot for [207]Pb/[206]Pb ages of BD-9/2 granite sample. (b-c-d) Upper intercept U-Pb zircon ages with statistically separable groups are shown for the sample BD-9/2 granite of BGC granitoids, respectively. (f) The concordia plots of U-Pb isotopic compositions of BD-2/2 granite samples of BGC granitoids. (e-g) CL images of representative zircon grains from BD-9/2 and BD-2/2. Concordant age ([207]Pb/[208]Pb ages) of individual analyzed grains are marked in CL images. MSWD – mean square weighted deviation.

normalized multi-element patterns show pronounced LILE enrichment of Rb, Ba, Th, LREE and HFSE depletion of Nb, K, P and Ti. The Zr–Y–Nb–Th relationships indicates that both the rock type were derived from the plume source whereas, low Nb/La

(<1), similar high large ion lithophile element concentrations and pronounced negative Nb, Zr, P and Ti anomalies suggests that components other than mantle plume must have been involved in the generation and evolution of both the rock types i.e. most likely
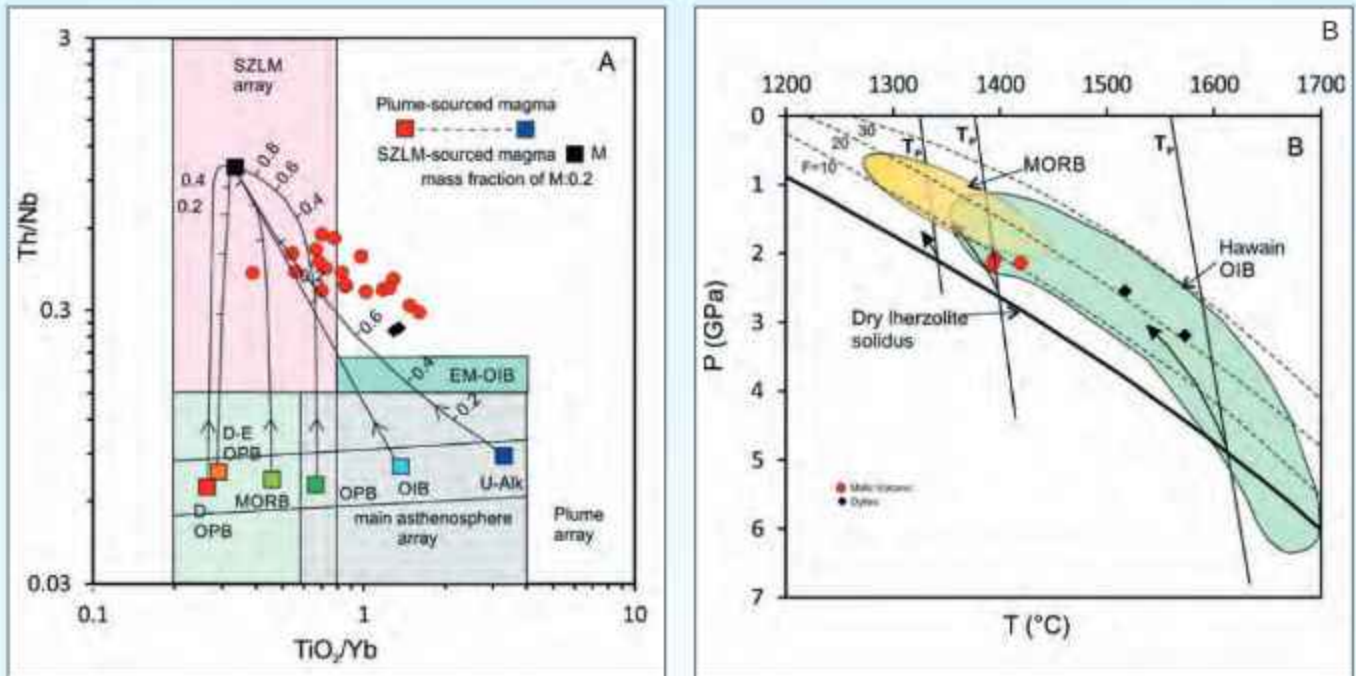
Fig. 3: (A) TiO₂/Yb versus Th/Nb plot (after Pearce et al., 2021) majority of the NKS mafic volcanic straddle in the plume-SZLM area has a diagonal trend, indicating that the source of their magma was an enriched plume that interacted more with the SZLM than dykes, which were primarily formed from the plume source. MORB: mid-ocean ridge basalt, N-MORB: normal mid-ocean ridge basalt, E-MORB: enriched mid-ocean ridge basalt, OIB: ocean island basalt, CAB: continental arc basalt, IAB: island arc basalt, OPB: oceanic plateau basalt, SZLM: subduction zone-modified lithospheric mantle; (B) Melting temperature (°C) versus pressure (GPa) calculated from primary magma composition estimated using major element molecular species defined by Lee et al. (2009). The P-T estimates for NKS volcanic rocks show a magma temperature range of 1392-1419° C, pressure of 2.1 GPa, and lie in the MORB-OIB interaction zone whereas, dykes have a larger temperature range of 1517-1573°C and a pressure range of 2.6-3.2 GPa, which is comparable to Hawaiian basalt formed by plumes. Range of melting temperature and pressure for mid-oceanic ridge basalts from East Pacific Rise and Mid-Atlantic Ridge, and ocean island basalts from the Hawaiian hotspot calculated by Lee et al. (2009) is also shown for comparison. The thick dark line and thin dotted grey line representing dry lherzolite solidus and melt fraction isopleths respectively are from Katz et al. (2003). Dark continuous curved arrays represent melting adiabats (from Lee et al., 2009). Mantle potential temperature for MORB (Tp^MORB) and OIB (Tp^OIB) are also taken from calculations by Lee et al. (2009).

plume and sub-continental lithosphere mantle (SCLM) interaction. The genesis of parent magma for the NKS volcanic and dykes were derived by 4-6% and 10-20% partial melting from spinel+garnet lherzolite stability field. The majority of the studied samples correspond spinel+garnet peridotite melting on (Gd/Yb)ₙ vs. CaO/Al₂O₃ diagram thereby corroborating residual garnet in the mantle restite. All the basalts and dykes from the NK section did erupt/intrude in an intracontinental rift setting based on geochemical discrimination. The key petro-tectonic processes attributed to the formation of these rocks are as follows: (i) the melting of the ascending plume by adiabatic decompression; (ii) the partial melting of this plume-SCLM source in the melting regime, which produces basaltic magma with a tholeiitic composition; and (iii) the release of heat that provides the thermal condition for melting of SCLM and interaction between

upwelling mantle plume and subduction metasomatized SCLM (Fig. 3).

Nature of pre-existing continental crust

The Bandal Granitoid Complex (BGC) constitutes the core of the Manikaran Formation within the Kulu-Larji-Rampur tectonic window in the northwestern Himalaya. This complex comprises a polyphase suite of granitoids intruded into the metasedimentary and metavolcanic assemblages of the Lesser Himalayan Crystalline Belt. Field observations, petrographic features, and geochemical signatures collectively indicate the composite nature of these granitoids and their emplacement within a tectonically dynamic regime. Geochemically, the BGC samples display variable strontium (Sr) concentrations ranging from 37 to 392 ppm, low yttrium (Y) contents (23–42 ppm), and high rubidium (Rb) abundances between 177 and 511
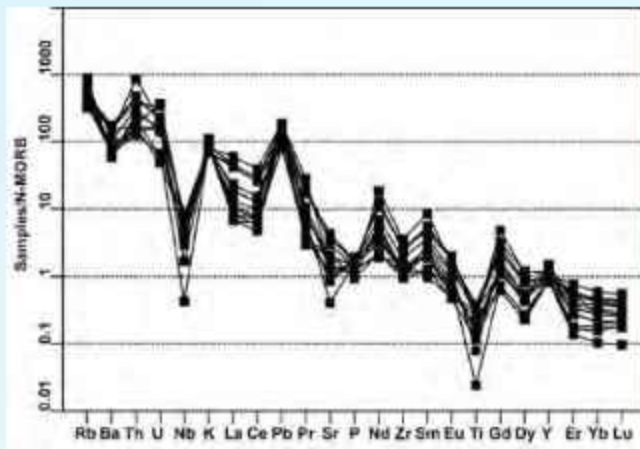
Fig. 4: N-MORB-normalized (after Sun & McDonough, 1989) trace-element pattern of the BGC granitoids, Himachal Pradesh.

ppm. The Rb/Sr ratios, spanning from 0.67 to 10.08, reflect significant magmatic fractionation. When normalized against N-MORB values (Sun & McDonough, 1989), the BGC granitoids exhibit marked enrichment in large-ion lithophile elements (LILEs), including Rb, Th, K, Ba, and Pb, and depletion in high-field strength elements (HFSEs) such as Nb, Sr, P, and Ti (Fig. 4). The presence of strong negative anomalies in Ti, Nb, Sr, and Zr, coupled with elevated LILE/HFSE ratios, suggests derivation from a sedimentary protolith and points to a post-collisional or extensional tectonic environment, likely involving the remelting of pre-existing continental crust.

Evidence of Intra Oceanic Island Arc in Gabbro

Supra-subduction zone (SSZ) ophiolites are significant in unravelling the source composition, extent of fluid/melt interaction in the mantle wedge, and thereby the tectonic history of the subduction complex (Dilek & Furnes, 2019). Clinopyroxene is an important crystallizing mineral phase in mafic-ultramafic rocks, and preserves crucial information about the parental mantle source composition (Batki et al., 2018; Li et al., 2020). Its compositional variation depends on the tectonic setting of the host magma related to the ophiolite sequences (Nisbet & Pearce 1977; Beccaluva et al. 1989; Nayak & Pal, 2021). It has been demonstrated that the clinopyroxene mineral chemistry can be used as a proxy for determining thermo-barometry, petrogenesis, and tectonic setting of ophiolites (e.g., Nisbet & Pearce, 1977; Leterrier et al., 1982; Beccaluva et al., 1989; Yaliniz & Goncuoglu 2000; Moazzen & Oberhansli, 2008; Ovung et al., 2018; Barnes et al., 2020; Vind et al., 2021; Khare et al., 2022).

In low-grade metamorphosed rocks, the magmatic signatures of clinopyroxenes are well preserved, and usually remain unchanged (Fodor & Thiede, 1977; Beccaluva et al., 1989). High-Ti clinopyroxenes generally occur in the mid-ocean ridge, back-arc basin, and Fe-depleted magmatic environments (Nisbet & Pearce, 1977; Beccaluva et al., 1989), while low-Ti clinopyroxenes are associated with the intra-oceanic island arc magmatism above subduction zones (Beccaluva et al., 1989). In clinopyroxenes, Al and Ti concentration generally increases from tholeiitic to per-alkaline magmatic affinities (Le Bas, 1962). In addition, clinopyroxene exhibits systematic and subtle chemical differences related to crust-mantle processes, melt-peridotite interaction, host magma composition, and tectonic affinity (Leterrier et al., 1982; Beccaluva et al., 1989; Putirka et al., 1996; Yogodzinski & Kelemen, 2007; Chen et al., 2018; Vind et al., 2021).

In Ladakh Himalaya, Late Jurassic to Early Cretaceous ophiolites are exposed along the Indus Suture Zone (ISZ) representing remnants of the eastern portion of the Neo-Tethys Ocean (Ahmad et al., 2008; Bhat et al., 2019a, 2019b; Buckman et al., 2018). Although, extensive whole-rock geochemical data is available on the ophiolitic rocks of the western Ladakh viz., Dras, Thasgam, Suru Valley, Shergol ophiolitic slices (e.g., Bhat et al., 2019a, 2019b, 2019c, 2021, 2023) however, limited studies are available on the mineral chemistry to understand the petrogenesis and tectonic affinity of the host ophiolitic rocks. In western Ladakh, the Thasgam ophiolitic gabbro offers distinct insights into the geodynamic evolution of SSZ magmatism. In the Thasgam ophiolitic gabbros, the clinopyroxene composition is characterized by lower concentration of TiO_2 (0.18 to 0.31 wt.%), and Al_2O_3 (1.74 to 2.51 wt.%), and higher concentration of CaO (21.2 to 24.5 wt.%), MgO (15.5 to 16.4 wt.%). These clinopyroxenes reveal restricted compositional range from $Wo_{43.5-51.2}$, $En_{50.6-38.2}$ and $Fs_{24.8-16.0}$, indicating limited degrees of iron enrichment. They show diopside compositional affinity in the Wollastonite (Wo)–Enstatite (En)–Ferrosilite (Fs) pyroxene ternary classification diagram similar to Thasgam ophiolitic pyroxenites (data after Bhat et al., 2021). In comparison, the Nidar ophiolitic gabbros (data after Nayak & Pal, 2021), and Shergol ophiolitic gabbros (data after Bhat et al. 2019c) along the ISZ shows more augitic compositions. Due to lower TiO_2 concentration in the studied clinopyroxenes, we designated them as low-Ti clinopyroxenes.

RESEARCH ACTIVITIES

The progressive crystallization of clinopyroxene from a magma is reflected in the variation of its elemental concentrations with respect to the fractionation index i.e., MgO. In MgO versus Si^{4+}, Al^{4+}, Ti^{4+}, Cr^{3+}, Fe^{3+}, and Ca^{2+} binary plots (Fig. 5) the studied clinopyroxene composition shows an overall coherent linear magmatic trend thereby indicating their magmatic nature with least probability of post-magmatic alterations. In MgO versus Si, Al, Ti, Cr, and Fe plots, the studied clinopyroxene shows slightly decreasing trend indicating an overall decrease of these elements in clinopyroxenes and their host magma with progressive clinopyroxene crystallization. While in MgO versus Ca plot, clinopyroxene shows an increasing trend reflecting Ca enrichment in the host magma during clinopyroxene crystallization.

In mafic rocks, the clinopyroxene composition is primarily controlled by the composition of host magma (Brown, 1967). According to Leterrier et al. (1982), clinopyroxene mineral composition such as Ca, Ti, Al, Si, Mg, etc. can be used to decipher the tectonic setting of the parental magmas. The high CaO, and MgO concentrations along with low TiO_2 and Al_2O_3 concentrations of the Thasgam gabbro clinopyroxenes reflect their derivation from depleted mantle sources (Pearce & Norry, 1979; Hebert & Laurent, 1990). In addition, the presence of low-Ti contents in the studied clinopyroxenes from the Thasgam ophiolitic gabbros reflect their origin in a SSZ setting (Beccaluva et al., 1989).

The activity of an element in clinopyroxene crystallizing from magma is proportional to that in the melt. The orogenic rocks, i.e., the subduction zone rocks, are depleted in Ti and Cr, while magmatic rocks from mid-ocean ridges, continental rifts, and passive continental margins are enriched in Ti and Na (Leterrier
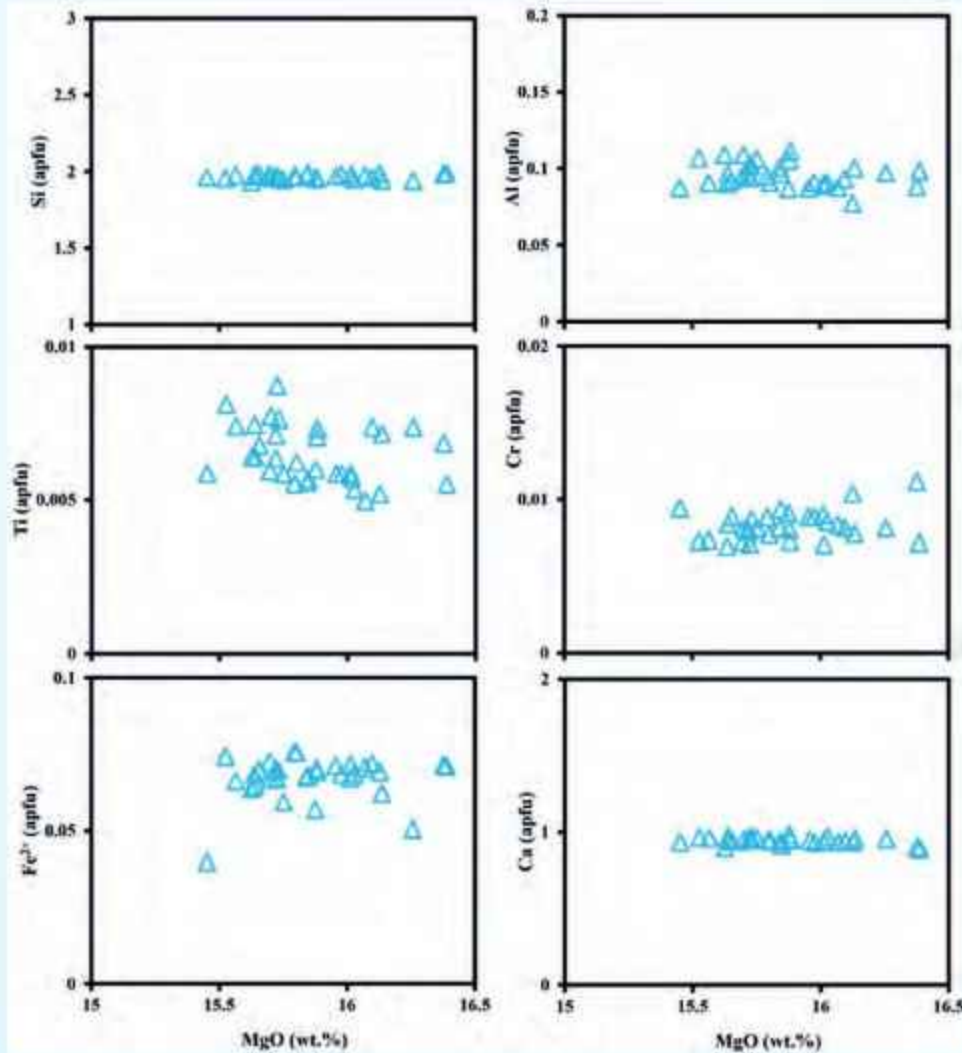

Fig. 5: Binary plots of MgO versus Si, Al, Ti, Cr, Fe^{2+}, and Ca for clinopyroxenes from the Thasgam ophiolitic gabbros.
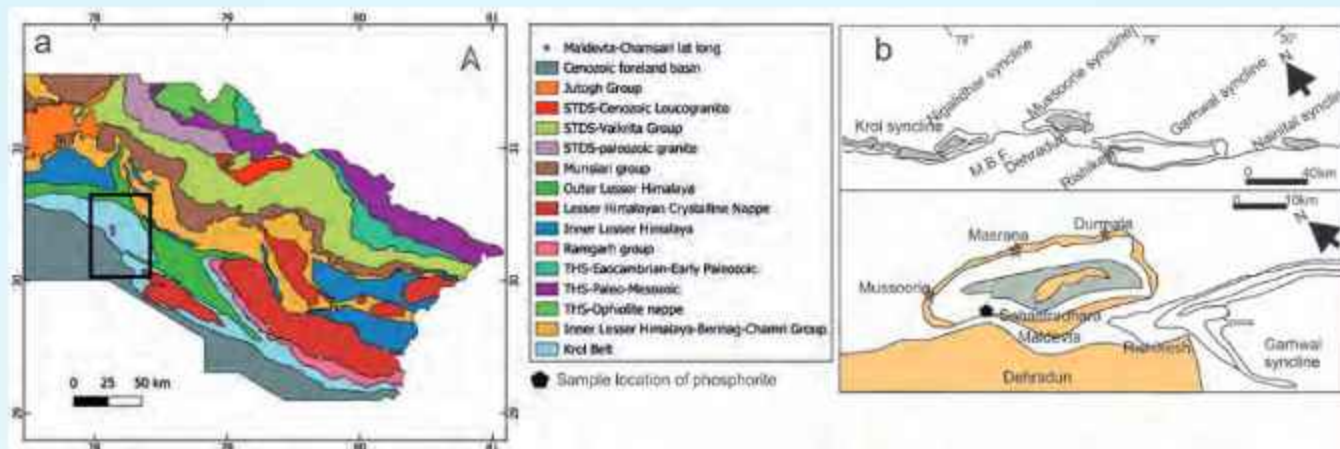
Fig. 6: Geological map of the a) Uttarakhand state, and b) Mussoorie region, Lesser Himalaya (Valdiya, 1980; Ghosh et al., 1991).
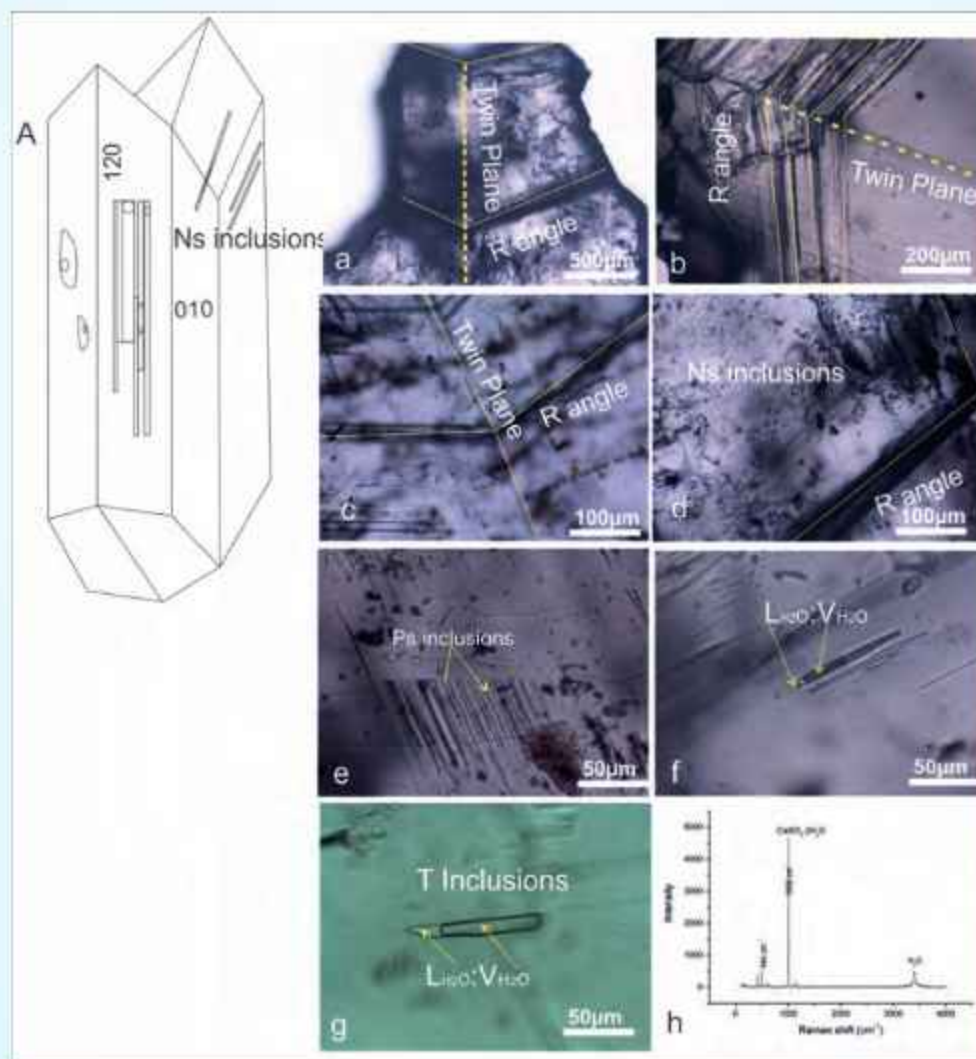

Fig. 7: Photomicrographs of Fluid inclusions in gypsum: A, The gypsum crystal morphology with inputs of needle-shaped (Ns) inclusions from the current study. a, b, c, d, show the re-entrant (R) angle and twin plane of gypsum with Ns inclusions. e, Pseudosecondary inclusions (Ps) along the plane. J,k, Fine neddle-shaped inclusions (Fns) of liquid –vapor of aqueous composition. g, Tabular aqueous inclusions and its h, Laser Raman spectra of the fluid inclusion.

RESEARCH ACTIVITIES

et al., 1982). Also, high MgO content in these clinopyroxene is consistent with pyroxene compositions reported in other ophiolite complexes of island arc affinities (De Bari & Coleman, 1989). Further, low-Ti clinopyroxenes from the Thasgam ophiolitic gabbros are comparable with the contiguous ophiolites of Ladakh Himalaya, and therefore highlighting the SSZ tectonic affinity.

Lower Ti, and Al contents characterize these clinopyroxenes, while higher concentrations of Mg, and Ca supports derivation from a depleted mantle source, typical of SSZ tectonic environments. In addition, recently published whole-rock geochemical study of the surrounding ophiolitic rock types emphasizes the sub-alkaline tholeiitic nature, with enriched large-ion lithophile elements (LILE) and depleted high-field-strength elements (HFSE), suggesting subduction-related geochemical signatures (Bhat et al., 2021). Therefore, the present petrographical and mineral chemical study of the clinopyroxenes from the Thasgam ophiolite gabbro aligns with the broader context of the Ladakh Himalayas, where ophiolitic remnants bear similarities to intra-oceanic island arc subduction system with in the Neo-Tethys Ocean.

Imprint of marine water in the Lesser Himalaya Gypsum

Gypsum formed in marine environments and fluid inclusions (FIs) are a particularly helpful tool for studying the depositional and diagenetic environment. Microthermometric analyses can provide information about the temperatures of formation of minerals precipitated in the marine environment unless the FIs were changed after entrapment. Gypsum occurs in the host rock shale and carbonate that is present in the Krol belt, Lesser Himalaya, Sahastradhara (Fig. 6). In the study area, gypsum comes in two varieties: anhydrite and as translucent platy encrustations of gypsum on the surface of shale.

The present study reported fluid inclusions in gypsum ranging in size from a few μm to >300 μm as clusters, isolated, and pseudosecondary trails (Fig. 7). FIs present along the twin re-entrant angle and parallel to crystallographic planes and primary FIs. They have a low salinity of 0.4–4.46 wt% NaCl equivalent. The Liquid to Vapour phase (L:V) ratio in biphase fluid inclusions is variable. The present study shows that a relationship exists between salinity and size of FIs: low salinities occur in large FIs. This is interpreted here as a likely alteration of FI contents during the crystallisation of gypsum. It is inferred that gypsum precipitated from a marine water body but secondary low-salinity fluids were introduced into the primary FIs, altering the parent brine composition.
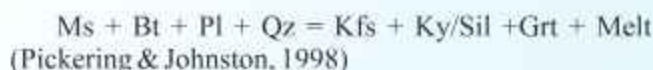
Activity: 1B

Mantle upwelling, fluid circulation, metasomatic processes: Implications on fluid-rock interaction
(Koushik Sen, S.S. Thakur, Saurabh Singhal, Aditya Kharya, C. Perumalsamy, and Pramod Kumar Rajak)

The Badrinath Formation constitutes the structurally upper part of the Higher Himalayan Crystalline Sequence (HHCS) in the Dhauliganga Valley, Garhwal Himalaya has undergone partial melting during the Cenozoic Himalayan metamorphism. The study shows that the partial melting of metasedimentary rocks in the Badrinath Formation results initially from the dehydration breakdown of mica as per the following reaction (Thompson, 1982):

$$Ms + Pl + Qz = Kfs + Ky/Sil + Melt$$

The detailed thermobarometry study suggests that the rocks of the Badrinath Formation have attained the peak P-T condition of ~11.9 kbar and ~800 °C. The petrological study shows that both muscovite and biotite have participated in the dehydration reaction. The following mica dehydration reactions have been suggested for the partial melting in the HHCS rocks:

$$Ms + Bt + Pl + Qz = Kfs + Grt + Melt \text{ (Le Breton \& Thompson, 1988)}$$

$$Ms + Bt + Pl + Qz = Kfs + Ky/Sil + Grt + Melt \text{ (Pickering \& Johnston, 1998)}$$

The dehydration melting in the rock is considered to have resulted from prograde heating in the stability field of kyanite. The muscovite dehydration melting was followed by the biotite dehydration melting during prograde metamorphism. The P-T pseudosection modelling suggests that the metapelites of Badrinath Formation have undergone at least ~15 vol% of partial melting (Fig. 8).

The development of LA-ICPMS and LA-MC-ICPMS enabled zircon geochronology with 20- to 60-μm laser spot sizes. Due to complexly zoned zircons, U–Pb dating at smaller sizes is essential. However, reducing spot size increases downhole fractionation (DHF), leading to inaccuracies. This work aims to determine ages with resolutions below 20μm using MC-ICPMS's high sensitivity. Zircon standards (91500, GJ-1, and Plešovice) were tested with smaller spot sizes. Optimization of laser settings and shot counts reduced the DHF effect. Static ablation at 35- to 15-μm spots with 150 shots achieved less than 1.5% precision and less than 2% age offset. At 10μm, DHF resulted in a 4%
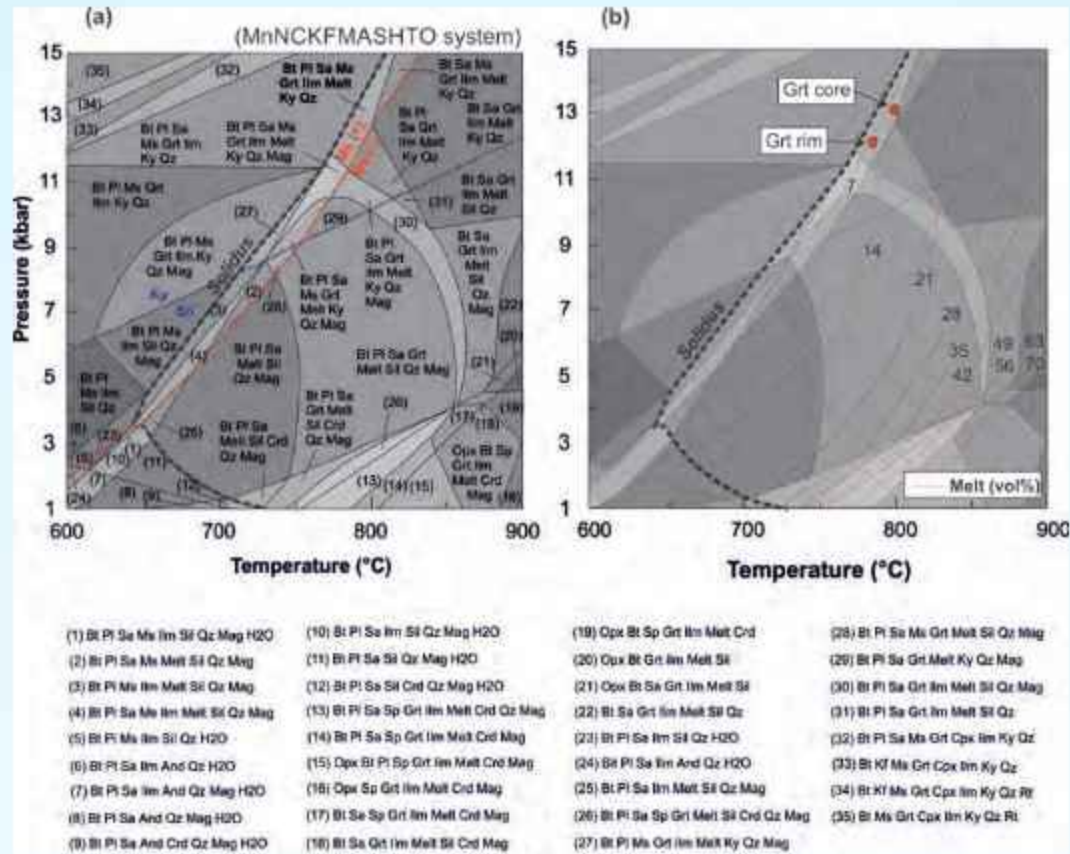
RESEARCH ACTIVITIES

Fig. 8: Phase diagrams for sample HH31 (Badrinath Formation) in the MnNCKFMASHTO system. Oxide mole proportions used are: $SiO_2 = 62.45$, $TiO_2 = 0.87$, $Al_2O_3 = 12.64$, $FeO = 7.27$, $MnO = 0.083$, $MgO = 5.56$, $CaO = 0.50$, $Na_2O = 0.98$, $K_2O = 3.72$, $H_2O = 7.00$, $O_2 = 0.30$. (a) *P–T* pseudosection with solidus marked by thick, black dashed line. Peak assemblage is shown in bold letters. Ms-in and Ms-out line is shown in red line; (b) Isomode contours of Melt in vol%.; please see P-T values measured for core and rim composition of garnet using isopleths intersection method.

age offset. Masking shot counts improved accuracy, especially at lower counts. With 75 shots, precision improved to 1.4%, and age offsets for $^{206}Pb/^{238}U$ reduced to 1.6% (Fig. 9). This method minimizes shot counts to avoid sampling multiple age groups, though DHF variability at smaller sizes may affect results.

All U–Pb zircon data of the Kausani Granite Gneiss within the inner Lesser Himalayan Sedimentary Zone (iLHS) is modelled for obtaining the upper and lower intercept lines. The upper intercept shows the peak ca. 1920 Ma (Fig. 10a). The 2-D map of likelihood shows the Pb-loss event 45 Ma to the recent time indicated by the blue region of the map which corresponds to ca.1920 Ma upper intercept (Fig. 10b). The Pb-loss event is prolonged due to different activity of the Himalayan Orogeny at this time.

The study provided new evidence supporting the existence of a metamorphic sole within the Spontong ophiolitic mélange. We utilize thermodynamic modeling and fluid inclusion studies, alongside petrographic and mineral chemistry analyses, to investigate a selection of mafic rocks that have undergone varying degrees of amphibolite facies metamorphism.

The rocks exhibit a range of reaction textures, such as hornblende encasing clinopyroxene, along with some plagioclase, which corresponds to hydration processes. The reaction can be represented as:

$$Cpx + Pl + H_2O = MgHbl + Ilm + Qz.$$

The results indicate that water-rich conditions were prevalent during the metamorphism of mafic gabbro. Phase equilibria modeling of the analyzed samples reveals that the peak metamorphic event occurred during a hydration episode at temperatures ranging from 678 to 790 °C and pressures between 7.1 and 11.28 kbars (0.71–1.13 GPa), as well as at approximately 640–670 °C under water-rich conditions (i.e., 2.5-3.2 mole% or 0.7 wt% H_2O).
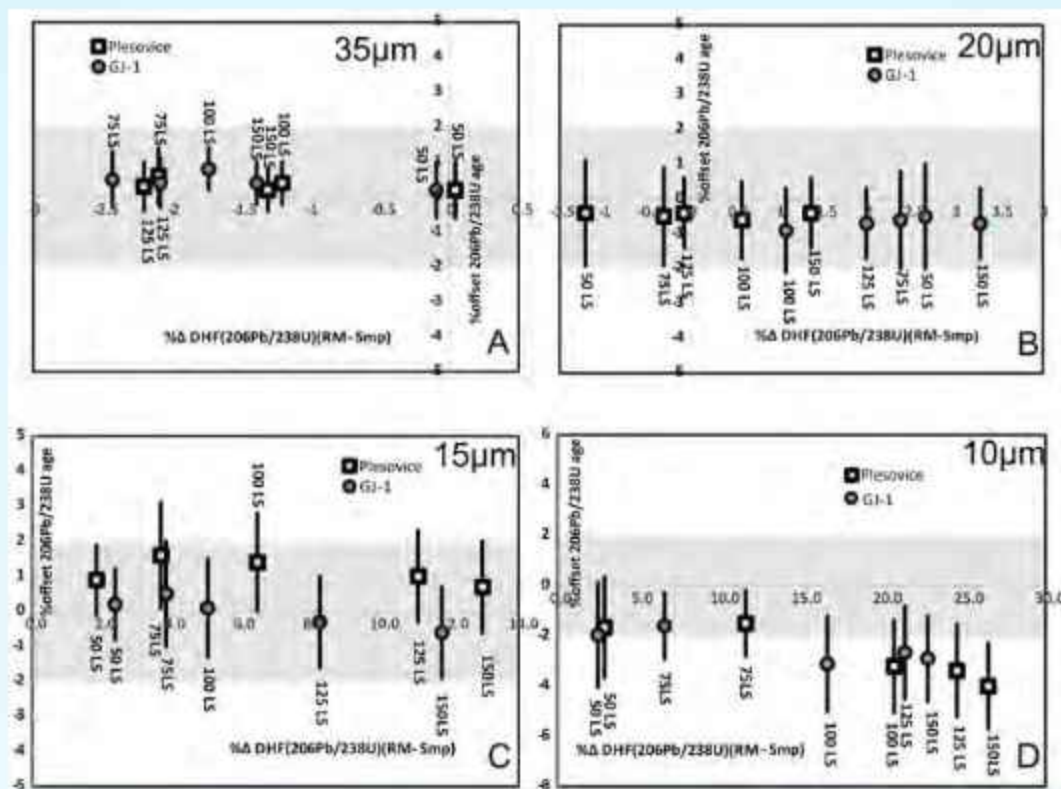
Fig. 9: Percentage (%) offset of $^{206}Pb/^{238}U$ age versus % difference in DHF for $^{206}Pb/^{238}U$ ratio for primary standard (Z91500) and unknown (Plesovice and GJ-1) for (A) 35 μm, (B) 20 μm, (C) 15 μm, and (D) 10 μm. The uncertainty is 2σ level.

The identification of two-phase aqueous-carbonic inclusions and carbonic inclusions suggests an initial eutectic temperature of approximately -56.6 °C, indicating the presence of pure CO_2. The isochores of the H_2O–CO_2 inclusions imply their formation at peak pressure-temperature conditions of 10.9-7.1 kbar and 790-680 °C, while the isochores of the carbonic inclusions indicate they were re-equilibrated in the phase following peak metamorphism due to density reversal. Additionally, two-phase aqueous inclusions were trapped in quartz at 450 °C and 4.2 kbar.

TQ-ICP-MS 8900 is a leading-edge analytical instrument capable for meeting trace elemental determination with high precision and accuracy. This study incorporates the measurement of different level elemental concentrations (0.01 ppb, 0.1ppb, 1ppb, 10, 100 ppb) CRM standards the batch calibration and validation by using MassHunder 5.2 software. By utilizing tuning gas cell modes, including on-mass and mass-shift modes, we demonstrate the effectiveness of He, H_2 , and O_2 in interference mitigation. The use of ^{103}Rh as an internal standard further corrected for matrix suppression and signal drift, significantly enhancing data reliability and reproducibility. The objective of this study includes, i) the accurate determination of REEs including Li, and Th with reduced interference removal, ii) the validation of SLRS-6 (pure water standard) through CRMs and across diverse different river water samples, and iii) the demonstration of the robustness of ICP-MS/MS for routine REE analysis.

In this study, the river water samples were collected at Bhagirathi, Alaknanda and Ganga rivers at different locations, where the numerous tributaries merging with rivers. The pre-cleaned polypropylene (PP) bottles were dipped at a few feet depth, collected the water samples and sealed immediately. The water temperature, pH, total dissolved solids and electrical conductivity (EC) were recorded using a portable multi-parameter instrument of water quality meter (DR1900, Hach, USA). The samples were stored in a refrigerator at 2°C and processed within a week. In laboratory, the samples were homogenized and filtered in 50 ml pre-cleaned centrifuge vials using 0.22μm cellulose membrane filter papers to avoid suspending particulate matters. The filtered samples were acidified with 2% HNO_3 and measured the major, minor and trace elements using ICP MS/MS (Agilent Technologies) at TQ-ICP MS Lab, Wadia Institute of Himalayan Geology, Dehradun (India). The alkaline nature, low TDS and high concentration of elements (Ca>Mg>Na>K>Al>Fe>B>Zn>As>Sr
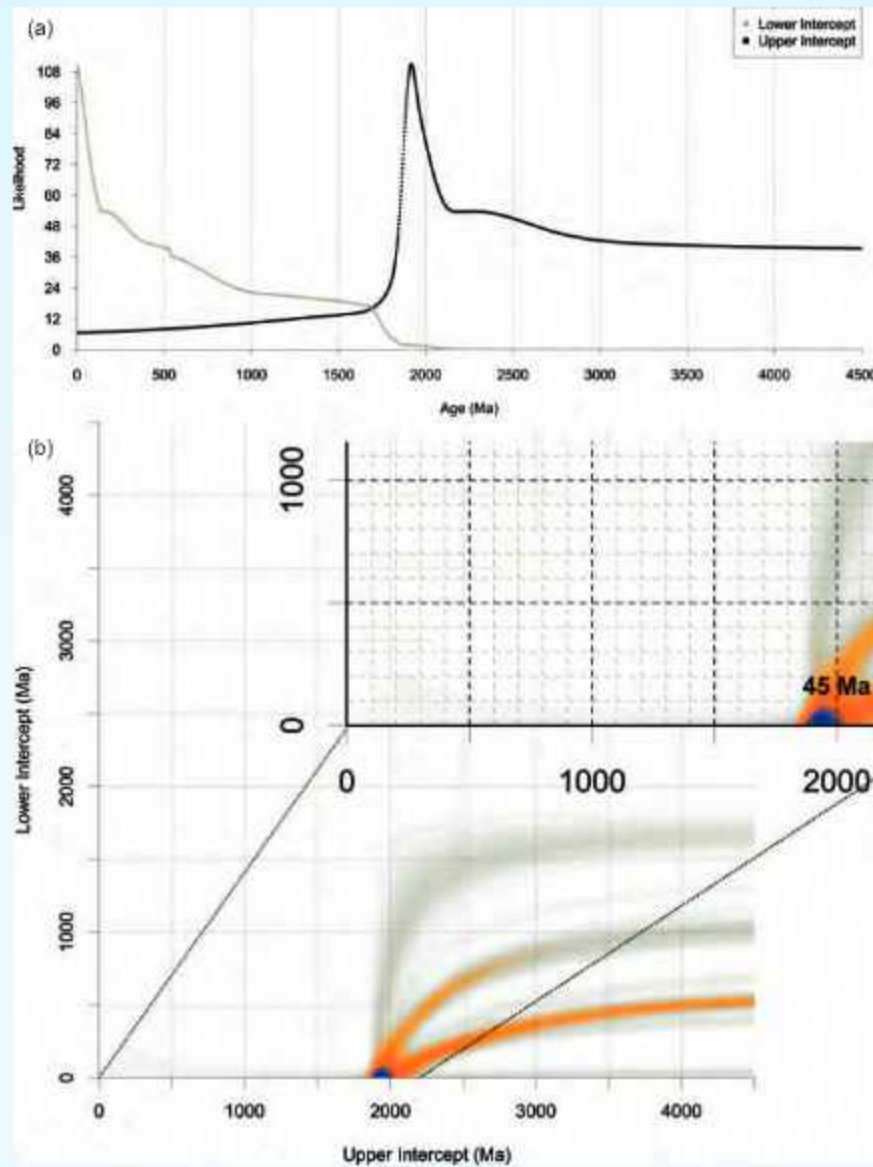
Fig. 10: (a) Likelihood plot for Pb-Loss model U –Pb age showing upper intercept and lower intercept, (b) The 2-D likelihood map indicates upper intercept age ~ca.1920 Ma with the Pb-loss event approximately 45 Ma(b).

>Ba>Rb) reflect the constant weathering of the surrounding lithologology of dolomitic limestone, metabasaltic rocks, slates, phyllites and clay minerals in the sediments and contribute to the water chemical compositions.

The Himalayan metamorphic core exposed in the Bhagirathi Valley of North India is characterized by three principal tectonic zones. The Main Central Thrust zone (MCTz) defines the boundary between the Paleoproterozoic Lesser Himalayan Crystalline rocks and the Proterozoic to Cambro-Ordovician Greater Himalayan Sequence (GHS). Superiorly, the High Himalayan Discontinuity (HHD) separates the lower

inverted metamorphic sequence from the upper anatectic portion of the GHS. The northernmost limit of this metamorphic core is demarcated by the Jhala Normal Fault (JNF). Microstructural analyses of quartz throughout this metamorphic core reveal that lower-temperature dynamic recrystallization has overprinted earlier high-temperature deformation fabrics, as further indicated by prevalent prism (A) slip in quartz. Notably, the strength of quartz crystallographic preferred orientation (CPO) is also maximal at these locations. Vorticity analysis suggests a partitioning of deformation, with simple shear dominating along the JNF and MCTz, while pure shear is inferred for the remaining areas. The exhumation of the Himalayan

metamorphic core is interpreted to have been accommodated by simple shear along the JNF and MCTz. Furthermore, thrust propagation south of the MCTz is proposed to have compensated for adjustments in the Himalayan wedge taper angle resulting from activity along the JNF.

A research initiative focused on analyzing 25 composite coal samples from Kalakot, Metka, and Moghala in Jammu & Kashmir was conducted across four institutions. At WIHG, Dehradun, the geochemical components were analyzed using ICP-MS, XRF for major oxides, XRD for mineralogical analysis, and TOC analysis to understand paleo-history, chemical anomalies, and hydrocarbon potential of these and other Cenozoic coal deposits in India. Simultaneously, the Department of Geology at B.H.U., Varanasi, undertook petrological analysis of the same 25 samples between May 25 and June 16, 2024, focusing on vitrinite reflectance, macerals, microlithotypes under white light, and liptinite under fluorescence light. Complementary geochemical analysis was performed at CIMFR, Dhanbad, during the same period, where proximate, ultimate, and Gross Calorific Value (GCV) were determined using advanced instruments. Finally, biomarker analysis of the 25 composite coal samples was conducted at IISER, Mohali, from September 18th to October 2nd, 2024. This multi-faceted approach aims to provide a comprehensive understanding of the geochemical and petrological characteristics of the Jammu & Kashmir coal deposits.

Activity: 2A

Development of Machine Learning approach to geoscientific data from Himalaya and adjoining region

(Naresh Kumar, Priyadarshi Chinmoy Kumar, Bappa Mukherjee and Jitender Kumar)

Tectonic Subsidence Modelling

Designed and computed tectonic subsidence curves (Fig. 11) using borehole stratigraphic data from the Upper Assam Basin to investigate its tectonic evolution. This modelling approach allowed quantification of the total subsidence experienced by the basin over time. Overall, the basin experienced tectonic subsidence of ~2 km throughout its lifespan with an average subsidence rate of ~30 m/Ma. This case study prominently elucidates the tectonic history of the basin, which occured during the Cenozoic time. Our findings stress the importance of subsidence analysis through the backstripping technique as a potential approach for untangling the geohistory of sedimentary basins worldwide.

Seismic Attribute-Based Machine Learning (ML) Workflows

Designed and implemented seismic attribute-assisted machine learning workflows utilizing high-quality seismic data to interpret the subsurface sedimentary environments effectively.
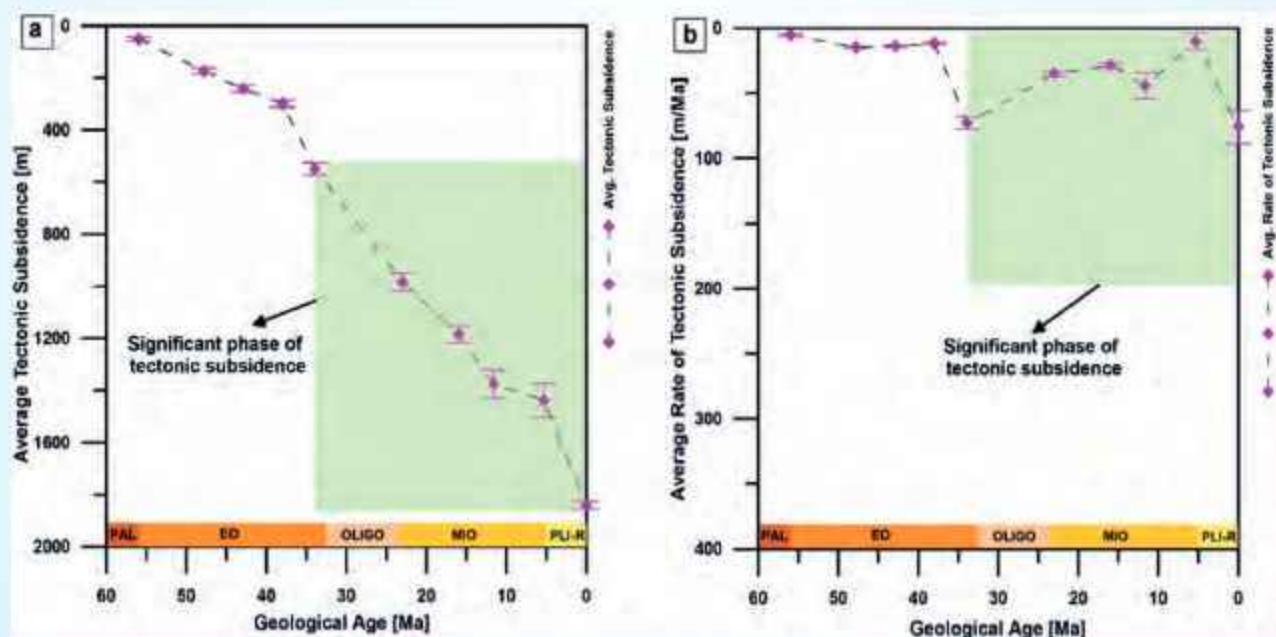

Fig. 11: (a) Average tectonic subsidence, and (b) average rates of tectonic subsidence over the geologic time compiled from the backstripped stratigraphic details of the studied boreholes. The standard error is highlighted using pink vertical bars.
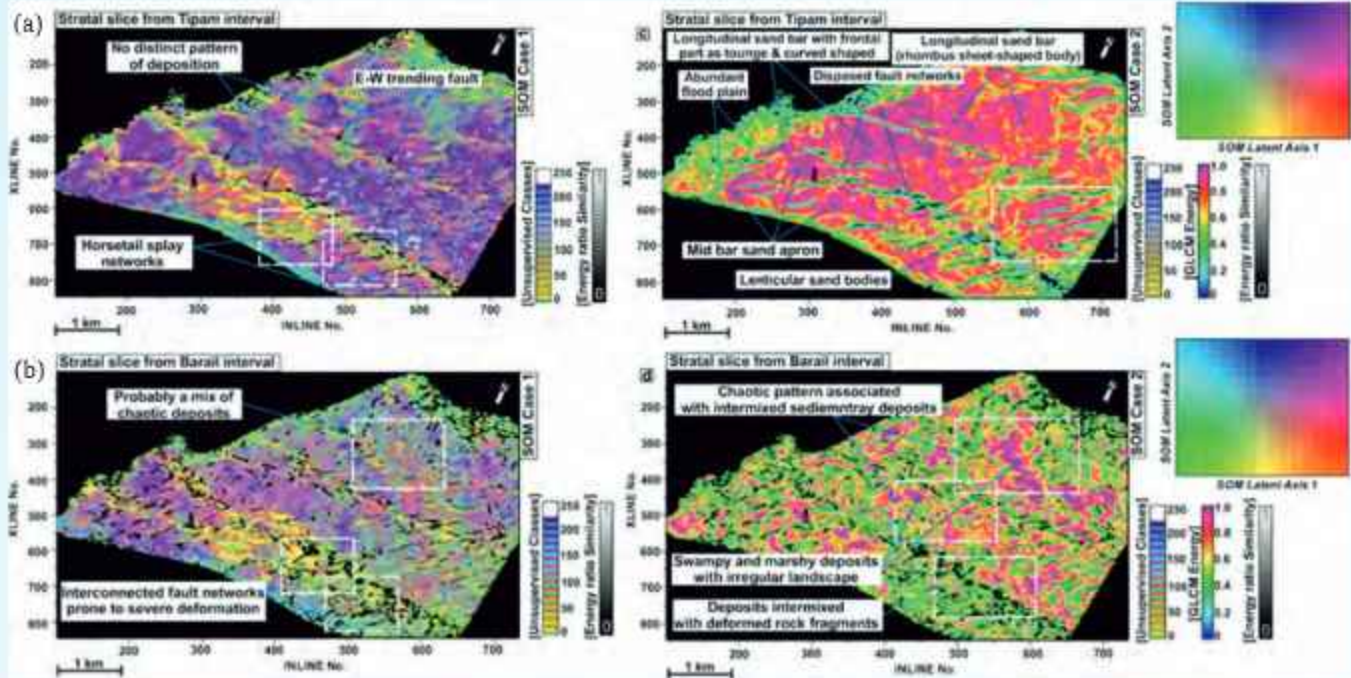
RESEARCH ACTIVITIES

Fig. 12: (a-b) Stratal slices from the Tipam and Barail intervals displayed for SOM Case 1 co-rendered with energy ratio similarity attribute. The display highlights the presence of fault networks (marked using solid black arrows); (c-d) Stratal slices from the Tipam and Barail intervals, displayed for SOM Case 2 co-rendered with GLCM energy and energy ratio similarity attributes. The model clearly highlights the geometry of several geomorphic features associated with the fault-bounded sediments within the interval of interest.

A series of seismic attributes, including geometrical, spectral, amplitude, and GLCM-textures (Grey Level Co-occurrence Matrix), are extracted using high-resolution three-dimensional seismic data acquired from the upper shelf of the basin. These attributes are amalgamated into two different cases to compute the self-organizing maps (SOM) models (Fig. 12) with an aim to highlight the subsurface structures and reveal sedimentary deposits engulfed within these structures. It is observed that the model SOM Case 1 highlights subsurface fault networks that structurally control the Oligocene-Miocene intervals. However, the model SOM Case 2 not only hints at the presence of these structures but also illuminates different patterns of seismic reflections and geomorphic features associated with sediment entrapped within the fault-bounded structures. Through this research, we envisage that for the SOMs to be optimal, geologically meaningful sets of seismic attributes should be used as an input, such that attributes assisting seismic interpreters could successfully identify relations or patterns within the data.

Basement Structure Interpretation

Interpreted the geometry and disposition of basement structures using advanced seismic attributes and ML-assisted workflows. These methods, applied across the upper shelf regions of NE India, can be adapted for seismic interpretation in other global onshore and offshore sedimentary basins.

The basement in the Upper Assam foreland basin, NE India, is severely deformed and buckled. It is compartmentalized into several structural compartments. These compartments are breached with minute flexures (or fractures) that developed over the geologic period due to tectonic modifications by fault networks and overlying sediment loads. Flexure anomalies dominant within the basement interval are interpreted using high-quality three-dimensional seismic data acquired from the basin. Attribute maps obtained by computing legacy seismic attributes such as energy-ratio-similarity and curvature are integrated to interpret flexure networks and associated deformed structures. An advanced seismic attribute called aberrancy is computed to complement the interpretations of the above legacy attributes (Fig. 13).

Application of ML for interpreting Basement faults

Accurately characterizing the basement faults, including their patterns and movements, holds paramount importance for engineers and seismologists in designing foundations and geotechnical structures
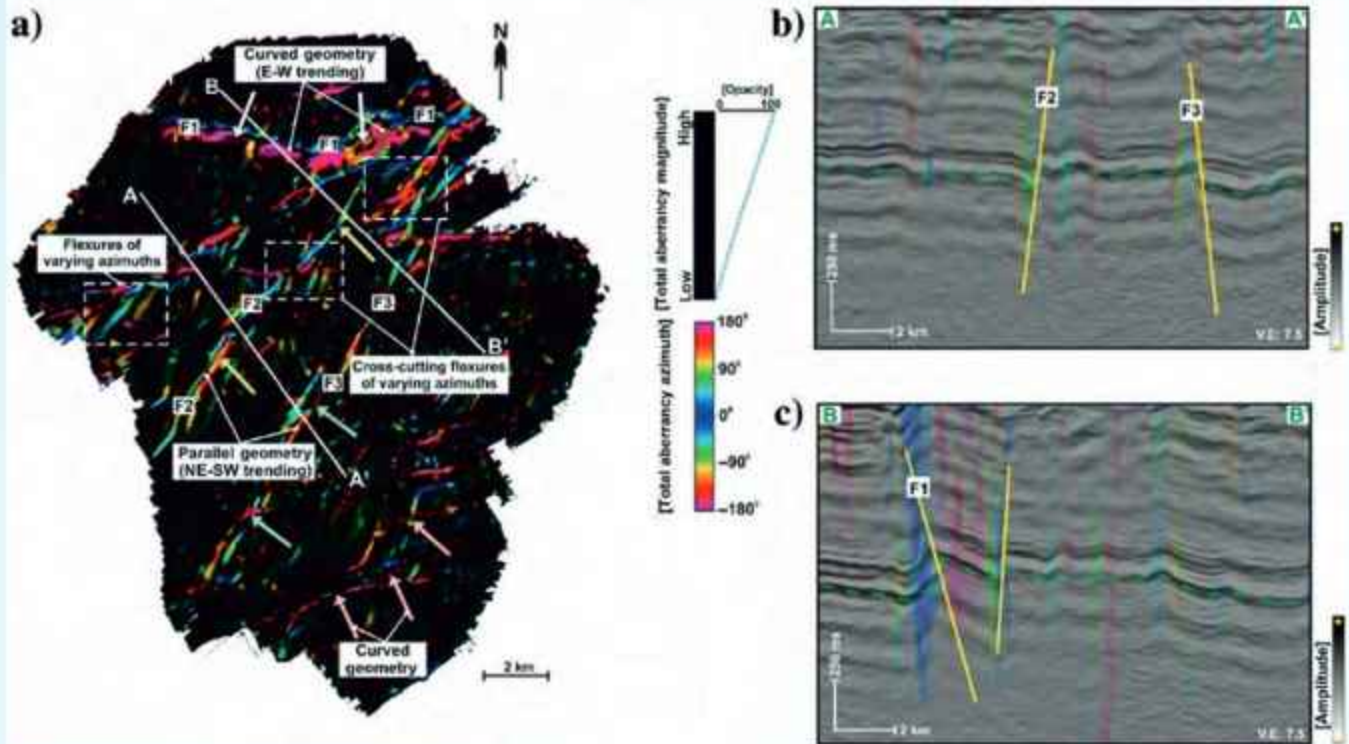
Fig. 13: (a) Aberrancy attribute map displayed for the basement top. The display is prepared by co-rendering the total magnitude and azimuth components of the aberrancy attribute. Fault networks and several crosscutting flexures of varying azimuths structurally deformed the basement in the study area. Major faults are highlighted using solid arrows in different colors; (b-c) Arbitrary seismic lines are displayed by co-rendering the amplitude volume with the aberrancy attribute, which in turn highlights the presence of such subtle anomalies within the basement interval.

and exploring resources. This research explores the efficacy of unsupervised machine learning models to uncover fault networks that structured and deformed the basement interval in the Dibrugarh region of northeast (NE) India. High-quality three-dimensional seismic data from the upper shelf of northeast India is utilized to extract a comprehensive set of geometric attributes. These attributes are analysed and amalgamated using two distinct unsupervised machine learning models: the self-organizing map (SOM) and the generative topographic mapping (GTM). Each of these models is interpreted and compared to determine the most effective unsupervised machine learning model for illuminating basement faults and associated deformations (Fig. 14).

Machine learning assisted state-of-the-art petrographic classification from geophysical logs

Accurate lithology classification is a fundamental task in the exploration and production (E&P) industry, as it aids in understanding reservoir characteristics and guiding extraction strategies. Traditional methods, such as core logging, are costly and time-consuming. In contrast, geophysical logs provide high-resolution petrophysical properties, making them a valuable tool for lithology prediction. However, conventional methods often struggle with precise lithology classification, especially in complex geological formations. In this study, we explore the use of six machine learning (ML) algorithms, namely k-Nearest Neighbors (kNN), Support Vector Machine (SVM), Decision Tree (DT), Random Forest (RF), Extreme Gradient Boosting (XGBoost), and Artificial Neural Networks (ANN) to predict lithology from geophysical log data.

The study focuses on the Lakadong-Therria formation of the Bhogpara oil field, located in the Assam-Arakan Basin, a petroliferous region with rich subsurface lithology. Figure 15(a) shows the geographic location of the Bhogpara oil field, while figure 15(b) depicts the distance between the studied wells, providing an overview of the spatial arrangement of the wells within the field. The general stratigraphy of the Lakadong-Therria formation is illustrated in figure 15(c), outlining the lithological sequence that serves as the geological context for this study.
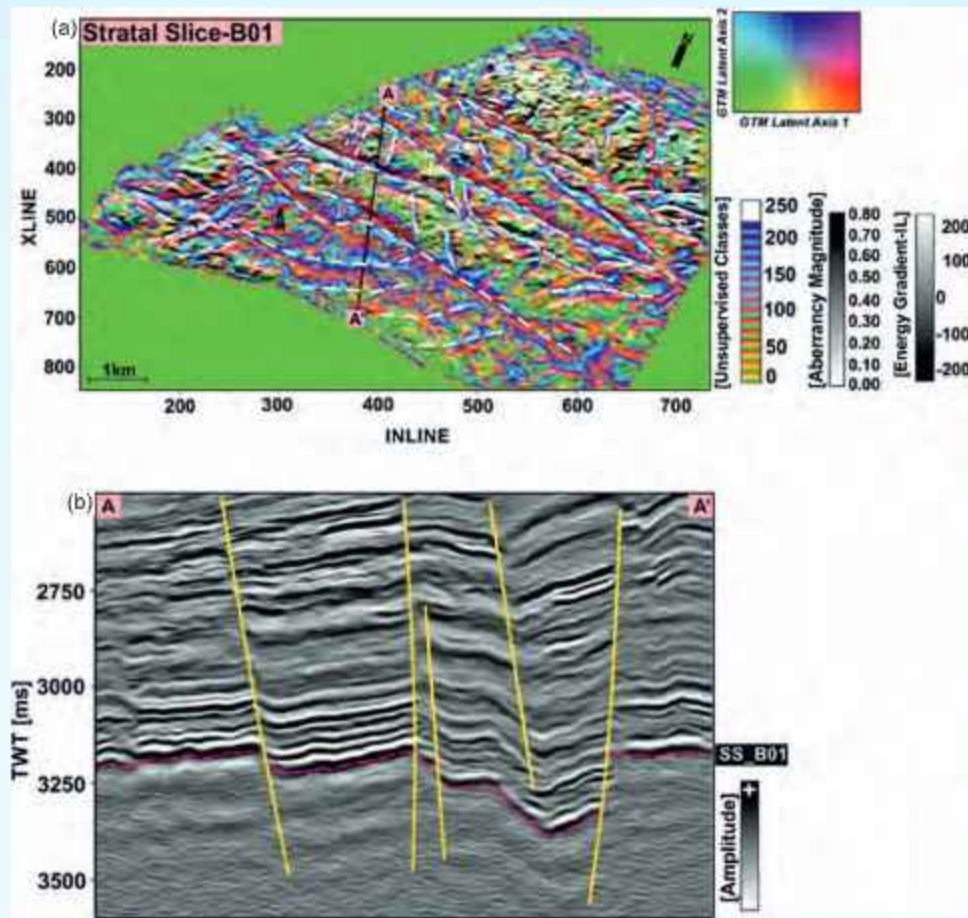
RESEARCH ACTIVITIES

Fig. 14: (a) Strata slices displayed for the basement interval using the GTM. The slices prominently illuminate the rugged and deformed structural environment of the studied basement; (b) Arbitrary seismic line AA' demarcating the position of the stratal slices extracted from the basement unit. Faults are marked using yellow solid lines in the cross-sections. The geometry and distribution of fault networks are highlighted using dotted white curves in the strata slices. The wellbore is marked using a black tripod.

The study utilised wireline log data from eight wells in the Bhogpara oil field, representing various lithologies such as claystone, sandstone, calcareous sandstone, shale, calcareous shale, carbonaceous shale, coal, and limestone. The wireline logs and core-derived lithological sequences from Well-2 and Well-4, as exemplified in figures 16 and 17, respectively. These figures show the wireline log responses, including caliper log, gamma ray (GR) log, laterolog deep resistivity (R_t) log, neutron porosity (Φ_N) log, bulk density (ρ_b) log, photoelectric factor (PEF) log and core-derived lithological sequence. These wireline logs serve as the input features for training the machine learning models. The task is to predict the lithological classes based on these features, providing a mapping between the physical log responses and the lithological types identified in core samples.

We applied six machine-learning models (kNN, SVM, DT, RF, XGBoost and ANN) to predict lithology from the geophysical log data. These models were evaluated based on several performance metrics, including accuracy, precision, recall, F1-score, and the receiver operating characteristic (ROC) curve. The results demonstrated that the ANN and XGBoost models performed the best, achieving the highest accuracy during both the training and testing phases. The accuracy hierarchy was ANN > XGBoost > RF > SVM > DT > kNN during training, and ANN/XGBoost > kNN > DT/RF > SVM during testing. Figure 18(a-g) illustrate the predicted lithofacies classification at Well-2, based on the six ML classifiers, alongside the core-derived lithological sequence. Figure 18(a) shows the true lithological sequence derived from core logging, while figure 18(b-g) display the predicted lithofacies classification from each model. The comparative

RESEARCH ACTIVITIES
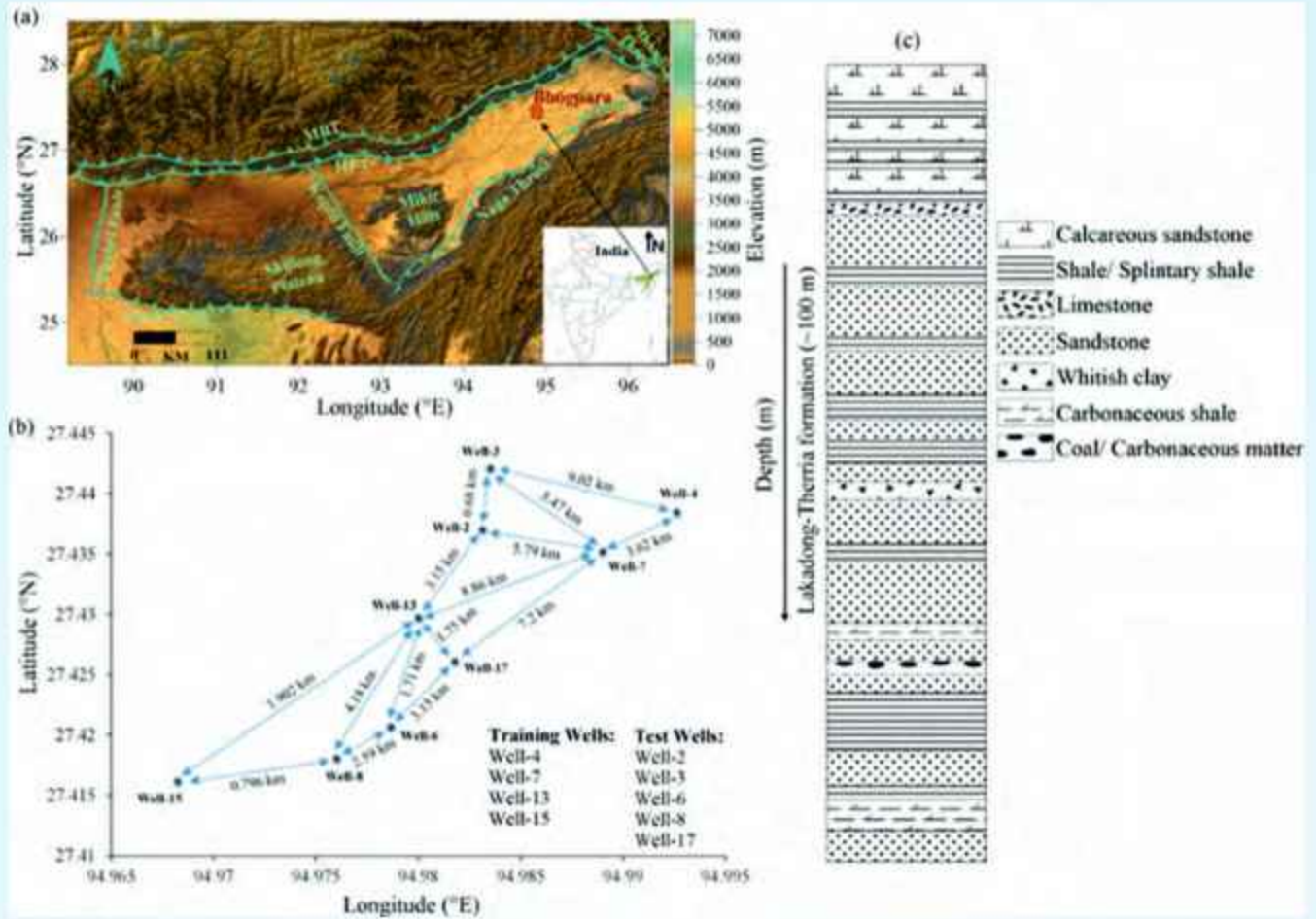
Fig. 15: (a) Geographic location of the Bhogpara oil field, (b) distance among the studied wells, and (c) representation of the generalised stratigraphic column of the Lakadong-Therria formation.
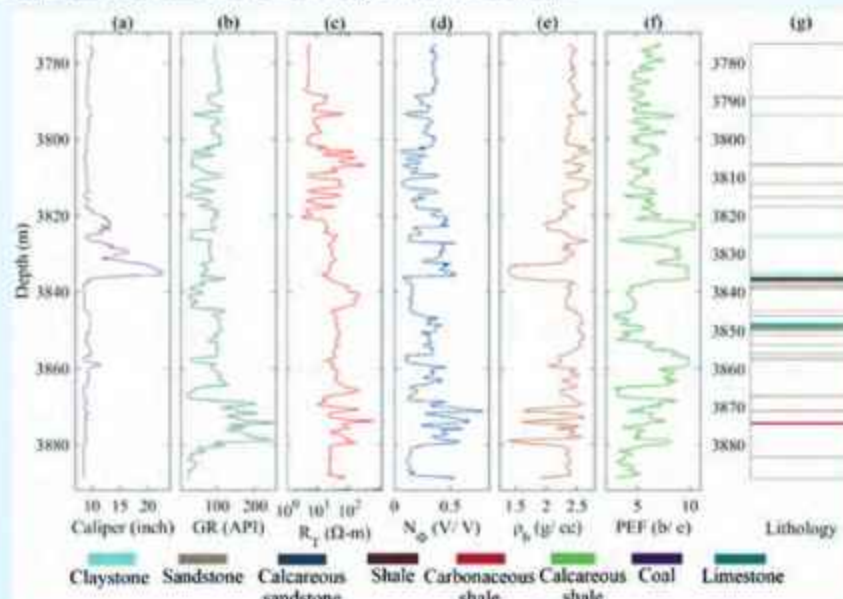
Fig. 16: Wireline log responses and core-derived lithological sequence at the well-2. (a) Caliper, (b) gamma ray (GR), (c) laterolog deep resistivity (R_t), (d) neutron porosity (Φ_N), (e) bulk density (ρ_b), (f) photo electric factor (PEF) log, and (g) core derived lithological sequence, respectively.

Fig. 17: Wireline log responses and core-derived lithological sequence at well-4. (a) Caliper, (b) gamma ray (GR), (c) laterolog deep resistivity (R_T), (d) neutron porosity (Φ_N), (e) bulk density (ρ_s), (f) photoelectric factor (PEF) log, and (g) core-derived lithological sequence, respectively.
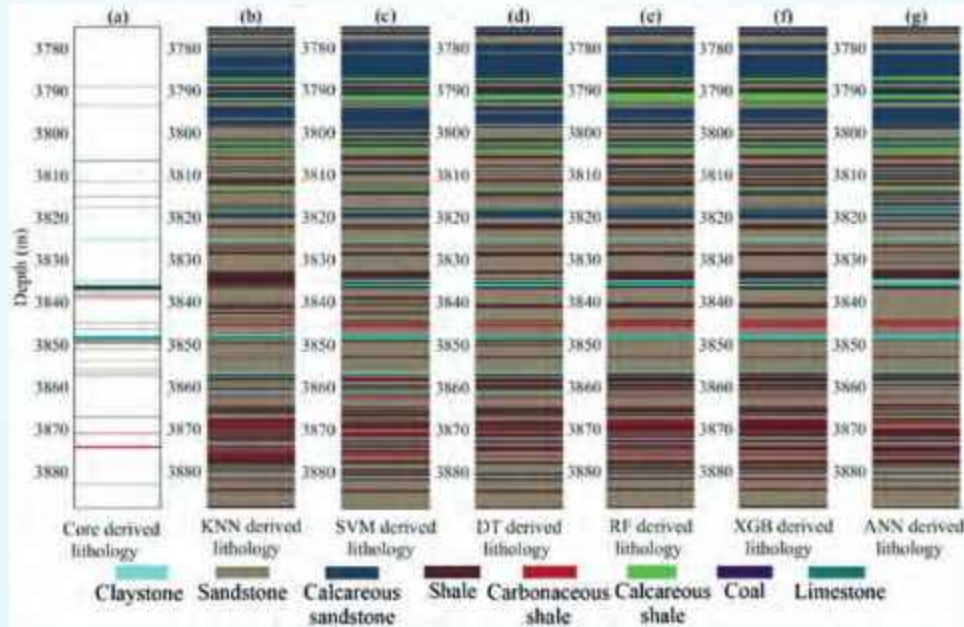
Fig. 18: Core-derived and predicted lithofacies classification from all six ML classifiers at well-2 (a) core-derived lithological sequence, (b) kNN predicted l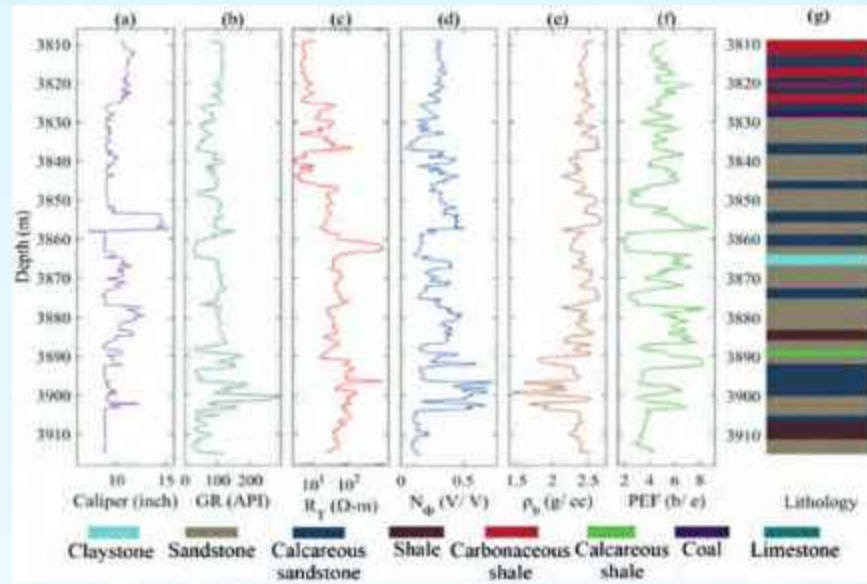ithofacies classification, (c) SVM predicted lithofacies classification, (d) DT predicted lithofacies classification, (e) RF predicted lithofacies classification, (f) XGBoost predicted lithofacies classfication and (g) ANN predicted lithofacies classification.

analysis demonstrates that XGBoost and ANN produced the most accurate lithofacies classification, closely matching the core-derived lithology. These models not only provide high accuracy but also offer a robust approach to lithology prediction in complex geological formations.

This study highlights the application of machine learning models for predicting lithology from geophysical logs, demonstrating the effectiveness of advanced algorithms like XGBoost and ANN in achieving high prediction accuracy. The results suggest that machine learning can significantly improve the

RESEARCH ACTIVITIES
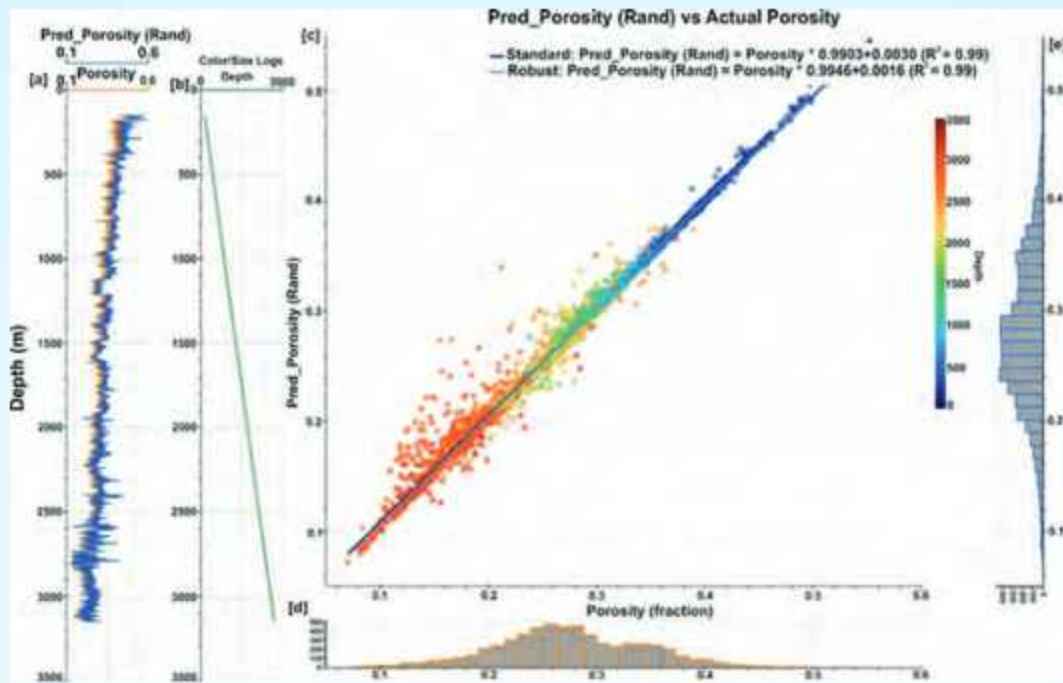
Fig. 19: Cross plot between actual and predicted outcome for the Random Forest algorithm of machine learning. The R^2 error between actual and predicted porosity is 0.99. (a)The first Panel represents the over lay of actual and Random Forest predicted porosity; (b) second panel represent the data availability throughout the studied depth interval; (c) third panel represents the actual porosity vs Random forest predicted porosities at different depth interval; (d) fourth panel shows the histogram representation of the actual porosity and (e) fifth panel shows the histogram representation of the predicted porosity.
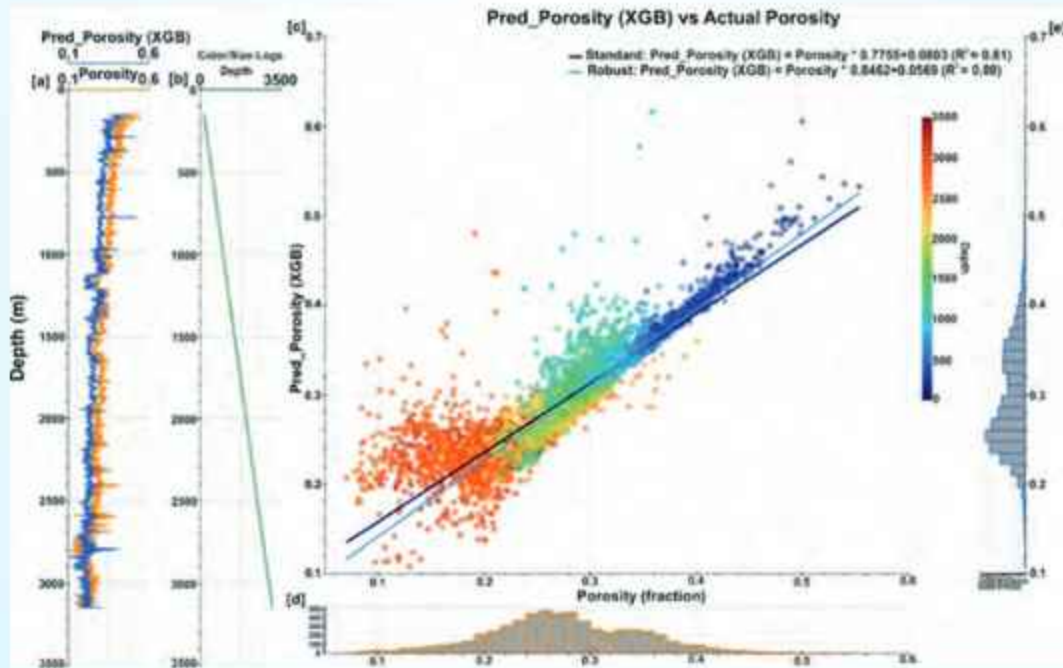
Fig. 20: Cross plot between actual and predicted outcome for the XGBoost algorithm of machine learning. The R^2 error between actual and predicted porosity is 0.81. (a)The first Panel represents the over lay of actual and XGBoost predicted porosity; (b) second panel represent the data availability throughout the studied depth interval; (c) third panel represents the actual porosity vs XGBoost predicted porosities at different depth interval; (d) fourth panel shows the histogram representation of the actual porosity and (e) fifth panel shows the histogram representation of the predicted porosity.

efficiency and accuracy of lithology classification, providing a valuable tool for geologists and reservoir engineers. Furthermore, the use of geophysical logs combined with ML techniques can supplement core-derived lithological sequences, enhancing the overall understanding of subsurface geology and aiding in better decision-making for exploration and production.

Porosity prediction through an ensemble ML approach

In petroleum exploration, it plays a crucial role in reservoir characterization, petrophysical studies, and geological analysis. However, in practice, porosity logs are not enumerated in the recorded logs for the entire well, either due to instrumental error or borehole environmental issues. Thus, the prediction of porosity log is essential to perform a better petrophysical analysis and reservoir characterization. In the present study, we emphasize the implementation of machine learning (ML) approaches in the prediction porosity log at the missing data interval. The outcome of the present study is satisfactory enough as we have seen the correlation coefficient values of the actual and predicted porosity vary between 0.8 to 0.9 (Figs. 19 and 20). Thus,

ensemble ML approaches could provide other petro-physical parameters at the missing data interval.

Activity: 2B

Geometry and rheological assessment of the MHT, lithospheric flexuring - Implications toward seismogenesis, deep earth processes

(Naresh Kumar, Devajit Hazarika, Gautam Rawat and Vandana)

Stress field implications in the Himalaya-Karakoram-Tibet based on Stress Tensor Inversion

The stress regime patterns of high seismically active regions within the western part of the India plate (IP) and Eurasia plate (EP) collision, spanning the parts of Himalaya-Karakoram-Tibet, are elucidated through analysis of 684 Focal Mechanism Solutions (FMS) from 1962 to 2021. Eighteen seismically active zones (Fig. 21) used for the stress tensor inversion, are defined based on the spatial extent of the seismicity, the depth distribution of seismic events, focal mechanisms and seismotectonics. Distinct regimes demarcated are: (1) Sulaiman Ranges and Lobe Region, (2) Hindukush, (3)

RESEARCH ACTIVITIES
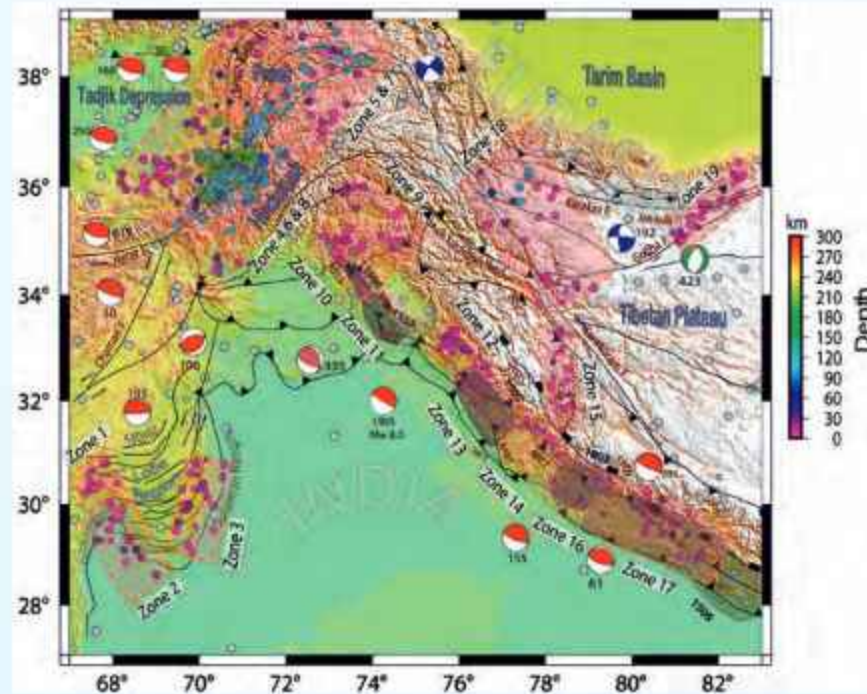
Fig. 21: Seismotectonic map of the study region. Major faults, strong and major earthquakes, seismicity and the zones for Stress Tensor Inversion (STI) are shown in the map: The areas defined with dotted line is showing the zones considered for the STI. The used events for STI are shown as the filled circle with colour inside the zones, the colour of the event represents the corresponding focal depth (km). Events with grey colour indicating the unused events for this study. Some of the past strong and major events (M≥6.5) are shown as beachball representations. The different colour of the beachball indicating different mechanisms (red: thrust, green: normal, blue: strike-slip, brown: thrust + strike-slip).

Pamir, (4) Nanga Parbat Syntaxis (NPS), (5) Hazara Syntaxis, (6) Kashmir-Zanskar region, (7) Kangra-Chamba, (8) Kinnaur and Kaurik-Chango Fault Zone (KCFZ), (9) Garhwal, (10) Kumaon, (11) Karakoram Fault Zone (KFZ), and (12) Gozha-Ashikule Fault Zone. Most of the seismicity is concentrated in the upper crust, except in the Hindukush and Pamir, where seismicity extends to the uppermost mantle (~280 km). Seismicity is clustered into three depth zones (up to 70 km, 70 - 160 km and 160 - 280 km) with distinct seismicity groups in this part of the Hindukush and Pamir. Stress Tensor Inversion (STI) of FMS visualise the stress pattern on the tectonic and sub-surface crustal-scale structure (Fig. 22).

The stress regimes and corresponding maximum horizontal stress axis (SH_{max}) orientations of different zones indicate north and NE thrusting in NW Himalaya, strike-slip in KFZ and extensional in areas which closely associated with Tibetan plateau (Zones 15 and 19, Fig. 1). The SH_{max} directions obtained from this study align with the horizontal principal strain-rate directions reported earlier. Furthermore, the results reveal a discernible gradient in stress regimes along the boundaries of the Tibetan plateau. Stress regimes shift from compression in the southern boundary (Zone 12 to Zone 17) to transpression in the central part (Zone 18) and to extensional stress on the northern edge (Zone 19). The same type of transition in the stress regime from SW to NE direction in the Hindukush-Pamir (HP) region is also evident. Based on the findings of this stress inversion study, there was no discernible difference between the Right Dihedron and Rotational Optimization approaches except for the zones where the vertical PSA has high uncertainty in orientation. The Rotational Optimization approach may produce more accurate results because it reduces any inherent error in the PSA orientation.

In the Hindukush region, the clockwise rotation of SH_{max} in the compressive regimes with respect to increasing depth reflects the rotational nature of the thrusting plate vis-à-vis with the increase in depth (Fig. 23). Simultaneously, in the Pamir region, anti-clockwise rotation of SH_{max} together with a change in stress regimes with respect to increasing depth has been observed. An effective conceptual model that highlights the depth-wise regional stress environment is provided
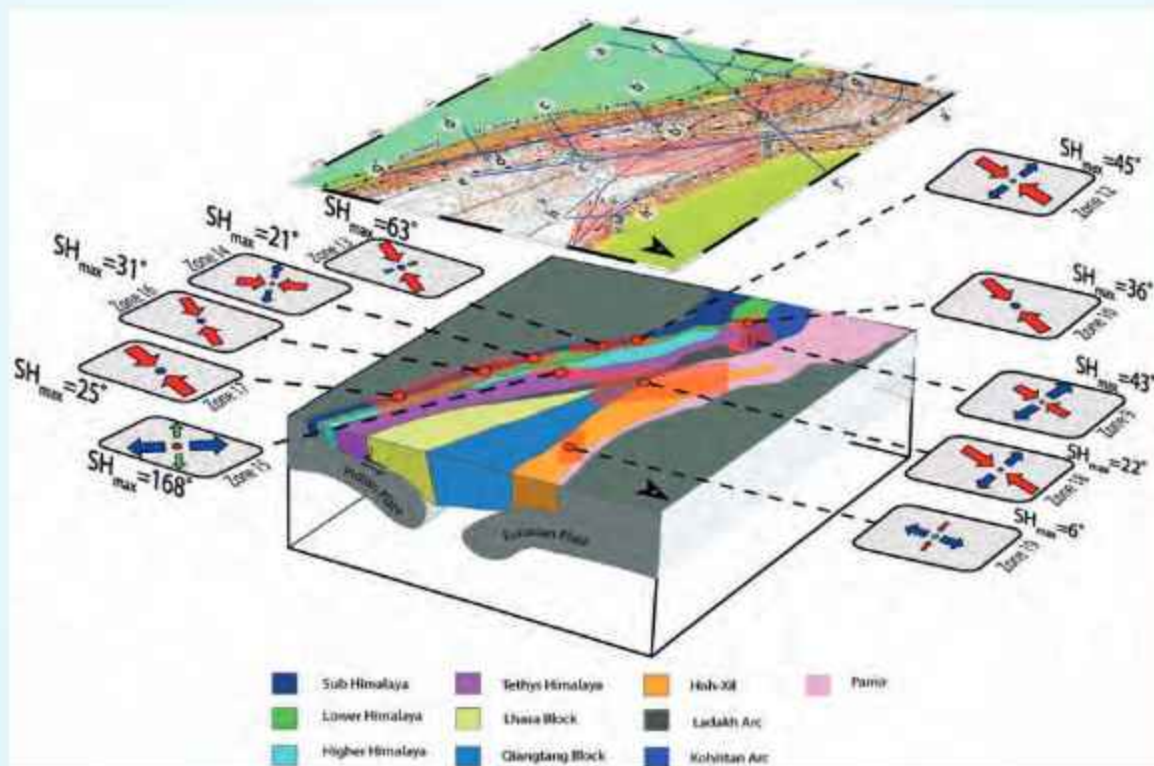
Fig. 22: A 3D illustration of tectonic model showing the stress regimes and corresponding SH_{max} orientation in NW Himalaya, Karakoram and Gozha-Ashikule regions. Major crustal blocks are shown in different colour according to legend (Modified after Parsons et al., 2020). The blue lines (a-a', b-b', c-c', d-d', e-e', f-f', g-g' and h-h') represents the cross-section profiles.
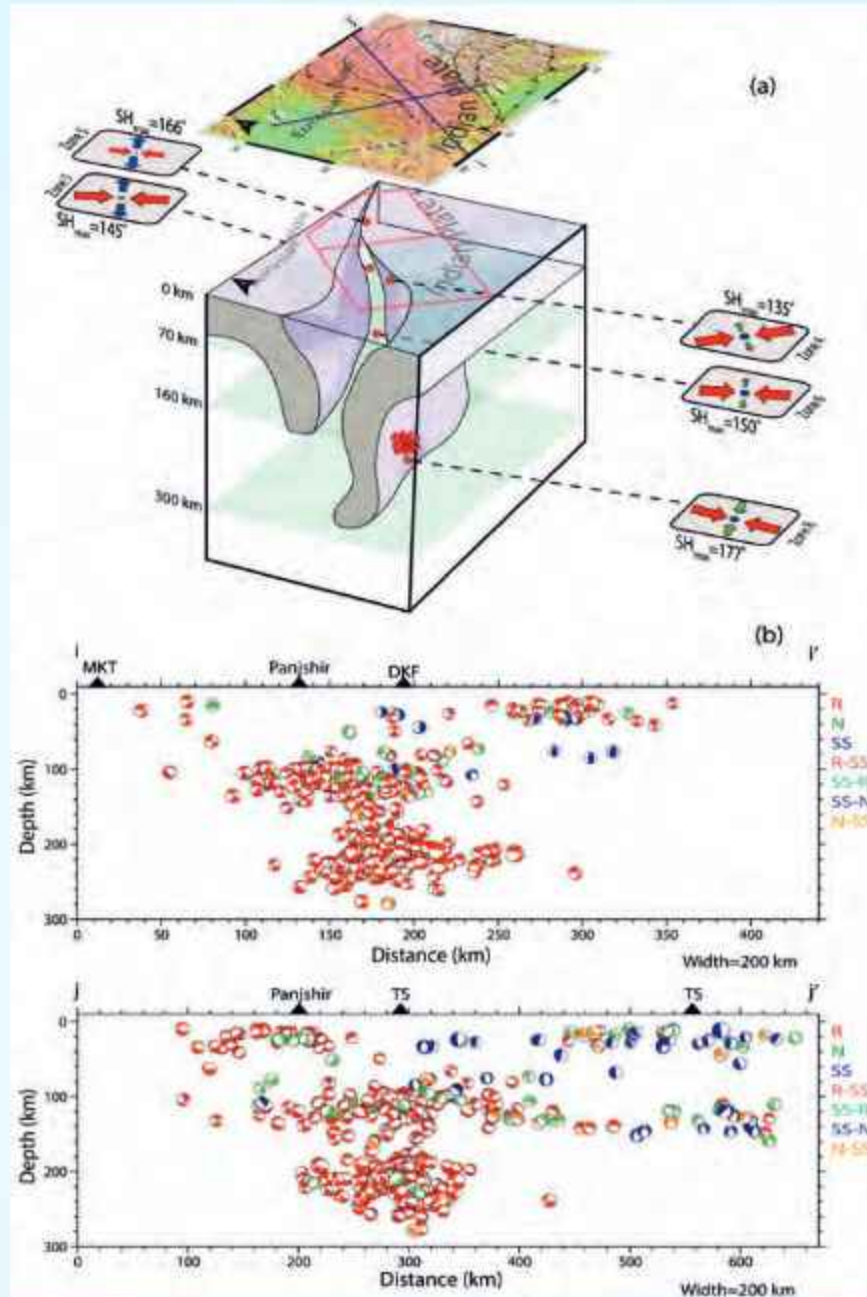
Fig. 23: (a) A 3D illustration of the tectonic model showing the stress regime and corresponding SHmax orientation in Hindukush- Pamir region in depth-wise manner. The blue lines (i-i' and j-j') represents the cross-section profiles. (b) Projection of FMSs along the i-i' and j-j' cross-sections as beachball representations. Different colours of beachballs indicate the different type of FMS as shown in the legend. Filled triangle at the top represents the major faults that intersect with the respective profiles.

by the seismicity and STI results in the HP region (Fig. 23). It gives effective information on the IP-EP collision and additional data in the future will strengthen the results. In the NW Himalayan arc, the tectonic convergence force is acting as the major driving force that controls the nature of the stress regime. However, regions like the NPS, Kinnaur, KFZ, and Zanskar are exceptions to this, where dominating extensional and transformational tectonic forces are dominating. It also indicates complex tectonics on a local scale. The SH_{max} orientation is nearly perpendicular to the plate boundary where thrusting/subduction occurs which implies that convergence tectonics is the major driving force for the seismotectonics processes in such regions. In the NW

Himalayan arc, the seismic gap zones exhibit thrust regimes in general. The KFZ and GAFZ are located in the Tibetan plane where the plate convergence force has less effect on defining the stress regime.

The investigation of seismic discontinuities in the Earth's upper mantle is vital for understanding the mantle process that influences the geodynamic evolution of a tectonically active region. Earth's mantle plays an important role in the evolution of the crust and provides the thermal and mechanical driving forces for plate tectonics. Unlike the crust, the chemical and mineralogical composition of the mantle is straightforward. The upper mantle is largely a peridotitic metamorphic complex that is comprised of olivine minerals, orthopyroxene, clinopyroxene, and an aluminous phase (e.g. plagioclase, spinel, or garnet as a function of pressure). The crystallographic structure of minerals changes with the pressure and temperature of the upper mantle leading to phase transitions. Several

seismological studies detected primary global discontinuities of the upper mantle (e.g. 440 and 660 km), however, second-order discontinuities such as the Hales discontinuity in the lithospheric mantle (Hales, 1969, EPSL, vol: 7, pp: 44–46) is poorly studied.

A shallow mantle seismic discontinuity (Hales) beneath northeast India

This study, reported Hales Discontinuity for the Upper Assam Valley or Brahmaputra River Valley (BRV), and parts of IBR and Bengal Basin based on teleseismic receiver function (RF) inversion and Common Conversion Point (CCP) imaging at 11 boradband seismological stations of National Center for Seismology, MoES, New Delhi (Fig. 24). The waveform data of teleseismic earthquakes with a high signal-to-noise ratio (> 3.0), body wave magnitude (Mb > 5.5), and epicentral distance (Δ) of ~30-95° were used (Inset, Fig. 24). Example of RFs at IMP station shows P-
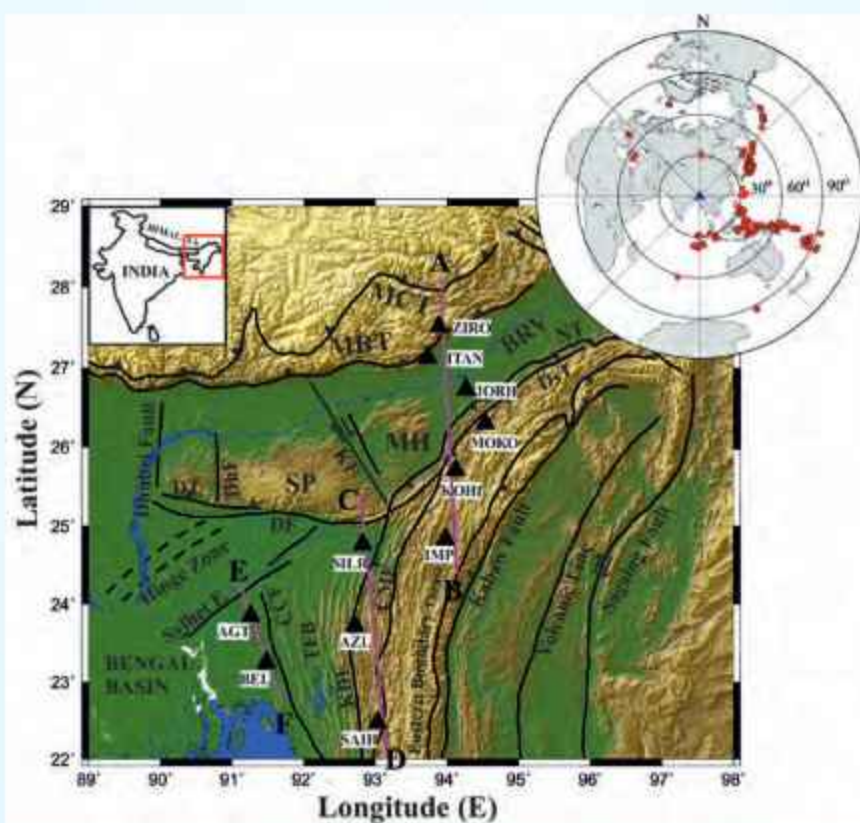
Fig. 24: Tectonic map of the northeast region (NER), India, showing the location of seismological stations (black triangles) used in this study. Major tectonic features e.g., Brahmaputra River Valley (BRV), Shillong Plateau (SP), Mikir Plateau (MP), Chittagong Coastal Fault (CCF); Churachandpur-Mao Fault (CMF); Dauki Fault (DF); Dudhnoi Fault (DhF); Disang Thrust (DsT); Dapsi Thrust (DT); Kaladan Fault (KDF); Kopili Fault (KF); Main Boundary Thrust (MBT); Main Central Thrust (MCT); Naga Thrust (NT); Tripura Fold Belt (TFB); The inset at the top left shows sketch map of India marking the study region by a red box. The epicenters of the teleseismic earthquakes used in this study are shown in the inset at the top right corner.

to-S conversion at Moho (P_ms) and Hales (P_hs) discontinuities (Fig. 25). The first strong positive arrival observed at 0 s in the RFs is the direct P-arrival (Pp phase) followed by the positive arrivals at ~3.2 s, ~6 s, and ~7 s. The positive arrival at ~3.2 s represents a shallow mid-crustal discontinuity and can not be attributed to the Moho discontinuity as it would imply
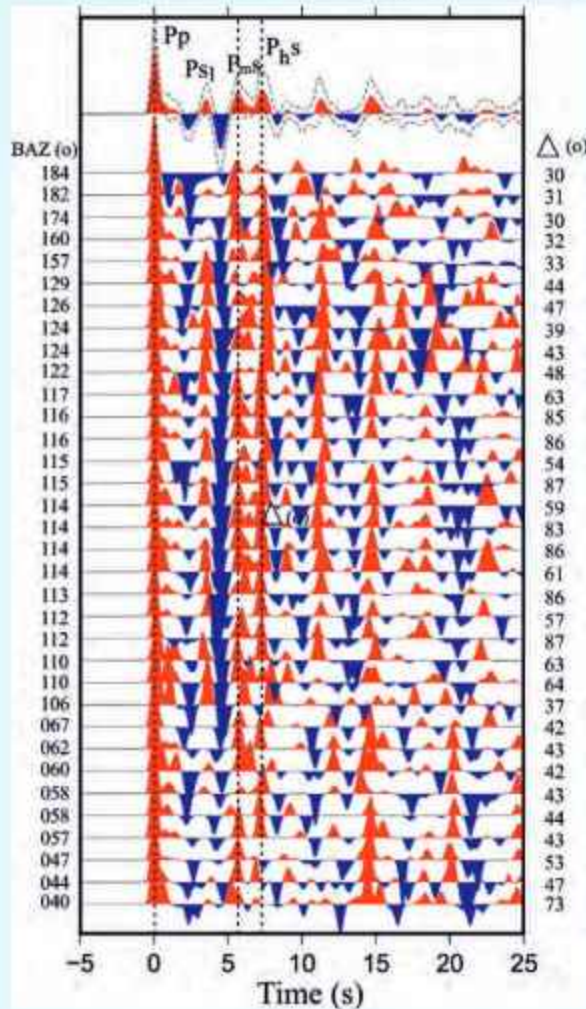
Fig. 25: Receiver functions (move-out corrected) plot of Gaussian width 2.5 for the Imphal (IMP) stations with increasing back azimuth (BAZ) marked at the left. The corresponding epicentral distance (Δ) is shown on the right. The direct P-wave (Pp), P-to-S conversions from the Moho (Ps), and the Hales (Ph) discontinuities are marked by dashed lines, respectively. The stacked receiver function is shown at the top with ±1 Standard Deviation bounds. The Ps_1 is a mid-crustal phase which may be a possible conversion at the Main Himalayan Thrust (MHT).

an unusually thin crust. Based on arrival time and polarity, as well as comparing with previous studies, the positive arrival at ~6 s is considered as Moho discontinuity. The strong positive arrival observed after the Ps phase, labeled as Phs, is recognized to originate from a shallow mantle discontinuity (i.e. Hales discontinuity). The Neighborhood Algorithm (NA) inversion method has been applied to radial RFs. Example of inversion has been shown considering data from IMP station (Fig. 26). The velocity model shows a low-velocity zone (LVZ) in the upper crust (~10-22 km). The Ps1 phase corresponds to the base of the LVZ. A sharp change in Vs is observed at ~42 and ~57 km with Vs ~4.1 and ~4.6 km/s, respectively. Based on shear wave velocity and previous studies in the region, the step jump at ~42 km is considered as Moho whereas the next step jump is identified as a shallow upper mantle discontinuity interpreted as the Hales discontinuity.

The study reveals a thin crust (~35 km) beneath the Brahmaputra Valley (at JORH station) with a surface sedimentary layer of ~4 km thick. The crustal thickness is observed to increase towards the north in the Himalaya (~40 km at ZIRO and ITAN) and to the south (up to ~46 km at KOHI). The crustal thickness near the Tripura fold-belt and Bengal Basin varies within ~36-40 km. The study reveals the existence of a shallow mantle discontinuity (Hales discontinuity) at a variable depth range of ~54-78 km characterized by a step increase (~7.5-11%) in shear wave velocity observed in the inverted models (Fig. 27). The mineralogical phase transformation from spinel to garnet is considered as the origin of this discontinuity. The shallow depth of the discontinuity indicates an increase in upper mantle temperature which conforms to the high geothermal gradient reported in the region. The variation of depth of the discontinuity can be interpreted in terms of the addition of Cr^{-3} which shifts the spinel-garnet stability field to higher depths whereas Fe^{-2} shifts it to lower depths. Despite the high temperature in the upper mantle, the observed low Vp/Vs ratio (1.65-1.75) below the Hales discontinuity can be explained by the presence of a high fraction of orthopyroxene.

Multiparametric approach to surface dynamics of rock-ice avalanche

The observation of precursory signals of the 2021 Chamoli rock–ice avalanche provides an opportunity to investigate the multidisciplinary analysis approach of rock failure. On 7 February 2021, a huge rock–ice mass detached from the Raunthi peak at Chamoli district in Uttarakhand, India (Fig. 28). It causes more than 200
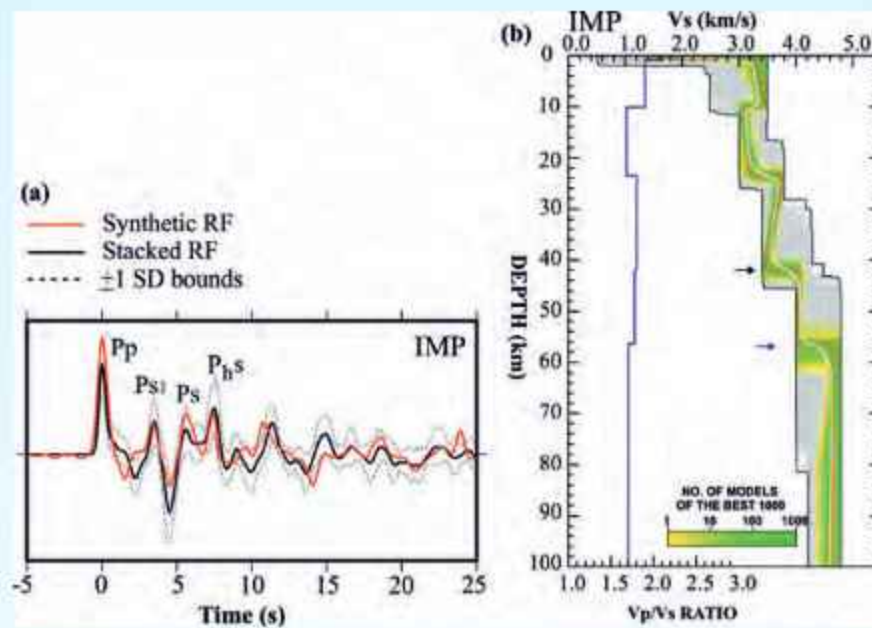
RESEARCH ACTIVITIES

Fig. 26: Examples of NA inversion technique applied at IMP station. (a) The left panel shows the stacked receiver functions. The comparison of stacked (red waveform) and synthetic RFs (black waveform) obtained from NA inversion is shown in (a). The grey dashed lines mark the ±1 standard deviation bounds. The direct *P*-phase (*Pp*) as well as Moho converted *Ps* phase and P-to-S converted phase in the upper mantle (*Ph*) are marked. The intra-crustal phase is marked by *Ps*. The velocity models obtained from NA inversion are shown in the right-hand panels. (b) The total range of initial models is marked by the grey area, out of which the best 1000 models are shown in the green area with minimum misfit between observed and synthetic RFs. The best-fitting and average models are marked by red and white lines, respectively. The variations of Vp/Vs values with depth for the best-fitting model are shown by a blue line to the left. The possible positions of the Moho and upper mantle discontinuity are marked by black and red arrows, respectively.

deaths and significant economic losses. Radon concentration and seismic signals are utilized to characterise the potential precursory anomalies prior to the detachment. This study not only characterises abnormal signals but also models the rock failure mechanisms. The analysis unveils three time-dependent nucleation phases, physical mechanisms of signal generation and a complete scenario of physical factors that affected the degree of criticality of slope failure. Gradual progression of rock cracks/joints, subsequent material creep and slip advancement acceleration preceded the final failure. On the correlation of radon data with temperature records (from the AWS station at Auli, 2900 m asl, 23 km away from the source) and atmospheric pressure (Ghuttu station), we prepared a schematic model of factors affecting the wedge failure (Fig. 29). The BBS deployed in the Rishiganga-Dhauliganga catchment and one station incidentally lies very close (10 km—TPN [Tapovan town] BBS) to the source zone.

This catastrophe was preceded by the gradual progression of material creep, ruptures and fractures 2 days prior to the event, which accelerated as time got closer to material failure. These abnormal changes possibly contribute to the enhancement of radon emanation due to additional stress–strain changes in the rocks close to the MCT and other local tectonic discontinuities of the Himalaya. Changes observed in the radon time series and the seismic signatures of creeping suggest interrelated effects of different parameters. The collective study of the recorded precursors allowed us to reconstruct the precursory dynamic nucleation phases, factors affecting the wedge failure, rock failure mechanisms and physical mechanisms of precursory signal generation which intensified as time got closer to the main detachment (Fig. 29). The degree of criticality of material failure depended on several physical parameters like stress–strain advancement, overburden pressure that increased radon gas migration along the fault zone, freezing–thawing cycle, fracture and creep propagation, slip acceleration and multiple small detachments along the wedge failure plane. Considering the criteria for
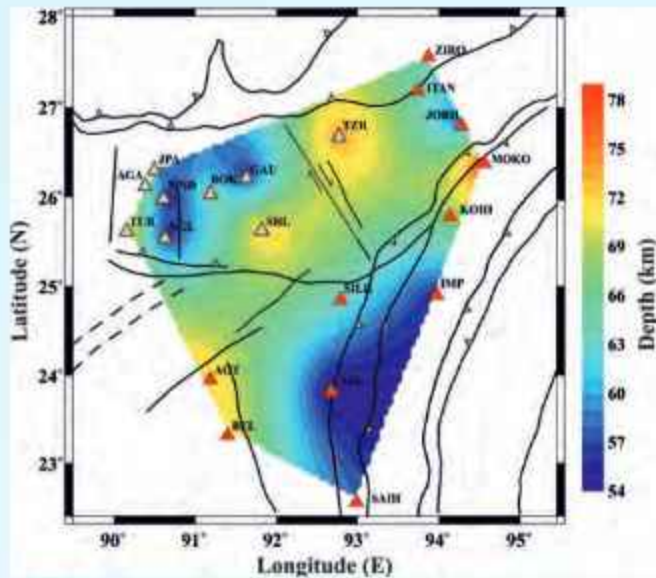
Fig. 27: Contour plot representing the variation in depths of Hales discontinuity in and around the study region based on results obtained from the 11 seismological stations of the present study (red triangles) as well as from previous work carried out in the Shillong Plateau and Assam Valley by Anand et al. (2018, JAES, Vol. 154, PP. 238–247). The seismological stations used by Anand et al. (2018) are shown by grey triangles.

distinguishing the three time-dependent nucleation stages, we primarily focus on CC threshold, SNR and wavelet analysis. A sequence of repetitive weak signals is accompanied by changes in amplitude amplification and a reduced duration between seismic signals, signifying static to dynamic transitions along developed cracks and fractures. Here, our observations do not reveal significant time-dependent changes in radon signals directly describing factors affecting rock or slope failure. The systematic and integrated study is crucial because we did not find any precursory seismic signatures on 5–6 February but found continuous m + 2σ anomalies in radon concentration, which is restricted in this time frame. We observed that rock dynamics played a significant role in controlling this Himalayan catastrophic event of 2021 (Fig. 30). For accuracy and to avoid false alarms, we need a dense integrated multiparametric network with real-time monitoring.

Earthquake source characterization and scaling relation in the central seismic gap, NW Himalaya

Earthquake source parameters of 52 local earthquakes of Mw1.5–3.3 are evaluated using the waveform data of 8 broadband seismograph in the Garhwal Himalaya through shear wave spectral inversion. This iterative technique is based on Brune's ω-square circular source

RESEARCH ACTIVITIES
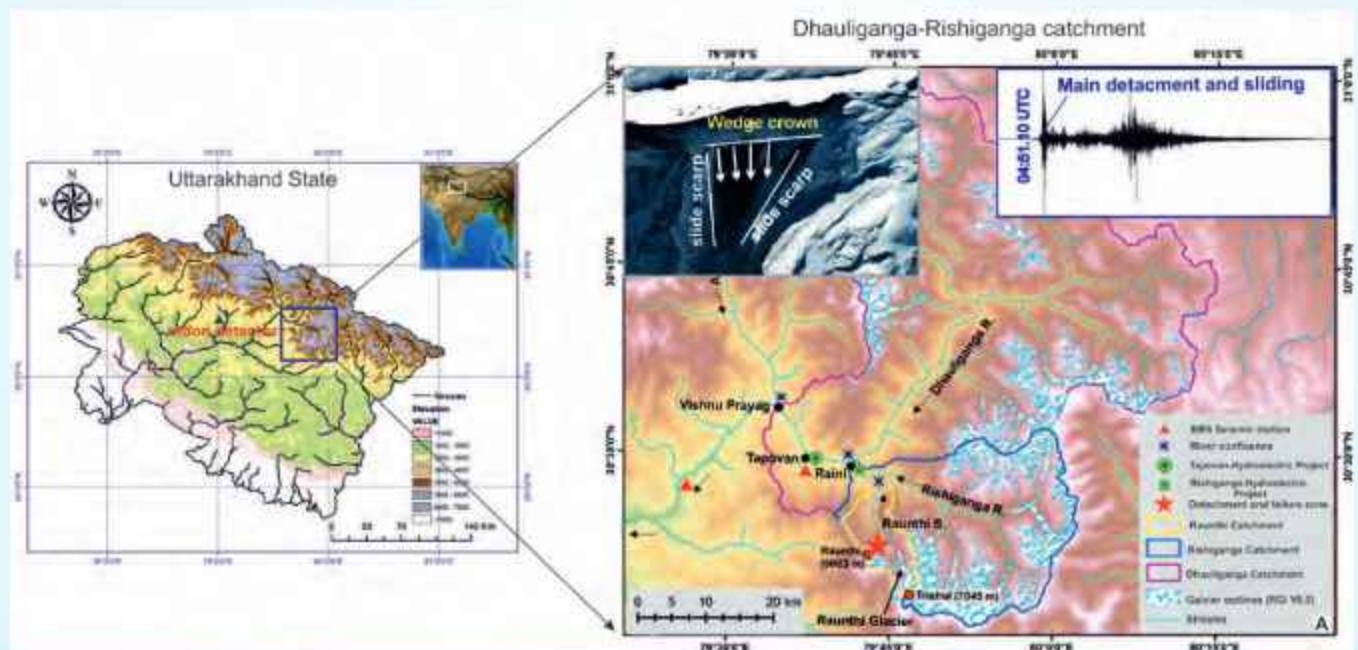
Fig. 28: Map of the study region, with satellite image and location of material failure/rock–ice avalanche in Dhauliganga Rishiganga catchment. The seismic waveform shows the record of main detachment at 04:51.10 UTC. Map was generated using ArcGIS software licenced version 10.5 (https://www.arcgis.com/index.html).
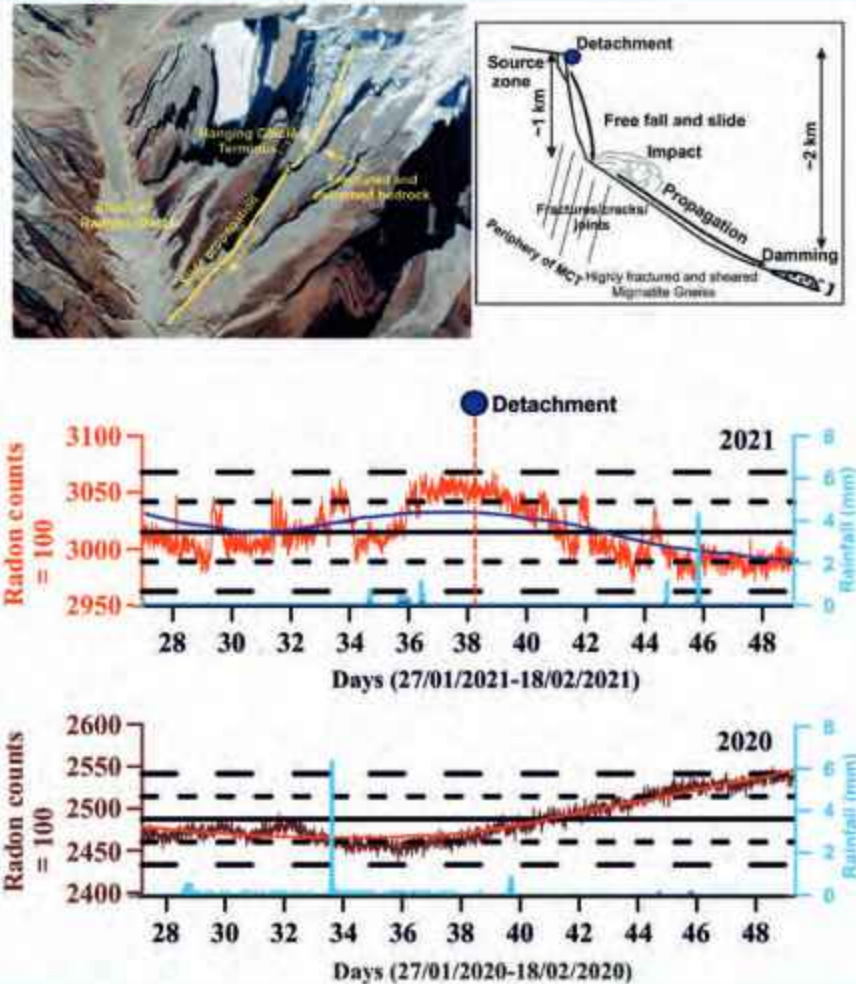
Fig. 29: The graph depicts the radon distribution and 21 days moving average (red and blue colour smooth curves) along its mean value distribution in 2020 and 2021 over a similar time period. The satellite imagery depicts the source zone of the main failure, as well as a rough sketch indicating the reconstruction of the material failure and its propagation.

spectral model. The displacement spectra on multiple stations is utilized to estimate the corner frequency and the displacement amplitude for the lower frequency having constant amplitude. The modeled source parameters, including corner frequency (fc), source-radius (r), stress drop ($\Delta\sigma$), seismic moment (Mo), and moment magnitude (Mw), varied in the ranges of 1.3–11.58 Hz, 117.6–1054.4 m, 0.004–36 bar, 2.83E+11–1.33E+14 N-m, and 1.5–3.3 respectively (Table 1). The estimation of earthquakes source parameters through waveform spectrum is an important component for the study of seismogenesis and obtaining scaling relations is crucial for understanding seismic hazard assessment. The scaling relations are used to develop ground motion prediction equations (GMPEs) that relate earthquake source parameters to ground shaking characteristics (e.g., peak ground acceleration, spectral acceleration). The significant result is that our

modelling indicates a scaling relationship between Mo and fc suggesting Mo $fc^{2.6} \propto$ Constant for Garhwal Himalaya based on local earthquakes of Mw 1.5 to 3.3. These scaling relationships derived from our current study could enhance earthquake hazard modelling for the Garhwal Himalayan region. This, in turn, could allow earthquake engineers to construct more resilient buildings in the area.

The observed difference in the relationship between seismic moment (Mo) and corner frequency (fc) in this study could be associated with the narrow range of magnitudes (Mw 1.5–3.3). Our modelling also gives a scaling relation (Log ($\Delta\sigma$) = 0.605 log (Mo) - 17.34). In 1967, similar linear scaling was observed for interplate earthquakes in the Uttarakhand and N-E Himalayan regions of India. We suggest that the earthquake scaling relationships derived from our current study could enhance earthquake hazard modelling for the Garhwal
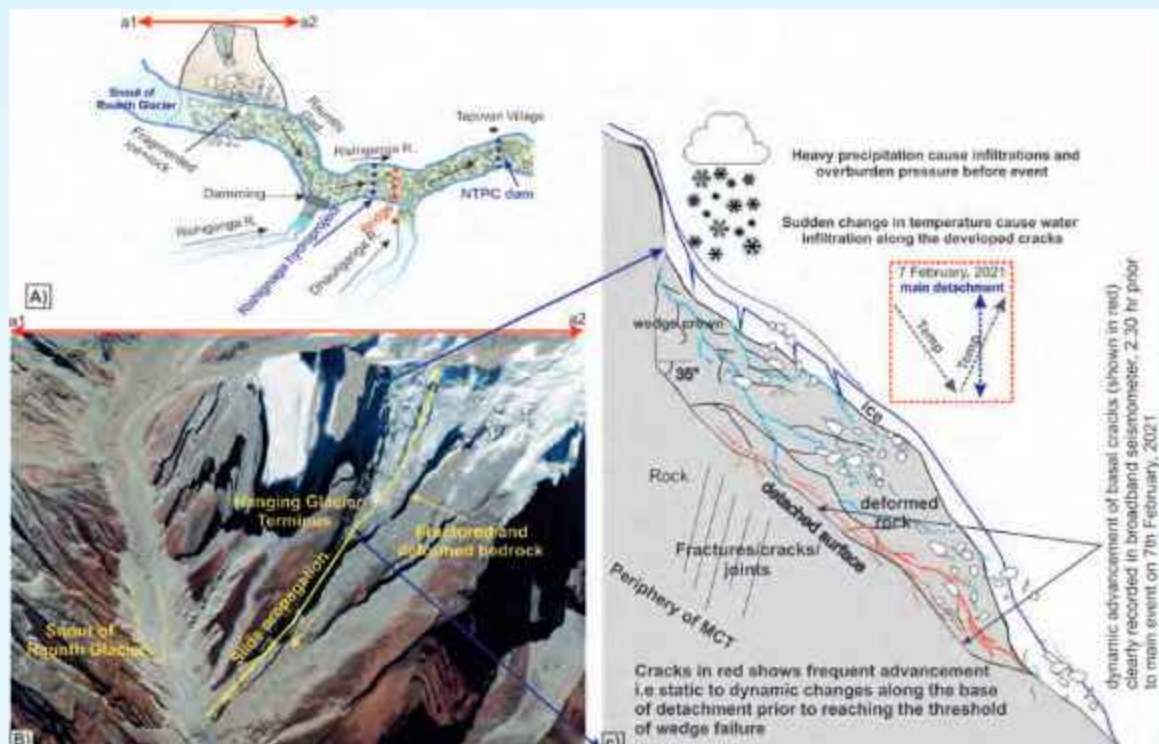
Fig. 30: Complete scenario of factors responsible for failure and related dynamic changes and readjustments within the source region. (a) A schematic diagram showing the debris-flow's progression, (b) satellite image of Raunthi peak and valley before failure, and (c) representation of critical loading and subsequent dynamic changes in rock mechanism.

Himalayan region, Uttarakhand. This, in turn, would aid earthquake engineers in constructing more resilient buildings in this region. The scaling relations are used to develop ground motion prediction equations (GMPEs) that relate earthquake source parameters (e.g., magnitude, distance, depth) to ground shaking characteristics (e.g., peak ground acceleration, spectral acceleration). GMPEs are essential tools for seismic hazard assessment, earthquake engineering, and building code development, providing probabilistic estimates of ground shaking for a given earthquake scenario.

Magnetotelluric (MT) investigations along the Nahan-Kaurik-Chango transect

Magnetotelluric (MT) investigations along the Nahan-Kaurik Chango transect in the Satluj River Valley, northwest Himalaya (Fig. 31), provide insight into the subsurface electrical properties. The geometry of the Main Himalayan Thrust is a flat-ramp-flat geometry in this sector of the Himalayas. Beneath the lesser Himalayan crystalline sheets, a thin conductive layer exists, which is present up to the STD. The presence of this thin conducting layer bears its implication in the translation of the Lesser Himalayan crystalline sheets.

In the geoelectrical model, medium to highly metamorphosed crystalline rocks in the Lesser and the Higher Himalayas are observed as high-resistivity features. At a depth of approximately 5–15 km, an intracrustal low-resistive layer is consistently present along the entire profile. The geometry of this dipping intra-crustal layer signifies the presence of the Main Himalayan Thrust, which represents the base of the accretionary wedge where all the major thrusts of the Himalayan tectonics sole down. The geometrical differences and distinct resistivity of this layer compared to the adjacent regions of Garhwal-Kumaon and Nepal Himalaya indicate the variability of tectonic processes in this part of the Himalaya. Another significant observation is the existence of a thin, highly conducting layer at a shallow depth (approximately 1–3 km). The spatial extent of this layer, along with the bending extent of the main central thrust toward the south, suggests its role in the southward translation of crystalline sheets during Himalayan tectonics.

Assimilation of seismic attenuation model of NW Himalaya and its surroundings

In this study, we analyze the seismic attenuation characteristics of the Northwest Himalaya and adjacent regions using a dataset of 2,716 earthquakes ($2.5 \leq$ Mw

Table 1: The earthquake origin time and the estimated source locations along with different parameters.

| Date (YYYY-MM-DD)	Oigin Time (Hr:Min:Sec)	Latitude (°N)	Longitude (°E)	Depth (km)	Moment Magnitude (MW)	Seismic moment (Mo in N-m)	Source Radius (m)	Stress Drop (bar)	Corner Frequency (Hz)
2020-12-01	04:11:51.56	30.150	77.977	37.6	3.305	1.33E+14	386.784	10.604	3.500
2020-12-01	22:34:57.15	28.776	77.263	1.9	3.027	5.42E+13	701.292	0.684	1.896
2020-12-03	15:16:12.71	31.366	77.988	8.8	2.841	2.44E+13	147.006	35.997	8.893
2020-12-03	16:03:21.25	31.317	77.961	6.3	2.156	2.82E+12	308.069	0.792	5.889
2020-12-04	04:51:10.07	30.100	76.975	19.9	2.643	1.15E+13	252.217	3.905	5.400
2020-12-04	22:4645.03	31.253	78.358	7.1	1.832	1.37E+12	195.517	0.571	6.868
2020-12-06	11:3129.8	30.722	77.921	21.1	2.793	2.07E+13	144.614	30.471	9.392
2020-12-07	18:57:42.76	29.223	77.182	4.5	2.723	1.70E+13	799.927	0.183	1.862
2020-12-17	12:05:51.81	31.261	78.461	39.3	1.900	9.25E+11	302.874	0.378	5.184
2020-12-20	02:04:59.04	30.049	80.772	23.5	2.426	5.63E+12	254.381	2.898	5.775
2020-12-25	23:06:27.04	31.883	78.322	2.8	2.490	8.03E+12	335.522	1.479	4.426
2020-12-28	15:16:50.71	30.394	80.073	1.1	2.462	8.05E+12	273.606	2.593	5.557
2021-01-01	22:41:56.41	30.480	79.195	10	1.918	1.14E+12	224.996	1.008	6.331
2021-01-02	16:15:54.73	32.616	77.763	0.1	2.311	5.87E+12	574.919	0.127	2.321
2021-01-02	18:39:02.89	30.843	77.385	34.1	1.746	9.23E+11	456.364	0.087	4.865
2021-01-04	05:24:40.76	30.493	79.234	6.8	1.923	1.30E+12	166.408	1.343	8.264
2021-01-04	06:09:24.02	31.466	77.016	0.7	2.142	2.19E+12	217.994	1.107	6.131
2021-01-05	20:14:54.33	31.419	77.389	1.3	2.342	5.26E+12	205.602	2.946	6.628
2021-01-08	04:35:16.93	30.077	79.811	3.2	3.008	4.49E+13	347.739	6.411	3.953
2021-01-09	05:57:24.98	31.083	78.699	35.1	2.928	3.53E+13	444.775	2.418	3.399
2021-01-09	19:33:27	31.514	77.608	10.7	1.769	5.81E+11	181.244	0.505	7.708
2021-01-14	14:49:13.29	30.392	79.477	15.7	1.900	1.18E+12	205.296	0.682	7.436
2021-01-20	07:14:08.64	30.517	79.306	14.8	2.825	2.18E+13	310.396	7.120	4.996
2021-01-26	02:02:03.5	30.237	79.553	1.9	1.958	1.25E+12	272.263	0.352	5.566
2021-01-27	15:28:28.01	31.613	78.164	13.8	2.119	2.69E+12	227.133	2.785	6.863
2021-01-27	19:14:29.47	30.376	79.536	29	1.847	7.54E+11	176.526	1.049	7.919
2021-01-30	12:28:19.1	30.490	80.608	6	2.344	5.16E+12	251.383	1.813	5.772
2021-02-03	07:37:28.95	31.123	78.936	1.8	2.389	8.47E+12	219.333	6.119	7.214
2021-02-04	20:31:46.77	31.328	78.215	49.4	2.155	2.52E+12	248.759	0.734	5.687
2021-02-05	22:34:21.82	30.786	78.884	43.8	2.867	2.59E+13	464.413	1.125	2.843
2021-02-07	13:32:51.44	31.417	79.356	29.3	1.959	1.22E+12	139.229	2.639	10.893
2021-02-09	12:41:42.64	31.616	80.142	31.3	1.730	6.20E+11	117.659	2.115	11.582
2021-02-09	18:10:55.54	31.579	78.707	10	1.573	3.49E+11	344.301	0.124	5.619
2021-02-10	21:03:49.54	31.502	78.337	48.2	1.998	1.46E+12	205.481	3.859	8.330
2021-02-11	14:31:33.79	31.416	78.511	10.1	1.887	1.19E+12	368.579	0.673	5.230
2021-02-11	16:53:18.99	30.963	78.562	77.1	1.810	1.09E+12	1054.372	0.004	1.313
2021-02-12	10:58:01.38	31.050	78.156	15.9	2.088	1.77E+12	208.553	1.082	6.434
2021-02-14	10:19:52.96	31.281	77.095	0.1	2.709	1.59E+13	228.789	6.214	5.983
2021-02-14	18:20:59.07	31.495	80.107	23.1	1.938	2.05E+12	221.515	1.800	6.289
2021-02-14	19:56:04.09	29.447	76.946	17	1.953	1.35E+12	334.218	0.174	4.066
2021-02-15	22:40:07.22	29.774	80.376	43.6	1.711	6.26E+11	304.928	0.112	4.463
2021-02-15	23:56:36.91	30.438	77.507	20	1.607	4.55E+11	147.049	0.745	9.490
2021-02-16	20:00:39.1	32.021	79.693	7.9	1.801	9.23E+11	334.136	0.425	5.062
2021-02-17	22:20:47.95	31.044	78.058	9.1	2.024	1.75E+12	244.921	0.844	6.559
2021-02-18	20:50:30.02	31.097	78.060	41.5	1.845	7.70E+11	235.740	0.378	5.930
2021-02-18	22:35:51.58	31.282	77.945	15.7	1.773	8.90E+11	243.557	0.321	6.034
2021-02-19	04:01:04.34	30.495	79.161	12.2	1.713	5.31E+11	194.310	0.366	7.015
2021-02-19	11:08:34.31	30.157	79.990	14.8	2.828	2.51E+13	309.790	5.826	4.760
2021-02-19	20:56:06.78	30.486	79.162	5.9	2.310	4.14E+12	263.901	1.088	5.332
2021-02-19	22:25:48.21	30.760	76.785	5.3	1.969	1.16E+12	313.593	0.644	5.348
2021-02-21	14:19:1.53	30.653	77.041	28.5	1.601	3.93E+11	164.769	0.584	8.826
2021-02-26	19:53:54.05	30.565	79.306	8	1.560	2.83E+11	153.397	0.405	8.650

≤ 5.0) recorded from 2008 to 2015 by a network of 30 broadband seismographs (Fig. 32). The single backscattering model was applied to estimate the quality factor of coda waves (Q_c) across three lapse time windows (LTWs) at varying frequencies. Our results reveal that Q_c increases with both frequency and LTW, suggesting a depth-dependent nature of seismic attenuation in the region. The average attenuation relationships for Q_c, Q_a, and Q_β across the Northwest Himalaya are determined as follows for LTWs of 20, 30, and 40 seconds, respectively: $Q_c = (74 \pm 14)f^{1.27\pm0.06}$, $Q_a = (103 \pm 26)f^{1.16\pm0.08}$, and $Q_c = (140 \pm 41)f^{1.16\pm0.06}$. Our

(a)

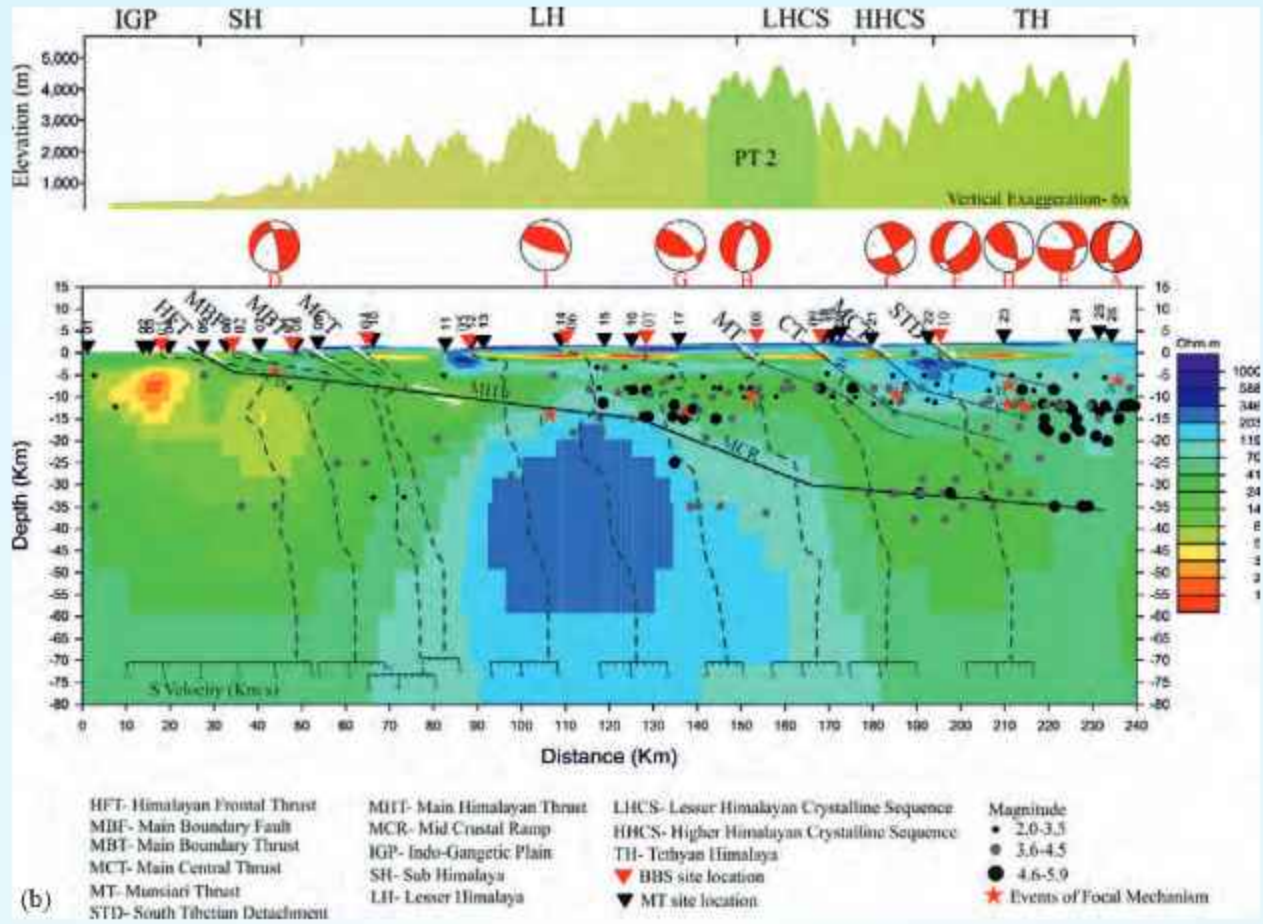RESEARCH ACTIVITIES
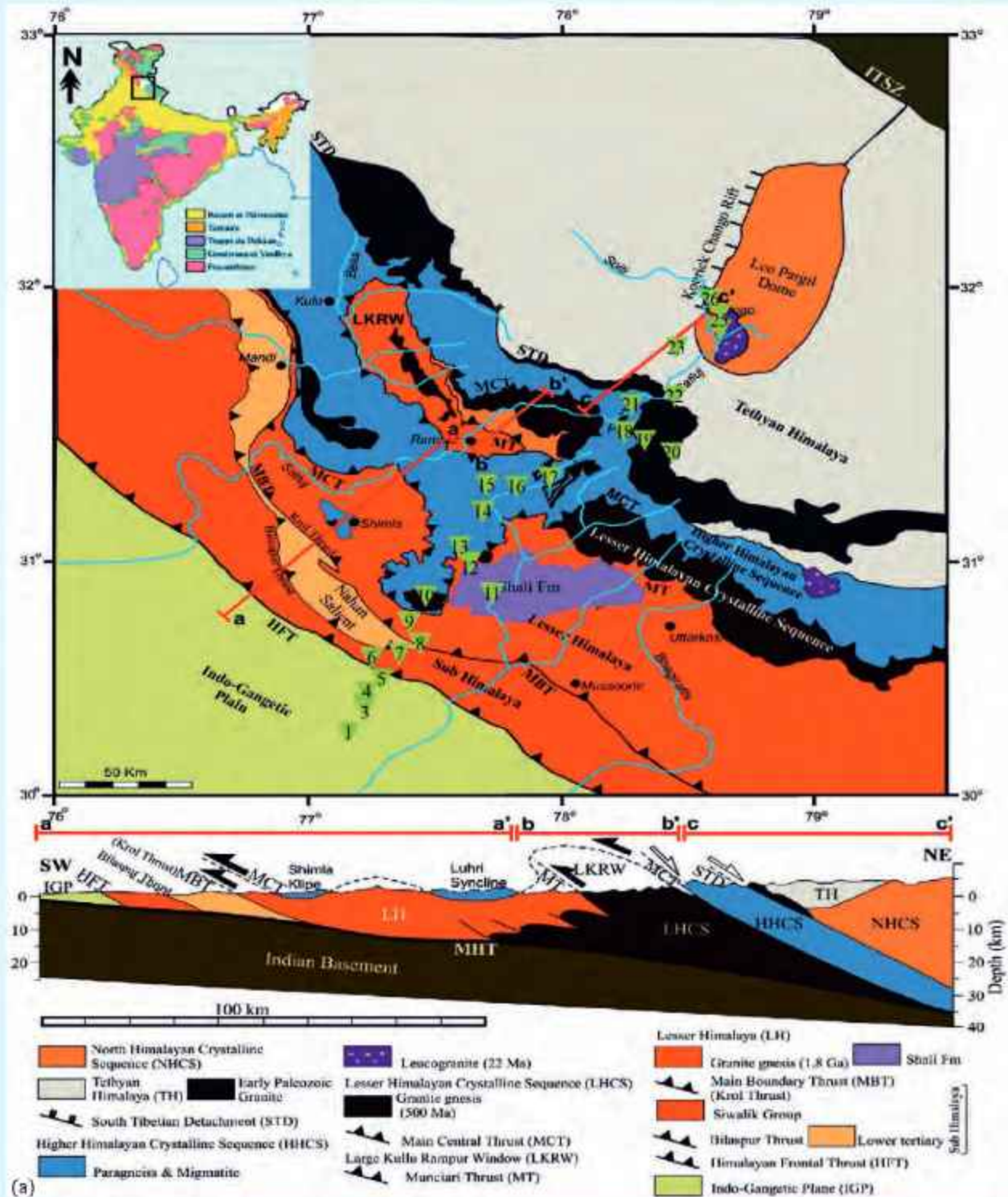
Fig. 31: (a-b) MT profile location and Geoelectrical section in Satluj Valley.

findings reveal significant variability in Q_c, Q_α, and Q_β across the Tethys (TH), High (HH), Lesser (LH), and Shiwalik (SH) Himalaya regions, as well as the adjacent Indo-Gangetic Plains (IGP), with this variability strongly linked to structural heterogeneity and seismogenic processes in each region. We further establish attenuation relations for distinct tectonic units, observing the following hierarchy: $[Q_{\alpha,\beta,c}^{-1}(HH) < Q_{\alpha,\beta,c}^{-1}(SH) < Q_{\alpha,\beta,c}^{-1}(IGP) < Q_{\alpha,\beta,c}^{-1}(LH) < Q_{\alpha,\beta,c}^{-1}(TH)]$. The Tethys Himalaya exhibits high attenuation, likely due to its sedimentary structure, while the Higher Himalaya shows low attenuation. These insights into attenuation characteristics across geotectonic segments in the Northwest Himalaya contribute to a more comprehensive seismic hazard assessment for the region.

The Himalaya region is characterized by high seismic activity due to its position in the India-Eurasia collision zone. While the attenuation of seismic waves is not directly linked to seismotectonic features, high attenuation is often associated with greater geological heterogeneity, resulting in frequent earthquake activity (Kumar et al., 2005). In this study, we evaluate and compare the attenuation characteristics across different geotectonic units of the NW Himalaya and surrounding regions, where 'P-wave (Q_α) and S-wave (Q_β)' hold significant seismotectonic relevance. The analysis of attenuation for various zones reveals patterns that can be linked to the geological composition of these regions. The average attenuation characteristics, including the average coda wave quality factor (Q_c), and the quality factors for P-waves (Q_α) and S-waves (Q_β), show that the Higher Himalaya (HH) exhibits the highest values compared to the Sub-Himalaya (SH), Indo-Gangetic Plain (IGP), Lesser Himalaya (LH), and Tethys Himalaya (TH). Conversely, the inverses of these quality factors-denoted as Q_c^{-1}, Q_α^{-1} and Q_β^{-1} as: $Q_c^{-1}(TH) > Q_c^{-1}(LH) > Q_c^{-1}(IGP) > Q_c^{-1}(SH) > Q_c^{-1}(HH)$; $Q_\alpha^{-1}(TH) > Q_\alpha^{-1}(LH) > Q_\alpha^{-1}(IGP) > Q_\alpha^{-1}(SH) > Q_\alpha^{-1}(HH)$ and $Q_\beta^{-1}(TH) > Q_\beta^{-1}(LH) > Q_\beta^{-1}(IGP) > Q_\beta^{-1}(HH)$. These results suggest that the Tethys Himalaya has the highest attenuation, followed by the Lesser Himalaya, Indo-Gangetic Plain, Sub-Himalaya, and Higher Himalaya in decreasing order. The high attenuation observed in the Tethys Himalaya is likely due to its sedimentary deposits, primarily formed by
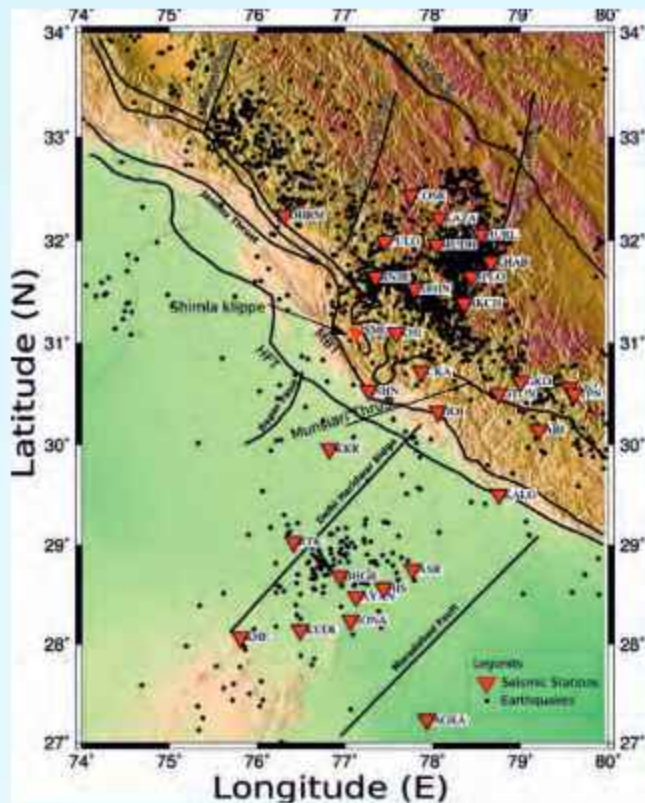
Fig. 32: A map illustrating the tectonic features of the NW Himalaya and surrounding regions. The tectonic features are represented by lines, including the Main Boundary Thrust (MBT), Main Central Thrust (MCT), Himalayan Frontal Thrust (HFT), Munsiari Thrust, Jammu Thrust (JT), Lesser Himalayan Crystalline Nappe (LHCN), South Tibetan Detachment System (STDS) and Indus Tsangpo Suture Zone (Tectonics after GSI (2000)). Solid triangles indicate the locations of seismograph stations in the network, while solid circles mark the epicentres of earthquakes analyzed in this study. The earthquake epicentres are sourced from the International Seismological Centre (ISC) catalogue (https://www.isc.ac.uk/).

gravity-driven erosion at the tectonic contact with the Higher Himalayan Crystalline sequence (Liu & Einsele, 1994; Garzanti, 1999; Srivastava et al., 2013). According to Spudich & Iida (1993), the upper few kilometers of sedimentary basins exhibit strong scattering, which contributes to the high attenuation observed in the Tethys region. The distinct geological separation between the Tethys Himalaya and the Higher Himalayan Crystalline (HHC) sequence, along with the boundary transition, leads to differences in attenuation properties, particularly in areas with significant tectonic discontinuities (Kumar & Yadav, 2019). In contrast, the Lesser Himalaya, situated south of the Greater Crystalline Himalayan sequence and bounded by the

Main Central Thrust (MCT) to the north and the Main Boundary Thrust (MBT) to the south, displays varying attenuation characteristics due to its complex geological composition. The region is predominantly made up of Proterozoic and low Paleozoic sedimentary rocks that have been metamorphosed to greenschist facies, along with Paleocene-Eocene limestone and shale formations (Subathu Formation), and outliers of Greater Himalayan metamorphic rocks. These factors likely contribute to the high attenuation observed in the Lesser Himalaya (Fig. 33). As it separates terrigenous carbonate rocks from overlaying metamorphic rocks including gneiss and mica schists, the MCT, a significant longitudinal thrust fault that separates the Higher and Lesser Himalaya, may be responsible for the observed variations in attenuation (Sinha, 1987). The different attenuation behaviour between the two zones is further explained by the existence of retrograde metamorphic series in the MCT zone, which include Paleozoic sediments in the Lesser Himalayan zone and crystalline rocks in the Higher Himalayan zone. The research area's southernmost region, the Indo-Gangetic Plain (IGP), shows greater attenuation than the Tethys Himalaya and Lesser Himalaya.

The IGP, an active foreland sedimentary basin, is filled with alluvial deposits from the Indus, Ganga, and Yamuna rivers (Lyon-Caen & Molnar, 1985). These sedimentary deposits are underlain by a thick sequence of Siwalik sediments, which rest on Precambrian granitic rocks of the Indian Craton (Raivermann, 1983). As noted in Das et al. (2024), the western IGP is particularly characterized by thick sedimentary layers contributing to significant seismic wave attenuation. The presence of soft alluvial sediments with low shear wave velocities (Vs < 0.5 km/s) and high Vp/Vs ratios (~2.5–3.0) within the uppermost 400-700 meters leads to substantial absorption and deceleration of seismic waves. As these sediments thicken towards the northeast, the attenuation effect intensifies, with basement depths reaching up to ~3.8 km near the Himalayan Frontal Thrust (HFT), making the IGP a seismically vulnerable zone where energy from Himalayan earthquakes can cause considerable damage.

In contrast, the Sub-Himalaya (SH), or Himalayan foreland, shows low attenuation compared to the IGP, Lesser Himalaya, and Tethys Himalaya. This is due to its composition, which mainly consists of dense, low-porosity rocks such as quartzites, phyllites, and schists, which are more compact and crystalline. This composition leads to reduced absorption and dissipation of seismic energy, resulting in low attenuation.
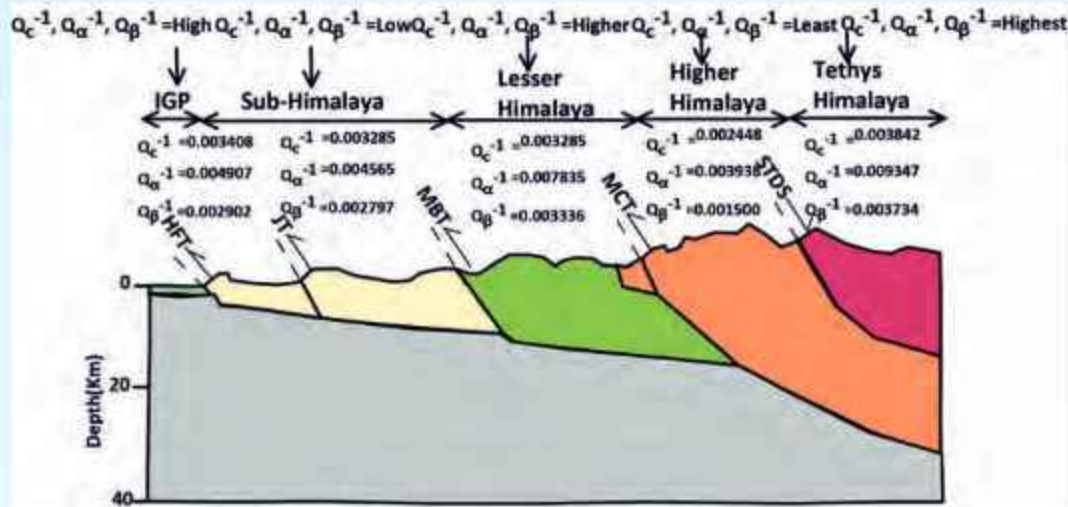
RESEARCH ACTIVITIES

Fig. 33: Comparison of Q_c estimates for (a) the NW Himalaya region, the Kinnaur Himalaya region, and the Garhwal Himalaya region (b) the whole dataset of the NW Himalaya. The abbreviations are the same as in figure 32.

Furthermore, the presence of higher-grade metamorphic rocks, such as those in the Chail Group, also contributes to the low attenuation, as these rocks are more rigid and stable, minimizing energy loss. Unlike the IGP, the SH lacks thick layers of soft, unconsolidated sediments, which typically amplify and attenuate seismic waves. Although the SH is affected by complex geological structures, such as thrusts and tectonic windows, they do not significantly increase attenuation, leading to low attenuation levels in this region. The Higher Himalaya, with its HHC formations, shows the low attenuation among all these regions. A layer of medium- to high-grade metamorphic rocks, including meta-sedimentary rocks intruded by Ordovician (about 500 Ma) and Miocene (approximately 22 Ma) granites, makes up the Higher Himalayan Crystalline (HHC) sequence. The layer is 30 km thick. These rocks show an inverted metamorphic field along the Satluj River, with migmatite Barrovian mineral groups at the bottom, garnet-staurolite rocks at the base, and kyanite and sillimanite in the centre (Vannay & Grasemann, 1998). Even at low pressure, the mica schist, quartzite, paragneiss, migmatite, and leucogranite rocks found in the HHC demonstrate multiphase deformation (Sorkhabi, 1999). This complex geology supports the conclusion that the Higher Himalayan experiences the least attenuation (Fig. 33). Furthermore, oblique-oriented faults, either crossing or aligned obliquely to the Himalayan longitudinal strike, have shown recent seismic activity. Particularly where these transverse faults meet the Himalayan thrust band, earthquakes in these areas are caused by both thrust and strike-slip faulting. Along these transverse faults, strike-slip movement is also linked to the Quaternary activity seen in some areas of the MCT zone.

Activity: 2C
Seismicity and Seismic Hazard Assessment in the Himalaya
(Dilip Kumar Yadav, Narendra Kumar, Praveen Kumar and Chinmay Haldar)

Attenuation Tomography in the Uttarakhand and Himachal Himalaya

This work proposes the shear-wave attenuation tomography of the Garhwal and Kumaun regions, Uttarakhand Himalaya, to investigate the crustal state. Based on attenuation characteristics, the highly attenuated layer identified starts at ~10km in the Garhwal region and ~5km in the Kumaun region (Fig. 34). The obtained model revealed that quality factor (Q) values vary from 16 to 664 and 49 to 866 at 1 Hz frequency for the Kumaun and Garhwal regions, respectively. The high attenuation rate (1/Q) in the Kumaun region compared to the Garhwal region may be due to the high attenuated layer at a shallower depth in the Kumaun region. The comparatively low attenuation rate of the Garhwal characterizes it as a region with high seismic hazard potential. Pioneeringly, layered frequency-dependent attenuation models are proposed up to a depth of 30 km for six different layers with 5km thickness each, which will provide new insight into seismic hazard evaluation.

The three-dimensional attenuation structure and
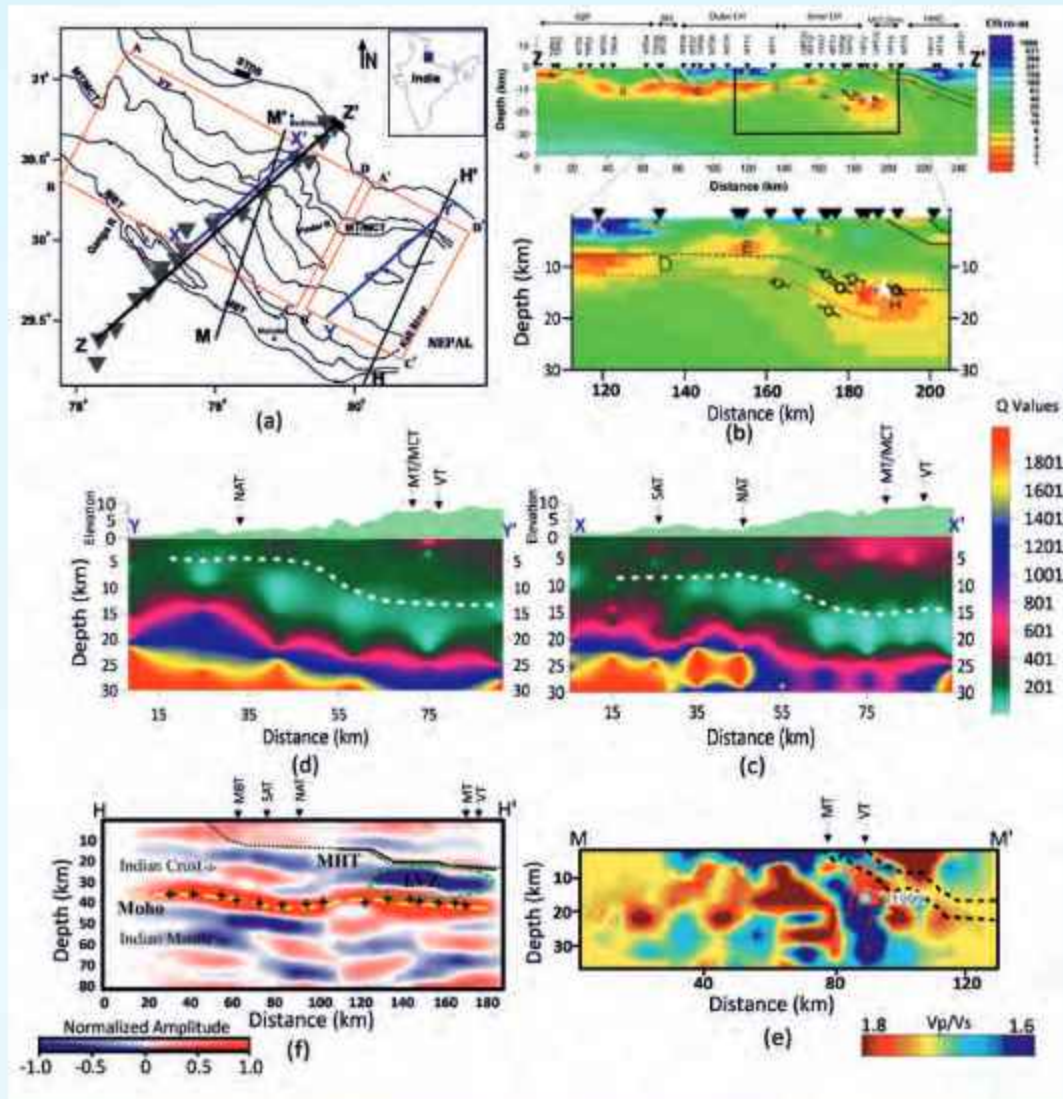
Fig. 34: (a) The locations of the profiles considered in the Uttarakhand Himalaya, and (b) the geoelectric model beside the profile ZZ' projected by Rawat et al. (2014). The attenuation model along the profile (c) XX' in the Garhwal region and (d) YY' in the Kumaun region. (e) P-wave by S-wave (Vp/Vs) ratio proposed by Mandal (2021; Sci. Rep. 11 (1), 14067) along the profile MM' and (f) common conversion point stacking image using the receiver function suggested by Hazarika et al. (2021; GJI, 224, 858–870) along the profile HH'. The white dashed line in (c) and (d) shows the starting depth of the fluid or partial melt zone.

frequency-dependent attenuation layered model are also proposed for constraining seismic hazards and exploring the presence of an intra-crustal high conductive (ICHC) layer in the Himachal Himalaya, India. Using acceleration data recorded in the Himachal Himalaya, this work quantifies the attenuation characteristics in the form of shear-wave quality factor (Q_β). This work suggests a frequency-dependent shear wave attenuation model for six different layers of 5 km thickness each, up to a depth of 30 km (Fig. 35). The low Q_β values (ranging 10–60) depict an aqueous fluid zone starting from a depth of ~11 km (Fig. 35). This aqueous fluid identified in the study region closely resembles the ICHC layer identified by other researchers in its adjacent area. The presence of an aqueous fluid zone identified at 11-20 km depth may be one of the possible reasons for high seismicity in the Himalayan seismic belt.

Crustal structure variation beneath the Indo-Gangetic Plain and Himalaya

This study investigated the structure of the sedimentary layer beneath four stations in the Chandigarh–Ambala

RESEARCH ACTIVITIES
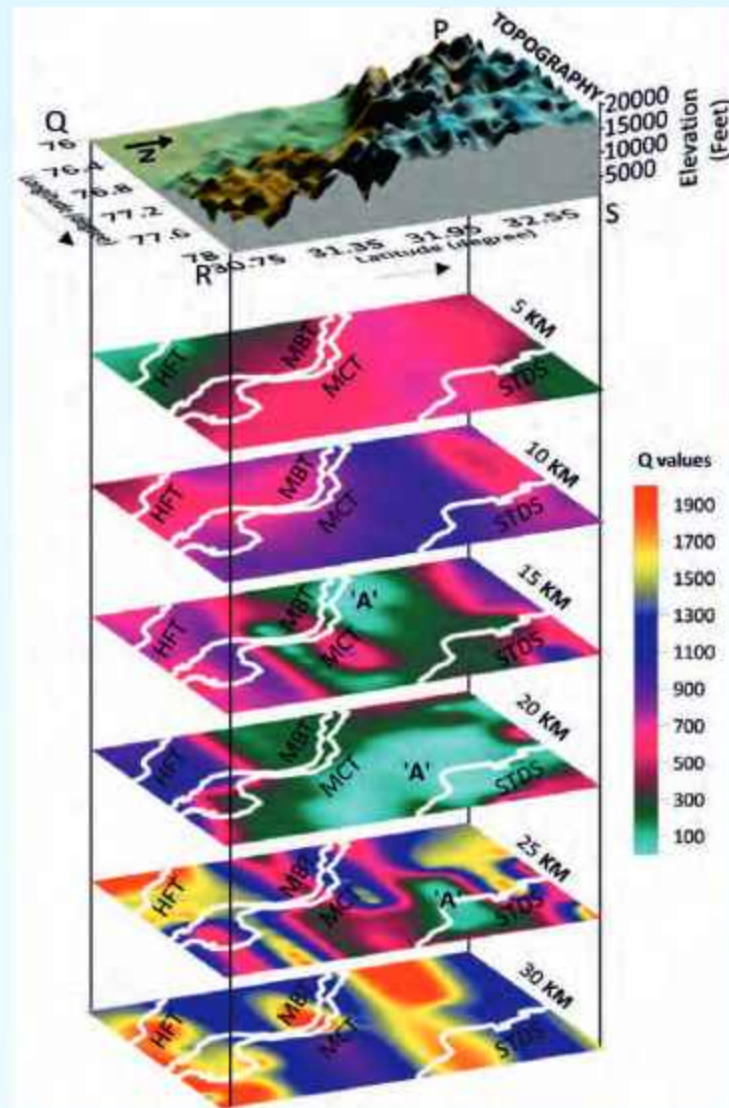
Fig. 35: The quality factor distribution at different depths at 5 Hz frequency along with the topography of the Himachal Himalaya. The white line represents the surface major tectonic. HFT, MBT, MCT, and STDS describe the Himalayan Frontal Thrust, Main Boundary Thrust, Main Central Thrust, and South Tibetan Detachment System, respectively. The zone marked by 'A' corresponds to the fluid region.

region in Indo-Gangetic-Plain using the receiver function (PRF) technique. The study found that the sedimentary layer thickness varies significantly, with values from 2.0 to 3.0 km beneath the IGP and increasing northward (Fig. 36). Shallow shear velocity (Sv) at the base of the sedimentary layer below the Siwalik Himalaya ranges from 2.8 to 2.9 km/s, which can be utilized for assessing earthquake ground-motion sites. Crustal thickness values vary between 44 and 50 km in the Indo-Gangetic Plain. From the Siwalik Himalaya to the higher Himalaya, it ranges from 44 to 65 km (Fig. 37).

Moho geometry and its driving mechanisms in the North-West Himalaya: insights from shear-wave velocity contrast across Moho

To estimate $\delta\beta_M$, a novel technique that utilizes P-to-s converted wave amplitude data was applied. The values of $\delta\beta_M$ range from 0.7 km/s to 1.3 km/s across the area under investigation. The $\delta\beta_M$ values beneath the Himalaya region vary from 0.7 to 1.0 km/s, whereas with the presence of sedimentary layers, it jumps up to 1.3 km/s (Fig. 38). This indicates that the presence of sediments influences the $\delta\beta_M$ values. The crustal thickness (H) varies in the study from 44 to 63 km. The
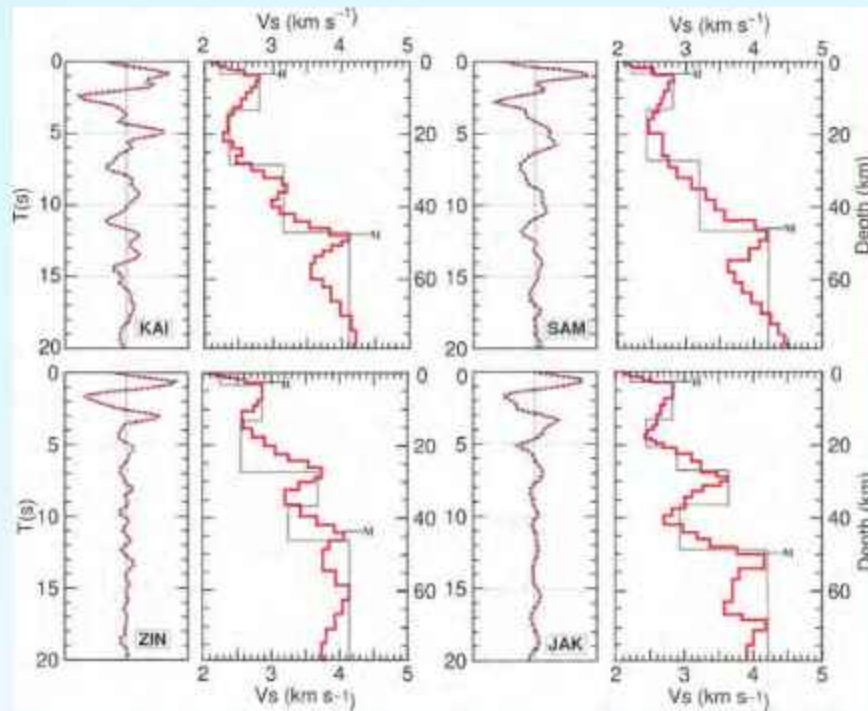
Fig. 36: Shear wave velocity models obtained by inversion of stacked PRFs are shown beneath 4 BBS stations (KAI, SAM, ZIN, and JAK). The red line represents the observed waveform at different stations, and the blue colour represents the synthetic waveform obtained from the final velocity model using the inversion of stacked PRF. The grey line in the right panel shows the 1-D starting velocity model used to invert the data.

scaling relation between $\delta\beta_M$ and H is positive, which indicates the thick crust associated with a high $\delta\beta_M$ meaning that the presence of a low-velocity material may be fluid at the lower crust beneath the Himalayan region. It is proposed that the fluid, connected with the weak zone, may have activated pre-existing faults, leading to the generation of earthquakes. It is suggested that the accumulation of strain in the crust-mantle transition zone, which is rich in fluid, might be sufficient to generate seismicity in the lower crust.

Fault Plane Solutions of local earthquakes and its depth distribution in Siang Valley and adjoining region of Arunachal Pradesh, NE India

The Siang Valley of Arunachal Pradesh, North-East India, is one of the seismotectonically very active regions of the world that lies in the Eastern Himalayan Syntaxis (EHS). We have investigated seismicity, fault plane solutions (FPS), and P (Pressure) axis orientation in this region. 756 local earthquakes of magnitude range ($1.0 \leq M_L \leq 5.9$) are analysed in the region during the period from January 2019 to December 2021. The location of earthquakes in the current study shows the seismically active tectonic structure of the region. An evaluation of 11 earthquakes over the magnitude range ($3.2 \leq M \leq 5.4$) to study the source mechanism is

undertaken. In addition, we choose earthquakes located near the seismic network (epicentral distance $\leqslant 50$ km). The space-depth distribution of hypocenters has been investigated beneath the region along three profiles A-B in WNW-ESE, C-D in NE-SW, and E-F in NW-SE that pass across the significant tectonic features, e.g., MBT, MCT, Lohit Thrust (LT), Mishmi Thrust (MT), and Walong Thrust (WL), respectively. The depth distribution of earthquakes in these sections is plotted along depth-projected major tectonic features. To visualize the distribution of seismicity with respect to depth, we have taken three profiles, A-B, C-D, and E–F (Fig. 39a, b). The A-B profile is across the western limb of the Siang window, the C-D profile on the eastern limb, and the E–F profile is taken across the crest of the Siang window. In profile A-B, it is seen that the major thrust MBT, MCT, shows a dipping trend towards NW, and the projected view of FPS no. 4 shows the orientation of one of its nodal planes along the dip direction of MCT, and it is a thrust faulting type; another distribution of seismic events is associated with MCT2. FPS no. 1, 3, and 2 are lying NW of MBT where FPS numbers 4 and 3, are shallow depth with thrust type, and FPS no. 2 is shallow depth with normal type faulting. In profile C-D, Bomdo Thrust (BT), Ramgarh Thrust (RT), and Lohit Thrust (LT) are dipping in the NE direction.
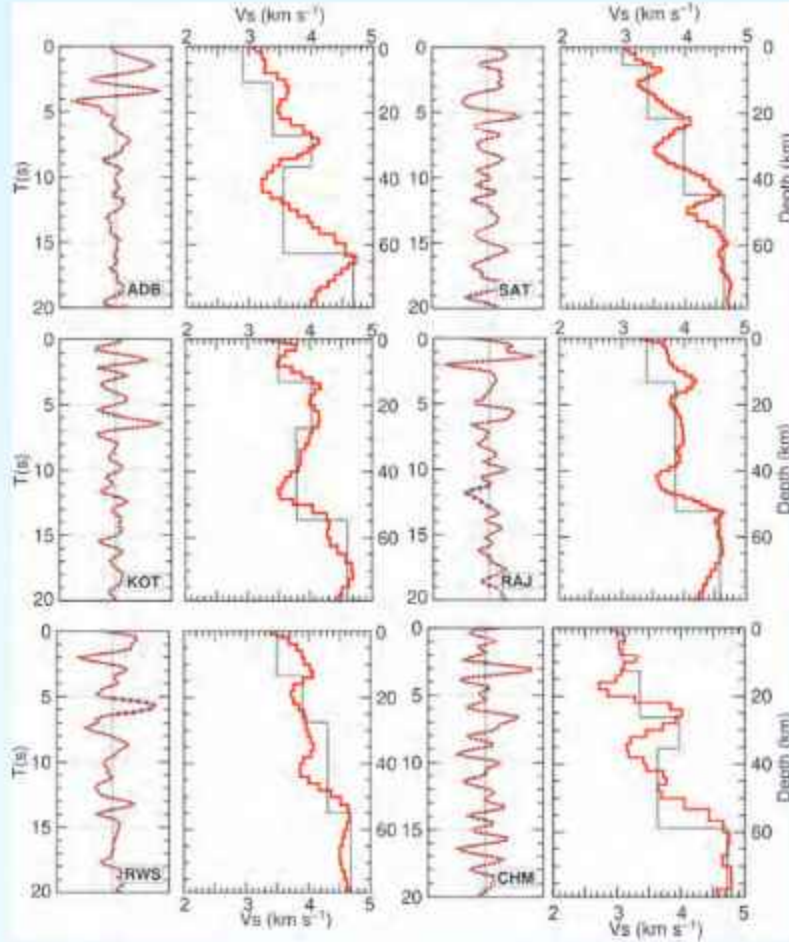
Fig. 37: Shear wave velocity models obtained by inversion of stacked PRFs are shown beneath 6 BBS stations (ADB, SAT, KOT, RAJ, RWS and CHM. This is similar to figure 36 but pertains to different stations.
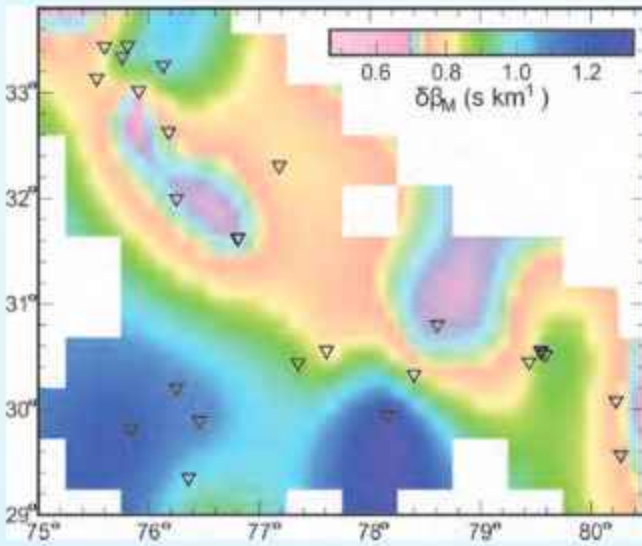
Fig. 38: Shear-wave velocity contrast map across the Moho in the study region. Inverted triangles indicate the BBS station locations.

One of the nodal planes of the fault plane solutions (events no. 6, 5, and 7) is associated with a dipping trend of tectonic lineaments (BT, RT, and LT). FPS no. 6 is thrust type of faulting, 5 is Normal type of faulting, and 7 is thrust with strike-slip faulting. In profile cross-section E–F, which is trending NNW-SSE, its tectonic lineaments are dipping toward NNW and SSE. FPSs no. 10 and 9 are associated with MCT, and FPS 11 is probably associated with Lohit thrust. FPS no. 10 is a Normal type, 9 is a thrust type, 8 is a strike-slip type, and 11 is a Normal type of faulting.

Eleven fault plane solutions (FPS) are determined using waveform Inversion (ISOLA). The inversion scheme is illustrated for an earthquake of M_L 4.5 with a focal depth of 15.3 km (event no. 7). Waveform data from six stations (BLNG, GLNG, JNGG, MRNG, PADU, and YING) are used to perform the inversion with a frequency band of 0.06–0.09 Hz. The MT solutions are computed considering 10 trial depths
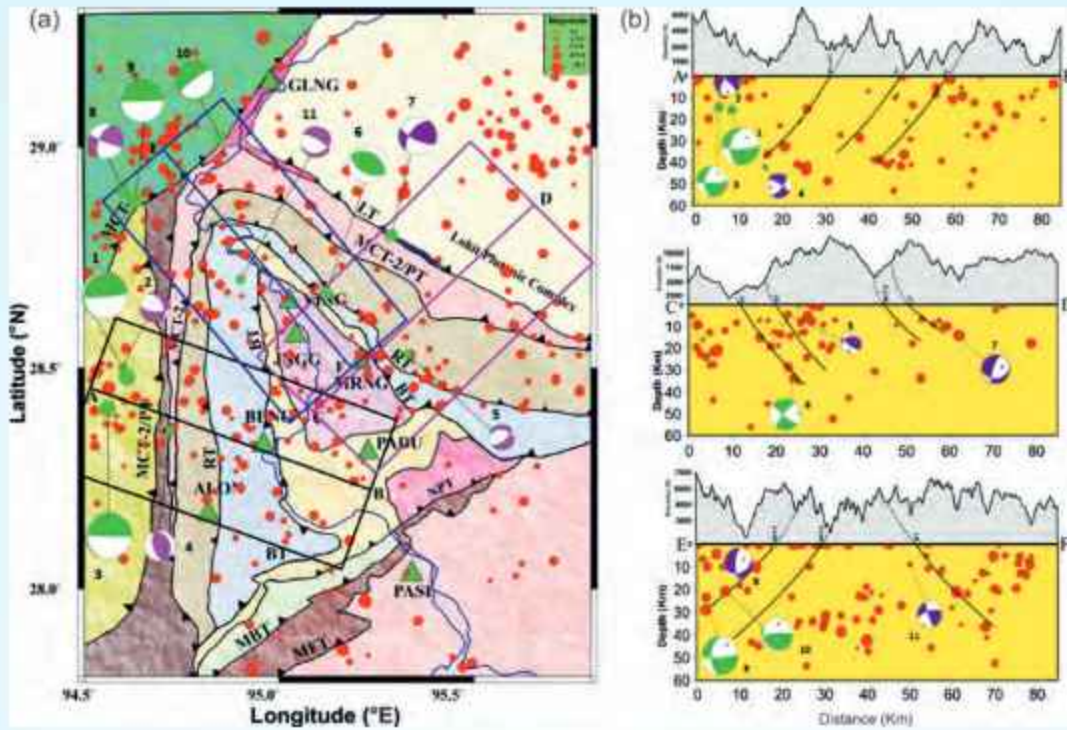
Fig. 39: (a) Seismicity and beach ball distribution of focal mechanism solution (FMS) in and around Siang Valley, Arunachal Pradesh, based on earthquakes recorded by eight broadband seismic stations (green triangles). Tectonic features in the region are LT (Lohit Thrust), RT (Ramgarh Thrust), BT (Bomdo Thrust) and NPT (North Pasighat Thrust) Green beach balls (Event no. 6, 1, 10, 9 & 3) events taken form the ISC catalogue and purple (Event no. 11, 5, 4, 2, 7 & 8) are from the present study, (b) Present day elevation, tectonics, and depth cross-section of seismic activity are shown along profile A-B, C-D and E-F. The depth projected view of the inferred FMSs of the local earthquake.
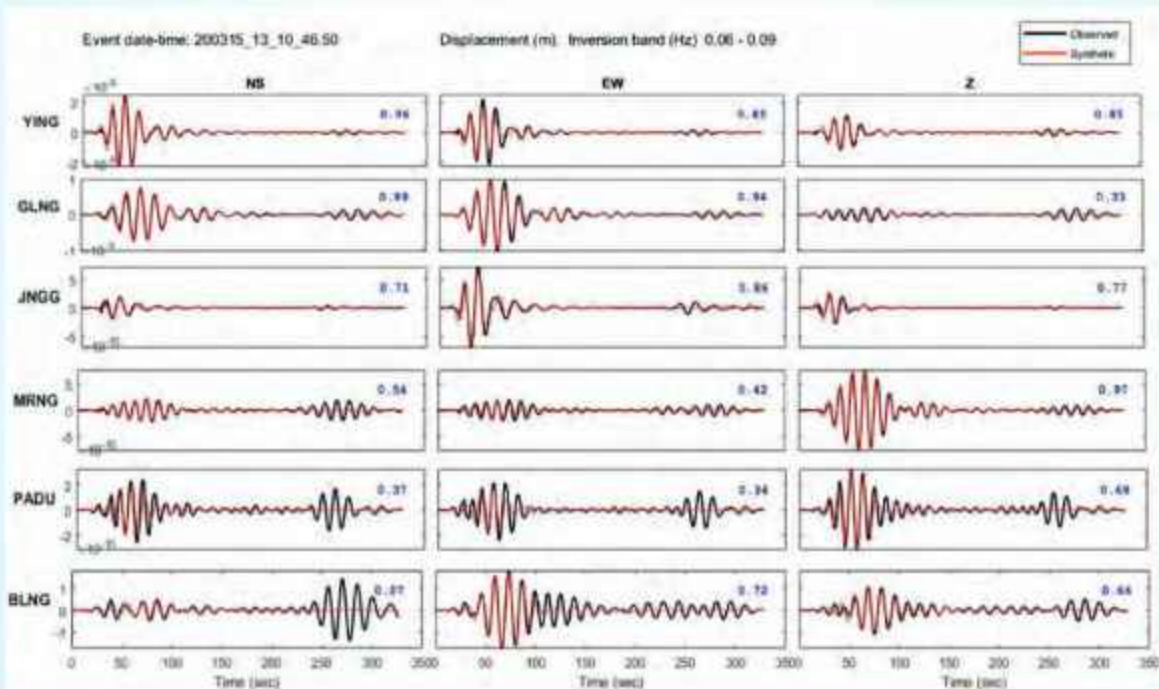
Fig. 40: Waveform fit at several stations for a moment tensor solution of a M_L 4.5 earthquake (event date: 15th March, 2020, origin time: 13h 10m 46.5s, event no. **7**). The observed and synthetic waveforms are represented by black and red lines, respectively. The variance reduction factor is written in blue numbers.

RESEARCH ACTIVITIES
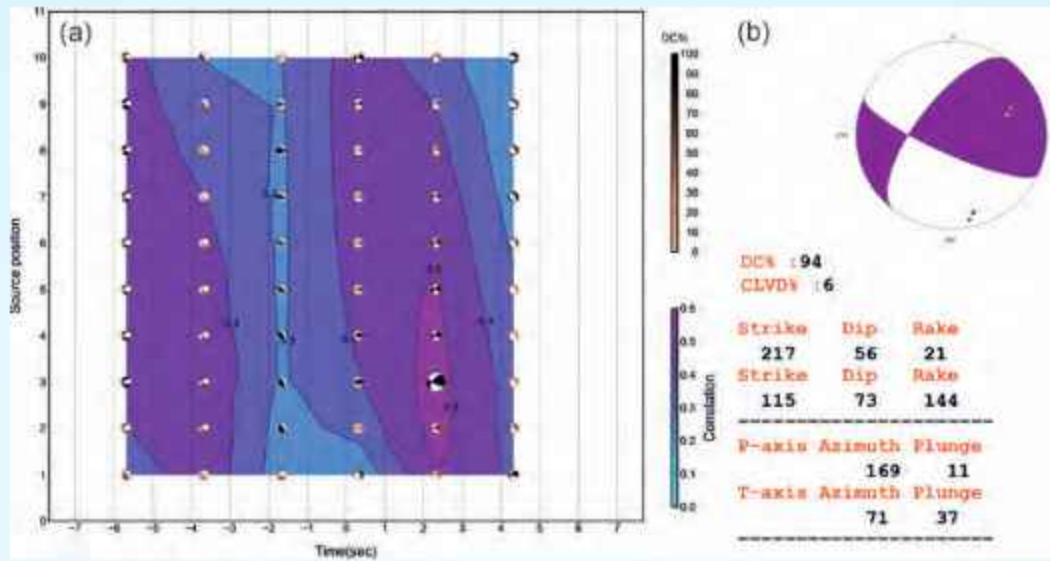
Fig. 41: Solutions of moment tensor inversion of Event No. 7. (a) The correlation plots reveal the source depth vs origin time shift correlation. The biggest black beach ball is the response for FPS with the maximum correlation values. The trial source depth is indicated on the vertical axis. The temporal grid search between -7 and + 7 s with regard to the origin time is indicated by the horizontal axis. (b) plot showing the obtained focal mechanism for the best-fit solution.

ranging from 3 to 15 km in 3 km steps. Figure 40 shows the observed and synthetic seismic waveform correspondences for the optimal moment tensor solution. Average variance reduction (VR>0.66), condition number (CN<2.7) and two additional parameters – the space – time variability index (STVAR<0.14), which evaluates the stability of the source position and time in a grid search as well as the focal-mechanism variability index (FMVAR<31°), which represents uncertainty in the focal mechanism solution are used to identify the best fit solution (Sokos & Zahradnik, 2013). A black beach ball represents the best-fit solution at a depth of 3 km and a time shift of ~ 2s, and the DC ratio corresponds to the highest correlation value, 94%. On the vertical axis, the trial source depth is displayed. The horizontal axis represents the temporal grid search between – 7 and + 7 s with respect to the origin time (Fig. 41a & b). Based on the geology and tectonics of the seismically active region, the fault plane is studied using two nodal planes produced by the waveform inversion technique. The beach ball representation shows the compressional quadrant (shaded area) and dilatational quadrant (unshaded area), where the P and T axes are orthogonal. The nodal plane's strike, dip, and rake are 217°, 56° and 21°, respectively. To obtain the above parameters, the same approach is used for the other selected earthquakes. The DC% of the studied earthquakes was found in the 65–94% range, much higher than the percentage of compensated linear vector dipole

(CLVD%). Previous research (Sipkin et al., 1986, Frohlich et al., 1994) has examined how the orientations of sub-faults along a particular fault zone affect the presence of the CLVD component in the source mechanism.

Activity: 3
Biotic evolution with reference to Indo-Eurasian collision, evidences for global events
(R.K. Sehgal, Kapesa Lokho, Suman Lata Srivastava, and Ningthoujam Premjit Singh)

Additional analyses of stem catarrhine and hominoid dental morphology support Kapi ramnagarensis as a stem hylobatid

Kapi ramnagarensis was described as a stem hylobatid on the basis of an isolated lower right M3 from ~13.0-12.5 Ma deposits surrounding Ramnagar (J&K), India. This interpretation was recently challenged, with alternative hypotheses suggesting that it is instead a stem catarrhine or a strangely derived pliopithecoid that has converged on hylobatid morphology. A series of morphological features were said to distinguish *Kapi* from fossil and extant hylobatids; notably, however, none of these features were examined or compared using quantitative analyses. Then, we further examined the dental morphology of *Kapi* to critically evaluate the hypothesis that *Kapi* represents a stem catarrhine or pliopithecoid rather than a stem hylobatid. We conducted a series of quantitative analyses on dental features discussed by Ji et al. (2022) in the context of
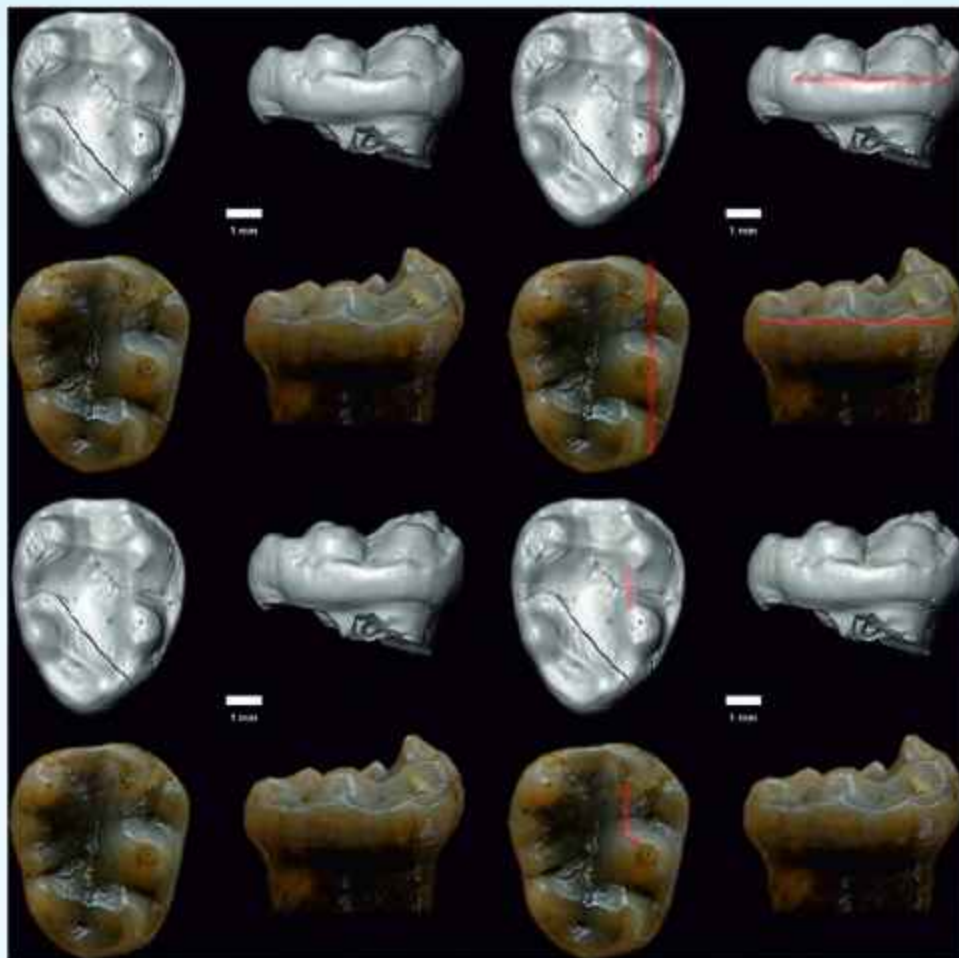
Fig. 42: Comparison between the M3s of *Kapi ramnagarensis* and *Yuanmoupithecus xiaoyuan*. Top left: comparison of *Kapi* (above) and *Yuanmoupithecus* (below) in occlusal and buccal views. Top right: the same comparison with the red line highlighting the development and extent of the buccal cingulum. Note that the buccal cingulum is longer and more extensive in *Yuanmoupithecus* than in *Kapi*, contra Ji et al. (2022). Bottom left: the same comparison as before, with *Kapi* and *Yuanmoupithecus* in occlusal and buccal views. Bottom right: the same comparison with the red line highlighting the orientation of the cristid obliqua. Note that the cristid obliqua is oriented mesiodistally in *Kapi*, even more so than is seen in *Yuanmoupithecus*, contra Ji et al. (2022). CT image provided for *Kapi* in all panels for better visualization; *Yuanmoupithecus* photograph from Ji et al. (2022). CT = computed tomography.

hylobatid, stem hominoid, and stem catarrhine evolution, namely entoconid size, hypoconid size, hypoconulid size, metaconid size relative to the protoconid, and metaconid orientation relative to the protoconid (Fig. 42). We also provided more detailed comparisons between *Kapi*, *Yuanmoupithecus*, and *Krishnapithecus* in terms of buccal cingulum development, pliopithecine triangle development, crown height, and cristid obliquid orientation. For these analyses, we built on the data set used in Gilbert et al. (2020a), again sampling numerous stem catarrhine and stem hominoid taxa representing propliopithecids (*Aegyptopithecus* and *Propliopithecus*), pliopithecids/ pliopithecoids (*Pliopithecus*, *Epipliopithecus*, *Laccopithecus*, *Egarapithecus*, *Anapithecus*, and *Platodontopithecus*), dendropithecids (*Dendropithecus*, *Limnopithecus*, *Simiolus*, and *Micropithecus*) and proconsulids/proconsuloids (*Rangwapithecus*, *Otavipithecus*, *Ekembo*, *Proconsul*, and *Kalepithecus*). We also sampled all living hominoid genera as well as *Kapi*, *Yuanmoupithecus*, and *Bunopithecus*. In addition to the quantitative analyses, we conducted 2D geometric morphometric (GM) analyses of M3 crown shape and cusp position, as quantified by 14 homologous landmarks. Our comparative morphometric sample is same as that documented in Gilbert et al. (2020a). Finally, we conducted a phylogenetic analysis using parsimony
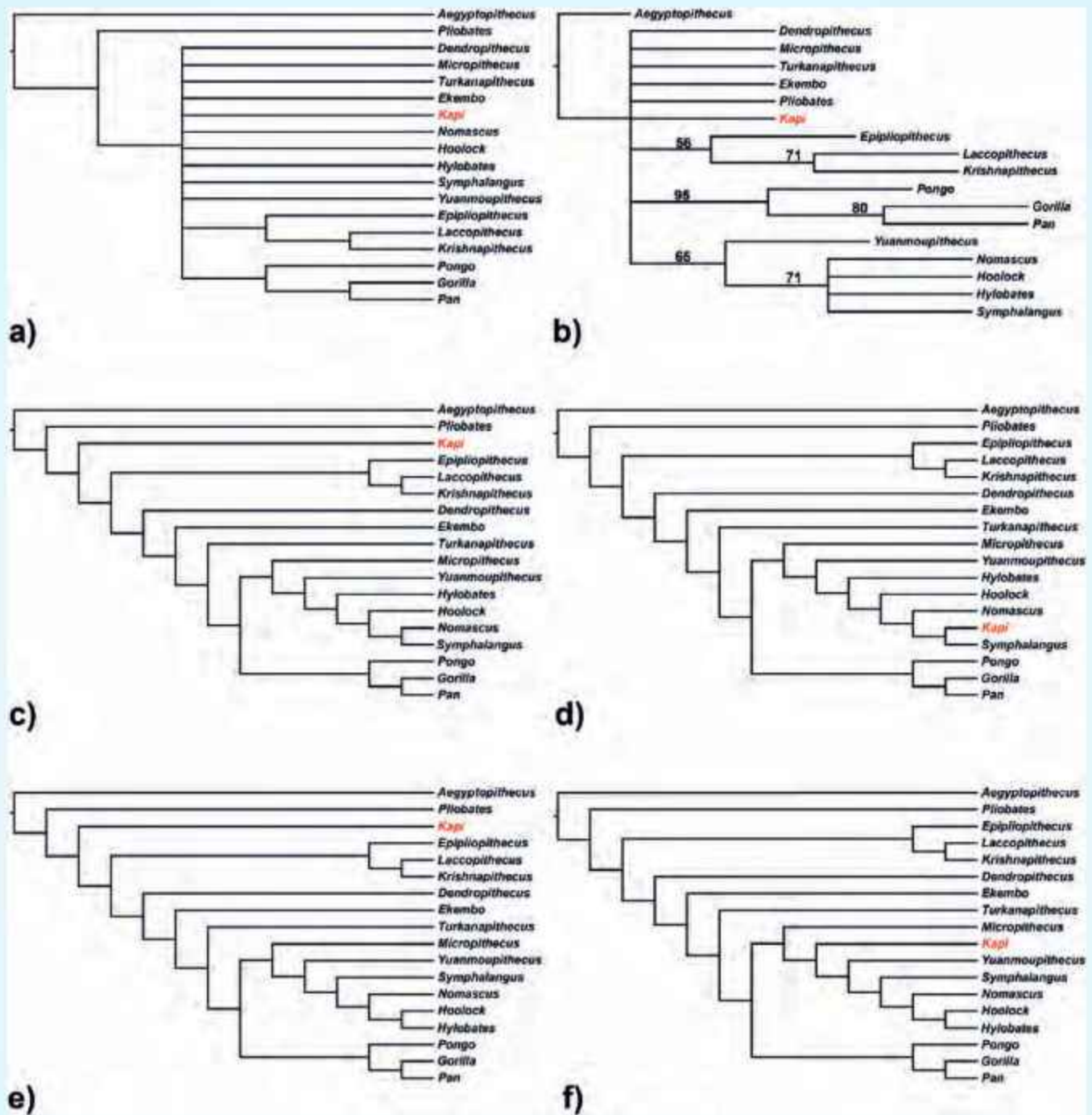
Fig. 43: Results from phylogenetic analysis of the corrected Ji et al. (2022) matrix including *Krishnapithecus*. a) Strict consensus of four most parsimonious trees (MPTs) resulting from phylogenetic analysis of eight stem catarrhine/stem hominoid ingroup taxa, eight crown hominoid ingroup taxa, and *Kapi*, including 163 characters (craniodental + postcranial), with *Aegyptopithecus* assigned as the sole outgroup. b) Majority-rule consensus of four MPTs. Numbers above branches indicate any bootstrap values over 50%. c) MPT 1 reconstructing *Kapi* as a stem catarrhine between Pliobates and a monophyletic pliopithecoid clade; d) MPT 2 reconstructing *Kapi* as a crown hylobatid, the sister taxon of *Symphalangus*; e) MPT 3 reconstructing *Kapi* as a stem catarrhine between Pliobates and a monophyletic pliopithecoid clade (note differing positions of crown hylobatids compared to MPT 1); f) MPT 4 reconstructing *Kapi* as a stem hyobatid between *Micropithecus* and *Yuanmoupithecus*. Tree length = 441 steps, CI = 0.5079, HI = 0.4921, RI = 0.6604; RC = 0.3354.

inference on a modified version of the Ji et al. (2022). Four MPTs were recovered, with *Kapi* placed as a stem hylobatid, a crown hylobatid, or a stem catarrhine branching off between Pliobates and a monophyletic pliopithecoid clade including *Epipliopithecus*, *Laccopithecus*, and *Krishnapithecus*. Bootstrap support is low for most clades, with only extant great apes, *Yuanmoupithecus* + extant hylobatids, and pliopithecoids (*Epipliopithecus* + *Krishnapithecus/ Laccopithecus*) receiving a bootstrap support over 50% (Fig. 43). *Krishnapithecus* is always reconstructed as a pliopithecoid, specifically as the sister taxon to *Laccopithecus* (among included taxa). Interestingly, Pliobates is not recovered in a monophyletic pliopithecoid clade, instead being recovered outside of the other pliopithecoids as a separate, earlier branching stem catarrhine.

It is important to note that while the totality of available evidence suggests that *Kapi* is most likely the earliest known hylobatid, it is difficult to be certain of its true affinities, given that it is only represented by a single lower right M3. While lower M3s are generally more variable than M1s and M2s, this variation can lead to greater evolvability, makingM3s more distinctive between taxa and thus, in some ways, more taxonomically informative (e.g., Mongle, 2019). This inference is also supported by our multivariate analyses demonstrating clear separation in M3 occlusal morphology between major groups. Thus, as long as the lone specimen of *K. ramnagarensis* preserves morphology close to the true species average (the statistically most likely scenario and default assumption), its overall similarity to extant hylobatids among non-cercopithecoid catarrhines is compelling.

Functional and Ecological Implications of the Late Miocene Siwalik Rodents based on Incisor Enamel Microstructure

Fossil rodent teeth are well known from the Neogene Siwalik Group of sediments and can provide insights into the evolution, taxonomy, diets, and adaptations to various ecological niches. However, data on the microstructure of rodent incisors from the Indian Neogene Siwalik sediments is sparse compared to that on molars. We have analysed the enamel microstructures (in both transverse and longitudinal sections) of a selected few rodent incisors from the late Miocene (~10-11 Ma) Siwalik sediments at Dunera, Punjab State, north India. Based on the microstructure analysis, the rodent incisors are identified as cf. *Progonomys* (murids), cf. *Democricetodon* (cricetids), cf. *Sayimys* (ctenodactylids), and cf. *Tamias* (sciurids).

The identified cf. *Progonomys*, cf. *Democricetodon* and cf. *Tamias* are represented by uniserial Hunter-Schreger Bands, whereas cf. *Sayimys* shows multiserial Hunter-Schreger Bands. Besides taxonomy, the functional and ecological significance of these rodents has been studied using enamel crystallite patterns; because the microstructural change(s) in incisor enamel is generally linked to the variety of diets consumed by these mammals. In our analysis, the absence of modified radial enamel in the incisors of cf. *Progonomys*, cf. *Democricetodon* and cf. *Sayimys* suggests that these rodents plausibly consumed a soft diet comprising of leaves, flowers, seeds, fleshy roots, and insects, while the presence of specialized three-layered Schmelzmuster in the incisors of cf. *Tamias* suggests that the rodents may have preferred a diet composed of relatively harder parts such as acorns, walnuts, and hazelnuts.

Quantifying the equatorial climate shifts in the Indo-Burma range using late Eocene–early Oligocene leaf fossils

The tectonic journey of the Indian Plate from its origin in Gondwanaland to its eventual position in the Northern Hemisphere is a remarkable geological odyssey spanning approximately 150 million years. During this period, India traversed an estimated 9000 km, crossing various latitudinal zones and experiencing a dynamic array of climatic regimes due to variations in insolation and land-ocean configuration (Chatterjee et al., 2013, Srivastava et al., 2023, 2024). The Paleogene epoch of the Cenozoic was characterized by significantly warmer global temperatures compared to the subsequent Neogene epoch. (Zachos et al., 2008; Westerhold et al., 2020). This pronounced warmth is largely attributed to elevated atmospheric concentrations of carbon dioxide (CO_2) (>1000 ppm), a potent greenhouse gas, which gradually declined from the early Paleogene onward (Anagnostou et al., 2016; Hönisch et al., 2023). The Paleogene also witnessed a series of prominent hyperthermal events, including the Paleocene–Eocene Thermal Maximum (PETM or ETM1), Eocene Thermal Maximum-2 (ETM2), the Early Eocene Climatic Optimum (EECO), and the Middle Eocene Climatic Optimum (MECO) (Zachos et al., 2008; Westerhold et al., 2020). Extensive research has been conducted on marine sediments to unravel the effects of Paleogene warming on oceanic chemistry and marine ecosystems, but studies focusing on terrestrial sediments are comparatively scarce and primarily concentrated in mid- and high-latitude regions (Wing et al., 2005; Zachos et al., 2010; McInerney & Wing, 2011; Krishnan et al., 2014; Willard et al., 2019; Li et al.,

Fig. 44: Fossil leaf floras utilized for the CLAMP analysis. A. OTU 1. B. OTU 2. C. OTU 5. D. OTU 10. E. OTU 13. F. OTU 3. G. OTU 7. H. OTU 6. I. OTU 4. J. OTU 8. K. OTU 12. L. OTU 9. M. OTU 14. N. OTU 11. O. OTU 15.

2023). We have quantitatively reconstructed the climate of the Laisong Formation using fossil leaf morphological traits deposited during the late Eocene–early Oligocene (Fig. 44). The reconstruction suggests a mean annual temperature (MAT) of 25.3 ± 2.3 °C and a cold month mean temperature (CMMT) of 19.2 ± 3.5 °C. Furthermore, the growing season (LGS) persisted throughout the year (12 months), with a mean annual precipitation (MAP) of 244.2 ± 64.3 cm, exhibiting distinct rainfall seasonality between the rainy summer (130 ± 40 cm) and dry winter (21.7 ± 9.8 cm) seasons. The study further reveals that the northward migration of the Intertropical Convergence Zone, driven by Antarctic glaciation, led to increased rainfall in low-latitude regions.

Paleolake sediments, Jankar Chu Valley, Lahaul (Himachal Pradesh)

A paleolake located at an elevation of 4010 meters above sea level in the Jankar Chhu Valley, Lahaul

(Himachal Pradesh), was investigated to reconstruct the late Quaternary climate and vegetation history. The Jankar Chhu Valley spans an area of approximately 695 km². The region has early Paleozoic granite (gneiss) and metasedimentary rocks of the Haimanta Group, including phyllite, schist, garnet schist, and graphitic schist. The valley's landscape has been shaped by a combination of glacial and fluvial processes during the Quaternary period. Positioned in the monsoon–arid transition zone, the region is influenced by both the South Asian Monsoon during summer and mid-latitude westerlies in winter.

A 165 cm-long sedimentary profile was sampled from the paleolake, with samples collected at every 1 cm intervals for multi-proxy analysis. The Jankar Chhu Valley remains largely unexplored, pristine, and free from significant anthropogenic disturbance. Its high sensitivity to climatic changes, particularly shifts in precipitation, makes it an ideal site for reconstructing the past climate and environmental conditions in the Lahaul region. The chronology of the Jankar Chhu paleolake was established using Accelerator Mass Spectrometry (AMS) radiocarbon (^{14}C) dating, conducted at IUAC, New Delhi. Analyses of total organic carbon (TOC) and grain size from the lake sediments reveal a climate history spanning the past ~19,890 calibrated years before present (cal yr BP). The deglaciation in the region has initiated the sediment deposition in the lake system prior to ~19.9 cal yr BP. During the post-Last Glacial Maximum (LGM) period (~19.9 to 16 kcal yr BP), strong Westerly influences and glacial control led to negligible total organic carbon (TOC) content and a high proportion of sand deposition in the lake. Between ~16 and 13 kcal yr BP, a decline in sand content alongside an increase in clay and silt suggests a more stagnant lake environment, characterized by low-energy transport and reduced meltwater input from the catchment. Despite this shift, TOC values remained low, indicating limited organic productivity in the region during this time. Between ~13 and 11.6 kcal yr BP, decreases in TOC, clay, and silt content, along with a slight increase in sand percentage, indicate arid conditions in the region. This period corresponds to the globally recorded cold-dry event known as the Younger Dryas period. During the Holocene Climatic Optimum (~11.6 to 8.5 kcal yr BP), TOC content began to rise gradually, while clay and silt percentages also showed an increasing trend. These changes suggest improved moisture availability and enhanced vegetation growth, likely driven by the strengthening of the Indian Summer Monsoon. During the mid-Holocene period (~8.5 to 4.2 kcal yr BP), the slight increase in TOC values and stagnant trends in clay and silt percentages and increasing percentages of sand were interpreted as a high sediment transport by persistent Westerlies and glacial meltwater input. In the late Holocene (~4.2 kcal yr BP to present), a significant increase in TOC levels, despite continued declines in clay and silt percentages, points to enhanced organic productivity, possibly driven by more favorable climatic conditions or localized ecological changes.

Activity: 4

Climate variability and landscape responses in selected transects in the NW and NE Himalaya

(Jayendra Singh, Som Dutt, Anil Kumar, Chhavi P. Pandey, Sudipta Sarkar, Subhojit Saha and Prakasam M.)

Sedimentological modelling of the Rautgara Formation, Lesser Himalayan Sequence

The Meso- to Neoproterozoic Rautgara Formation exposed in the Himalayan Orogenic Belt of NW India (Fig. 45a, b), offers a chance to study a well-preserved fluvial-marine transition to nearshore sedimentation. A detailed sedimentological analysis identifies six genetically linked facies associations (FA) probably deposited in a barrier, back barrier, and subtidal deltaic environments. The facies partitioning, observed in the present study, between wave-dominated and tide-influenced/ dominated deposits can be explained by an inshore tide-influenced/dominated and a shoreline dominated by swelling waves, respectively. During the Highstand System Tract (HST), north/northwestern (N/NW) flowing fluvial systems carried sediments to the east-north-east to west-south-west (ENE-WSW) shoreline (Fig. 46a,b). Later, through late HST, the shoreface-foreshore system was established by reworking the shoreline's sediments via longshore or storm currents (Fig. 46c). These wave-dominated shoreface-foreshore deposits (FA I and FA II) acted as a barrier, offering a mechanism for separating offshore and inshore processes. The fluvial system was transgressed during the Transgressive System Tract (TST, Fig. 46d). Erosively overlying FA III deposits at L5 with 'lag deposits' at the basal part and well-developed lateral accretion (LA element)/ point bar deposits, evince tidal reworking of the fluvial channels. With increases in tidal energy and spit formation within the barrier-shoreface system, the tidal inlet (FA IV) opens, and deposition occurs by flood tidal and wave or storm currents. The close association of the FA III and FA IV deposits evidences continuous, steady transgression. The relatively fine-grained sediments of the tidal flat (FA V) likely represent the filling of tide-dominated back-barrier environments. Subtidal sand

RESEARCH ACTIVITIES
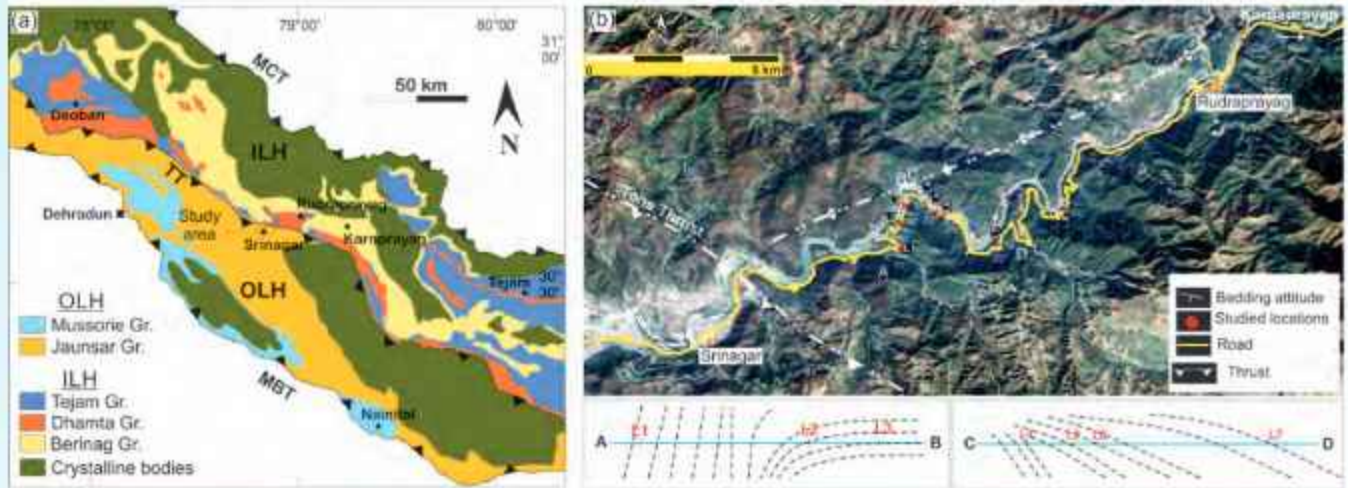
Fig. 45: (a) Detailed geological map of Lesser Himalaya (modified after Valdiya, 1980), Garhwal-Kumaon sector, where OLH (outer Lesser Himalaya) is separated from ILH (Inner Lesser Himalaya) locally by southward dipping TT (Ton Thrust) and crystalline bodies are the klippe overlying basinal sediments. Studied road section is marked. (b) Google Earth image showing the locations (L1 to L9) of the studied sections along the Srinagar-Rudraprayag Highway. Note that the studied sections are located in the southeastern limb of a regional antiform. Inset shows the cross-section along the A-B and C-D transects (marked in 'a'), respectively.
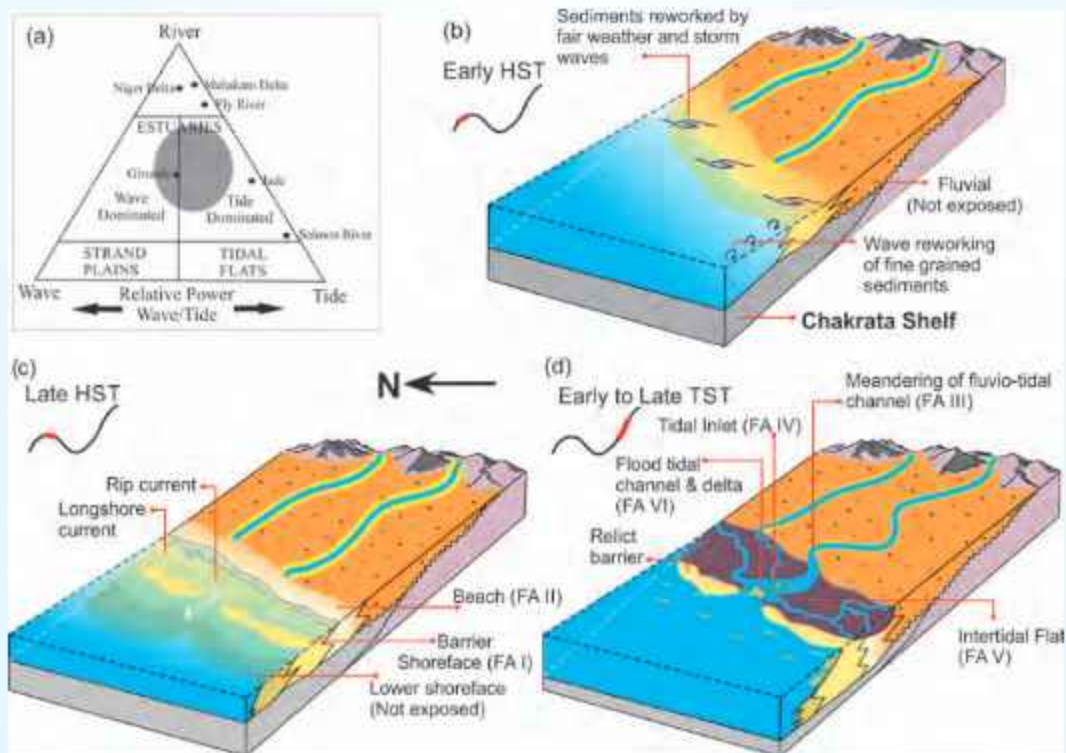
Fig. 46: a) Ternary process based classification of coastal deposits showing range of possible environments for the mixed energy nearshore clastic deposits. Consideration of relative influence of fluvial, wave and tidal current places Rautgara Formation in the middle part of the triangle (shaded area). Note that other modern day coastal systems are marked for comparison. Depositional model for the Rautgara Formation, b) during early HST NW flowing river system/s carried sediments to the ENE-WSW shoreline and reworked by the fair weather and storm currents. c) In the late HST barrier shoreface system was established. d) At early to late TST due to increases in tidal energy inlet developed and back barrier deposition took place.

bar (FA VI) with dominance of flood-dominated currents over the ebb current and wave influence, possibly deposited at a distal part (seaward compared to FA IV) with an open ocean connection during the late TST. However, wave-generated facies (FA I/ FA II) have not been encountered directly below the FA VI succession at L9. This may be due to the erosive action of the marine agents during transgression. As in macrotidal (> 4m) settings, barrier shoreface succession is generally suppressed, and the above-identified facies arrangement possibly indicates a mesotidal (2-4m) range. In addition, there is no evidence of a macrotidal barrier island/lagoon system in the literature. Besides, in a shoreline supplied by multiple rivers, there was likely extensive along-strike variability in coastal morphology, including lobate, linear and embayed shapes, and simultaneous coastal progradation and retreat. Therefore, the sedimentary facies identified in the study area support the interpretation of the depositional regime as a mixed wave-tide dominated barrier-back barrier (inlet) setting built on a roughly ENE-WSW paleoshoreline, where the sediments were brought down by the N/NW flowing river systems along an open coast.

Speleothem inferred Indian summer monsoon variability in the Himalaya

We have developed speleothem oxygen isotopes records of Indian summer monsoon (ISM) variability in the Himalayan regions during the past. A record from the Bhiar Dhar cave, Uttarakhand, Northwest Himalaya indicates ISM changes in northwestern Himalaya between 309 and 260 kyr BP. Weakening of ISM conditions occurred between 309 and 292 kyr BP and from 286 to 264 kyr BP (Fig. 47). A sudden and very strong phase of ISM-linked rainfall begun at ~291 kyr BP which continued till 286 kyr BP (Fig. 47). The orbital scale changes in the ISM rainfall from 309 to 260 kyr BP

in the study area appear to have been driven by the global ice cover and atmospheric CO_2 concentration superimposed by the northern hemisphere solar insolation. Another record has also been developed showing changes in ISM conditions during MIS-7 and MIS-6.

Landscape responses to climate change and tectonics

Uttarakhand state has experienced a rise in cloudburst catastrophes in the last few decades. The cloud burst occurred on 20-21 August 2022 in Dehradun district is examined for geological and geomorphological controls. The study reveals steep slopes, rapid peak flows, a sharp peak hydrograph, poorly developed (low drainage density) drainage and a short concentration time, worsening the impacts of the flood. The river discharge was 50 to 100 times higher during the event than normal monsoonal discharge (Fig. 48). Another study from Pangong Tso Lake, Ladakh Himalaya exhibits strong source-to-sink connectivity, prompt response to sediment supply and accommodation space changes. The deltaic evolution of Pangong Tso is controlled by a series of lake-level fluctuations along with a significant role of fluvial supply since 13 ka. The upper Satluj Valley is also examined to understand the responses of long-term tectonic-climatic coupling in landscape building processes using various morphometric analyses and field investigation. Results reveal that the Satluj Valley has dynamic tectonics, as indicated by geomorphic features such as dammed lake deposits, river ponding, deep gorges, high relief, fault scarps, and widespread landslides. These features underscore the landscape instability and topographic irregularities.

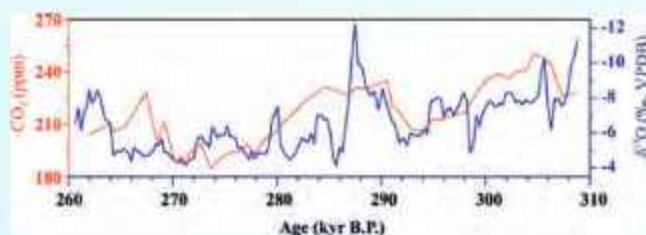**Fig. 47:** Reconstructed $\delta^{18}O$ time series from the Bhiar Dhar cave, Uttarakhand, northwest Himalaya (Present record in blue colour) in comparison with global CO_2 concentration in the atmosphere reconstructed from EPICA Dome C (Jouzel et al., 2007; red colour).
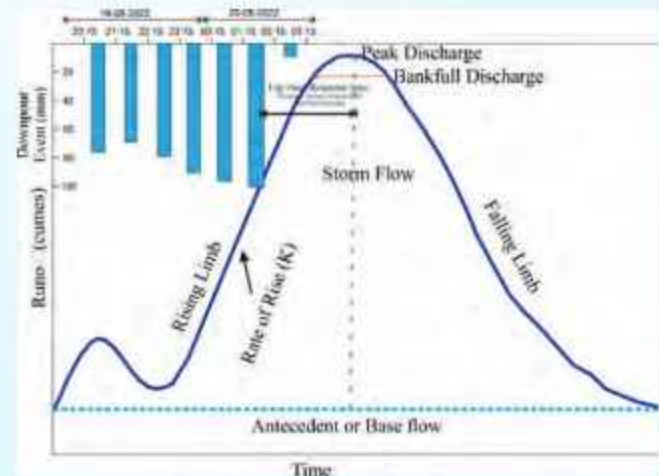
Fig. 48: Different components of the hydrograph during the flash flood on August 20, 2022.
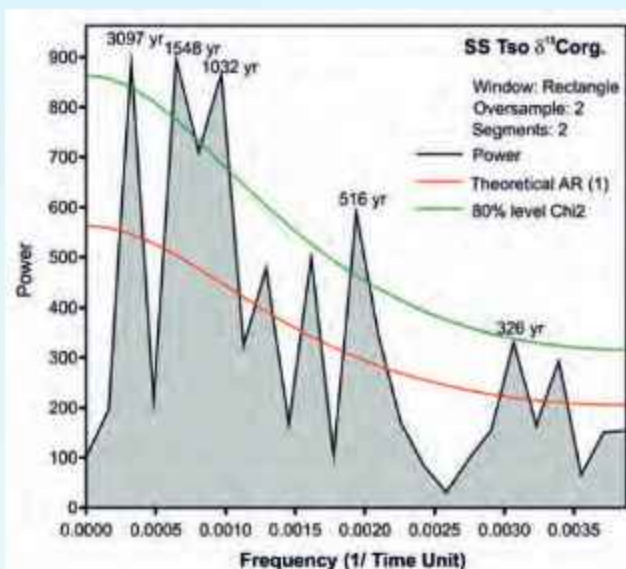
RESEARCH ACTIVITIES

Fig. 49: Results of spectral analysis using Past v 4.11 for SS Tso Lake sediment data during last 4500 years. Numbers shown above the peaks are periodicities in years.

Late Holocene climate history of the Spiti, Northwestern Himalaya

The multi-proxy records (quartz, calcite, muscovite, χlf, and $\delta^{13}C_{org}$) during the Late Holocene sediments at SS Tso Lake present a comprehensive picture of climate variability and environmental fluctuations in the Spiti area. Our results demonstrate that solar insolation has been the primary driving force behind climate fluctuations, with warmer periods receiving more precipitation (2600-2200 BCE, ~1500–900 BCE, ~700–100 BCE, ~900–1300 CE, and ~1800 CE to the Present) and cooler intervals receiving less precipitation (~2200-1500 BCE, ~900–700 BCE, ~100–900 CE, and ~1300-1800 CE). These climatic fluctuations have affected the lake environment and the sediment sources in the region, and caused fluctuations in weathering patterns and erosion through the watershed area. The highly significant correlation of the records to regional paleoclimate records illustrates the overall coherence of climate fluctuation in the northwestern Himalaya. The spectral and wavelet analysis of carbon isotopes highlights the contribution of the solar cycle (326, 516, 1032, 1548 and 3097-year) other large-scale oscillations to the lacustrine system (Fig. 49). This study provides a critical perspective on the environmental history of this fragile high-altitude environment during the last 4500 years.

Late Quaternary centennial to millennial-scale climate and vegetation changes of the Lahaul-Spiti Himalaya: a multi-proxy record

Chronologically constrained multi-proxy data sets have been developed to reconstruct the centennial to millennial-scale climate and vegetation history, especially, during the Holocene period from the north-western Himalaya and Indo-Gangetic Plain. Soil and peat samples from few study areas, located in the Lahaul-Spiti region of Himachal Himalaya have been analyzed for sedimentological and geochemical proxies. Radiocarbon age dating of samples at specific depths from these study locations was conducted at the Inter University Accelerator Centre (IUAC), New Delhi. The Falder Area of Spiti Valley will provide around 13000 years of paleoclimatic record. The soil profile from the study area provides a clear picture of decreasing concentration of finer grained particles (clay and silt) from older to younger sediments, which indicates the increasing energy condition of the depositional basin towards the top. The magnetic susceptibility (χlf) gradually increases, and the total organic carbon decreases towards the younger time scale, i.e., towards the top of the profile. The depositional basin gradually changed its depositional condition from low to high energy towards the younger time period. Moreover, increased organic matter (increased Total Organic Carbon values) at the lower part, i.e. older period of the section, indicates warmer and humid paleoclimatic condition of the area during the older period, when the organic productivity seemed to have increased due to favorable conditions.

Optical and physicochemical characterization of atmospheric aerosols from Uttarakhand Himalaya, India

Atmospheric aerosols are complex mixtures of solid and liquid particles suspended in the air, originating from natural or anthropogenic sources. The intricate composition strongly influences climate, air quality, and cryospheric processes, especially in sensitive environments such as the Himalayan region. The optical and chemical characterization of total suspended particles (TSP) acquired from Gangotri Glacier Valley during the pre-monsoon season in May 2016 was performed using Raman micro-spectroscopy. Our preliminary analysis revealed that aerosols contained a complex combination of carbonaceous species, including black carbon (BC) and organic carbon (OC), as well as oxidized functional groups such as carbonyl and hydroxyl, indicating the presence of secondary organic aerosols (SOA). Additionally, peaks associated
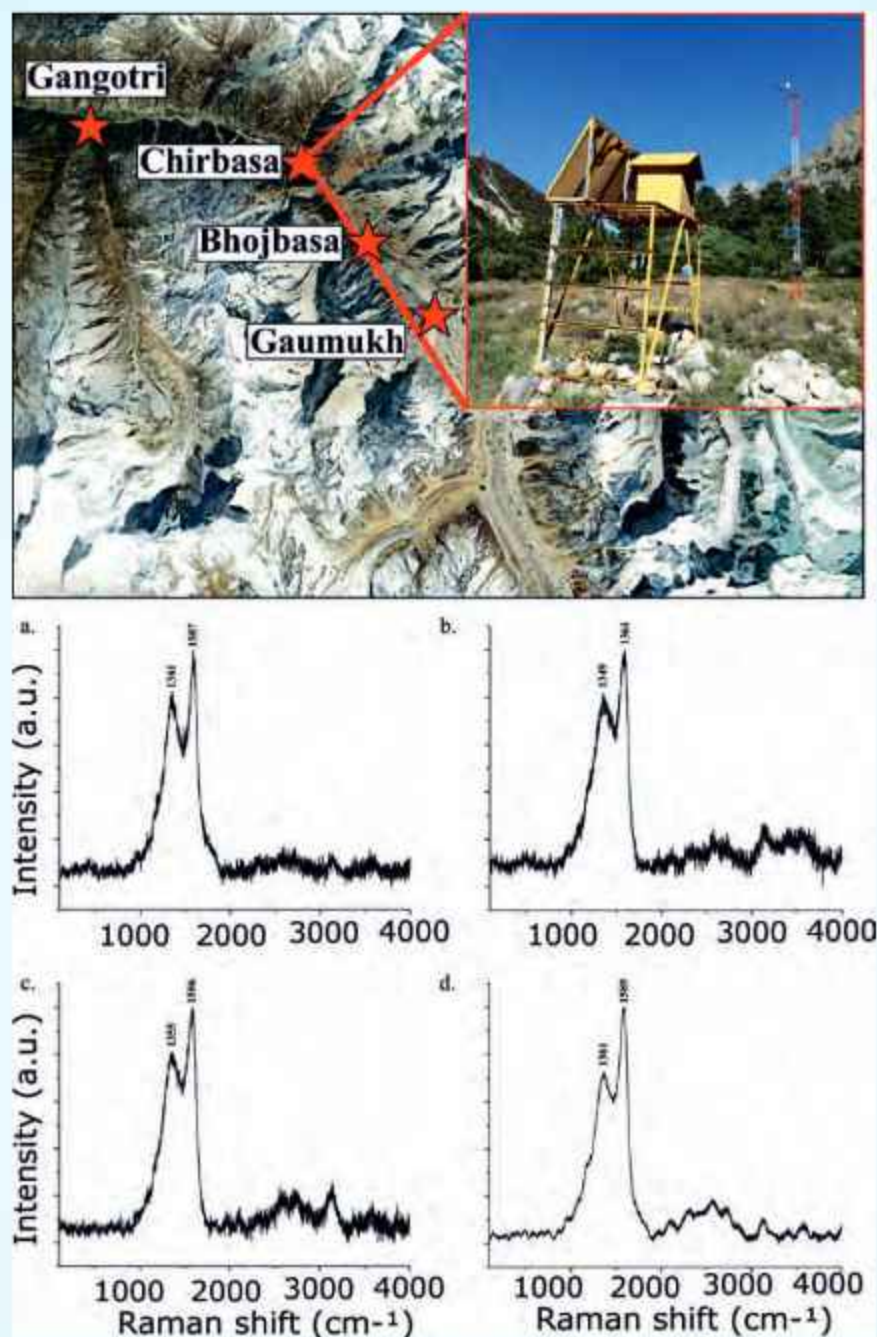
Fig. 50: Satellite image of sampling site along the Gangotri Glacier Valley (Gangotri, Chirbasa, Bhojbasa, Gaumukh) with an inset image showing the field image of Black Carbon monitoring setup at Chirbasa. (a-d) Raman spectra indicating the presence of black carbon with characteristic D and G bands.

with aliphatic hydrocarbons, ammonium, sulfates, nitrates, and mineral dust confirmed contributions from primary and secondary sources. This diverse chemical composition reflects the possible influence of regional transport, particularly from the Indo-Gangetic Plain, and atmospheric aging during long-range movement. Raman spectroscopy proved highly effective in identifying molecular-level aerosol components without complex sample preparation. These findings could enhance our understanding of aerosol behavior in high-altitude environments and their connections to glacier melting, radiative forcing, and regional climate variability. Figure 50 depicts the satellite image of the study site, and plots (a-d) show the Raman Spectra indicating the presence of D and G bands.

Tree ring record from the Lahaul region, Himachal Pradesh

Ring-width chronology (1670-2022 CE) was prepared using tree cores of the *Picea smithiana* [(Wall.) Boiss], growing on the right bank of the Chenab River in the Lahaul region, Himachal Pradesh. The chronology was truncated at 1838 CE based on the Expressed Population Signal (EPS) value ≥ 0.85 and used in further analysis. Tree-growth climate analysis revealed that tree growth has a direct (positive) relationship with precipitation, except in December of the previous year and in January, April, July, September, and October of the current year. In contrast, a significant relationship was observed between precipitation and tree growth in February through October of the current year. The temperature revealed an inverse relationship during most months. However, November of the previous year and June, July and September of the current year exhibited a positive relationship in tree growth. Notably, a significant relationship in tree growth was observed for the temperatures in March, April, and September of the current year. The significant relationship was observed in temperature in the March, April and September of the current year. Furthermore, analysis indicated that ring-width chronology has a strong positive relationship with seasonalized precipitation during February-March. Such a strong relationship in precipitation and ring-width chronology in February-March could be used to infer the precipitation variability during the past 185-years. The chronology captured the highest indices during 1951-1961CE and the lowest in 1858-1868CE, reflecting wettest and driest periods, respectively in the entire series.

Activity: 5
Geological and geomorphic controls on landslide for risk assessment and zonation in the Himalaya
(Khayingshing Luirei, Swapnamita C. Vaideswaran, Naveen Chandra and Tariq Anwar Ansari)

Neotectonic activity along the Main Boundary Thrust and Main Boundary Fault zones in the SE western Himalaya as evident from morphotectonic features

Neotectonic activity in the Main Boundary Thrust and Main Boundary Fault zones of the Sataun area is well discernible in the outcrops, Google Earth imagery, and topographic maps. Fault traces are observed in the Barthal-Sataun and Bhatrog-Nagetha sections that stretches for about 48 km long intervene by sections

Fig. 51: (a) Google Earth images showing fault trace of the Main Boundary Fault (MBF) between Sataun and Baila (marked by yellow triangles), the fault scarp is south dipping with development of sag ponds along the fault trace; (b) Google Earth image showing sag ponds in a linear arrangement along the fault trace; (c,d) highly sheared bedrock and stretching lineation observed in the footwall block of the MBF; (e,f) formation of sag ponds on the downthrown side of the fault; (g) south dipping fault scarp showing slickensides in the bedding planes indicating bedding parallel movement in the limestone.

where no tectonic landforms are developed. In the Barthal-Sataun area the fault trace measures more than 25 km in length (Fig. 51). The fault trace is formed along the MBF and across the ridge the dip of the bedrock and fault scarp changes from south dipping to NNW-NNE dipping. In the Baila-Kansar area the MBF zone is defined by highly sheared bedrocks of limestone, shale, and sandstone, comprising the hanging wall and footwall blocks, respectively. Along the fault trace between Baila and Chhichheti the fault scarp dips towards the south and is represented by small, linearly aligned hillocks. Parallel to it is the Kandon ka Khala Fault along which the Kandon ka Khala flows. Apart from these faults two other parallel lineaments are also observed, which are 7 km and 3.5 km long, respectively. The MBF at the Baila-Kansar area is north dipping, and the fault zone is defined by highly sheared bedrocks; in the footwall block stretching lineations are developed. East of Kansar the MBF becomes vertical to south dipping as observed during the present study. It is represented by fault trace and sag ponds. The fault scarp is observed in the limestone bedrock with an attitude 60° towards 185° and slickensides are also developed in the bedding plane indicating bedding parallel movement. The fault scarp measure about 34 m in height. The sag ponds here are formed on the downthrown side (footwall) of the fault, which can be explained to have formed due to relative downward movement of the hanging wall block with respect to the footwall block, followed by accumulation of water during the monsoon. At Achhaun, related structural fabric in the form of shear zone, fault scarps, and faults are observed in the alternation of limestone, sandstone, and carbonaceous shales and is exposed along the stream section where rocks of the pre-Siwaliks dip 62° towards the southeast-south. As the movement is parallel to the bedding no significant displacement is observed, but the rocks in the footwall-block are highly sheared. At Kyari, along the Kyari-ka-Khala, a steeply dipping fault scarp is observed upstream. Conjugate sets of the faults are also prominent in the highly indurated sandstones; one set dips towards the southwest while the other dips northeast. At Chhichheti, the fault zone is about 200 m wide, and a fault depression is formed at the hanging wall block. The footwall noted along the road-cut is made up of steeply (75°-85°) dipping sandstone that dip

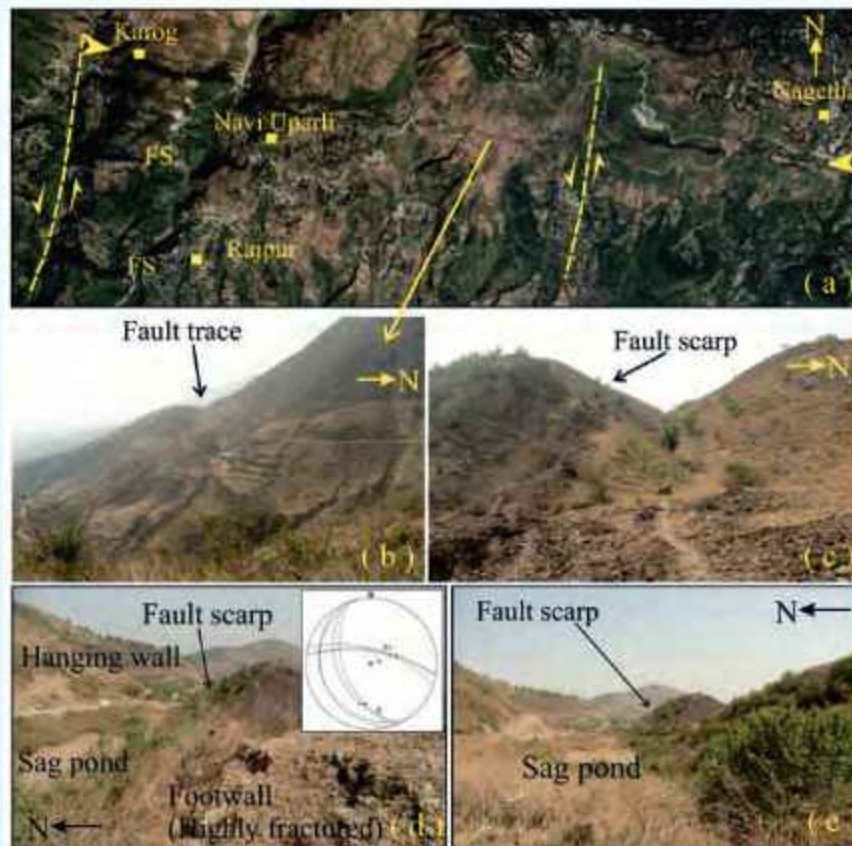**Fig. 52:** (a) Google Earth image showing the eastern part of the Bhatrog-Nagetha fault trace, the fault trace has been displaced by two sinistral strike slip faults in a later phase of faulting; (b,c,d,e) field photographs showing fault traces, fault scarps and sag ponds in the area, inset in figure (d) shows stereoplot representing orientation of the bedrock, fault scarp and fracture planes.

towards NW to NE, while the bedrock in the hanging wall dip moderately (40°- 44°) dip towards NW to NE. The fault zone is marked by highly crushed rocks; fault movement is parallel to the bedding. Down dip lineations are imprinted on the sandstone bedrock. Further eastward, this fault trace is parallel to the Kandon-ka-Khala; in the topographic map, it is marked by linear elevated hillocks, while in the Google Earth image, it is represented a linear depression of about 2-km in length.

Eastward of the Giri River, from Bhatrog to Kulthina, a curvilinear fault trace is observed; while from Karog to Nagetha in the east, the fault trace trending almost E-W is nearly straight (Auden 1934; Rupke, 194; Oatney et al. 2001; Virdi and Philip, 2006) (Fig. 52). The fault trace cut across the MBT obliquely near Bhatrog. There is change in the strike of the fault trace from NE-SW trending in the western segment to E-W trending in the eastern segment. The fault scarp trend also swings from the northwest to the north dipping. Between Bhatrog to Kulthina the fault trace is discontinuous and modified by the slope processes and streams. The maximum height of the fault scarp is about 70 m. In the westernmost portion of the fault trace near Bhatrog the fault scarp has been formed in old landslide debris, as observed at Sikna and Shilon. It is most prominent between Shilon and Kaner where the fault scarp is made up of bedrocks, while the fault trace at Shilon and westward is formed in the landslide debris and has degraded with time due to erosion. At Kulthina-Karog, the fault zone is marked by a wide depression of almost 50 m, and the fault scarp is about 45 m in height. The fault depression is most prominent along the spur. This depression, about 450 m wide in the eastern segment, has been modified by stream erosion. The beds in the footwall dip 25° towards the northeast while those in the hanging wall dip 22° southwest; the fault scarp dips steeply (75°) towards the north (355°). Further east of Kulthina, at NaviUparli, the fault trace is 800 m long and 60 m wide; the fault scarp is more prominent in the west. The fault scarp develops in slate bedrock at Agron, which dips north. Near Nagetha, where the rock beds dip steeply towards NNE, the fault scarp is very prominent. The footwall block is made up of slates that dip SW. Several fractures trend parallel to the fault scarp and numerous joint and fracture planes related to the fault are discernible in the footwall rock. The maximum height of the fault scarp here is about 80 m. Water accumulates in the sag ponds during the rainy season. On the footwall the bedrock dips gently to moderately (14°-44°) towards SW (242°-247°), and the fracture planes parallel to the fault scarp dip steeply (63°-67°)

towards NNE (8°-16°), while the hanging wall rock dips gently (15°) towards SW (235°). The displacement of the fault scarp at Bharli and Kulthina points to a later phase of tectonic activity. At Kulthina, the fault trace has been displaced by about 700 m by the sinistral, strike-slip STF. Similar observations were made based on the displacement of the MBT and Bilaspur Thrust. Near Bharli, the fault scarp is displaced by a NNE-SSW-trending sinistral strike-slip fault by about 150 m. This strike-slip fault trends parallel to the fault that displaced the fault scarp at Kulthina. To the south of Navi Uparli two small stretch of fault scarps parallel to the main fault scarp is observed, and at Lobhi and Hatwar-Panjabiwala. The fault deflects the stream, and the deflection is parallel to the trend of the fault scarp. It is about 40 m in height and 280 m in length. It dips towards the north, trending almost E-W. This fault scarp does not extend eastward, possibly due to erosion during the earlier phase and the deposition of the massive landslide debris in the later phase. East of Navi Uparli two traces of fault scarp merged at Kangra. The fault depressions are more prominent along the spurs.

Landslide risk assessment in the Ram Ganga Catchment, around Chaukhutiya and Tadag Taal, Uttarakhand

In the Himalayan region, the steep slopes and deep valleys create localised weather patterns, increasing the intensity and severity of rainfall events, thereby posing risks to slope failures. The Ram Ganga Catchment in the Almora, Chamoli and Rudraprayag districts of Uttarakhand is characterized by litho-structural units which are undergoing continuous denudational processes (Kaushik et al., 2023; Kothyari, 2008). Tadag Taal is a rain-fed lake in the Ram Ganga basin, close to Chaukhutiya. With the changing climatic patterns and the rise in extreme weather events, the possible risk of a lake outburst flood from the Taal Volcano may be a concern. To address such risk, a study was done to generate a geological database assessing the potential hazards in this region and the lake. Utilizing a comprehensive methodology, land use and land cover (LULC) change in the study area and susceptibility mapping are integrated for a risk assessment of the study area. Objectives also included analysing centennial and decadal climate patterns, understanding sedimentation rates over the past 1500 years, analysing the change in the lake area with fluctuating climate patterns and change in LULC to determine the anthropogenic effect in the study area. ArcGIS and Excel were used to process the data. The results reveal a decreasing trend in precipitation over the past century, with significant variability across different time scales. Additionally,

RESEARCH ACTIVITIES
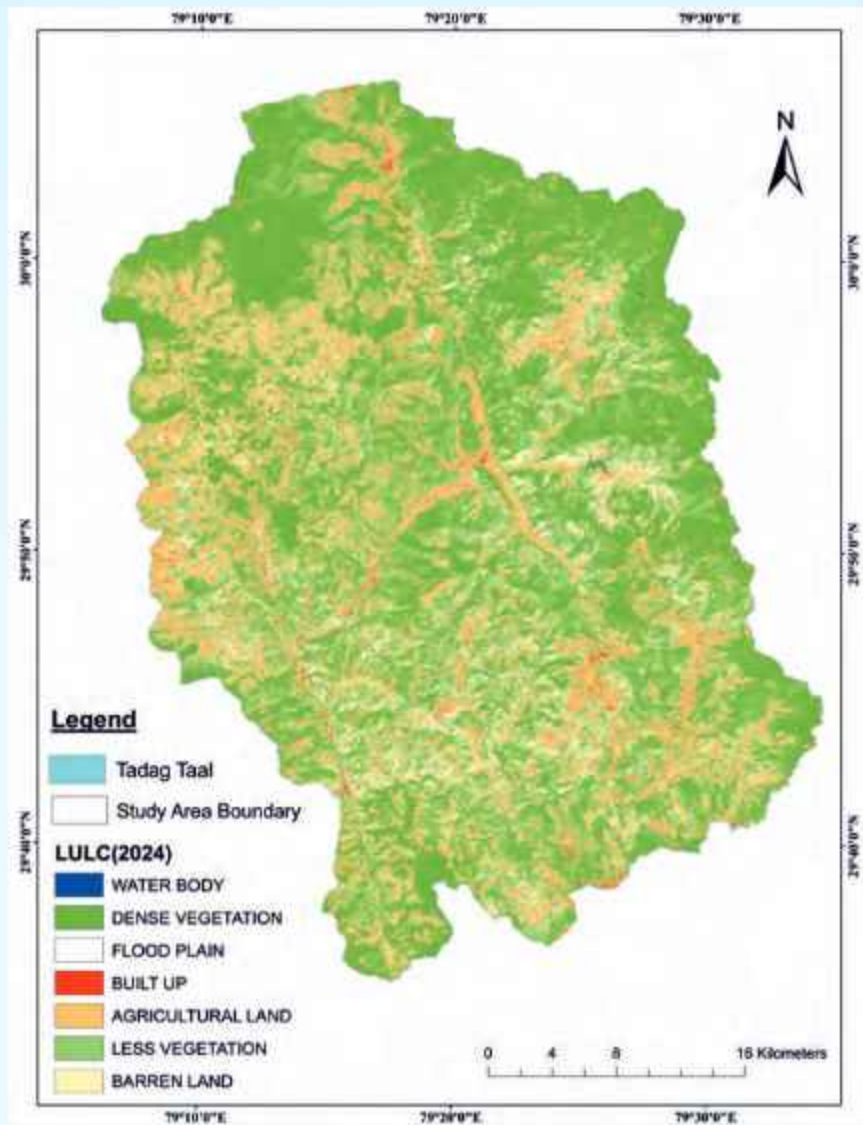
Fig. 53: LULC of the Ram Ganga catchment using Sentinel-2 imagery with a 10-meter resolution from April 25, 2024.

land use changes driven by human activities have contributed to alterations in the study area.

LULC map of the basin was created using ESA Sentinel-2 imagery with a 10-meter resolution from April 25, 2024. The supervised classification results for April 2024 are shown in figure 53. Dense Vegetation covers approximately 5,574 km², representing 34.21% of the study area. Agricultural land occupies about 3,182 km², making up 19.53% of the area, barren land spans approximately 2,018 km², making up for 12.39%. Water bodies, flood plains, and the built-up regions cover 3 km² (0.02%), 2.5 km² (0.02%), and 105 km² (0.65%) of the basin, respectively. A landslide susceptibility map was generated using the Frequency Ratio Method for the catchment by evaluating several factors, including slope, geology, soil type, land use, Vegetation, and rainfall (Fig. 54). The frequency ratio method involves a statistical analysis to estimate the probability of landslides in a given area. The results show that most of the area falls within the moderate susceptibility zone, followed by low and high zones. Although the very high susceptibility zone is relatively small, continuous changes in environmental conditions, topography, and climatic factors such as rainfall continually alter the lithology of the study area. The North Almora Fault, in particular, exhibits a higher susceptibility zone, indicating potential landscape uplift.

Geo-morphometric parameters are calculated considering the Ram Ganga River, which stretches 81km within the study area. To estimate Ksn, the drainage area is normalised for a given reach using a reference concavity theta, corresponding to the regional
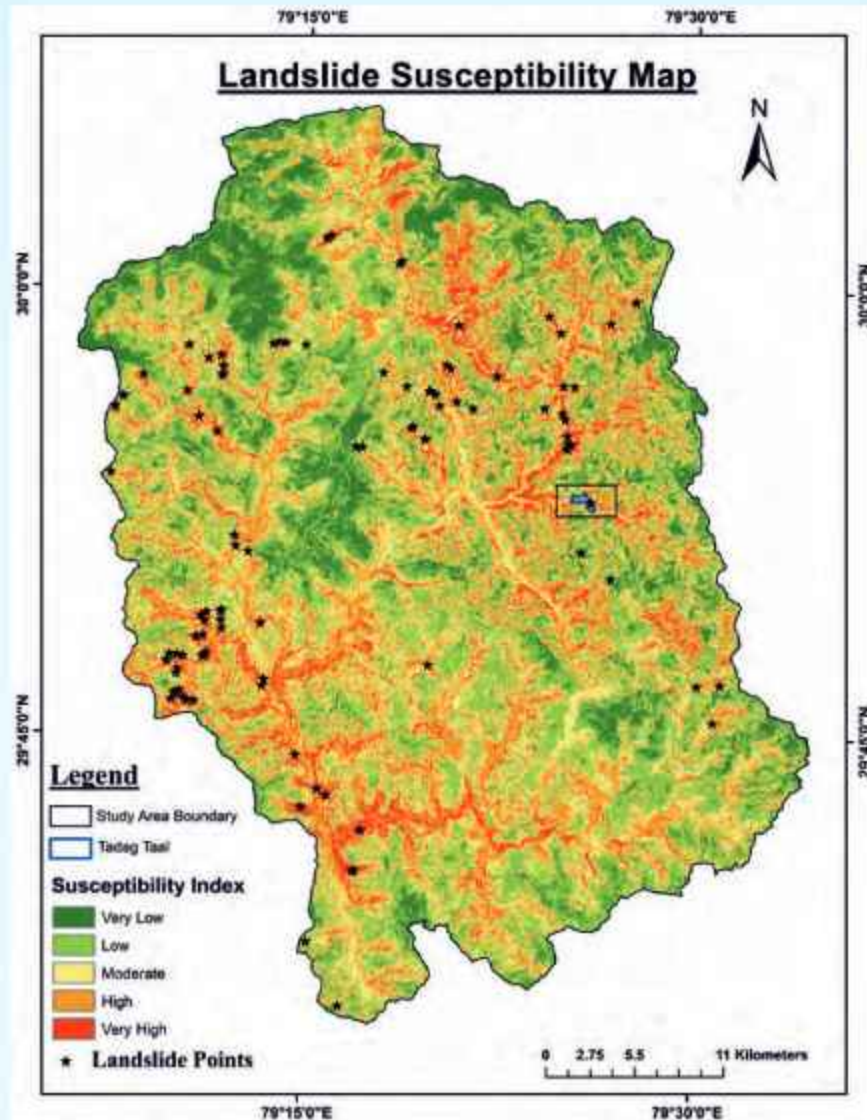
Fig. 54: Landslide Susceptibility Map of the Ram Ganga catchment with landslide inventory of the area for validation.

concavity in areas unaffected by tectonic influences (Wobus et al., 2006). The Stream Length-Gradient index, which provides a direct measure from a stream profile, has also been derived. The indices are seen to respond to the same geomorphic controls, such as lithological boundaries, tectonic uplift, or erosion processes. Peaks or changes in the graphs may represent knickpoints indicating tectonic activity or variations in rock strength. The SL Index, assessing the channel slope and length relationship, highlights regions with steep gradients that may signify active tectonic regions or variations in rock strength. Peaks in the SL Index along the tributaries feeding into the Tadag Taal suggest areas more susceptible to erosion and landslides. These steep tributary channels contribute to rapid water flow into the lake during heavy rainfall, influencing the lake water level and increasing the risk of overflow and flooding.

Geospatial landslide susceptibility mapping

Landslides are among the most recurrent and destructive geological hazards in mountainous regions, posing serious threats to life, infrastructure, and the environment. The Garhwal Himalaya in northern India is particularly prone to such hazards due to steep terrain, complex geological structures, intense rainfall, and increasing anthropogenic pressures. In this context, landslide susceptibility mapping (LSM) serves as an indispensable tool for identifying areas at risk and supporting effective disaster preparedness and mitigation strategies. This study presents a comprehensive LSM of Tehri District, Uttarakhand, employing two widely recognised statistical and multi-criteria decision-making models: the Analytical Hierarchy Process (AHP) and the Frequency Ratio (FR)
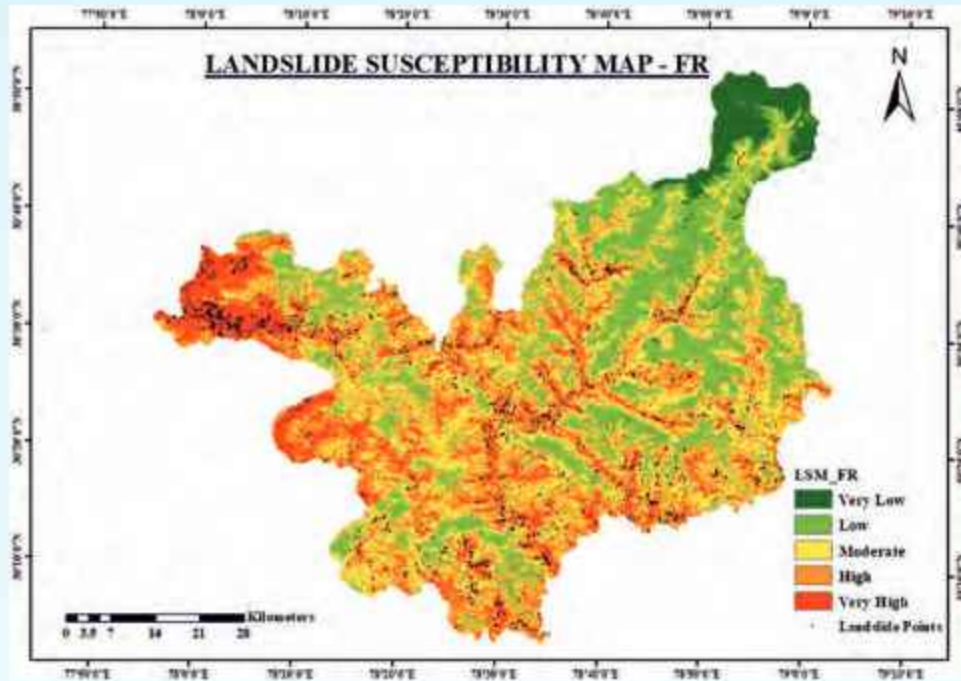
Fig. 55: LSM of Tehri District Using FR model.
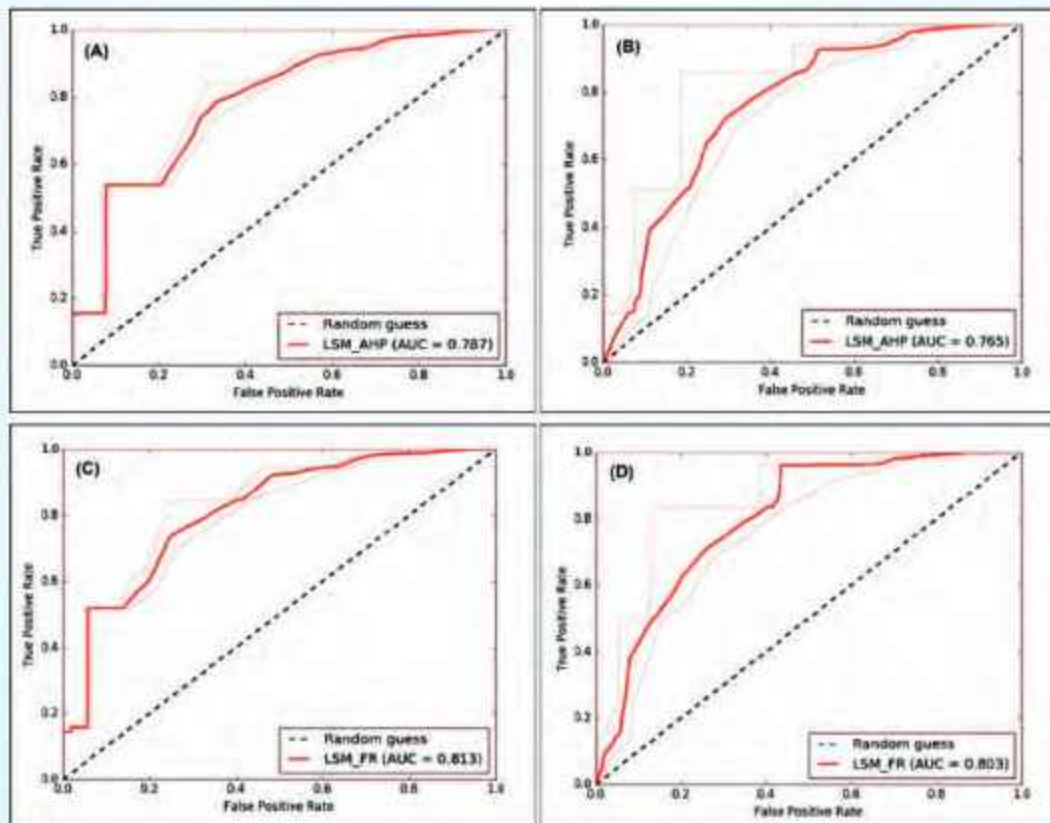
Fig. 56: Area under curve (AUC) of the produced LSM using AHP and FR methods, illustrating the success rate curve (SRC) (A and C), and prediction rate curve (PRC) (B and D).

RESEARCH ACTIVITIES

model. These models were integrated with geospatial tools within a GIS environment to analyse the spatial correlation between historical landslide events and various contributing factors. Fifteen causative factors were considered for thematic map preparation, chosen based on their geomorphological, hydrological, and environmental relevance. These include slope, elevation, aspect, relative relief, curvature, geomorphology, stream power index (SPI), geology, normalized difference vegetation index (NDVI), distance to lineament, land use and land cover (LULC), distance to stream, topographic wetness index (TWI), distance to road, and annual rainfall.

A comprehensive landslide inventory comprising 2,612 recorded landslide events was compiled using remote sensing data and secondary sources to support model development and validation. The dataset was split into a training set (70%) for model calibration and a validation set (30%) for performance evaluation. The susceptibility maps were generated through the FR model (Fig. 55). The performance of each model was assessed using success rate and prediction rate curves (Fig. 56). The AHP model achieved a success rate of 78.7% and a prediction rate of 76.5%, demonstrating good overall reliability. However, the FR model exhibited superior predictive capability, with a success rate of 81.3% and a prediction rate of 80.3%, confirming its robustness in capturing the spatial likelihood of landslide occurrence in the study area. These results underline the practical effectiveness of the FR model for landslide susceptibility assessment in complex mountainous terrains, where physical conditions and triggering factors vary significantly across short spatial scales. The final LSM outputs are highly beneficial for regional planners, disaster management authorities, and infrastructure developers, enabling them to prioritize

mitigation efforts and implement resilient land-use policies. In conclusion, this study contributes to the growing research on Himalayan landslide risk and demonstrates the value of combining statistical modelling with geospatial analysis to generate actionable insights for sustainable development and risk-informed decision-making in vulnerable regions.

An integrated approach combining physical and numerical models for the early prediction of landslides

Shallow landslides, oftenly referred as soil slips, are a common geohazard that occur in various geo-environmental contexts worldwide, leading to significant destruction. These events involve separating surface soil layers from shallow depths on slopes, mainly due to the rainfall. This research seeks to develop a slope monitoring system for the early detection of these shallow landslides or soil slips slope failures. Traditional landslide prediction systems generally consist of a wireless sensor network, a base station, and a remote monitoring system. This configuration monitors slope movements and detects shifts before failure, activating the warning alarms. The sensor system developed for this research incorporates multiple sensors to measure critical parameters, such as temperature, soil moisture, rainfall, and acceleration (Fig. 57). Further, we designed a routing protocol where each sensor node communicates with neighbouring nodes and uses multi-hop communication to send collected data to the station. These routing strategies can effectively reduce energy consumption, and future improvements in energy-efficient routing protocols will enhance coverage area and longevity. By analysing these measurements, our aim is to determine threshold values, allowing for the prediction of potential slope instability and subsequent landslide events. It requires
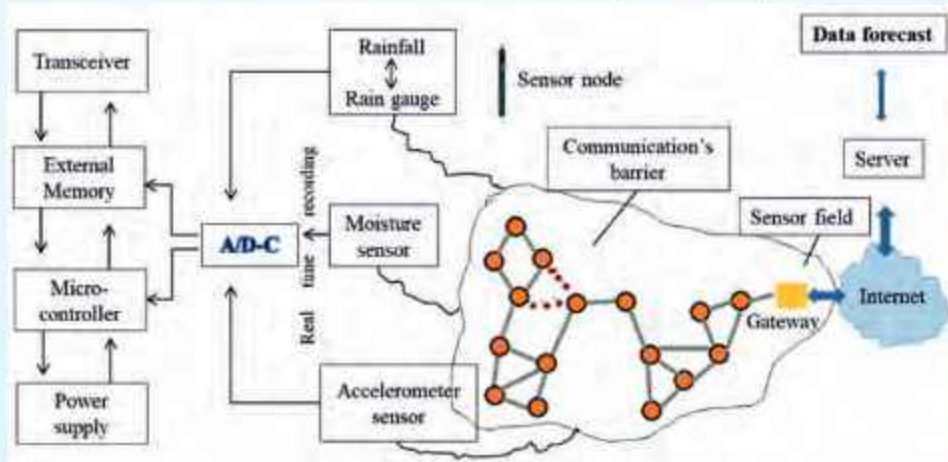
Fig. 57: Architecture of the wireless sensor network for landslide monitoring.

the formation of a small-scale physical model that utilizes wireless sensor networks to monitor slope failures. Also, it continues to underscore the crucial role of moisture changes caused by precipitation in influencing slope stability, highlighting the need to incorporate soil hydrological data into laboratory-scale landslide monitoring systems.

By employing a physical model at the laboratory scale and numerical simulations, the study indicates the significant effects of rainfall infiltration on slope behavior and stability. This was achieved by increasing simulated rainwater flow intensity over intervals (dry condition, from t=0 to t=30 min., 0.5 mm/min. from t=30 to t=60 min., 0.75 mm/min. from t=60 to t=91 min. and 1 mm/min. from t=91 to t=120 min.). The experimental results, obtained by incrementally increasing simulated rainwater flow intensity, reveal the progressive deterioration of the slope structure and the emergence of critical instabilities. As the experiment progressed, deep gullies formed and larger soil masses displaced, indicating a critical stability stage. Factor of safety (FoS) analyses through numerical simulations for different moisture content yielded outcomes aligning with physical model observations. The findings provide insights into slope stability and failure mechanisms under varying rainfall, highlighting the importance of continuous monitoring and early intervention in real-world scenarios to prevent catastrophic landslides.

Activity: 6A
Glacial dynamics, glacier hydrology, mountain meteorology and related hazard
(Manish Mehta, Vinit Kumar (on Lien), Sameer Tiwari, Pinkey Bisht, Amit Kumar, Rakesh Bhambri, Jairam Singh Yadav)

Status of Glacier Surface Changes in the Doda and the Suru River Basin: past and current status, priorities, and future prospects

The ablation-stake network measurements suggest that the Pensilungpa Glacier's (PG) net balance was negative in 2023-2024. During the measurement period, the net ablation of the glacier was ~ (-) 7.26 ×10⁶ m³ w.e., while the net accumulation of the glacier was ~(+) 0.94 ×10⁶ m³ w.e. However, the ablation and accumulation gradients of the glacier were ~(-)4 m/100 m and ~ (+) 1.5m/100m, respectively (Fig. 58). Our result also suggested that during the same period, the glacier's Equilibrium Line Altitude (ELA) was situated at a height of 5251 meters (m) above sea level (asl). Further, our result shows that most surface ablation was
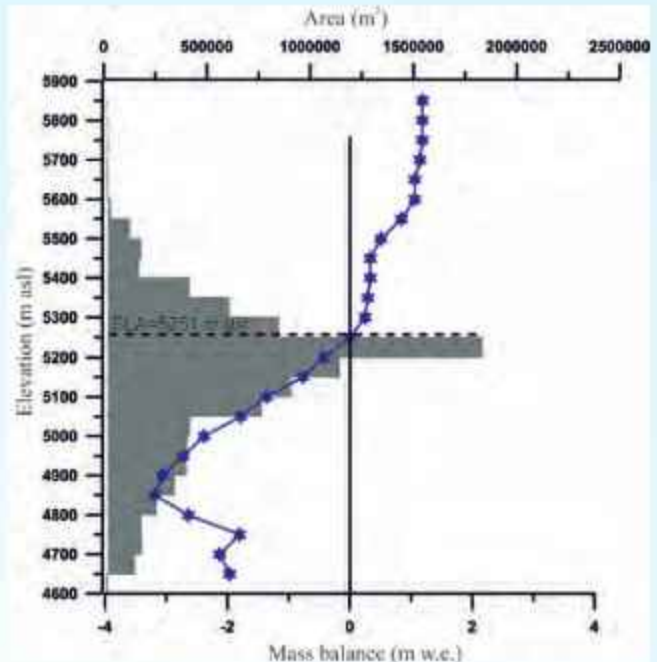
Fig. 58: Graph showing the mass balance, Elevation and area of the Pensilungpha glacier in 2023-2024 and the ELA of the glacier located at the elevation of 5251 m asl.

observed between altitudes 4800 and 5000 m, encompassing areas covered by thin and patchy debris up to 10 cm thick. We suggest that a thin cover reduces albedo without significantly introducing an insulating layer at the surface. While the lower areas between 4600 and 4800 m reduced the surface ablation due to thick debris covered.

The lack of long-term glacio-hydrological data for the Himalayas remains a significant constraint in addressing regional issues. From 2017 to 2023, the melt water discharge of the Parkachik river showed a continuous increase, with meltwater volumes of 1.7 ± 0.04 × 10⁸ m³, 5.7 ± 0.13 × 10⁸ m³, 16.03 ± 0.81 × 10⁸ m³, 10.32 ± 0.23 × 10⁸ m³, 11.39 ± 0.53 × 10⁸ m³, and 23.67 ± 0.34 × 10⁸ m³ for the respective years.

Seven peri-glacial lakes near the Pensilungpa Pass and two proglacial lakes near the front of the Durung-Drung Glacier (DDG) were studied. Peri-glacial lake dimensions showed a marginal rise of about 6.5% in surface area and around 7% in water volume, highlighting their dependence on non-glacial water sources. The expansion of the Proglacial Lake near the Durung-Drung Glacier was notable, with approximately a 177% increase in the area and 195% in water volume between 2004 and 2023 (Fig. 59). These substantial increments underscore intensified glacial melt processes, emphasizing the vulnerability of the

Fig. 59: Proglacial and periglacial lakes in the Doda and the Suru River Basin. (A) The photograph shows the two proglacial lakes that are formed near the front of the Durung-Drung Glacier. (B; B1-B4) The periglacial glacial lakes, which are situated on the Pensila, pass between the ablation valleys of two glaciers, showing a unique character. These lakes have no passage to the inlet and outlet of water. The source of the lakes depends on the snow melt and rainwater. (C) The secondary lake is positioned at a proximity of merely 1-kilometer from the Durung-Drung Glacier terminus, exhibiting a configuration reminiscent of a kidney.

region's glacial dynamics to climate change. Further, field observations from 2015 to 2023 revealed a total terminus retreat of ~ (-)165 ± 95 m with an average rate of -21 ±12 m a^{-1} for DDG and ~ (-) 80 ± 35 m with an average rate of -10 ± 4 m a^{-1} for the PG. These findings signify a concerning acceleration in glacier recession and an increase in glacial melt, potentially influenced by climate change.

Glacier lake changes in Uttarakhand, India from 2013 to 2023 using high resolution satellite images

The enhanced climate warming from the early 20th century caused large-scale glacier retreats and mass losses, which induced the formation of new glacier lakes and increased the extension of many existing glacier lakes. This study deals with the glacier lake changes in Uttarakhand from 2013 to 2023 using high-resolution Resourcesat LISS IV images. In this decade, the number of glacier lakes increased by 1.9%, while the area covered by them increased by 8.1%. This rise is mainly attributed to rising temperatures in the region over the last some decades. The number of glacier erosion lakes and moraine-dammed lakes increased, while the area of supraglacial lakes decreased. The glacier lakes were distributed between 2900 m, asl and 6100 m, asl, and 1001 counts out of 1290 (78%) were above 4500 m, asl. The Alaknanda basin had the maximum number and area of glacier lakes (580 counts), followed by the Bhagirathi basin (341 counts). In contrast, no glacier lakes have been found in the Ramganga basin. The total area of glacier lakes increased in all the ten river basins. However, in the Alaknanda basin, the number of glacier lakes decreased by 8.6% (Fig. 60), while the Dhauliganga and Pinder basins showed negligible changes in lake numbers. Elevation-specific changes revealed an expansion in lake areas above 4000 m, asl, whereas a decline in lake numbers was observed between 3500 m, asl and 4500 m, asl. Out of the 13 administrative districts in the Uttarakhand, glacier lakes are distributed only in six districts, corresponding to the presence of glaciers at high altitudes. The maximum number and area of glacier lakes were found in the Chamoli district, followed by Uttarkashi. Our study recommends field surveys and further investigations using high-resolution satellite data to understand the potential hazards posed by these lakes to infrastructure and human lives.

Abnormal melting of the Changmolung Glacier due to geothermal activity

Geothermal activity is a potential but underexplored driver of glacial dynamics in the Karakoram. The impact of such activity on glacier melting has not been systematically investigated in this region. Our study reports the first discovery of an undocumented geothermal spring at the terminus (~4,980 m, asl) of the Changmolung Glacier in the Nubra valley, during a field expedition in August 2022 (Fig. 61). To assess thinning of the Changmolung Glacier, four bamboo stakes were installed ~4 m into the ice in the lower ablation zone
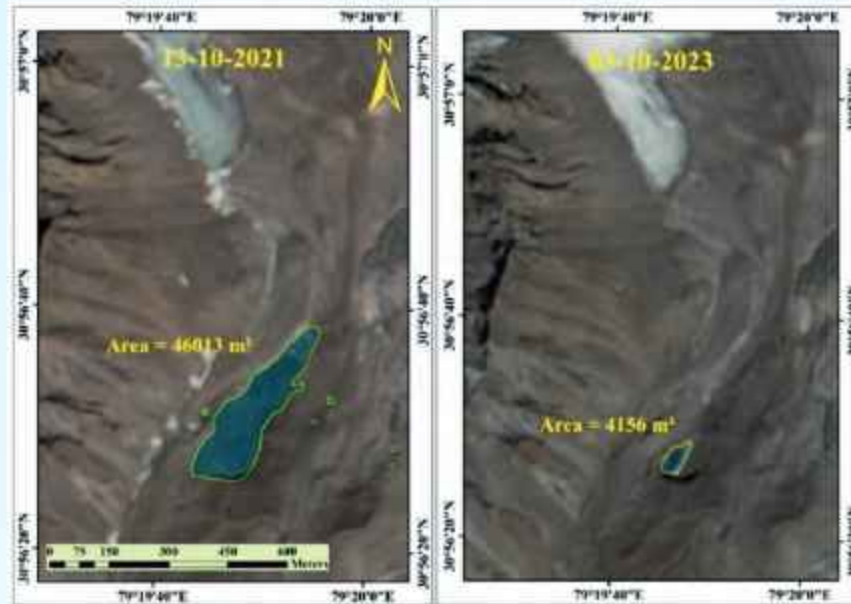
Fig. 60: Comparative satellite images of an unnamed glacier lake in the Uttarakhand on 13-10-2021 (left) and 03-10-2023 (right), illustrating a significant reduction in the lake's area. In 2021, the lake had an area of 46013 ± 3037 m², which dramatically decreased to 4156 ± 274 m² by 2023 (a reduction of ~91%). This drastic shrinkage reflects the dynamic nature of glacier environments and highlights the ongoing impacts of climate change, potentially including GLOF events or other geomorphological process.
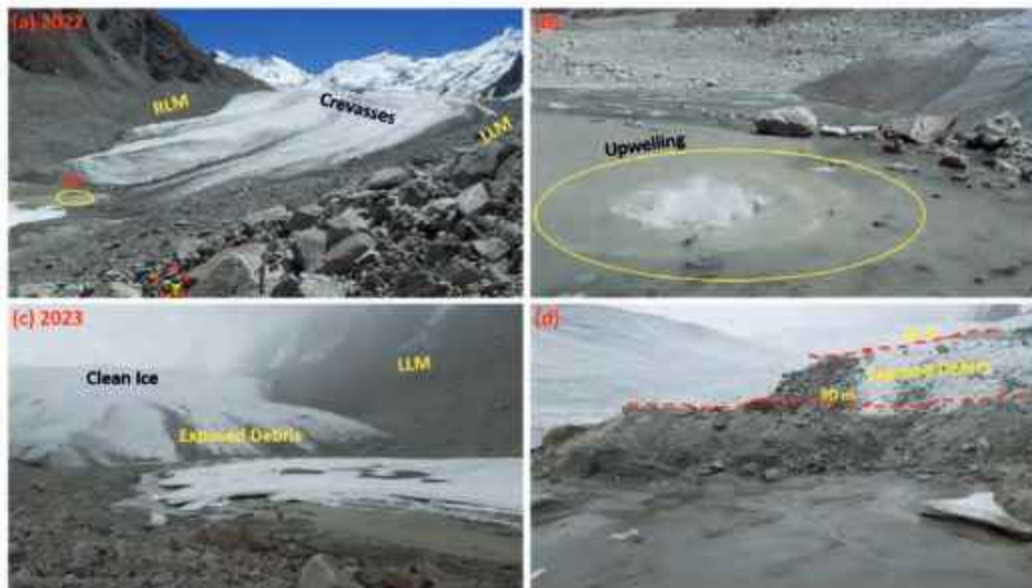
Fig. 61: Field photograph showing the upwelling of geothermal spring near the terminus of the Changmolung Glacier (a-b). A large debris-covered area was exposed in 2023, with varying thickness (2-60 cm). The dashed red line represents the central width of exposed debris (c-d).

(5063–5200 m, asl), extending up to geothermal spring-affected areas, using the direct glaciological method. Two stakes were placed on clean ice near the lateral moraines, and two in the debris-covered central zone. During the August 2023 survey, exposed stake heights indicated maximum surface melting (~390 cm) along the geothermal spring line, while lower melting (~190 cm) was observed near the lateral moraines. Geothermal melting exposed debris layers 2–60cm thick, contrasting with clean, unaffected ice on the glacier flanks (Fig. 61). This uneven melt pattern has altered glacier morphology, producing an undulating surface in the lowest ablation zone. This study emphasizes the influence of geothermal activity on glacial dynamics,

RESEARCH ACTIVITIES

highlighting the crucial need to integrate geothermal assessments into future glaciological research to better understand the heterogeneity in glacier response in the Karakoram.

Snow cover analysis (SCA) using NDSI and SWI indices in Pindari-Kafni Glacier Valley's, Kumaon Himalaya

This study analyzed seasonal SCA dynamics in the Pindari and the Kafni Glacier Valleys (Kumaon Himalaya) using Landsat satellite images during the winter accumulation period for the last two decades (2008–2009, 2015–2016, and 2021–2022). We employed the Normalized Difference Snow Index (NDSI) and the recently developed Snow Water Index (SWI) to delineate and compare SCA across these adjacent basins. Validation against MODIS data, high-resolution Google Earth imagery, and field observations yielded accuracies exceeding 70% and 72% for both
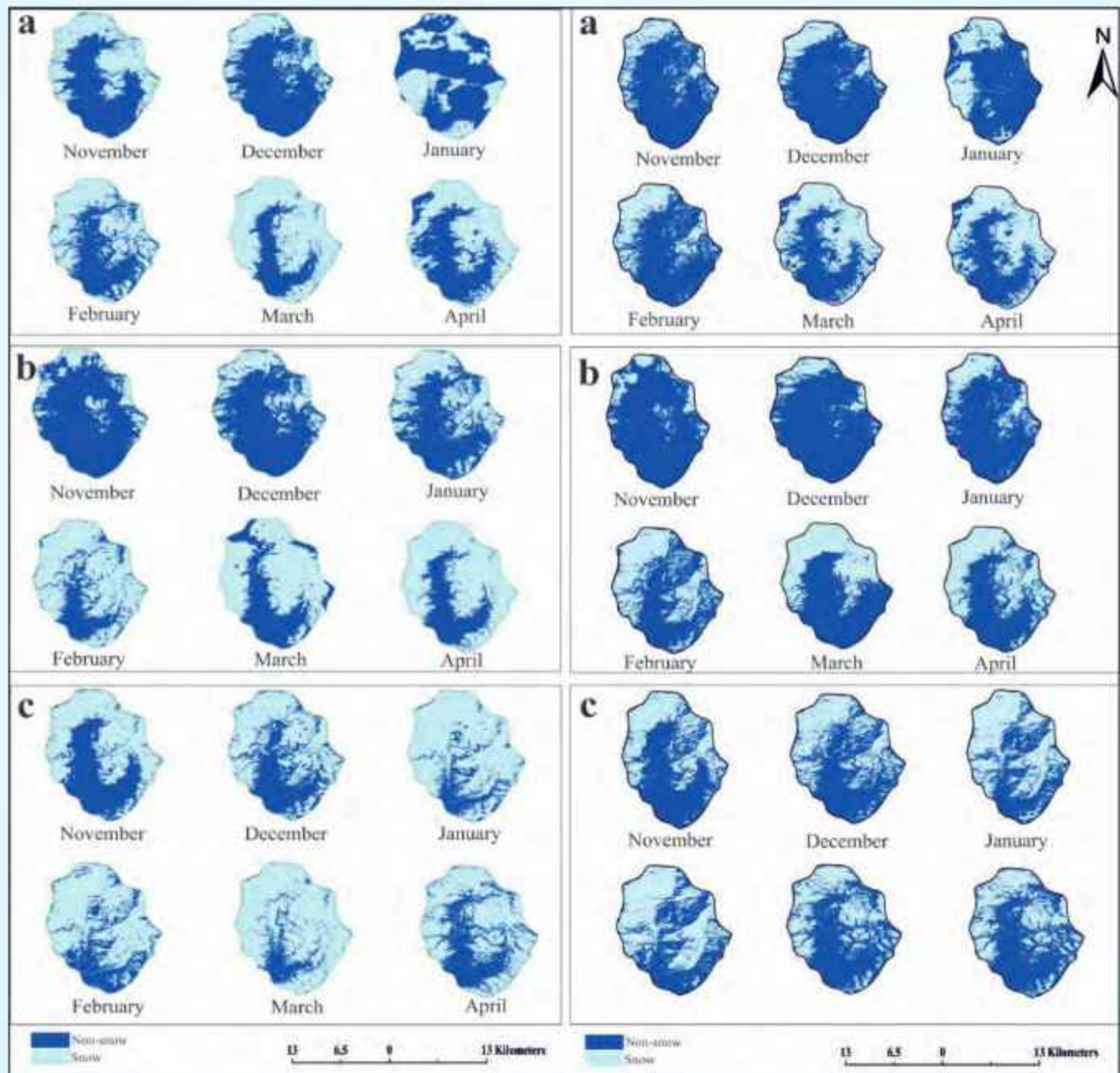
Fig. 62: Classified NDSI from Landsat-5 & Landsat-8 (FCC) satellite images of the accumulation period for the years (a) 2008-2009; (b) Year 2015-2016; (c) Year 2021-2022. The left panel (a-c) shows the snow cover area computed using NDSI, and the right denoted SWI results.

RESEARCH ACTIVITIES

NDSI and SWI indices, respectively (Fig. 62). Our results indicate an overall increase in SCA, consistent with snow mass trends observed in neighbouring regions of the Indian and Nepal Himalaya. Specifically, year-wise SCA exhibited an increasing trend: 461.17 km² (2008-09), 491.87 km² (2015-16), and 601.01 km² (2021-22). NDSI and SWI analyses revealed minimum SCA in December and maximum SCA in April, with a remarkable exception of 2021-2022, which showed minimum SCA (87.09 km²) in April and maximum SCA (123.3 km²) in January. These findings underscore an increasing sensitivity of SCA to climate warming in recent years, leading to rapid snow melt. While our results suggest a subtle increasing trend in SCA, a highly possible shift in water phenology, and the trend may not compensate for the increasing water demand, particularly during the lean melt season, deserves further investigation.

SCA trend analysis using Normalised Difference Snow Index (NDSI)

The analysis of NDSI in 2015-16 revealed that the minimum (25.62 Km²) and maximum (128.55 Km²)
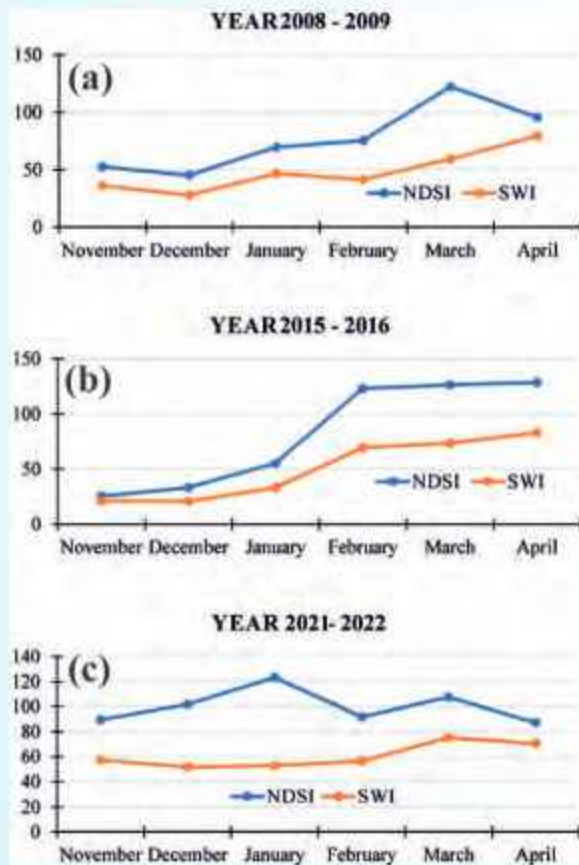
Fig. 63: SCA change in the accumulation period. (a) 2008-2009; (b) 2015-2016; (c) 2021-2022.
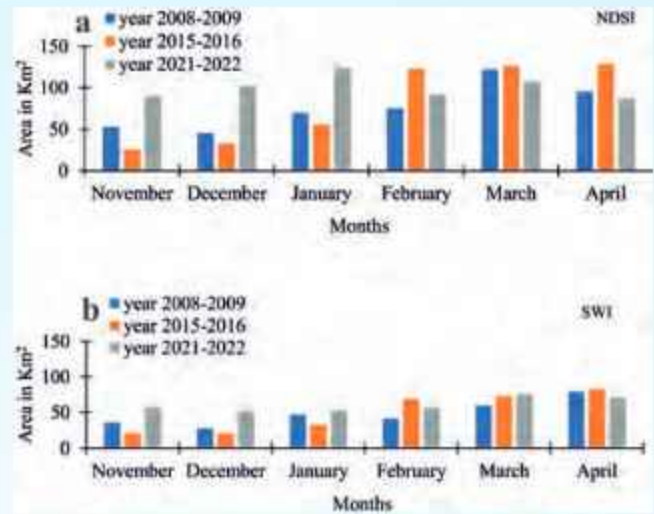
Fig. 64: The snow cover area using NDSI (a) and SWI (b) for 2008-09 to 2021-22.
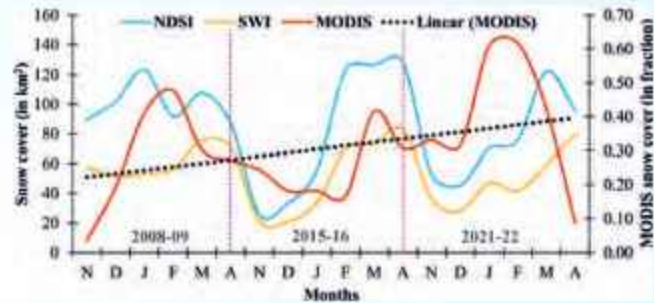
Fig. 65: The accumulated SCA trend correlation with MODIS modelled data shows a good correlation and an increasing trend of the quantified SCA from NDSI and SWI.

SCA were in November and April 2015-16, respectively. There was a total difference of 491.71 Km² of snow coverage area between the onset and end of the accumulation period. However, in 2021-22, the minimum (87.09 Km²) SCA was recorded in April and the maximum (123.3 Km²) in January. These findings align with previous studies over the Himalaya, showing peak snow accumulation between January and February. We also noticed an increasing seasonal trend during the study period 2008-09, 2015-16, and 2021-22, as (461.17 km²), (491.87 km²), (601.01 km²), respectively. The seasonal sum of SCA during 2021-22 was higher (601.01 Km²) than the previous period; the detailed illustration is presented (Figs. 63-65). Our findings were consistent with other recent studies conducted in the Himalayan region, suggesting that localized SCA increases are caused by changing precipitation patterns in specific areas. In contrast, few have reported that the diminishing SCA trend is due to warmer temperatures, confirming that local climate

RESEARCH ACTIVITIES

RESEARCH ACTIVITIES

variation is essential in moderating snow accumulation. Further, the difficulty originated due to snow mixing with shadow, cloud, debris, vegetation, and others, frequently affecting snow cover mapping over areas of rocky terrain with highly changeable physical and atmospheric circumstances. As a result, a competent technique unaffected by the challenges presented by land cover variables is required.

SCA analysis through Snow Water Index (SWI)

The study compares the SWI for the first time in the Pindari-Kafni region. In this study, the SWI was used to estimate the area of snow cover regions for three different time intervals: 2008-09, 2014-15, and 2018-19. We used the SWI method for the seasonal SCA change from November to December and January to April. The period 2008-09 depicted the maximum SCA in April (79.41 km^2). The total SCA was reported as 291.34 km^2, followed by the minimum coverage (27.96 km^2) in December. An almost similar seasonal change was observed during 2015-16, with a minimum SCA (20.74 km^2) in December and a maximum (83.13 km^2) in April. The total SCA during the period 2015-16 was 301.23 km^2. Further, 2021-22 showed the minimum SCA in December as 51.73 km^2, while the maximum SCA was 75.33 Km^2 in March, with a total snow area of 364.05 km^2. We have observed that the estimation of SCA was seen to be increased from 2008-09 to 2021-22 using the SWI method. Because SWI can remove the influence of prominent neighbourhood classes, including cloud, soil, plant, and water, this index provides a more complex process of removing the influence of nearby water pixels.

An increasing seasonal trend was observed from 2008-09 to 2021-22, similar to the trend in NDSI usage. A graphical comparison of the result data indicates a huge difference in the month (January 2009; January and November 2016; February 2022) with reference to clouds (Fig. 61). Figure 62 shows the year and month-wise SCA pattern compared to NDSI and SWI for the years 2008-09 (Fig. 63a), 2015-16 (Fig. 63b), and 2021-22(Fig. 63c). Additionally, Figure 64 shows the snow cover area (Km^2) for 2008-2009, 2015-2016, and 2021-2022 using NDSI and SWI indices.

MODIS-modelled snow cover (fraction) data were used to understand the annual and inter-annual trends and patterns of the NDSI and SWI. The trend line shows a good correlation between MODIS data and quantified SCA from NDSI and SWI. The MODIS linearity illustrated the increasing trend of the snow cover during the study period. The overall month and year-wise SCA trend can be seen in figure 62. Based on the study, the SWI-based approach may be helpful for long-term snow cover monitoring, advancing knowledge of glacier mass balance, hydrological processes driven by snowmelt, and the effects of climate change. Improved remote sensing methods are helpful for cryospheric research, and certain SCA variations are significant for hydrological modelling since they can affect regional water supply (Figs. 64 and 65).

Integrated impacts of climate change and anthropogenic activities on glaciers: a case study of the Byans Valley, Kumaon Himalaya, Uttarakhand

Climate change poses a significant threat to the local communities of the Higher Himalayan regions. These impacts include food security, water availability, natural hazards, agriculture, and livelihoods. Tourism, which has become the backbone of the economy, has also affected these regions environment, livelihoods, culture, and food habits. The present study explores the effects of climate change on glaciers and lakes. Also, the perceptions of local communities about climate change and their impacts on their lives and environment in the Byans Valley of the Kumaon region, Uttarakhand (Fig. 66). The Primary data analysis (questionnaires) are based on approximately 110 household's interviews regarding the community's perspective of climatic and cryosphere variability (Fig. 67). We discovered that a large majority of respondents believe that summer and winter temperatures are rising, and snowfall has decreased during the last 10 years. The climatic data also reflect rising temperatures and decreasing precipitation, which is consistent with most respondents. Highlighting these changes is the first step in reducing the mounting pressure on climate-sensitive high-latitude valleys that are historically and culturally important.

The findings show a general agreement between the scientific observations of climate change and the opinions of the local people. The knowledge of public opinion can also assist policymakers and decision-makers in creating policies that effectively address climate change as well as local adaptation measures. One of the most attractive tourist destinations are the glaciers. Since they are the most delicate specific tourism resources, their development needs additional focus. The development of the area is significantly influenced by tourism and location. The management and observation of the environment in the tourist's area are essential. This is the only way to eventually grow glacier tourism sustainably.
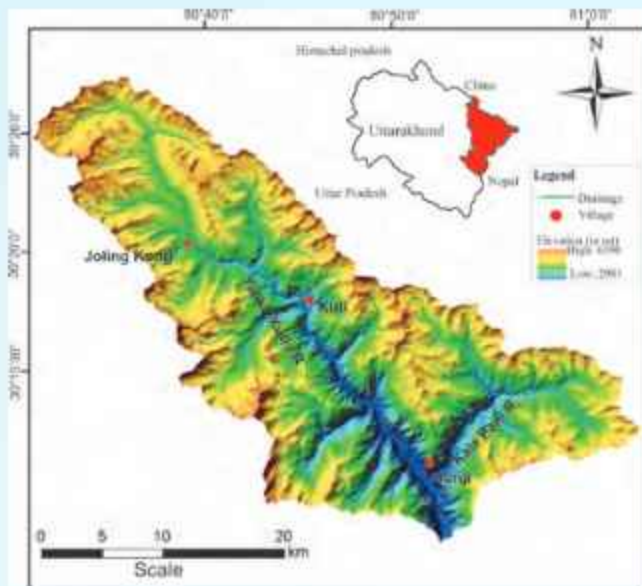
Fig. 66: Location map of the study area.

Fig. 67: Flow chart of the methodology undertaken during the present study.

The emphasis should be put on the following:

- Regulation of travel and vehicular movement and support and promotion of environmentally friendly planned infrastructure development.

- To maintain a suitable distance between glaciers and visitors.

- To create tourism activities that cause the least amount of environmental harm.

- To increase the climate change awareness in the villages and through an outreach program.

With a responsible tourism system, stakeholders can effectively handle the challenge, internalize sustainable development goals, and collaborate to fulfil the public duty of achieving sustainable development of tourist destinations without affecting the environment, especially the cryosphere.

Glacier changes and fragmentation in Birahi Ganga Basin, Garhwal Himalaya: Implications for water resources

Glacier changes in the Himalaya are unequivocal under a changing climate, making them susceptible to water availability in the future. Given the significance of glaciers for hydrology and the dangers they pose, the current study examines the state of the Birahi Glacier in the Birahi Ganga Catchment (BGC), Alaknanda Basin, Uttarakhand, from 1968 to 2020 (Fig. 68). From 1968 to 2020, the glacier retreated by 329 ± 15 m, averaging a rate of 6.3 ± 0.3 m per year, and vacated an area of approximately 5000 m^2 annually. Based on satellite images, glacier separation began in 1994, as demonstrated by the small patches exposing the bedrock. It eventually grew and detached the lower debris cover zone from the upper clean ice zone in 2019. The recent satellite image reveals snow and ice avalanches occasionally feed the lower, disconnected debris-covered portion. The lower zone with an area of 0.59 ± 0.03 km^2 behaves differently than the rest of the 3.6 ± 0.06 km^2 clean glacier zone. Glacier detachment is influenced by topography, steep slopes along its central flow line, rising snowlines, and increased melting in the transition between debris-covered ice and clean ice. During the period between 1994 and 2020, the glacier shows pronounced shifting of snout elevation from ~3910 to ~4000 m asl (~90 m; 2.8 m a^{-1}) and snowline
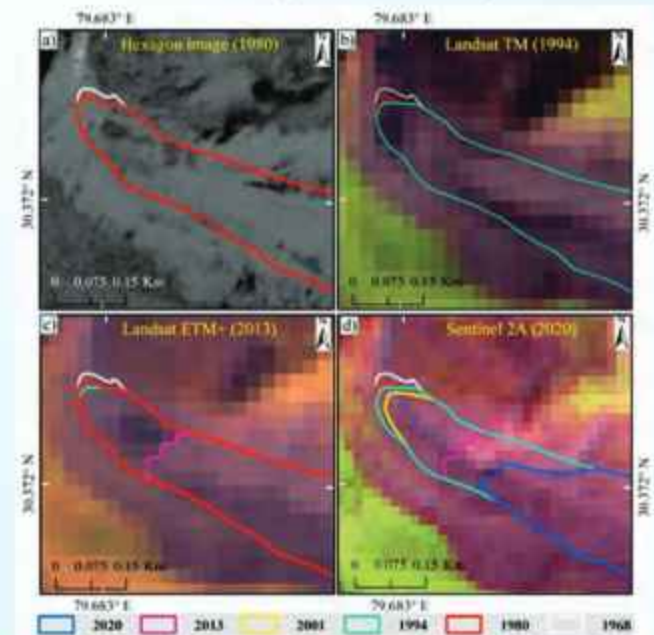
Fig. 68: Changes in the Birahi Glacier from 1968 to 2020. (a) Hexagon (1980), (b) Landsat-5 TM, (c) Landsat-8 OLI, and (d) Sentinel-2A (2020) images are in the background with FCC.

RESEARCH ACTIVITIES

from 5143 to 5335 m asl (192 ± 17 m; 7.3 ± 0.65 ma^{-1}). Deglaciation in BGC may pose an alarming situation for water availability downstream for drinking, agriculture, and hydroelectric power projects in the future (Fig. 69).
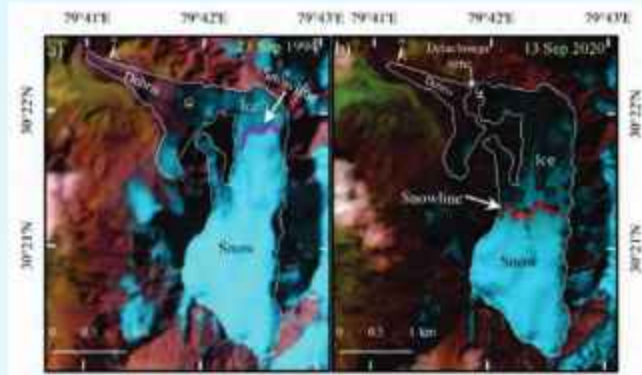
Fig. 69: Snowline altitudes (SLA) of the Birahi Glacier during September, 1994 (a), and 2020 (b).

Anticipating the impact of glaciers, landslides and extreme weather events on vulnerable hydropower projects and the development of an integrated multi-hazard warning system (IMWS)

The Himalayan river basins offer great potential for hydropower development, but they are also vulnerable to various hazards such as debris flows, landslides, avalanches, glacial lake outburst floods (GLOFs) and landslide lake outburst floods (LLOFs) (Fig. 70). Despite these hazards' regional and global significance, there is a lack of information and data on different aspects, including their meteorology, hydrology, geology, and seismology. Many hazards often go unnoticed or receive little attention until they start affecting humans and their activities, like damage to buildings, infrastructure, and other human-made structures. It is important to recognize that hazards can have severe and long-lasting impacts on society, even when they do not directly affect humans. Flash floods can disrupt ecosystems, destroy habitats, and threaten
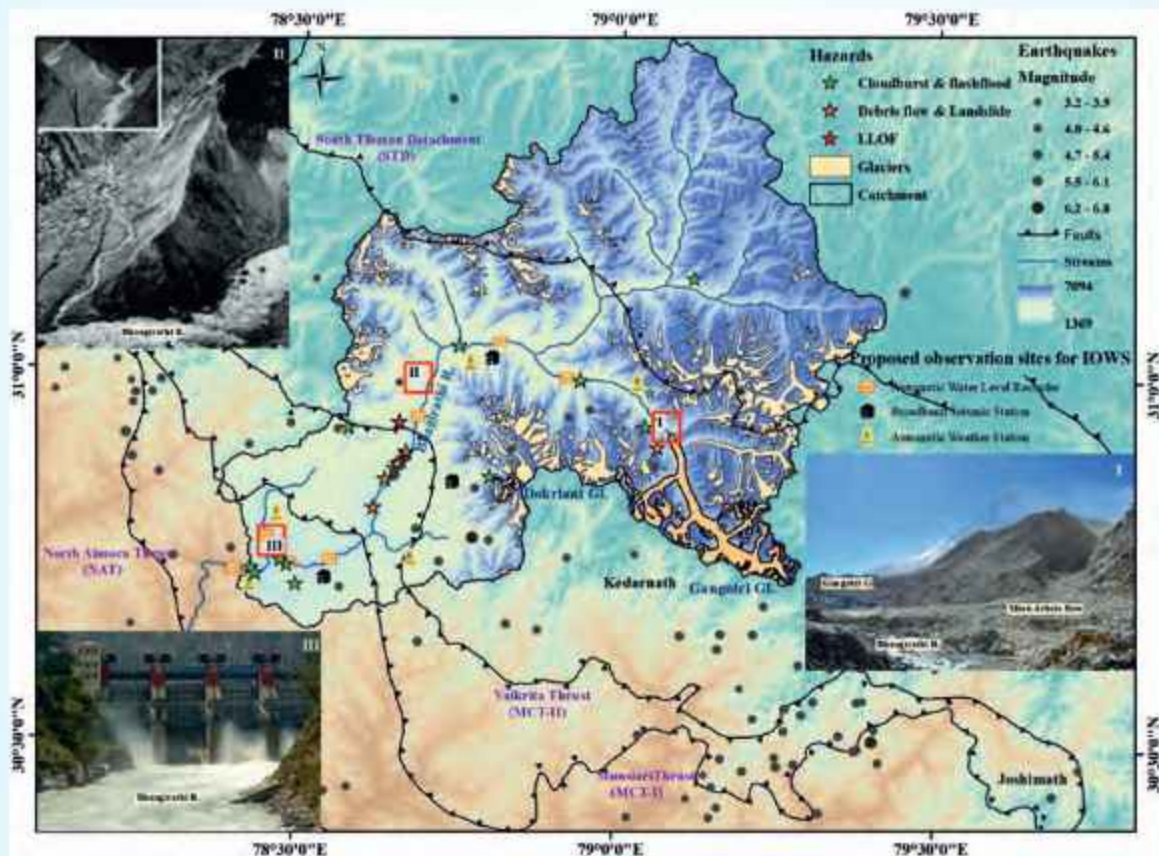
Fig. 70: Distribution of glaciers and major hazards like cloudbursts, debris flow, flash-floods, landslide lake outburst floods (LLOF), landslides in the basin and earthquakes associated with major tectonic boundaries around nearby. Locations of major extreme events in the basin including (I) debris flow (moraine failure) near the snout of Gangotri Glacier, (II) cloudburst followed by a landslide and LLOF at Kanodia gad and (III) cloudburst in the Assi Ganga River.
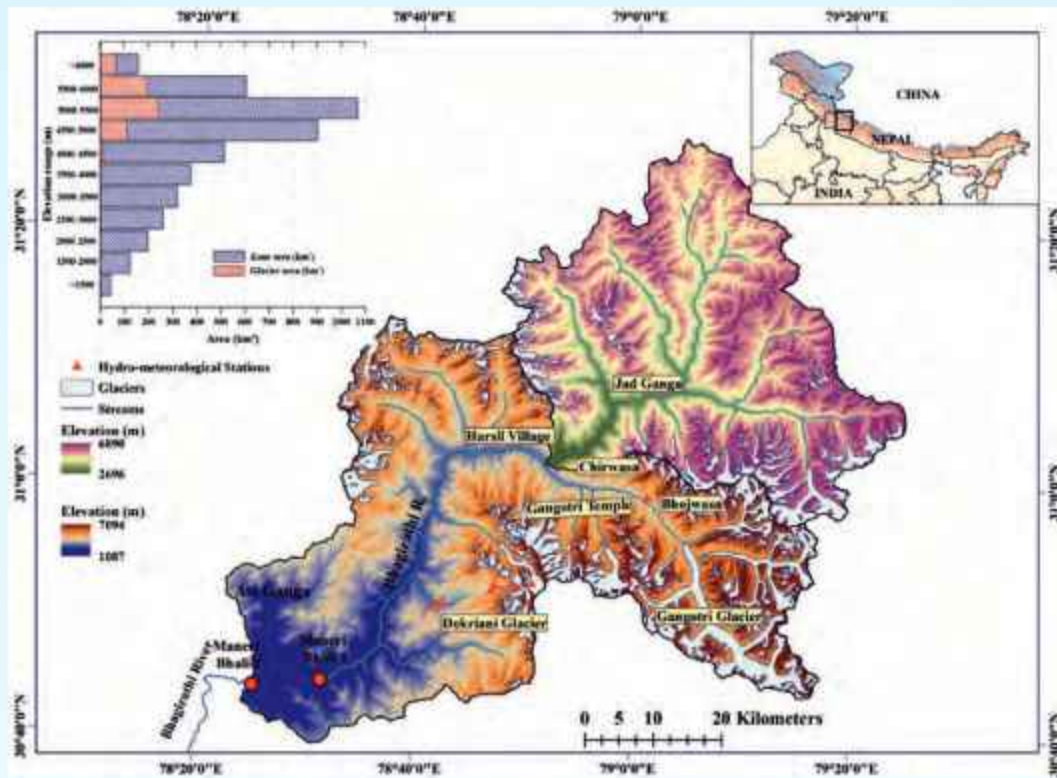
Fig. 71: Digital Elevation Model (DEM) of the Bhagirathi basin up to Maneri Bhali II dam site with Jad Ganga sub-basin showing the distribution of glaciers, major tributaries, locations, and photographs of existing hydro-meteorological stations. Area-elevation information for the glaciers and the basin in the inset.

biodiversity. It is crucial to consider the complex climatic influences on both regional and local scales. Therefore, we emphasize the importance of continuous long-term monitoring across entire river basins in the Himalayas. For this purpose, we selected the Bhagirathi basin, extending up to Maneri-Bhali, for detailed investigation. The total catchment area of the basin up to the Maneri Bhali–II HEP is about 4557 km², with a total of 403 glaciers, covering an area of 625.5 km². The minimum and maximum elevations of the basin vary from 1100 to 7100 m, asl, respectively. The hypsometry (area-elevation curve) shows that the maximum basin and glacier area lies between 5000 to 5500 m, asl (Fig. 71). Followed by 4500 to 5000 m and 5500 to 6000 m for the basin and glaciers, respectively (Fig. 71). The study recommends that the highest hydropower in the glacierized basin should have its network of hydro-meteorological observatories at different altitudes, providing real-time data transmission and deploying a multi-hazard warning system (IMWS) for flash floods.

Seismic and Radon signatures: A multiparametric approach to monitor surface dynamics of a hazardous 2021 rock–ice avalanche, Chamoli Himalaya

Observing precursory signals of the 2021 Chamoli rock–ice avalanche provides an opportunity to investigate the multidisciplinary analysis approach of rock failure. On 7 February 2021, a huge rock–ice mass detached from the Raunthi peak at Chamoli district in Uttarakhand, India. The tragic catastrophe resulted in more than 200 deaths and significant economic losses. Here, we analyse radon concentration and seismic signals to characterise the potential precursory anomalies prior to the detachment. Continuous peaks of radon anomalies were observed from the afternoon of 5 to 7 February and decreased suddenly after the event, while a cumulative number of seismic tremors and amplitude variations are more intensified ~2.30 h before the main event, indicating a static to dynamic phase change within the weak zone (Fig. 72). This study characterises abnormal signals and models the rock failure mechanisms. The analysis unveils three time-dependent nucleation phases, physical mechanisms of

RESEARCH ACTIVITIES
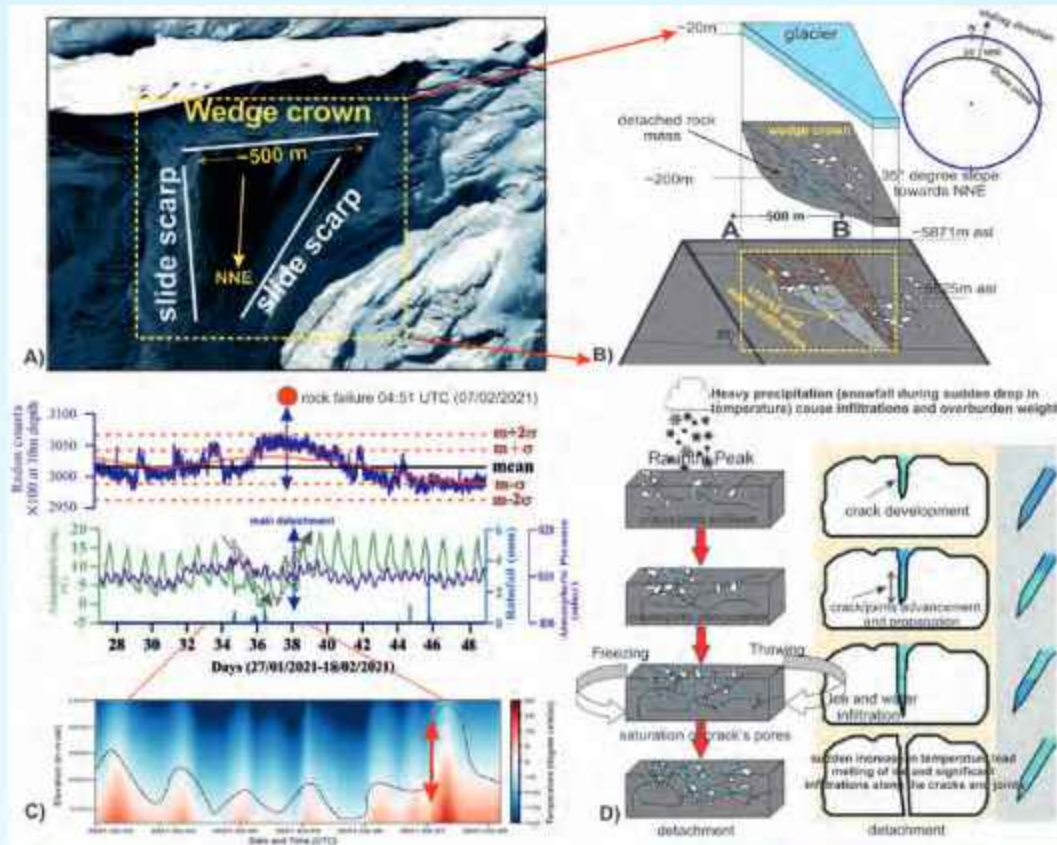
Fig. 72: A schematic physical model explains the radon and temperature variability along with the physical changes in the source zone. (a) Figure shows satellite image of source zone, (b) geometry of detached wedge, (c) observed geophysical parameters and (d) physical changes that affected rock dynamics during precursory signals generation.

signal generation, and a complete scenario of physical factors that affect the degree of criticality of slope failure. The results of this study suggest a gradual progression of rock cracks/joints, subsequent material creep and slip advancement acceleration preceded the final failure. Furthermore, the study highlights the importance of an early warning system to mitigate the impact of events like the 2021 Chamoli rock–ice avalanche.

Quantification of post-monsoon CO_2 degassing flux from the headwaters of the Ganga River: emphasis on weathering pattern of the basin

Research on the carbon-cycling process in high-altitude streams is crucial for understanding whether carbon acts as a source or sink for the atmosphere during global climate change. In this study, we have quantified the post-monsoon CO_2 flux (FCO_2) from the Bhagirathi and Alaknanda rivers, with the help of analytical hydrochemistry and PHREEQC software (version 3.7.3). Our results show that FCO_2 values of 88 $gCO_2m^{-2}d^{-1}$ and 175 $gCO_2m^{-2}d^{-1}$ from the upstream of the Bhagirathi and

Alaknanda Rivers, respectively, which is significantly greater than the fluxes observed in the downstream (18 $gCO_2m^{-2}d^{-1}$ and 4.1 $gCO_2m^{-2}d^{-1}$, respectively). This difference in FCO_2 is attributed to the major variation in gas transfer velocity (kCO_2) along elevation, with the upstream section exhibiting approximately eight times higher kCO_2 than the downstream. The steeper bed slope increases turbulence and energy dissipation at higher altitudes, enhancing the kCO_2 values. The partial pressure of CO_2 in the rivers was approximately 2.5 times greater than that of the atmosphere. Our findings suggest that form-drag turbulence, instead of bed friction, prevalent in the high-gradient reaches of the rivers, is the main driver of CO_2 degassing into the atmosphere. This study shows that Ganga headwater streams are sources of CO_2 in the atmosphere and underscores the need to monitor other Himalayan streams for CO_2 flux (Fig. 73).

Mountain-building processes release more CO_2 than they absorb (Liu et al., 2023; Bufe et al., 2021; Torres et al., 2016; Zhang et al., 2009), highlighting the
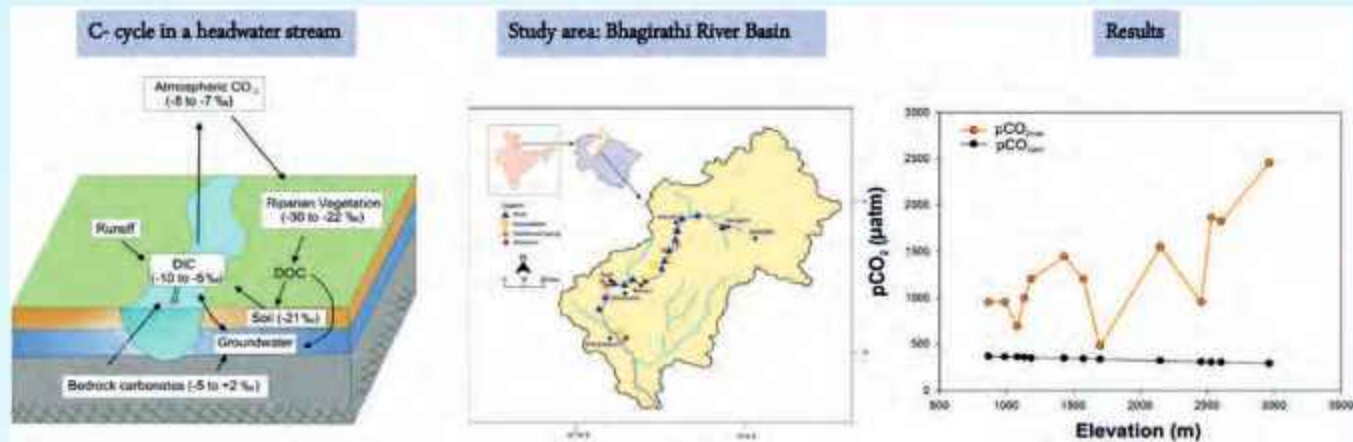
Fig. 73: Graphical abstract of the research (Methodology>Implementation>Findings).

need to study the carbon cycle in mountain streams. Globally, high-altitude streams often show elevated pCO_2 levels compared to the atmosphere (Clow et al., 2021; Horgby et al., 2019; Marx et al., 2017; McDowell & Johnson, 2018; Natchimuthu et al., 2017; Rocher-Ros et al., 2019). While CO_2 flux (FCO_2) in rivers has been widely studied (Cole et al., 2007; Lauerwald et al., 2015; Liu et al., 2022; Raymond et al., 2013; Sawakuchi et al., 2017), headwater streams remain underexplored due to challenges in estimating gas transfer velocity (kCO_2) using floating chambers or tracers (Alin et al., 2011; Natchimuthu et al., 2017). Existing equations (Alin et al., 2011; Raymond et al., 2012) are not ideal for high-altitude streams, though Ulseth et al. (2019) proposed improved models based on global data. pCO_2 can be measured with sensors or estimated using software like PHREEQC or CO_2SYS (Li et al., 2012, 2013; Lauerwald et al., 2015; Upadhyay et al., 2024). In the Ganga River system, few studies have focused on CO_2 dynamics in the Upper Ganga Basin (UGB). Research by Manaka et al. (2018), Nayna et al. (2022), and Upadhyay et al. (2024) provided CO_2 flux estimates for larger river sections, relying on equations from Alin et al. (2011) and Raymond et al. (2012), though often with limited spatial resolution. This study analyzes hydrochemistry and CO_2 degassing in the Bhagirathi and Alaknanda Rivers in the Garhwal Himalaya. While previous research has examined water chemistry (e.g., Kumar et al., 2009; Singh et al., 2014), comprehensive assessments that include groundwater are lacking. Geothermal springs suggest high CO_2 emissions (GSI, 2000; Tiwari et al., 2016, 2020), but riverine carbon dynamics remain uncertain. Using PHREEQC, we estimate that post-monsoon river pCO_2 is approximately 2.5 times higher than atmospheric levels. The CO_2 fluxes from the upstream Alaknanda and the

Bhagirathi Rivers are 88 $gCO_2 m^{-2} d^{-1}$ and 175 $gCO_2 m^{-2} d^{-1}$, respectively, which are much higher than the downstream values. This gradient is driven by higher kCO_2 in the steep upstream sections (123 vs. 16 $m\,d^{-1}$), likely due to turbulence created by large roughness elements. Our findings highlight the significance of small Himalayan catchments in regional CO_2 emissions. Limitations of this study include indirect estimation of pCO_2 and kCO_2, as well as assumptions regarding carbonate alkalinity. Future research should focus on direct measurements and assess the contributions of soil organic carbon to refine flux estimates.

Activity: 6B

Hydrogeology-Himalayan Fluvial System & Groundwater

(Santosh Kumar Rai and Rouf Ahmad Shah)

Geohydrology and chemometric appraisal of karst and fissured springs in the Lesser Himalaya

Ascertaining the geohydrology and chemometrics of springs in hilly areas with limited hand pump access is essential for protecting and sustainably managing groundwater from mountain aquifers. Towards this, first and detailed insights into the geohydrology, elemental sources, and quality characteristics of karst and fissured springs in a previously understudied region (Chakrata) of the Lesser Himalaya, India were provided. The study indicates that the Deoban and Chakrata rock formations, covering 285 km^2 and 208 km^2 respectively, are the primary hydrogeological units with moderate to high yields, in which karstification and fracturing greatly regulate the flow patterns and spring distribution (Fig. 74a). The electric resistivity tomography (ERT) model shows two main resistive zones: a lower zone (10-200 $\Omega.m$) at 10-20m depth, associated with thick saturated soil and weathered

<div style="text-align:right">RESEARCH ACTIVITIES</div>
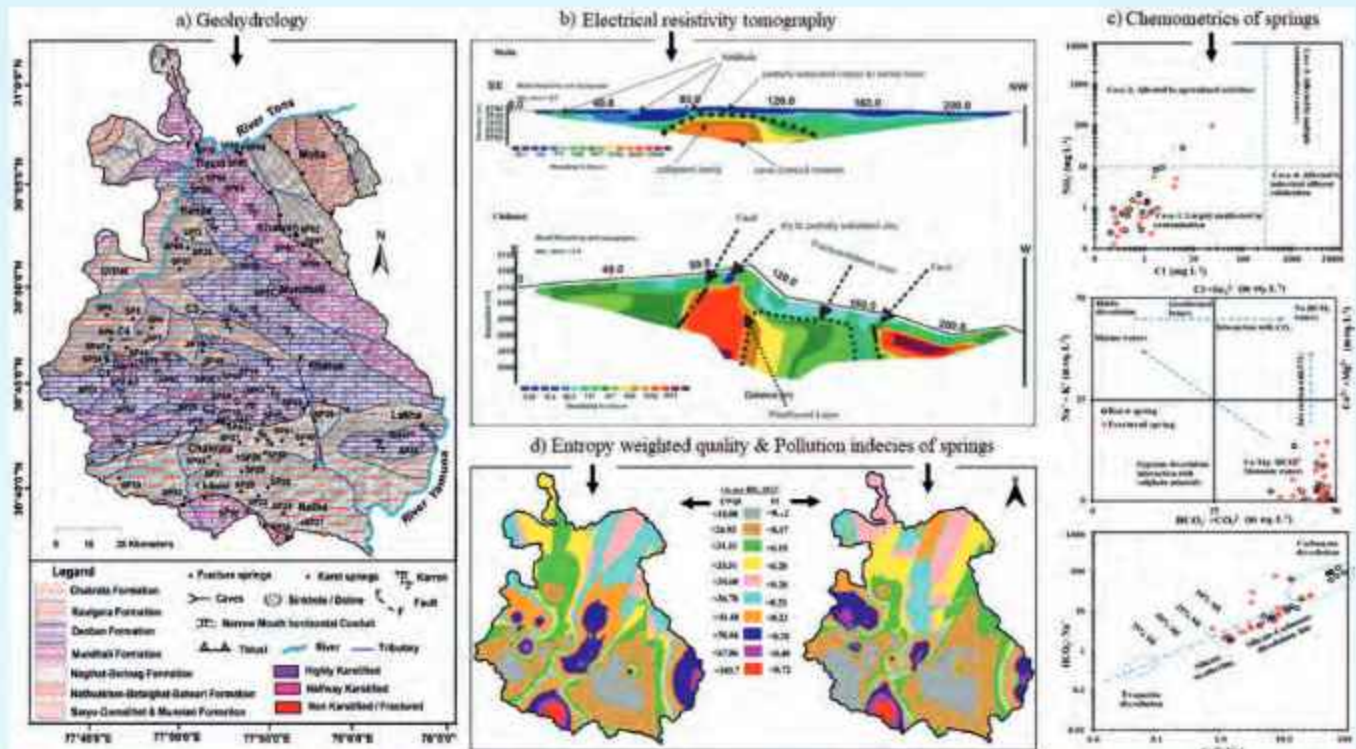
Fig. 74: (a) Map of the study region depicting the geohydrological information, (b) Scatter plots depicting geogenic and anthropogenic source mechanism and major geochemical processes occurring along flowpaths, (c) Subsurface resistivity distribution beneath the Moila and the Chilmiri ERT sections, (d) Springs water quality status based on the EWQI and PI of monitored karst and fissured springs.

materials or hydraulic impedance, and a higher localized zone (1000 Ω.m to 50,000 Ω.m) at 20-50m depth, which is an indicative of high transmissivity network including voids, conduits, caves, mostly air filled or dry (Fig. 74b). Chemometric analysis suggests that spring are alkaline (pH: 7.8 to 9.4), low to moderately mineralized (TDS: 10 to 317 mg L^{-1}) and their ionic composition regulated by multiple geogenic dissolution processes, classifying them as Ca-HCO$_3$ and Ca-Mg-HCO$_3$ facies (Fig. 74c). Further, karst springs are mostly carbonate oversaturated and fissures springs are mostly under-saturated; however, both attain higher pCO$_2$ (2×10^{-3} to 8.9×10^{-3} atm.), suggesting active dissolution–precipitation processes along the flow paths. The findings reveal that springs have excellent water quality, with entropy water quality indices and pollution indices well within safe thresholds for human consumption (Fig. 74d); however, positive correlation of cropland with NO$_3^-$ (R^2: 0.68) and Cl$^-$ (R^2: 0.63) in some springs in the south-eastern and south-western parts is a matter of concern. The study recommends that since groundwater is critically connected to achieving sustainable development goals (SDG$_s$), particularly SDG-06 (safe water and sanitation) and SDG-13

(climate action), a sustainable effort by involving local communities in implementing sustainable land management practices in springsheds and /or recharge catchments can truly contribute to safeguarding the groundwater systems in this hilly tribal region.

Decoding the climate-tectonic control on sediment source budget of the Teesta River Basin

Erosion of the Himalaya mountain and subsequent deposition of sediments in the flood plains, and distal fans are primarily regulated by tectonics, climates, lithology, and regional relief. These eroded sediments preserve their chemical and isotopic compositions in their depositional archive, which can be used to trace the erosion processes and to assess the relative role of controlling factors. The present study has analysed the ^{87}Sr/^{86}Sr and ε_{Nd} in the silicate phase of sediment recovered from a ~ 40 m long sedimentary core representing ~8 ky of sediment accumulation in the Teesta River mega fan (Fig. 75). The lithostratigraphy of the core indicates a rapid aggradational nature of the Teesta mega fan. The ^{87}Sr/^{86}Sr and ε_{Nd} display wide variability with depth, which ranges from 0.75700 to 0.89294 and − 15.1 to −25.0, respectively. The observed ^{87}Sr/^{86}Sr and ε_{Nd} values in the core sediments

Fig. 75: Geological and drainage map of the Teesta basin along with the location of the sedimentary core Position of Rangeet window is marked by the area within the black dashed line.

have been interpreted in terms of differential sediment contribution from the higher and the lesser Himalayan lithologies. The $^{87}Sr/^{86}Sr$ and ε_{Nd} isotope profiles and estimated fractional sediment contributions identify the Lesser Himalaya as the major sediment contributor to the Teesta basin since the mid-Holocene, unlike the other Himalayan river basins, which are dominated by sediments from the Higher Himalaya after the Last Glacial Maximum. The rapid exhumation and erosion of the tectonically active Rangeet window with the focused precipitation and presence of rock types vulnerable to weathering in the Lesser Himalaya of the basin appear to be the major factors resulting in the sedimentary budget of the Teesta River Basin over at least by last 8 ky. Our assessment suggests that tectonic activity and climate

have a competitive effect on the observed sedimentary budget, with an additional role of lithology.

Activity: 7

Quantification of strain accumulation/release rate along Main Himalayan Thrust (MHT) at different time scales

(R.J. Perumal, P.K.R. Gautam, Rajesh S., Vikas Adlakha, Shubam Bose, Rajeeb Lochan Mishra and Mahesh Kapawar)

Geometry of the MHT, quantification of strain release, and seismic hazard in the Eastern Himalaya

Whether the Main Himalayan Thrust can host a single surface-rupturing event in the Himalaya with a rupture

RESEARCH ACTIVITIES

RESEARCH ACTIVITIES
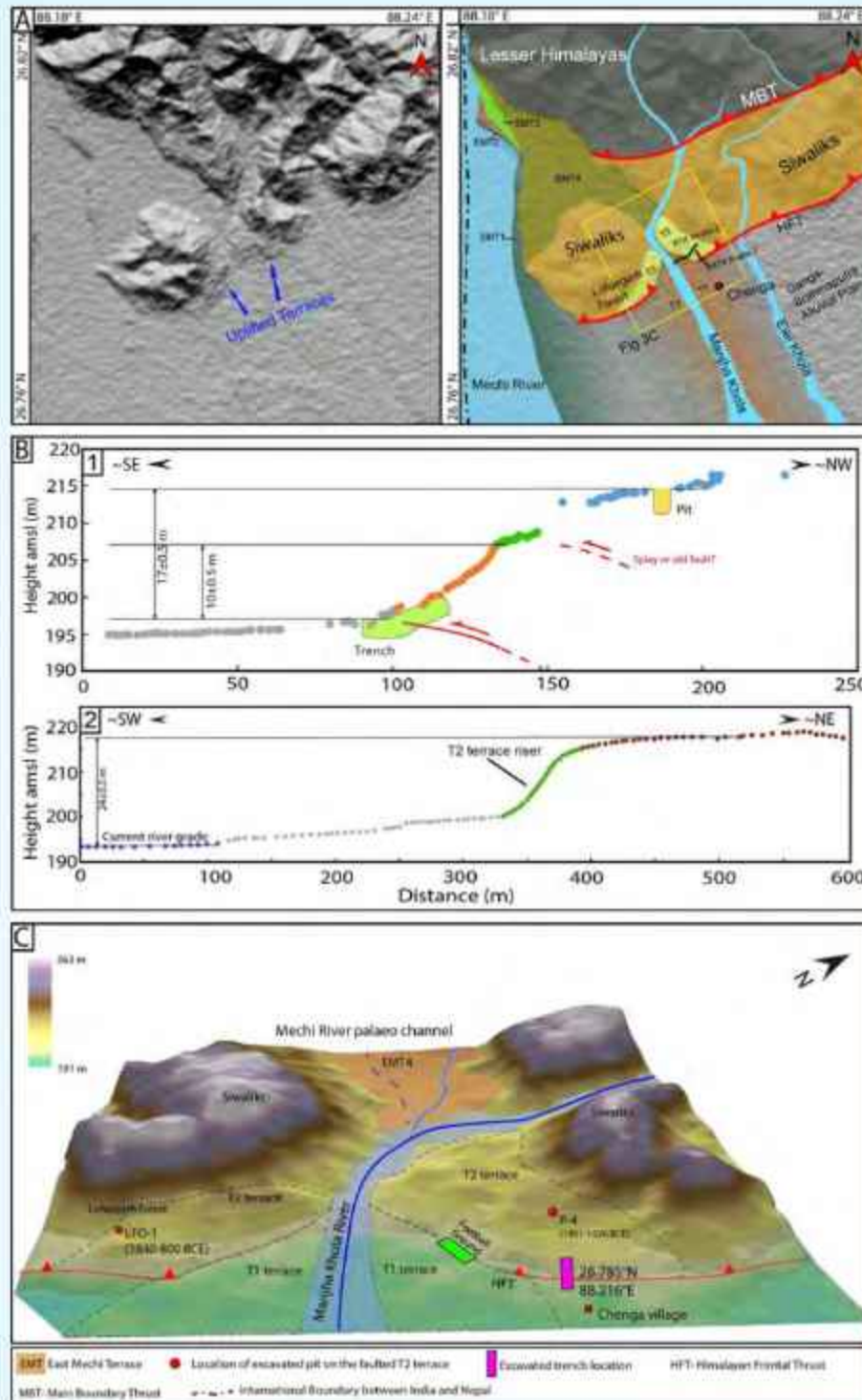
Fig. 76: (A) Study area mapped on 12.5 m resolution ALOS-PALSAR DEM,. Red line: HFT (Himalayan Frontal Thrust). The first image is a raw DEM with uplifted segments and topography; the second is the same region with mapped features. EMT- East Mechi Terrace, LF-Lohargarh Forest. (B1) 10 m and 17 m high scarp profiles extracted from the RTK-GPS survey. Yellow polygon: location of a pit excavated on the hanging wall. (B2) Profile across the terrace riser from the current river grade to the surface of the truncated T2 terrace showing ~24m elevation difference. (C) A geomorphic map of the study area was created using Triangulated Irregular Network method (1.5x) extracted from 12.5m resolution ALOS-PALSAR DEM. Dashed lines mark two levels of terraces along the Manjha Khola River, where T2 terraces are truncated by HFT and T1 terraces are not cut by active fault (Brice et al., 2024).

Fig. 77: The top image is the bird's eye view of the fault scarp with an excavated trench location at the base of the scarp. The photograph was taken using the Ricoh GR digital camera, which was mounted on a DJI Phantom I unmanned aerial vehicle. The bottom left portion shows farmed flatland (footwall), and the top right portion is the uplifted fault scarp (forest and village area) (hanging wall). The bottom image is the view from the ground surface of the trench, carrying out scraping of the walls and collecting charcoal samples.

length of > 700 km remains controversial. Previous paleoseismological studies in the Darjeeling-Sikkim Himalaya (DSH) suggested medieval surface-rupturing earthquakes, correlating them with the eleventh–thirteenth century events from Nepal and Bhutan and extending the coseismic rupture length > 700 km. Conversely, there is no rupture evidence of the 1714 Bhutan and 1934 Bihar–Nepal earthquakes in the DSH, resulting in a discrepancy in the rupture extent of the great earthquakes. Consequently, we conducted a paleoseismological investigation across a ~ 10 m-high fault scarp on the Himalayan Frontal Thrust at Chenga village, DSH, revealing a surface-faulting event during 1313–395 BCE (Figs. 76-79). We suggest that the DSH is a 150 km-long independent segment bounded by a transverse ridge and fault and has a recurrence interval of ~ 949–1963 years, which is significantly larger than Nepal (~ 700–900 years) and the Bhutan Himalaya (~ 339–761 years).

Multidisciplinary approaches have been employed to understand the landforms associated with tectonic deformation, through detailed field investigation supplemented by the geodetic, chronological, and morphometric database in the southernmost extent of the southeast Kumaun Himalaya and western Nepal Himalaya. The velocity data acquired from published literatures (Mondal et al., 2016; Yadav et al., 2021), including our two CORS sites MUNS and PTH2 are transformed into a common reference frame ITRF08. This velocity indicates secular plate motion toward the NE direction with the range of 37.67 to 67.98 mm/yr and direction of motion varies from 28.83° to 52.76°. The velocity fixed with IISC site range from 0.71 to 19.26 mm/yr, is reducing toward the south, which indicates the continuous strain accumulation in the zone of the HFT and the region is being locked gradually. Generally, the Indian plate continues moves northward collide with the Eurasian plate, however velocity concerning the fixed IISC shows the clockwise motion from northwest to the northeast direction reflecting the crustal deformation in the study region. To perceive the behavior of local deformation in the study region, we estimated the velocity by fixed MUNS which is a permanent GNSS station and located in the study region. Here we have also observed the clockwise motion of the velocity field and non-linear pattern of the deformation with the velocity range 0.5 to 14.79 mm/yr. The site located in the core part of Almora Nappe exhibits a higher deformation rate comparatively up to 28.66 mm/yr, which may be the effect of present local active faults/thrusts. Overall our observation through this study is that the Tanakpur and its adjoining area in the NW Himalaya are tectonically active, however such intradisciplinary studies for tectonically active regions are needed for future infrastructure development.

Correlation of geomorphological indices and the inter-seismic geodetic deformation of Siwalik Hills in the Dehradun re-entrant

Apart from geodetic studies on the interseismic deformation of the Siwalik Hills and the adjoining HFT, we also carried out Geomorphological investigations in the study area through the analysis of established geomorphological indices like mountain front sinuosity and the stream-length gradient. The mountain front sinuosity (S_{mf}) is an index that connects the erosional and the tectonic forces. Mountain fronts associated with active faults are considered to have a linear geometry in

Fig. 78: (A) Photomosaic of the trench excavated at the Chenga site (B) Graphic representation of trench with unit description. Red lines: fault splays. (C) Illustrative log displaying the fabric of trench exposures (Brice et al., 2024).

RESEARCH ACTIVITIES
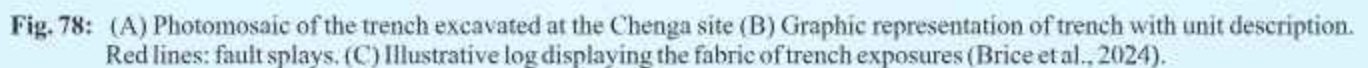
Fig. 79: Space-time correlation with previous studies. The segment between the MSR and DCFZ demarcates the probable break in the Himalayan segment and the rupture extent of the 1255 CE, 1714 CE and 1934 CE events. meisoseismal zones and possible hypocentre location (translucent blue) of great earthquakes in the past millennia dark blue polygons are the inferred rupture area of paleoearthquakes. Locations of previous paleoseismic investigation sites in Nepal, DSH and Bhutan region are allotted different colours that demarcate different segments. The vertical coloured bars are the age range of earthquake events inferred from numerous studies, and the bars with arrow head indicate no lower bound of the inferred earthquake, hence the event occurred post upper bounding age. The horizontal bars are the lateral extent of different paleoearthquake events. The dashed red bar of the penultimate event in DSH region implies a possible rupture beyond the DCFZ barrier. Three horizontal bars at the bottom of the figure with fuzzy (exact termination point unclear) ends represent the probable extent of different segments (Brice et al., 2024).

RESEARCH ACTIVITIES
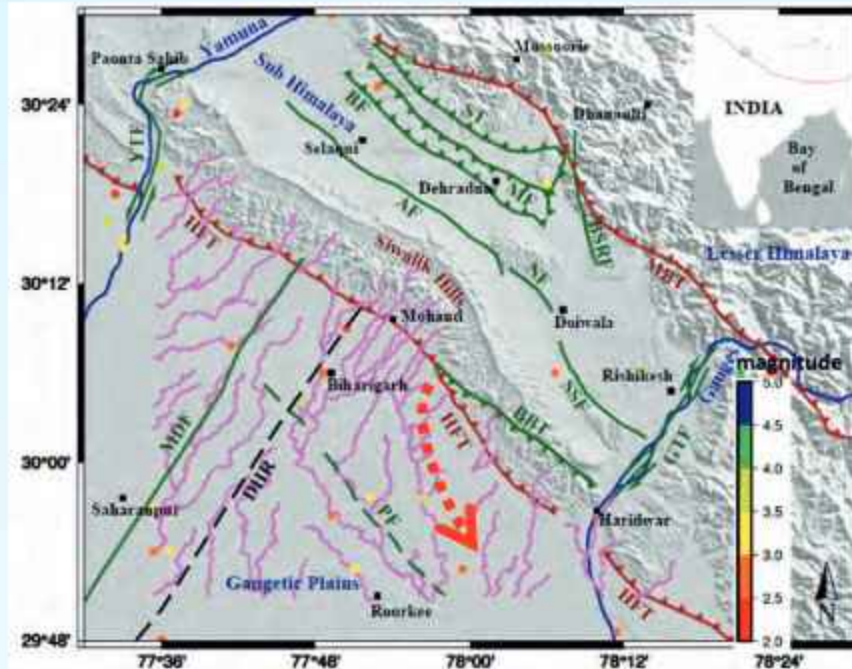
Fig. 80: The southeastward flows of the frontal river streams (red dotted arrow) which abruptly become sub parallel to the Piedmont fault (PF) indicate the corresponding block movement of the frontal shallow crust.

comparison with those bounded with inactive or dormant faults. In the study area, the obtained Smf value is close to 1 (1.25), which implies an active mountain front. So, the calculated mountain front sinuosity index of 1.25 at the foothills of Siwaliks and close to the HFT indicates that the mountain front is straight and active due to the activity of HFT. Further, the stream gradient analysis done along the river profiles crossing across the HFT also show an abrupt change in their flow at the HFT. It is inferred that the Siwalik anticlinal ridge exerts structural control on the south-eastward bounded flow of the streams. The sudden stream deflections causing the flow sub-parallel to the piedmont fault and their linear arrangement suggest that the piedmont fault, which lies south of the HFT is also active and contributes to the regional surface deformation processes (Fig. 80). The underlying cause of the southeastward movement of the river streams is also correlated with the estimated inter-seismic geodetic velocities at the frontal part of the Siwalik Hills within the footwall of HFT. Results show GPS stations south of HFT have predominant south-eastwardly movement of ~ 4 - 5 mm/a parallel to the strike of the HFT. These southeastward movement indicate the present-day kinematics of the HFT over the locked portion of the MHT; which is, mainly an arc parallel movement and the streams too have aligned their flow in conjunction with the southeastward horizontal movement of the shallow crustal block.

Land gravity data processing and generation of gravity anomalies

The processing of acquired land gravity data along Sahranpur to Mussoorie and other two sub-profiles from Mussoorie to Zeropoint and ITM/DRDO have been completed and the first version of free-air gravity, Bouguer anomaly and the Complete Bouguer anomalies are produced. Free-air anomalies in all these profiles are in complete agreement with the topography and their values vary from 66 mGal to -122 mGal with respect to the GRS80 ellipsoid. Datum conversion with respect to the msl has been done by calculating the orthometric height by using EGM2008 and the local gravimetric geoid. These gravimetric geoid models are computed based on 1) Moritz's analytical solution to Molodensky's problem through Curtin University of Technology approach 2) using Vanicek and Kleusberg modified Stokes kernel approach and 3) the method of Least Squared Modification of Stokes formula with Additive corrections. The EGM2008 model is obtained by using the fully expanded spherical harmonic solution coefficients up to degree and order 2160. The discrepancies among the gravimetric geoids are very low and <1 cm. While discrepancies in the local orthometric heights with respect to the global model in the elevated region varry from 75 to 80 cm. The Bouguer (BG) anomalies are produced by applying the Bouguer spherical cap correction (Bullard B) on Free-

air anomalies and obtained the GRS80 datum corrected anomalies. The BG anomaly varies from -125 mGal in the Gangetic plane to -167 mGal towards the elevated Mussoorie region and over the Shiwalik high it is around -145 mGal. The full scale topographic correction that includes the Bouguer spherical cap (Bullard B) and the terrain corrections (Bullard C) has been applied to the msl corrected Free-air anomaly and produced the Complete Bouguer (CBG) anomaly of the area. The CBG anomaly varies from -155 in the planes to -172 towards the elevated region. Major inference from the BG and the CBG anomalies is that the basement is showing a northward dip -as like the MHT- towards the MBT, where the Outer Lesser Himalayan rocks are overriding the basement. Further modelling work in progress.

Application of Deep Learning (ANN & LSTM) in the GPS time series data

GPS data is widely used for navigation, surveying, and environmental monitoring, but it often suffers from missing values due to signal disruptions or data recording issues. Common interpolation techniques, such as linear, polynomial, and spline methods, are generally employed to fill these gaps but often fall short when dealing with the complexities of time series data. This study investigates the use of machine learning models, particularly Artificial Neural Networks (ANN) and Long Short-Term Memory (LSTM) networks, to better estimate missing values in GPS data for the North, East, and Vertical components. Observations show that LSTM models outperform ANNs and traditional methods, achieving significantly lower Root Mean Square Error (RMSE) values, ranging from 0.0018 to 0.1082 mm. Among conventional interpolation methods, K-Nearest Neighbours (KNN) provided the best results for the North and East components. In contrast, linear interpolation was most effective for the Vertical component with an RMSE of 0.4051 mm. However, even the best-performing traditional methods were surpassed by deep learning approaches, highlighting the potential of LSTM models for more accurate GPS data interpolation. The study suggests that these models could be scaled up and enhanced with ensemble techniques, making them a powerful tool for improving GPS data accuracy across various applications. Supporting evidence from recent research also demonstrates that neural networks, particularly LSTM models, consistently deliver superior results in GPS error prediction and data interpolation.

Fission-track thermochronology study

Our study provides the first apatite fission track (AFT) and zircon fission track (ZFT) thermochronological record from the Gianbul Gneissic domes in the NW Himalaya. The dome is bounded by two extensional shear zones, namely the South Tibetan Detachment System (STDS) dipping towards NE and the Khanjar Shear Zone (KSZ) dipping towards SW. The AFT cooling ages range from 14.2 ± 1.2 to 5.7 ± 1.1 Ma, and ZFT ages range from 22.8 ± 2.2 to 14.6 ± 0.9 Ma. The ZFT ages get younger towards the bounding faults, while the AFT ages remain constant across the dome. The fission-track data, in combination with the published Ar-Ar and (U-Th)/He cooling ages, have been modelled using a thermo-kinematic inverse and forward model to analyse the processes that led to the exhumation of the dome. Various scenarios such as the river incision, lithology, deformation along faults like the Main Himalayan Thrust, the Main Central Thrust, the STDS, glacier control, and erosion control over exhumation have been tested. Our results suggest that the extension of the normal fault is the primary mechanism for the exhumation of the GD. The extension happened in two phases: (a) during the initial normal sense movement along the STDS when the reverse sense of shear was switched to the usual sense of shear during the early Miocene, and (b) during the Late Miocene. The initial phase of extension is a well-recognized phenomenon in the Himalayan orogen that has been explained through models like channel flow or ductile wedge extrusion. However, the first report of extensional activity along the STDS during the Late Miocene allows us to test whether it is a local phenomenon or a regional event that happened in the brittle stage. Thus, we compiled all the published geochronological and thermochronological data of all the prevailing gneissic domes in the Himalayas from west to east and ran the 3D thermokinematic model to assess the exhumation path of the rocks and brittle stage deformation history. Our results suggest that two phases of extension happened in the entire arc of the Himalayan orogen. The first phase facilitated the southwest migration of ductile materials of rocks from mid-crustal depths, accompanying the extension due to gravity. The second phase of extensional collapse happened during ~7-3 Ma ago in the brittle stage.

Rock magnetic studies

The rock magnetic, petrography, and petrofabric (AMS) analysis of Nidar ophiolitic rocks has been carried out to deduce the magnetic mineralogical characteristics and obduction dynamics experienced by the Nidar

RESEARCH ACTIVITIES

RESEARCH ACTIVITIES

ophiolitic rocks. Also, the rock magnetic signatures of the Middle Siwalik rocks collected from the Mohand region will be submitted to a suitable journal for publication. The oriented samples collected from the Upshi-Lato section of the Indus molasses are undergoing the paleomagnetic sample preparation process. Further, a fieldwork of 20 days has been performed at the Naga-Schuppen belt, NE India, for understanding its exhumation history through a magnetostratigraphy approach. In addition, the environmental magnetic study of Gangotri glacial sediments has been carried out as one of the proxies for source characterization, suggesting a single source for their existence, i.e., the Gangotri supraglaciers. Similarly, the topsoils of Dehradun city are examined for anthropogenic pollution and evaluated for their association mostly with traffic-related pollution rather than industrial pollution.

Structural and microtectonic studies

- Evolution of strain regimes across the Main Central Thrust Zone and the Greater Himalayan Sequence in the Garhwal Himalaya, India, through the geological to the decadal time scale.

- Quantification of crustal shortening across the Main Central Thrust and the Greater Himalayan Sequence in the Garhwal Himalaya, India.

- Established the mechanisms of extrusion of the Himalayan Metamorphic Core (HMC) in the Garhwal Himalaya, India, from the Oligocene through the Miocene.

- Carried out 14 days field-work across the Main Boundary Thrust Zone, northwestern Himalaya, India and 3 days of field work across the Munsiyari thrust Zone and the Inner Lesser Himalaya, Garhwal Himalaya, India

SPONSORED RESEARCH PROJECTS

High-resolution mapping of crust and upper mantle structure across the northwest Himalaya and Ladakh-Karakoram zone with special emphasis on the seismotectonic of the Shyok Suture zone and adjoining region
(Devajit Hazarika and Naresh Kumar)

Crustal Structure and Composition in the NW Himalaya and adjoining Indo-Gangetic Plain

The underthrusting mechanism of the Indian Plate beneath the Himalaya has not only resulted in variations in strain rates, slip deficits, and seismicity throughout the Himalayan arc but also led to enormous lateral variations in crustal thickness and its composition. Investigating such changes in crustal configuration is of paramount importance in the Himalayan region to understand seismic activity and the geodynamic evolution of the area. Despite a few studies in specific transects in the NW Himalaya, no efforts have been made to map the lateral variation of crustal thickness and composition. In this study, the average crustal thickness and Vp/Vs ratio were finalised at 38 broadband seismological stations across the NW Himalaya and adjoining Indo-Gangetic Plain (IGP) (Fig. 81). This work is an extension of the work reported in the last annual report. The standard H-k stacking technique of receiver functions has been applied (Zhu and Kanamori, 2000). However, its application in a sedimentary basin poses a challenging task due to the significant complexities within the low-velocity sedimentary layer. To overcome this issue, the sequential H-k stacking method of Yeck et al. (2013) has been adopted for the stations with a significant sediment cover (Fig. 82). Integrating our results with other published studies has facilitated the mapping of regional variations in crustal thickness and compositional changes.

For Receiver Function (RF) analysis, teleseismic earthquake data with magnitude $Mb \geq 5.5$ and signal-to-noise ratio (SNR) ≥ 3.0. Only events within $30°–90°$ epicentral distance were included to avoid mantle triplications and core-mantle boundary complexities. The epicentral distribution is shown with red circles in figure 81 (inset). Earthquake hypocentral data were obtained from the U.S. Geological Survey catalog (https://earthquake.usgs.gov/earthquakes/search/). We adopted Iterative deconvolution method for receiver function analysis.

The results of H-k stacking analysis from this study are combined with previous studies available in the region to portray the crustal structure, composition, and its relation to the tectonic features across different segments of the NW Himalaya. The most distinct feature of the NW Himalaya is the gradient from a thinner crust in the Kumaon Himalaya (~38-41 km) in the east, to intermediate crustal thickness in the adjacent Garhwal and Himachal Himalaya (~40-55 km), and a significantly thickened crust in the Kishtwar and Kashmir Himalaya (~55-60 km) to the west (Fig. 83a). The topography, geologic structure, rheological changes and seismicity of the Himalaya are a consequence of the collision and convergence of India and Eurasia. GPS studies have suggested varying convergence rates across the region, with a lower rate (~10 mm/year) in the Kumaon Himalaya, increasing to ~13-14 mm/year in the adjacent Garhwal Himalaya, and ~14-16 mm/year in the Kashmir Himalaya. These variations in convergence rates significantly impact the geometry of the underthrusting Indian Plate, which not only resulted in arc-normal variation but also caused arc-parallel segmentation. In addition, the subsurface structure in the Himalayan region is also influenced by the interaction of various transverse bathymetric structures on the underthrusting Indian plate and the rift and nappe structures within the overriding Himalayan wedge. In the Garhwal-Kumaon Himalaya, two N-S and NNE transverse zones were observed where the crust was markedly thin. This could be spatially correlated with the subsurface extension of the Delhi-Haridwar Ridge and the Moradabad Fault which may have significantly caused up-warping of the Moho structure (Mandal et al., 2021). Such structural complexity could lead to a redistribution of strain, potentially contributing to the observed variations in seismicity along the Himalayan arc.

The Vp/Vs ratio is considered a more effective diagnostic parameter for evaluating the mechanical properties of rocks than relying solely on *P*-wave or *S*-wave velocities, thus making it highly sensitive to variations in rock composition, fluid content, and deformation. In the NW Himalaya, the spatial variation in crustal Vp/Vs ratios (Fig. 83b) reveals a heterogeneous crustal composition that varies both along and across the strike of the Himalayan arc. These variations suggest a progressive transformation of the initial felsic crust of a craton (comprising granite and granodiorite) has been altered to an intermediate
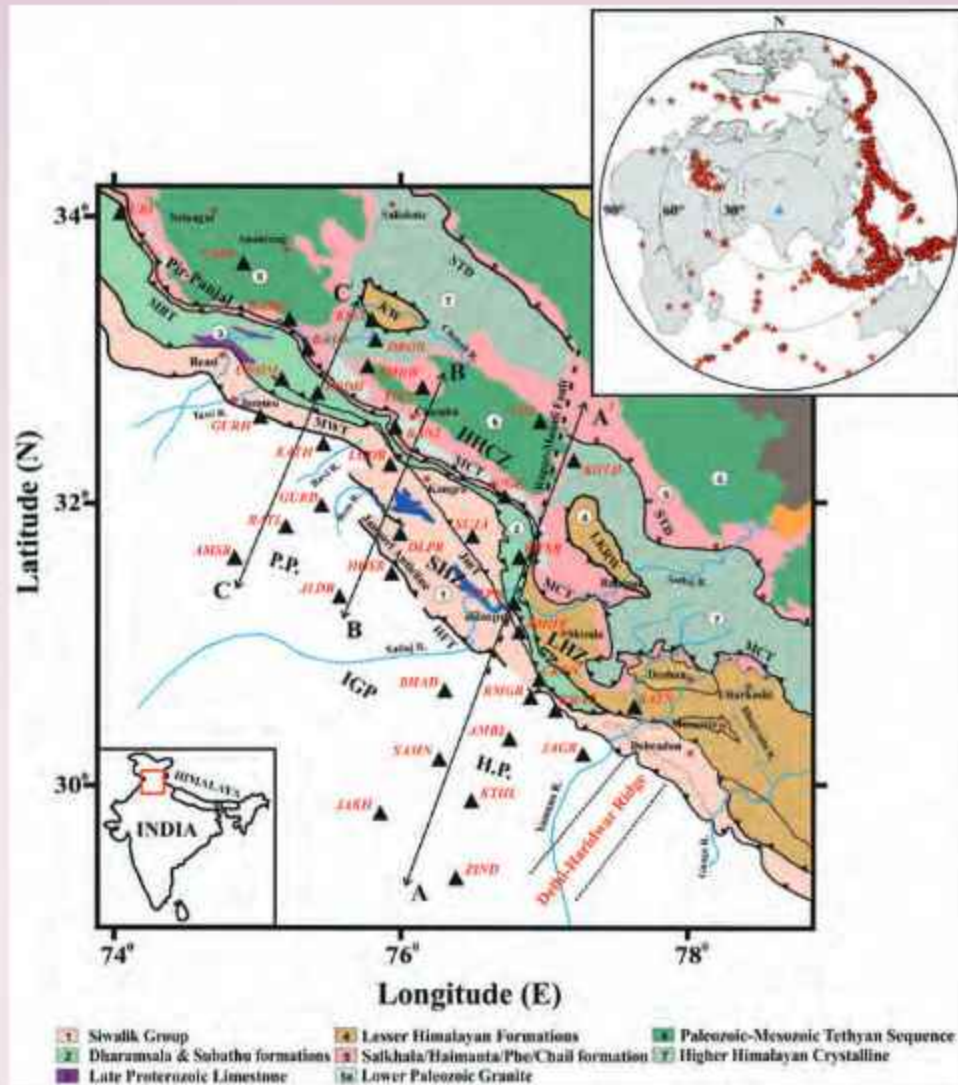
Fig. 81: Tectonic map of the northwestern part of the Himalaya. The major litho-tectonic domains from south to north are labeled as Indo-Gangetic Plain (IGP), Sub Himalayan Zone (SHZ), Lesser Himalayan Zone (LHZ), and Higher Himalayan Crystalline Zone (HHCZ). The principal thrusts and tectonic features are labeled as Himalayan Frontal Thrust (HFT), Main Boundary Thrust (MBT), Main Central Thrust (MCT), Southern Tibetan Detachment (STD), Medlicott-Wadia Thrust (MWT), Jwalamukhi Thrust (JmT), Kishtwar Window (KW), Larji-Kullu Rampur Window (LKRW), H.P. (Haryana Plain), P.P. (Punjab Plain). Locations of the 38 broadband seismic stations analyzed in this study (black triangles). The azimuthal distribution of teleseismic earthquakes (red stars) used in this study for the computation of receiver functions has been shown (inset, top right corner).

composition (diorite) and eventually into a highly mafic crust (including gabbroic rocks, mafic granulite, and subordinate serpentinite). This transformation is influenced by the addition of mantle-derived mafic materials (Zandt & Ammon, 1995), elevated heat flow facilitating partial melting and recrystallization, the serpentinization of ultramafic rocks through hydration, and the high-pressure and high-temperature metamorphism of mafic protoliths into mafic granulite. Together, these processes reflect the complex evolution of the crust under tectonic and thermal influences. The IGP and the adjacent Himalayan orogen suggest distinct compositional variations. In the study area, the tectonic units show the anti-correlations between crustal thickness and the Vp/Vs ratio. The high Vp/Vs and comparatively thin crust in the IGP indicate that the initial felsic to an intermediate crust of the Indian craton has been significantly altered by the intrusion of mafic materials into the lower crust. Over time, this process has transformed the lower crust into a predominantly
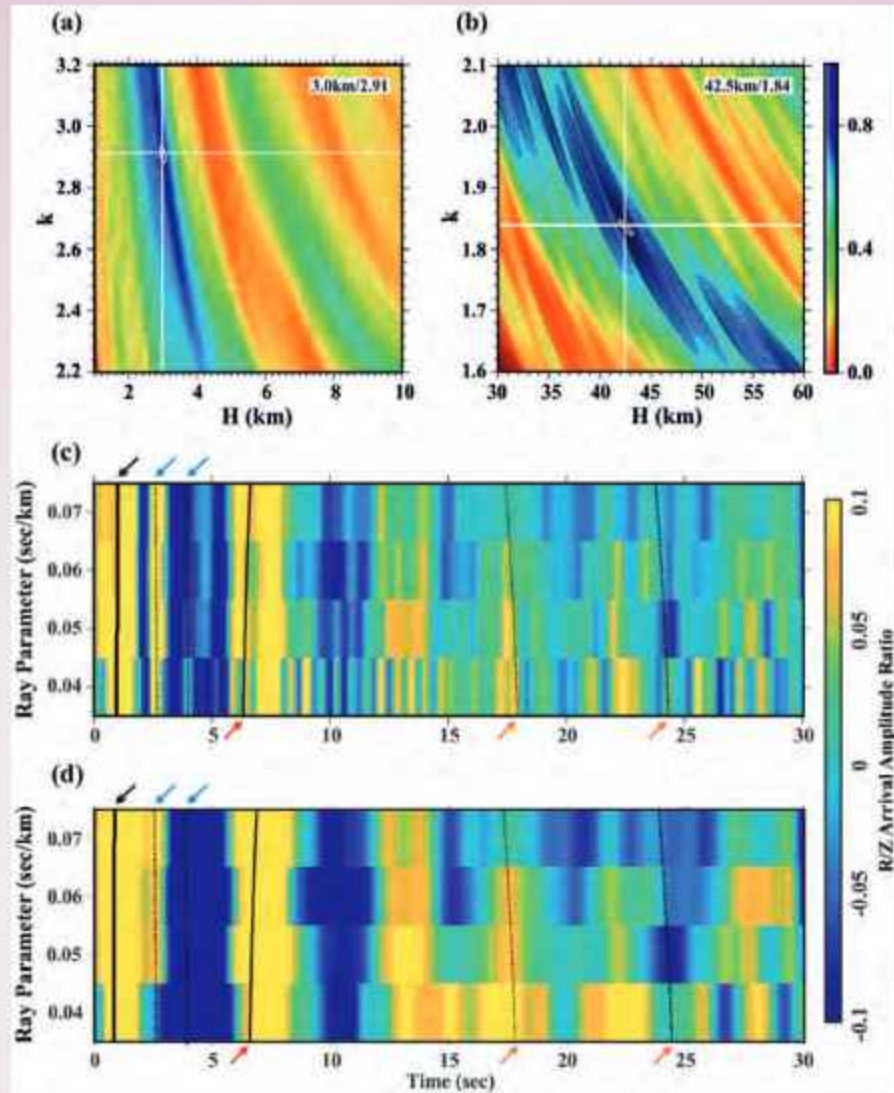
Fig. 82: Results of sequential H-*k* analysis for station AMBL, located in the IGP with sedimentary cover. a) presents the results of the sedimentary layer (first H-*k* stack) using RFs of Gaussian width 5.0. The best-estimated values of sediment thickness (3.0 km) and Vp/Vs (2.91). b) presents the crustal results (modified H-*k* stack) using the sequential H-*k* stacking with RFs of Gaussian width 2.0. The best-estimated values are H (42.5 km) and Vp/Vs (1.84). c) shows a high-frequency receiver function moveout image where sediment arrivals are prominent. Black and blue arrows indicate the sediment-basement converted (*Ps*) phase and multiples, respectively. The red and orange arrows indicate the Moho-converted (*Ps*) and its multiples, respectively. d) shows the moveout image using low-frequency receiver functions.

mafic composition, resulting in a stratified and bimodal crustal structure. The preservation of this mafic lower crust infers that it has not undergone significant destruction by any other mechanism. As we progress towards the Himalayan orogen, the Vp/Vs ratios decrease with increasing crustal thickness. In young Cenozoic orogens, processes such as folding and thrusting contribute to the recycling and refining of the existing continental crust. This leads to crustal thickening and may involve delamination processes that facilitate the removal of the mafic component from the

lower crust. This observation is further supported by the fact that the influence of the Indian cratonic crust is most prominent in the IGP, indicating a greater contribution from the mafic lower crust. However, the dominance of the mafic crust diminishes progressively towards the north which could be correlated with the increasing thickness of the Himalayan wedge, mostly composed of felsic to intermediate rock compositions. The high Vp/Vs ratios in the Kishtwar region and the Kashmir Valley can be attributed to the localized volcanic rocks and the presence of partial melts/aqueous fluids.
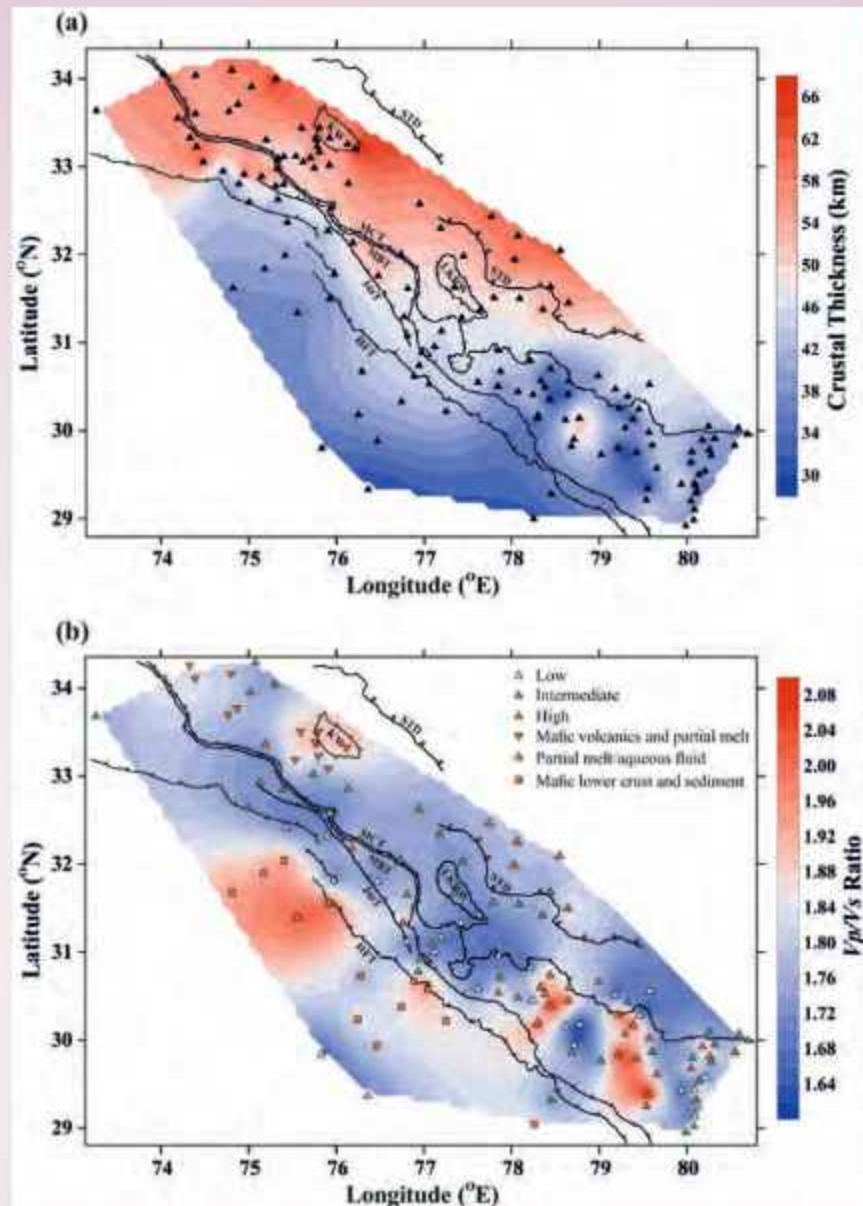
Fig. 83: Lateral variations (a) Crustal thickness and (b) Vp/Vs ratio in the NW Himalaya and adjoining IGP. The results from the present study beneath each station are combined with data from previous RF studies to obtain a comprehensive regional view of the crustal structure and composition. The black triangles in (a) mark the locations of all the broadband seismological stations used in the contour figure. In figure b, different symbols for the stations are used based on the classification of Vp/Vs values and their interpretation. The black lines mark the major tectonic features labeled as Himalayan Frontal Thrust (HFT), Main Boundary Thrust (MBT), Main Central Thrust (MCT), South Tibetan Detachment (STD), Jwalamukhi Thrust (JmT), Kishtwar Window (KW), Larji-Kullu Rampur Window (LKRW).

ANRF Sponsored Project

Development of an enhanced landslide detection model from remote sensing imagery through deep learning

(Naveen Chandra)

This study explores advanced deep learning models for automated landslide detection using satellite imagery.

In the first phase, we employ YOLOv10 and its variants integrated with four attention mechanisms: CBAM, ECA, GAM, and SA. These models were trained on an open-source landslide dataset and evaluated using precision, recall, F-score, and mean average precision (mAP). The YOLOv10m+CBAM model achieved the best performance with a mAP@50-95 of 78.5%. Our

Fig. 84: Results of the detected landslide by the proposed YOLOv10+ attention model.

results demonstrate a robust model capable of rapidly identifying and localizing landslide events (Fig. 84) with significant detection speed and accuracy improvements. In a related approach, we introduce a novel Generalized Efficient Layer Aggregation Network (GELAN) enhanced with CBAM and ECA at different integration points (Fig. 85). Tested on satellite images from the Nepal Himalaya, GELANc+CBAM achieved the highest F-score of 81.5%. These results highlight the effectiveness of attention-augmented models in accurate landslide mapping and support timely disaster response and early hazard prediction.

SPONSORED RESEARCH PROJECTS
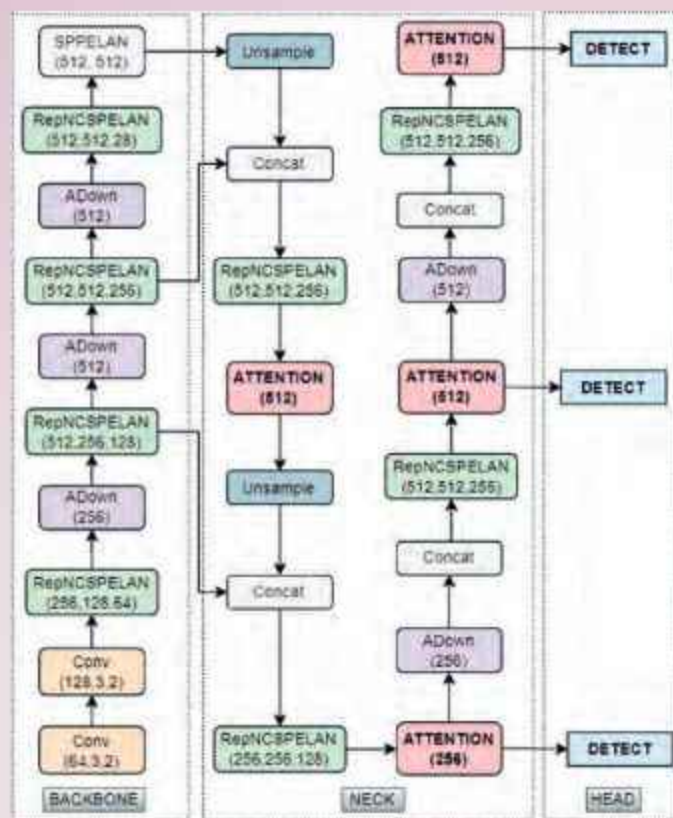
Fig. 85: Structure of the proposed model.

NCPOR Sponsored Project

Decoding South Atlantic paleoceanographic changes during the Plio-Pleistocene: insights from IODP Hole U1560A
(Prakasam M.)

This Internation Ocean Discovery Program (IODP) India post-cruise research project will investigate paleoclimate and paleoceanographic changes in the South Atlantic Ocean during the Plio-Pleistocene. The time interval (last 5 million years) has been marked by a dramatic change in Earth's climate and oceanography, from a warmer condition to the colder icehouse climate of the Pleistocene. During the Mid-Pleistocene Transition (MPT), Earth's glacial cycles changed drastically from 41 to 100 kyr cycles. The North Atlantic part is well-studied, whereas the South Atlantic part is relatively under-explored, especially its central part. This the South Atlantic plays a key role in global climate regulation via mechanisms such as the Atlantic Meridional Overturning Circulation and the Agulhas Current. This proposal seeks to fill this knowledge gap by examining multi-proxy records from IODP Hole 1560A in the South Atlantic (Fig. 86) to elucidate Plio-Pleistocene paleoceanographic evolution and its implications for future climate. Additionally, the proposal attempts to study the teleconnection of sea surface temperature anomalies in the South Atlantic and the Indian monsoon, a critical system to South Asia while, previous model studies indicate that warming of the South Atlantic can influence monsoon precipitation. By comparing IODP Hole U1560A data with Indian monsoon data, this research seeks to enhance our knowledge of these teleconnections to make better predictions about the monsoons and assess the impact of climate change on India's water resources and agriculture. Thus far, 52 samples have been processed for foraminifera faunal recovery and for measurement of total organic carbon, with planktic foraminifera being identified by microscopic analysis.
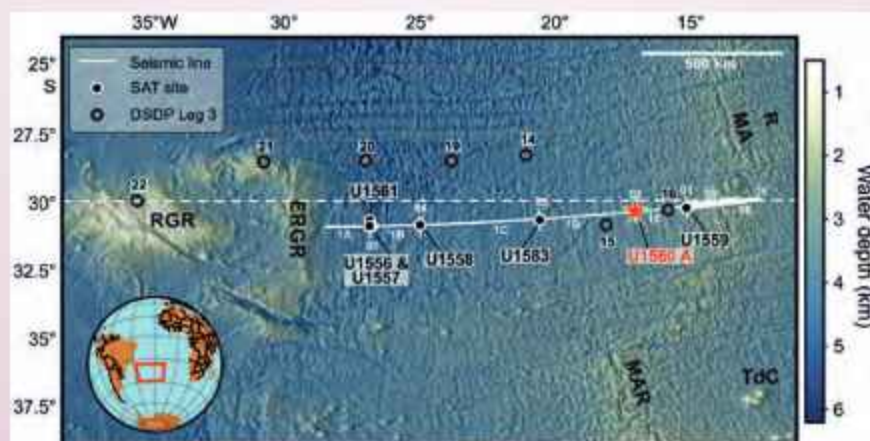
Fig. 86: Bathymetry map of South Atlantic Ocean (red star represents study Hole U1560A). Map modified from Coggon et al., 2022).

ANRF-DST Sponsored Project
Post-LGM precipitation and temperature variability in western Himalaya
(Som Dutt and Anil Kumar)

A 2.43 m sediment core from the Khajjiar Lake, Himachal Pradesh has been investigated for proxies of grain size characteristics, magnetic susceptibility and stable carbon isotopes in organic fraction to understand regional climate change in the past and regional and/or global forcing mechanisms. The chronology of the sediment core has been established using Accelerator Mass Spectrometry (AMS) ^{14}C dating of bulk sediments. The Khajjiar lake is a small lake situated at an altitude of 1900 m in Chamba district Himachal Pradesh. The lake has an area of 4500 m^2 and total catchment of 6 km^2. Geologically, the area is mainly comprised of Silurian rocks sales, schist and conglomerate. These rocks are underlain by granite, gneiss and conglomerate. The strata is conventionally known as Dalhousie Granite forming part of Dhauladhar Granite. The area is influenced by two moisture mechanisms, the Indian Summer Monsoon (ISM) and mid latitude westerlies. The ISM contributes major portion of the annual precipitation in the region and snowfall occurs during the winters. The dating results indicate the deposition of the 2.43 m sediments during the last ~6000 years.

Based on various proxy time series, the present record from the Khajjiar Lake can be categorized into three different zones.

Zone 1 (243 and 130 cm)

Between 243 and 130cm, sediments are dominated by silt size fractions, and within the silt fraction, sand concentration is low (Fig. 87). This can be interpreted as low energy transport linked with low water discharge from the catchment related to the weekend ISM. More depleted carbon isotopes suggest high contribution of organic content from the catchment having dense forest. This zone is showing weakening ISM and reducing precipitation in last phase of Northgrippian and early phase of Meghalayan. This phase is also visible in the lake records from western Himalaya and western India (Enzel et al., 1999; Dutt et al., 2018).

Zone 2 (130-90 cm)

Zone 2 suggests drastic increase of sand-size particles to more than 20 percent, which indicate a very high energy transport linked with the very high precipitation in the region that raised flash flood like conditions (Fig. 87). The deposition between 130 and 110 cm is a result of flashflood or cloudburst transport deposition. The angularity of the grains also indicates short distance transport and sudden deposition to the Khajjiar Lake (Fig. 88). The age reversal encountered in this zone can be interpreted as transport of dead carbon from the catchment and deposition in the lake.
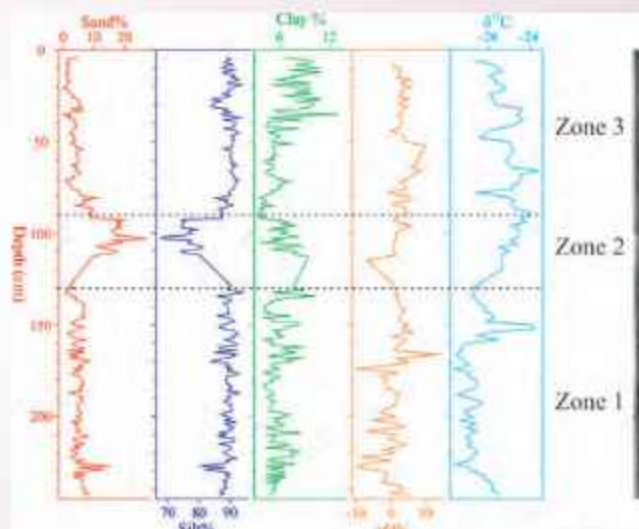
Fig. 87: Proxy records of grain size characteristics, χfd (%) and δ^{13}C isotope with ages w.r.t collected core sample from the Khajjiar Lake, Himachal Pradesh.
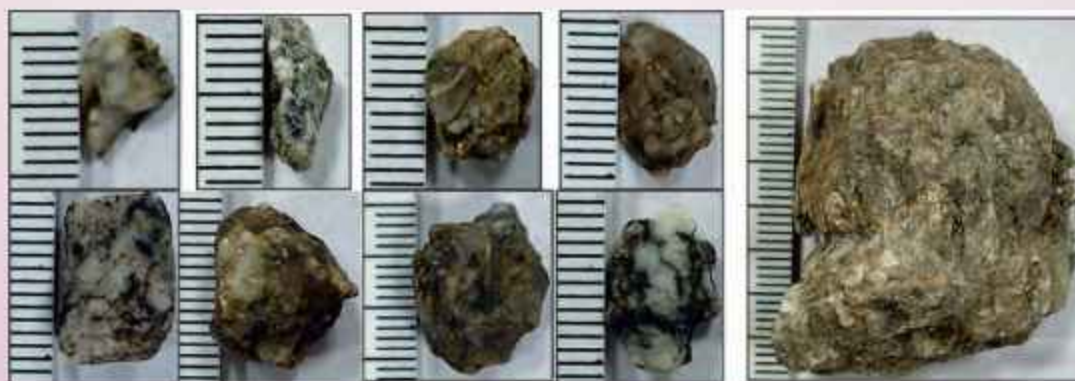
Fig. 88: Few grains of various sizes from the gravel-sized sediments zone (Scale: 1 unit = 1mm).

Zone 3 (90cm-Top)

After 90 cm, the sand fraction again decreased and silt increased. This can be referred to as decreasing high energy transport and decreased strength of ISM and less precipitation in the region. After 50 cm, clay fraction increased gradually which can be linked with the gradual decline in ISM strength that led to the stagnant and low water level in the lake. The deposition of the sediments on the coring site occurred during the high lake level after monsoon only.

ANRF-DST Sponsored Project
Optical characterization of atmospheric aerosols along Mandakini Valley, Garhwal Himalaya, India
(Chhavi Pant Pandey)

The project is aimed at the monitoring and analysis of black carbon (BC) concentration in the Mandakini Valley using field-based measurements and data-driven approaches. The primary objective is to understand the spatial and temporal variability of black carbon under different environmental and seasonal conditions. Three fieldwork campaigns have been conducted across different locations in the Mandakini Valley. In addition to periodic fieldwork, a continuous monitoring system has also been established in the valley to record real-time variations in black carbon concentrations. However, to comprehensively capture the variability of black carbon concentrations across different seasons, months, and meteorological conditions, further field campaigns are required. These future campaigns, combined with continuous monitoring data, will help to strengthen the dataset and provide deeper insights into seasonal dynamics, source attribution, and the potential impacts on regional climate and human health. The project is currently ongoing since May 2024. The findings will ultimately contribute toward developing mitigation strategies and informing local policy frameworks aimed at controlling black carbon emissions in the sensitive Himalayan region.

ANRF-DST Sponsored Project
Assessment of groundwater from hard rock aquifers in the Lower Himalaya, India
(Santosh Kumar Rai and Rouf Ahmad Shah)

The project aims to assess the groundwater resources from hard rock aquifers in the Chakrata hilly region through multiproxy approaches (Fig. 89). The primary objective is to prepare the spring inventory and understand the groundwater recharge processes and vulnerability. Five periodic field campaigns have been conducted to measure the spring flow rates and collect the water samples from surface (precipitation and streams) and groundwater (wells and springs) from different locations across the study region. About 104
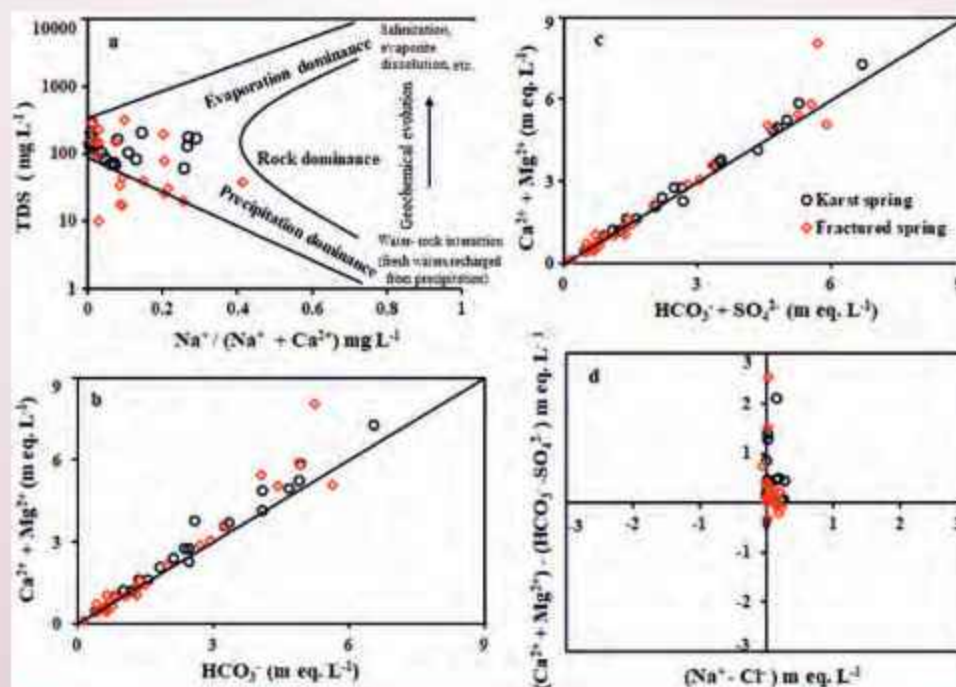
Fig. 89: Scatter plots show the relationships among major ions in monitored springs within the study area. The plots include: a) Gibbs diagram b) $Ca^{2+}+Mg^{2+}$ versus HCO_3^- c) $Ca^{2+}+Mg^{2+}$ versus $HCO_3^-+SO_4^{2-}$ d) Na^+-Cl^- versus $Ca^{2+}+Mg^{2+}-HCO_3^--SO_4^{2-}$. These relationships provide valuable insights into the geochemical processes occurring along the flowpaths of monitored springs.

springs with low to moderate discharge of 3-200 L/min, originating from these two rock formations, were traced; most of springs have been sampled for chemometric and isotopic analysis. The preliminary results suggest that springs are alkaline in character, and are low to moderately mineralized, showing ionic abundances follow the similar abundance order as: Ca^{2+} > Mg^{2+} > Na^+ > K^+ for cations, and HCO_3^- > SO_4^{2-} > Cl^- > NO_3^- for anions. Further, there is a noticeable variance in ionic concentrations among the springs at the spatial scale, which could be attributed to changes in local mineralogy in the corresponding host rock and/or changing weathering rates. The data plotted as Na^+ / Na^+ + Ca^{2+} versus TDS (Fig. 89a) shows that most samples lie within the rock dominance zone, particularly the karst springs, suggesting the ionic composition of spring waters is primarily regulated by natural mineralization of hosted rocks. Some water samples are from the fissured ones, with lower TDS or dissolved ions that fall along and/or below the rock-precipitation control zone. This suggests that the recharge water, which is lower in TDS, may have insufficient contact time to cause any significant geochemical change and/or to exert a geochemical effect on the host rock, along the flow path of these springs. The carbonate and silicate weathering is supported by Ca^{2+} + Mg^{2+} versus $HCO3$ (Fig. 89b), and versus HCO_3^- + SO_4^{2-} (Fig. 89c), where samples mostly lie along the equiline. However, few samples shift away from the equiline, suggesting some ionic exchange and /or silicate contribution during the carbonate dissolution that may have contributed to their higher Ca^{2+} and Mg^{2+} concentrations. The relationship between Ca^{2+} + Mg^{2+} -HCO_3^- -SO_4^{2-} and Na^+ - Cl^- (Fig. 89d), where samples fall very close to zero on the x-axis (i.e., Na^+ -Cl^-), supports minor role of ion exchange process in regulating the ionic content of the spring waters.

DST Sponsored Project
Development and Deployment of an Integrated Operational Warning System (IOWS) in Dhauliganga River Basin, Chamoli, Uttarakhand
(Kalachand Sain and Amit Kumar)

The project's objective is to develop a comprehensive Integrated Operational Warning System (IOWS) for the Dhauliganga Basin. The system will be initiated by deploying real-time monitoring tools, including Automatic Weather Stations (AWS), Automatic Water Level Recorders (AWLR), and Broadband Seismic
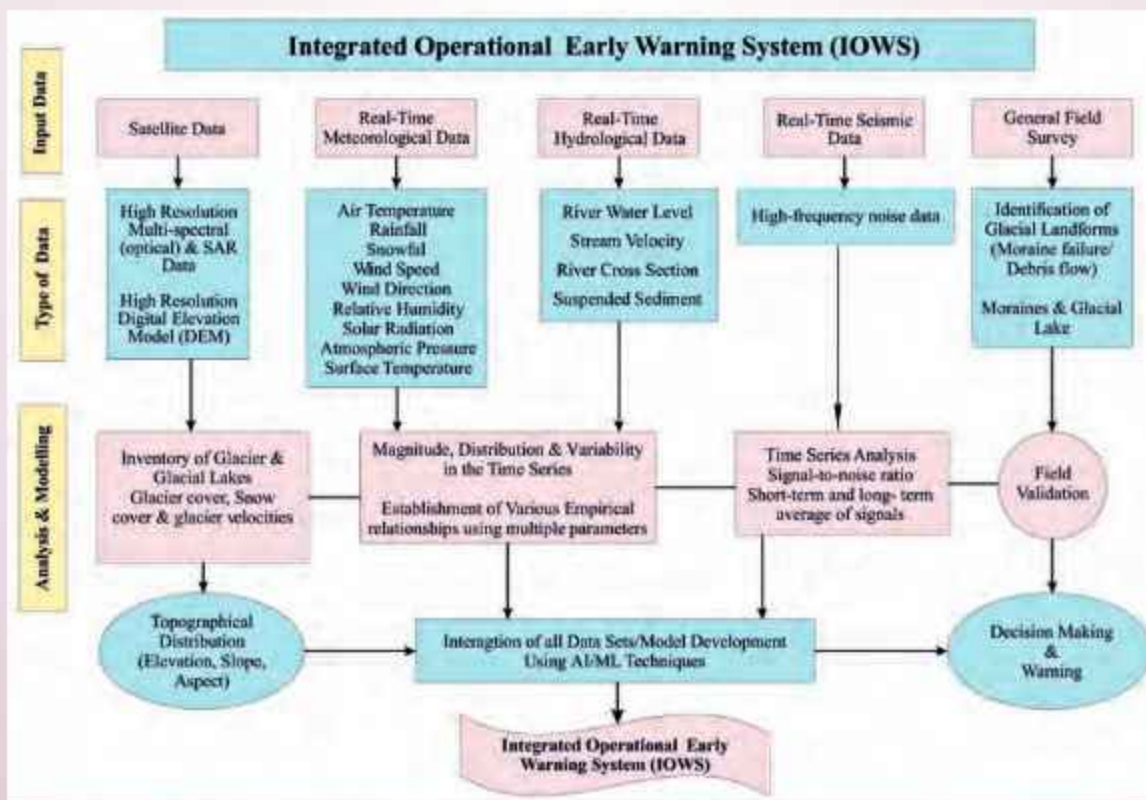
Fig. 90: Flowchart illustrating the methodology adopted in the development and deployment of the Early Warning System in the Dhauliganga Basin.

Stations (BBS). These instruments will continuously collect data on weather conditions, water levels and flow, and seismic activity observed during disasters. This real-time data will feed into an intelligent system that uses Artificial Intelligence (AI) to detect unusual patterns and predict potential flood disasters. To ensure the system functions accurately, it will be tested and calibrated using historical flood data (glacial lake outburst floods, landslides, avalanches and hydro-meteorological extremes) of the region. When a threat is identified, the system automatically sends alerts through sirens and other channels, helping people evacuate and protect lives and property. Disaster response agencies will also receive this information, enabling them to respond quickly and manage resources efficiently. Additionally, training and awareness programs will be conducted for local authorities and residents to ensure proper use of the system and its long-term sustainability. As part of the project, the Department of Science and Technology (DST) has approved and sanctioned the budget for the procurement of instruments, including Automatic Weather Stations (AWS), Automatic Water Level and Velocity Recorders (AWLR), Broadband Seismic Stations (BBS), and sirens/hooters. These instruments are to be integrated via a Very Small Aperture Terminal (V-SAT and GSM (Global System for Mobile Communications) or GPRS (General Packet Radio Service) telemetry system to enable real-time data acquisition and dissemination. The primary objective is to install and operationalise a robust monitoring network that allows real-time data transmission and helps mitigate regional risks. The methodology is illustrated in a flowchart, highlighting the various components to be adopted in developing and deploying the Early Warning System in the Dhauliganga Basin (Fig. 90).
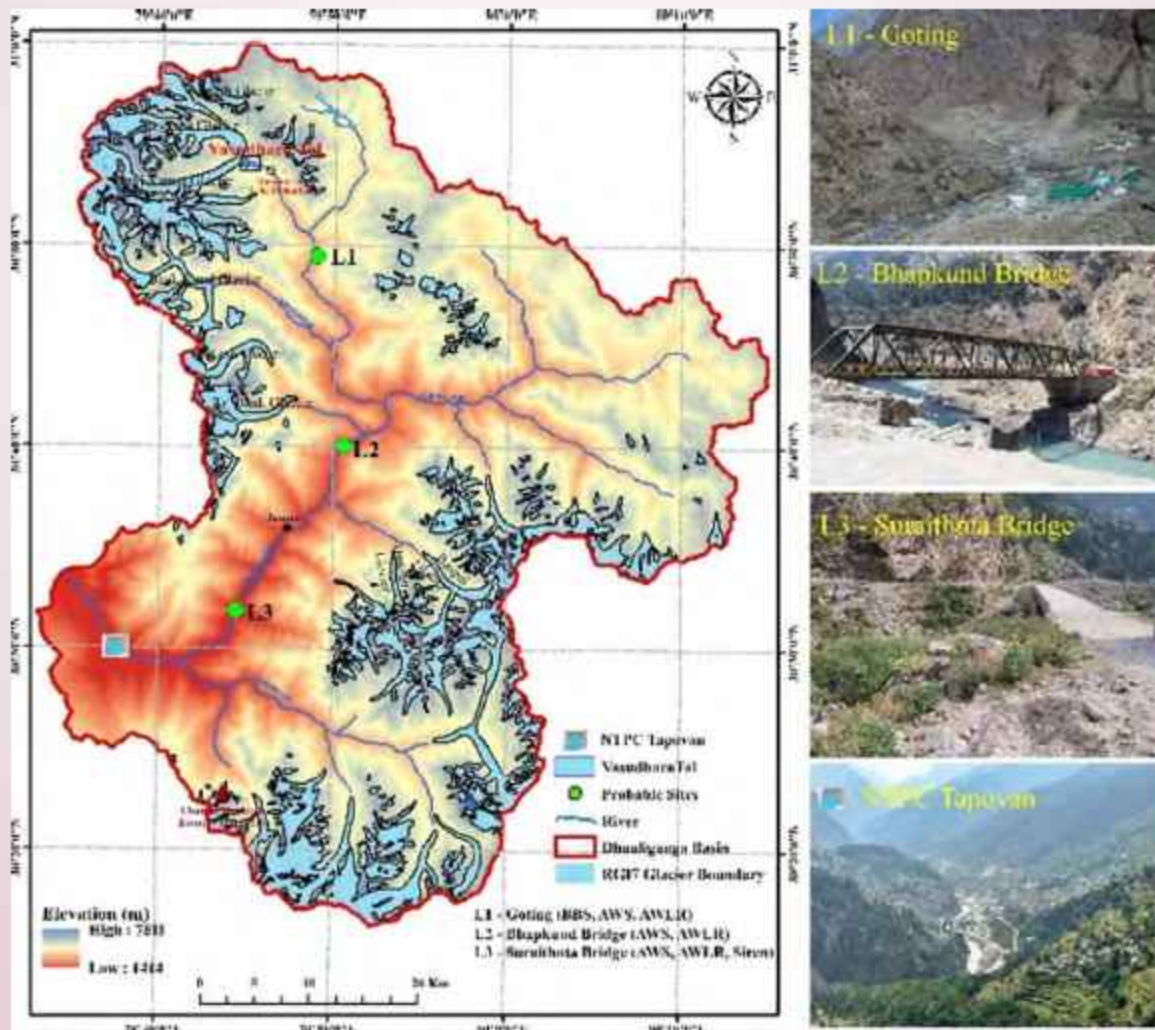
Fig. 91: Showing the locations of the instruments to be installed in the Dhauliganga basin, including the selected sites for AWS, AWLR, BBS, and sirens for real-time data acquisition under the IOWS Project, along with the vulnerable glacial lake and one damming site in the upper Dhauliganga basin.

Given the high susceptibility of the Dhauliganga basin to multiple hazards, including glacier-related events, landslides, avalanches, lake outburst floods, and extreme hydro-meteorological occurrences, the careful selection of sites is critically important. This basin has a documented history of such events and continues to experience several of them annually. Therefore, the project team conducted extensive field surveys to identify and finalize suitable locations for installing a network of AWS, AWLR, and BBS instruments. The methodology involved selecting the first site in the uppermost region of the basin, designated as Site L1 (Fig. 91), where the hazard potential is considered most critical. These surveys focused on highly glacierized areas in the upper Dhauliganga Basin.

A detailed assessment was conducted through ground reconnaissance and field expeditions, identifying glacial lakes, active landslides, and probable sites for developing landslide-induced lakes with potential outburst events. Based on this evaluation, one critical lake (Vansundra Tal) was selected for continuous monitoring (Figs. 91 and 92). It is important to mention that the lake (Vansundra Tal) selected for

monitoring is already included in the list of most vulnerable lakes of Uttarakhand, as identified by the National Disaster Management Authority (NDMA) under the National Glacial Lake Outburst Flood (GLOF) Risk Mitigation Project (NGRMP).

Similarly, two additional sites for the installation of the instruments mentioned above (Sites L2 and L3) have been selected further downstream, particularly at locations where major tributaries (sub-basins) merge with the Dhauliganga River (refer, Fig. 93). These sub-basins pose a significant hazard potential due to their extensive glacier-covered areas. One such example is the Dunagiri–Bangni sub-basin. To avoid duplication and ensure optimal coverage, it was verified that no other agency has installed similar instruments/networks at or near the selected locations. This was done through consultations, field checks, and reviewing existing observation networks in the basin. The information for the same has also been provided to different stakeholders/institutions working in this basin. The exact location for the installation of the Automatic Weather Station (AWS), Automatic Water Level Recorder (AWLR), and Broadband Seismometer (BBS)

Fig. 92: The fieldwork was carried out by two teams near Vasudhara Tal, covering both upstream and downstream areas. One team, consisting of project staff, conducted surveys using funds available under the project. The other team, from WIHG, was funded by the USDMA for the joint expedition. Additionally, members from the State Disaster Management Authority (SDMA) provided crucial support during the field visit, particularly in conducting the bathymetric survey. Their involvement ensured the successful completion of the survey by offering technical expertise, resources, and logistical assistance. Given the challenging high-altitude environment, SDMA was also available to manage any unforeseen situations, providing essential support in handling the harsh conditions and ensuring the safety and success of the fieldwork.

SPONSORED RESEARCH PROJECTS
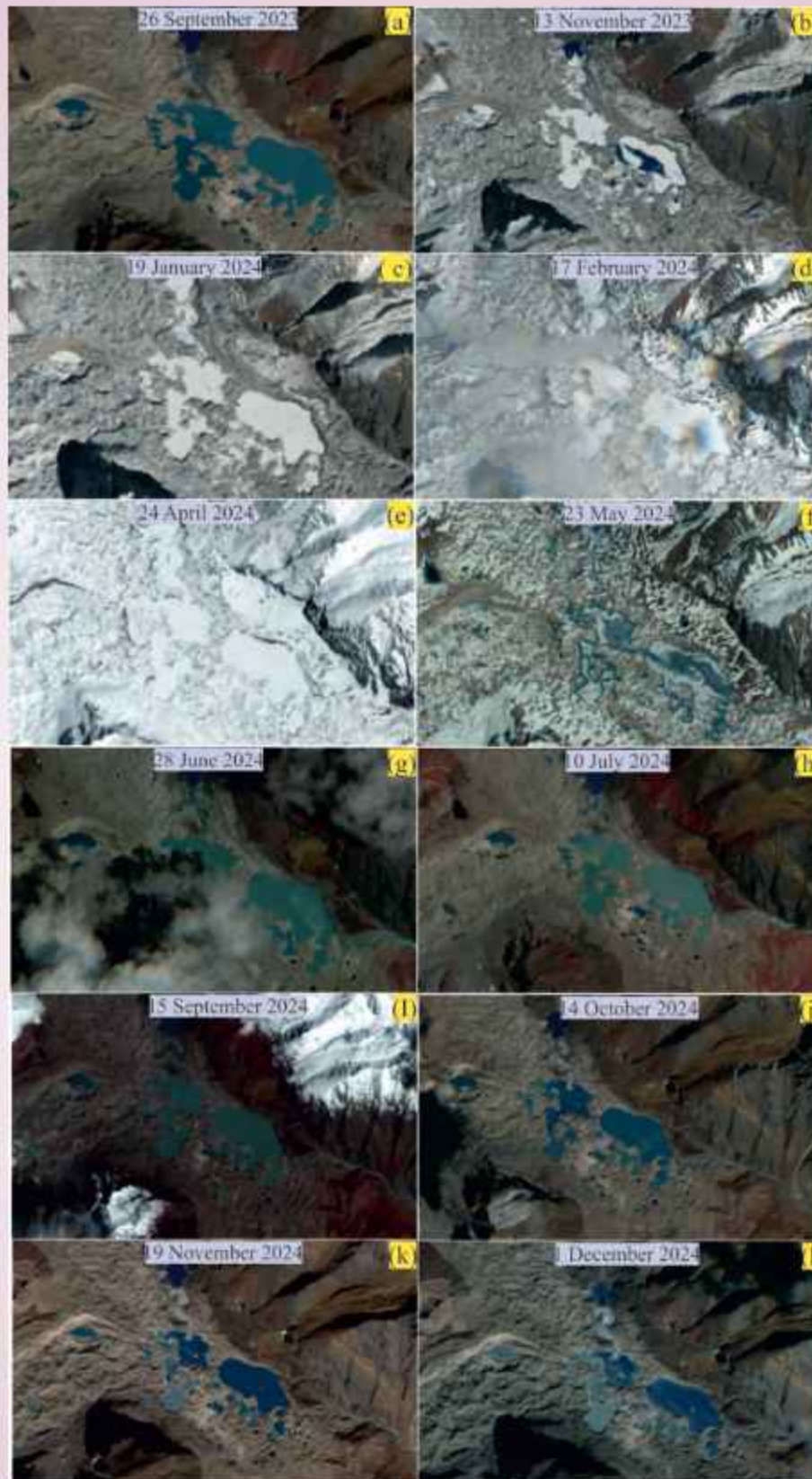
Fig. 93: Location of Vasundhara Lake in the Dhauliganga Basin and its surface area variation between 2023 and 2024, based on LISS IV data from September 26, 2023 and September 15, 2024.

was strategically selected near the confluence, where water from the lakes/dammed lakes would likely flow downstream in the event of an outburst (Fig. 91). The joint expedition was conducted by the Uttarakhand State Disaster Management Authority (USDMA) under the National Glacier and River Monitoring Programme (NGRMP), funded by the National Disaster Management Authority (NDMA), team from the WIHG visited the glacier and the associated glacial lake, confirming its vulnerability to outburst floods in the downstream region. As mentioned, Vasundhara tal, a prominent glacial lake located at an elevation of approximately 4,700 meters, is one of the largest glacial lakes within the study area. During the study period, high-resolution LISS-IV satellite imagery (with a spatial resolution of 5.8 m) was utilized to monitor changes in the lake's surface area. Observations from September 2023 to December 2024 reveal a clear seasonal pattern: the lake expands during the pre-monsoon and monsoon months (May to July), reaching its maximum extent in July. After the monsoon, the lake's area begins to shrink and remains completely frozen from January to April (Fig. 93). It has been noted that the area of Vashudhara Lake decreased by 5.7% over the past year, from approximately 0.50 km² on September 26, 2023.

ANRF-DST Sponsored Project
Long-Term Monitoring of Gangotri Glacier, Garhwal Himalaya
(Kalachand Sain and Amit Kumar)

This project aims to map and monitor the Gangotri Glacier and their associated glacial lakes, collect meteorological and hydrological data, assess glacial hazards, and disseminate information regarding potential threats to the USDMA. In this context, a network of two Automatic Weather Stations (AWS), one Automatic Water Level Recorder (AWLR), and two broadband seismic stations was installed in the basin during October and November 2023 (Fig. 94). The project staff visited the Gangotri Glacier several times during the entire study period from April 2024 to March
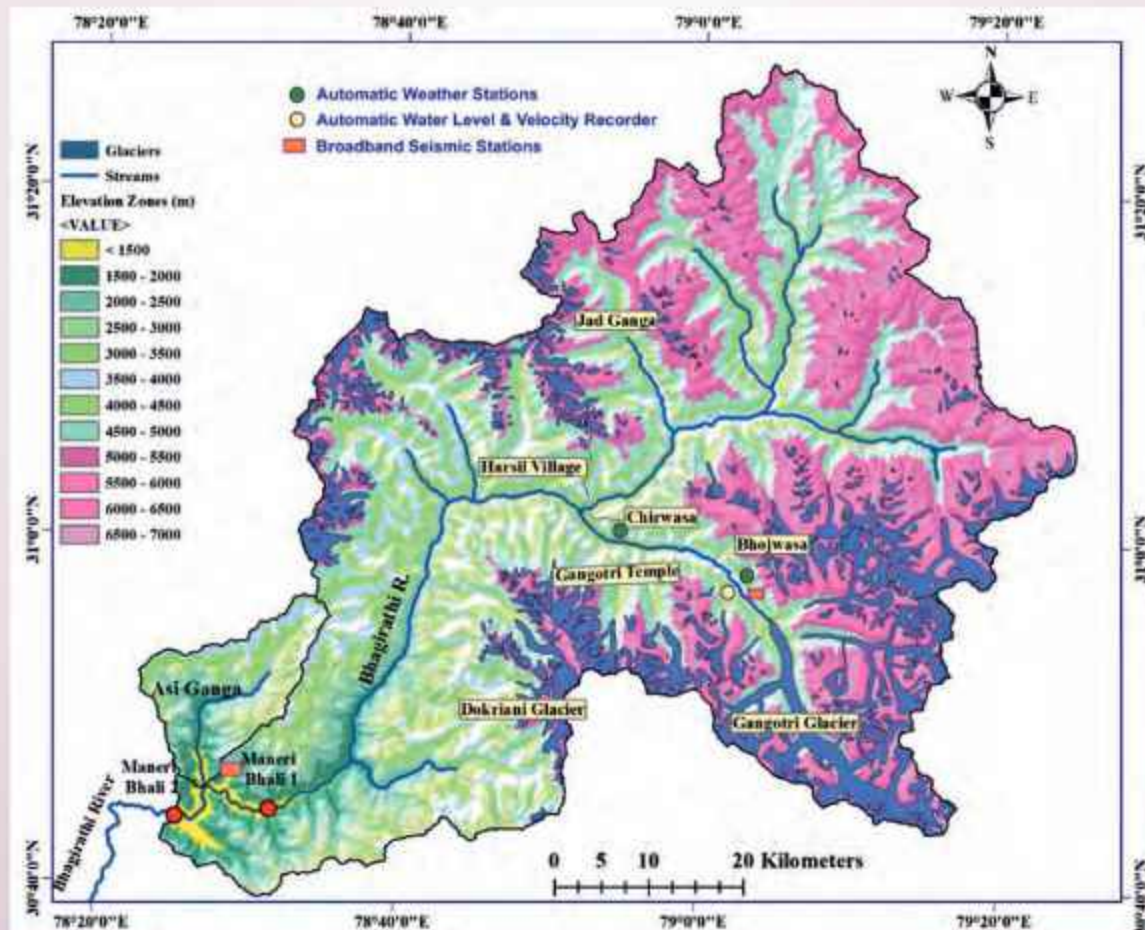
Fig. 94: Showing the elevation-wise distribution of the Bhagirathi basin and the location of the Automatic Weather Station, Automatic Weather Station, and Broadband Seismic Stations, installed in November 2023.

SPONSORED RESEARCH PROJECTS

2025. The water level of the Bhagirathi River began to increase in the first week of April. The channel originating from the Meru Glacier started discharging water into the main Bhagirathi River. Significant debris remains around the snout of the Gangotri Glacier following the debris event in 2017. During August 2024, all the instruments are functioning well; however, in the first week of August, continuous rainfall combined with glacier-related activities may have contributed to a flash flood event in the region. As informed by our watch and ward staff, on 4th August 2024, due to an unusually high water level and sediment in the river, our Automatic Water Level Recorder (AWLR) was washed away.

Despite efforts by the staff to retrieve the instrument, they were unsuccessful due to the high water and sediment in the river. A team from the WIHG visited the Gangotri Glacier in September 2024 to assess and understand the event's causes. During the visit, the team collected meteorological data from the Automatic Weather Stations (AWS) at Bhojwasa and Chirwasa and seismic data from the Broadband seismic stations at Bhojwasa and the Maneri Dam. In September 2024, a manual observatory was transported and established at the Bhojwasa to collect various meteorological parameters, including rainfall and temperature data, as shown in figure 95. The manual observatory was installed to collect meteorological data and to serve as a

Fig. 95: (A) Photograph showing the observatory at the base camp, equipped with an Automatic Weather Station, Broadband Seismic Station, and manual instruments such as maximum-minimum thermometers, an ordinary rain gauge, and a pan evaporimeter installed in September 2024. (B) The Automatic Weather Station at Chirwasa and (C) the Broadband Seismic Station at Maneri.

Fig. 96: (A) Snow-covered view of Bhojwasa during March 2025. (B) The hut and base camp, fully covered in snow. (C) The observatory at the base camp, equipped with an Automatic Weather Station and Broadband Seismic Station at Bhojwasa. (D) The Automatic Weather Station at Chirwasa.

backup in case of any malfunctioning of automated instruments. From October to November 2024, the project staff conducted field reconnaissance along the Bhagirathi River from Bhojwasa to the snout of the Gangotri Glacier.

From January to early March 2025, field activities in the Gangotri Glacier region were limited due to harsh winter conditions and heavy snowfall (Fig. 96). Significant snowfall occurred from January through mid-March, making access to high-altitude areas such as Bhojwasa extremely challenging. As a result, the project team operated from lower elevations during this period. In mid-March 2025, despite persistent snow and rugged terrain, the project team reached the Bhojwasa. During this visit, they inspected the instruments installed at both Bhojwasa and Chirwasa and confirmed that all systems were functional (Fig. 96). However, no data were retrieved at that time.

Snow cover in the glacier basin was monitored at regular intervals to understand the areal extent of seasonal snow distribution throughout the year. On 10th April, the glacier basin was 99.82% covered with snow up to the base camp (3800 m). By 27th May, this coverage had reduced to 73%, meaning 27% of the snow melted in just 47 days. It is expected to decrease to 67% by 12th June 2024, indicating an additional 6% melt over 16 days (Fig. 97). This data highlights a significant and relatively rapid reduction in snow cover in the glacier basin over a short period, with specific percentages of melt calculated for different time intervals. This trend may suggest accelerated snowmelt due to rising temperatures, seasonal variations, or other environmental factors. On 30th July, observations showed that the glacier basin was 45% covered with snow up to the base camp. By 31st August, this coverage had increased to 53%, marking an 8% rise in just 32 days. It increased to 81% by 24th September 2024,
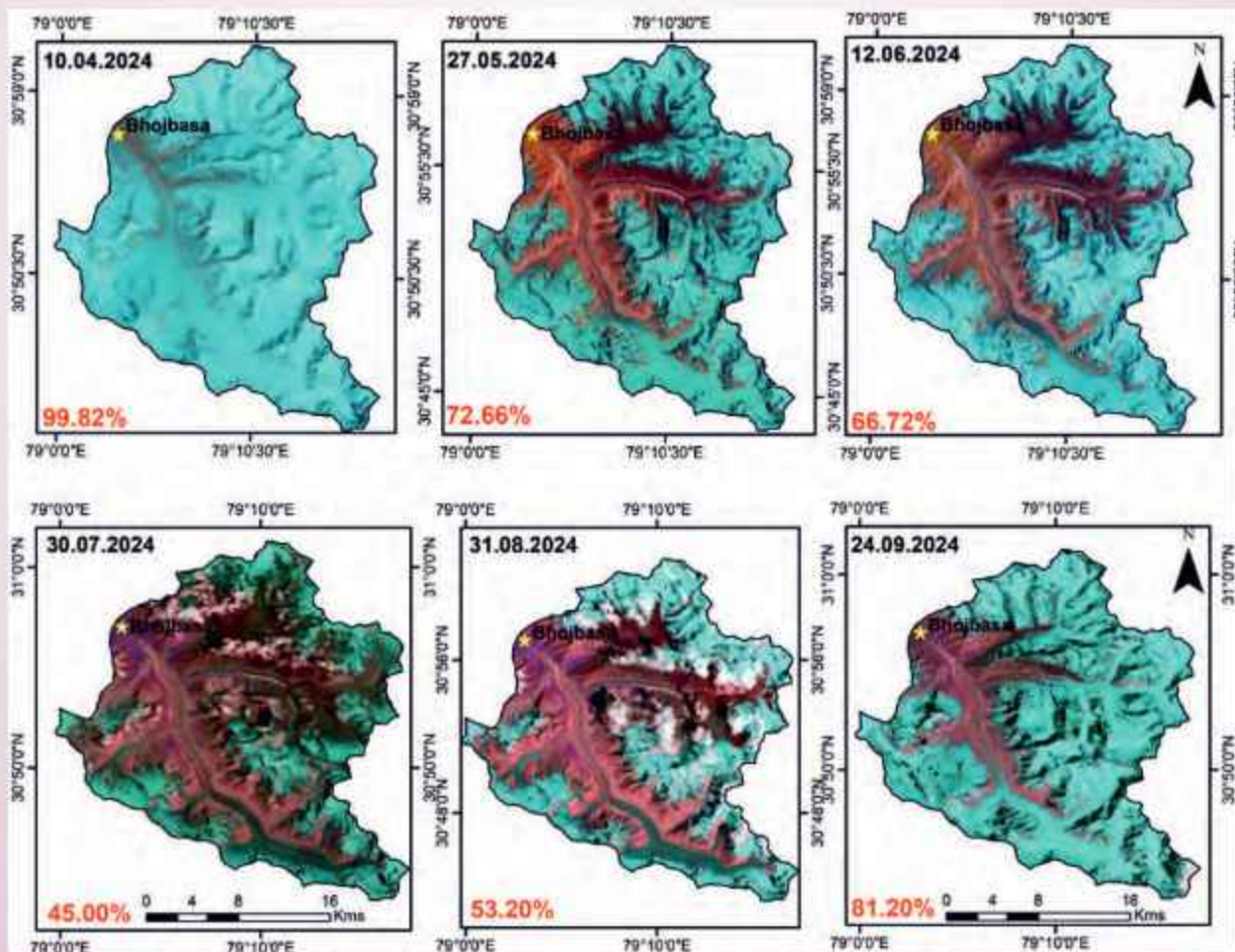
Fig. 97: Satellite images showing the distribution of seasonal snow cover up to Bhojwasa in the Gangotri Glacier basin from April to September 2024. Sentinel-2A and Landsat imagery were used for monitoring snow cover from April to June, while Landsat imagery was used to monitor changes from July to September.

indicating an additional 28% rise over the next 24 days (Fig. 97). This snow cover increase over a short timeframe suggests a snowfall event at higher elevations, likely driven by low temperatures and continuous rainfall during this period.

As detected through imagery, the observed decrease in snow cover from 44% on 1st November to 38% on 21st November highlights its effectiveness in monitoring seasonal snow changes. This trend indicates a gradual reduction in snow cover, likely due to increased temperatures, decreased precipitation, or enhanced solar radiation during this period. The snow cover percentage for the basin area up to the Bhojwasa has been calculated. Specifically, between 1st November and 11th November, the snow cover decreased from 44% to 41%, and from 11th November to 16th November, it decreased from 41% to 39%. Finally, from 16th November to 21st November, the snow cover declined from 39% to 38%, showing continued melting, likely due to increased temperature and clear sky conditions (Fig. 98). The analysis of snow cover in December, based on Sentinel-2 satellite data, offers valuable insights into snow's spatial and temporal dynamics. The data reveals an increase in snow cover from 36% on 6th December to 62% on 21st December, as identified through the imagery of Sentinel-2, emphasising its effectiveness in monitoring seasonal snow changes. This trend indicates a gradual accumulation of snow, likely influenced by factors such as lower temperatures and increased precipitation during this period. Between 16th and 21st December, the snow cover fluctuated between 45% and 41%, respectively, showing signs of melting due to clear sky conditions (Fig. 98). During the winter months of January to March 2025, snow cover in the Gangotri region was monitored at multiple intervals to assess seasonal variation and the extent of snow accumulation. The observations reveal notable fluctuations in snow cover throughout the period, influenced by prevailing weather conditions and episodic snowfall events. In January 2025, snow cover remained relatively high, with values ranging between 54% and 74%. On 10th January, the snow cover was recorded at 68%, increasing to a peak of 74% by 15th January. This was followed by a gradual decline to 63% on 25th January and 54% by the end of the month on 30th January (Fig. 99).

The initial increase in coverage likely corresponds to early January snowfall events, while the subsequent decrease suggests minor melting or settling of snow. February 2025 showed greater variability. Snow cover on 9th February was recorded at 66% but dropped sharply to 49% by 14th February, indicating a brief
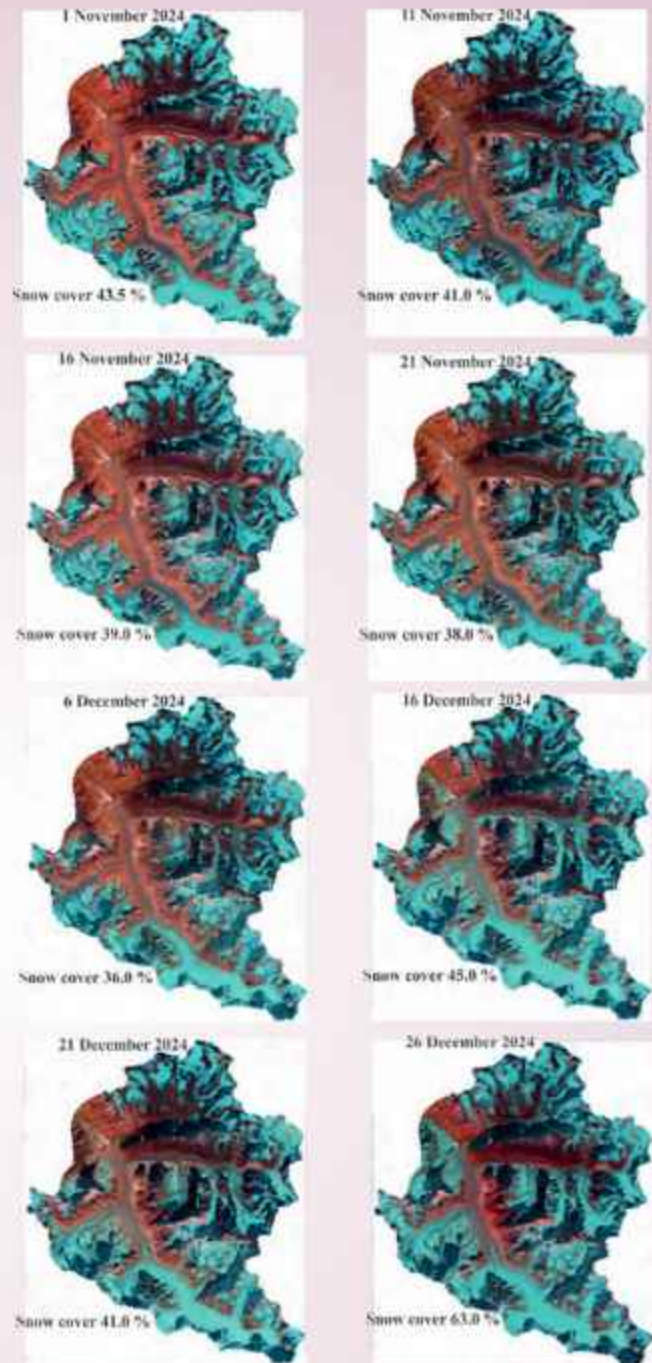
Fig. 98: Satellite images showing the distribution of seasonal snow cover-up to Bhojwasa in Gangotri Glacier basin from July to September 2024. Landsat imageries were used the monitor these changes.

period of warmer conditions or reduced precipitation. However, a significant increase followed in the month's latter half, with snow cover rising to 74% on 19th February and reaching 80% by 24th February. This sharp rise suggests renewed snowfall activity in the region. March 2025 marked the highest snow accumulation
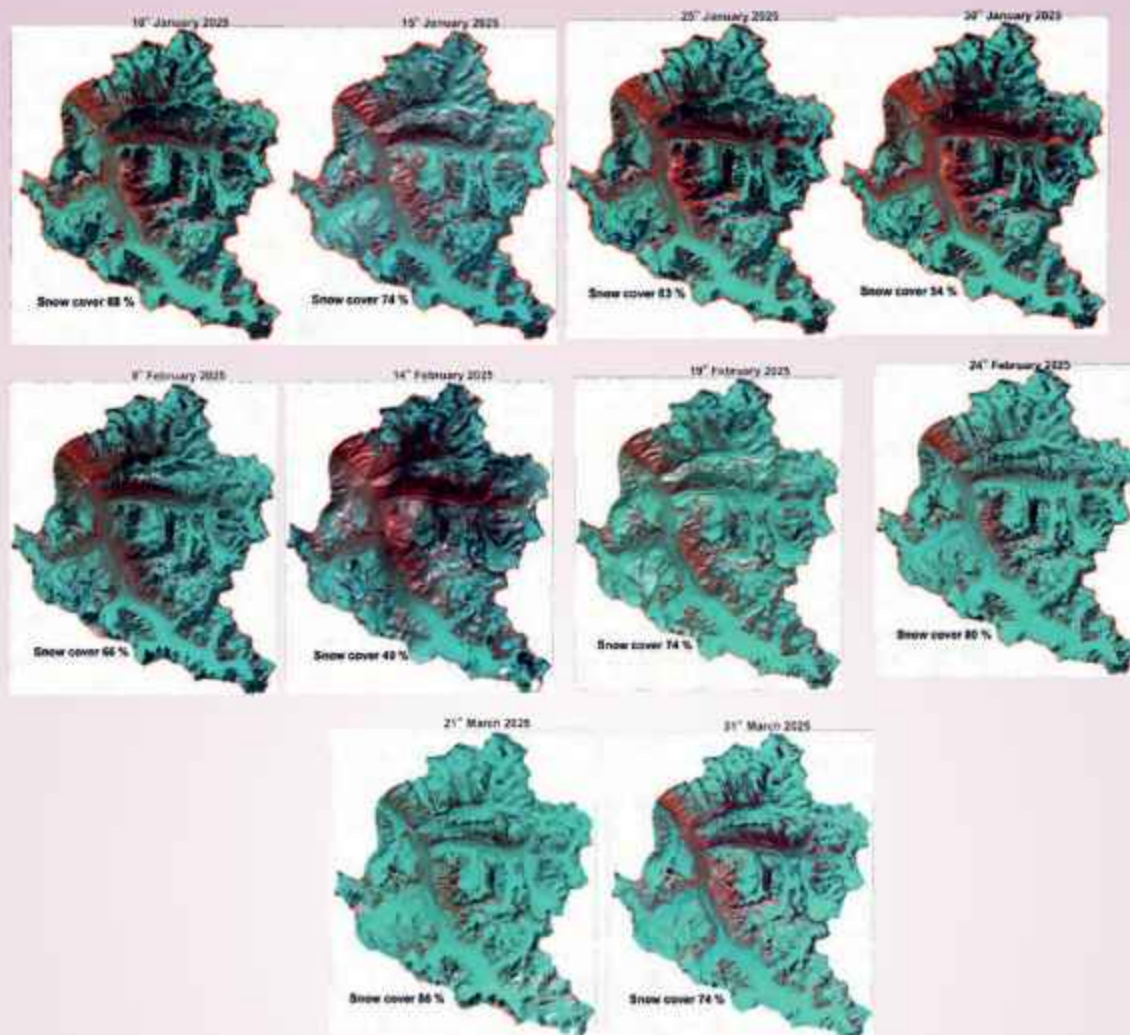
Fig. 99: Satellite images showing the distribution of seasonal snow cover-up to Bhojwasa in the Gangotri Glacier Basin from January to March 2025.

during the observation period. Snow cover reached 86% on 21st March, the peak value for the season. Although a slight reduction to 74% was recorded by 31st March, the overall snow presence remained substantial (Fig. 99). This persistent and heavy snow accumulation during March aligns with reported field challenges faced by the project team, particularly in accessing higher-elevation locations such as Bhojwasa. The data indicate consistent snow presence with episodic increases, reflecting active winter precipitation patterns. The high snow cover observed in late February and March would significantly impact glacier surface energy balance, melt timing, and spring runoff into the Bhagirathi River. These observations underscore the importance of continuous snow monitoring to better understand seasonal dynamics.

ANRF-DST Sponsored Project
Early Landslide monitoring of the Kondoi Village, Chakrata Block: with special emphasis on slope vulnerability investigation and suggestive measures
(Swapnamita Choudhury and Khayingshing Luirei)

The Kandi Village (Kondoi Bondur) has a population of approximately 400 people and 40 houses, which are at the risk of landslides due to natural and anthropogenic factors. Construction of the road has increased the frequency of landslides in this region, which are visible along the road cut section, and the presence of fractures and joints on the slope can facilitate the slide during the monsoon. Therefore, a prediction model using in-situ sensors and remote sensing was proposed and planned for a real-time operational Landslide Early Warning System (LEWS). Field work was conducted in the study area to study the litho-structural aspects and to collect soil and rock data for geotechnical analyses. The

samples were analysed for grain size, soil classification, and liquid and plastic limit at the WIHG Geotechnical laboratory. Geotechnical investigation is also crucial before the installation of the LEWS is initiated to plan the site, installation depths, and positions. Geotechnical analyses provide insights into the soil's behaviour and its suitability for various engineering applications based on the physical properties. Kandi (Kondoi Bondur) Village, located in a geomorphologically sensitive zone, has been increasingly impacted by hydro-geological hazards, including landslides, land subsidence, and structural damages such as cracks in residential buildings. Field observations have identified at least six active landslide points within and around the village, with a particularly critical active landslide zone posing direct threats to property and life. This report integrates long-term climatic analysis with geohazard data to understand how changes in rainfall patterns may influence or exacerbate these hazards. Rainfall and Temperature Trend Analysis for the Kandi (Kondoi Bondur) Village (1901–2024): Rainfall: the Mean Annual Rainfall graph (1901–2024) shows a declining trend in annual precipitation over the past 124 years. While the early 20th century recorded higher and more stable rainfall (peaking over 10 mm average), a steady decline is visible post-1960s, with annual means frequently dipping below 4 mm in recent decades. A linear regression model applied to the rainfall time series shows a negative –11.46 mm/year trend, reflecting a measurable and progressive decline in annual rainfall. To assess the statistical robustness of this trend, the Mann-Kendall test - a non-parametric test specifically suited for environmental time-series analysis was employed. The test results confirm a statistically significant decreasing trend, supported by a p-value of 0.0, indicating robust evidence against the null hypothesis of no trend.

Furthermore, the Kendall's Tau coefficient was calculated at –0.530, implying a moderately strong negative association between time and rainfall. The Theil-Sen slope estimator yielded a value of –11.20 mm/year, corroborating the regression outcome, offering a robust estimate of the trend's magnitude. Recent Rainfall Trend Analysis 2024-2025: the 2024 high-resolution daily rainfall analysis reveals distinct patterns. Prolonged dry periods characterized the early months of the year, while late July to mid-September saw abrupt and sharp rainfall spikes, peaking at 66 mm in a single event. During the monsoon, moderate to heavy rainfall clusters were evident, increasing the risk of slope saturation. Although the total annual rainfall remained low, the concentration of intense rainfall events significantly heightens the risk of slope failures. The decreasing rain could be attributed to monsoonal dynamics, increased dry spells, land use changes, deforestation, and rising regional temperatures. This trend is consistent with climate change patterns in Himalaya. The changing nature of precipitation is less frequent but more intense, combined with geological fragility and human activity, leading to increased landslide and subsidence risks. The active landslide zones and structural damages in Kandi are likely not solely a result of cumulative rainfall but of hydro-climatic stress concentrated over shorter periods, exacerbated by local terrain and development practices. Proactive intervention through integrated climate and hazard assessments is urgently required to protect lives and infrastructure in this vulnerable Himalayan village.

ANRF-DST Sponsored Project
High-resolution rodent biochronology and vertebrate based palaeoecology and palaeobiogeography of the Ladakh Molasse Group, North-West Himalaya
(Ningthoujam Premjit Singh)

A 10 days detailed field work was carried out in Ladakh during October 6-15, 2024 to delineate sections containing micro-vertebrate fossils and use them to reconstruct the biostratigraphy of Ladakh Molasse. The findings would be important as they will help to rebuild the paleoecological condition that prevailed at the time and make comparisons with local, regional and sub-continental deposits to understand the ecological continuity/discontinuity. With the stated objective, the undertaken fieldwork comprised of 4 days in Leh and 3 days in Kargil. The first part of the field was in Leh from 7-10 October, 2024. First, we visited the Taruche and Saspochey villages (Fig. 100) first and started reconnaissance of the exposures of Ladakh Molasse in the area. Based on the available literature and previous work done in Leh, the region was selected as one with the most potential for yielding micro-vertebrates fossils and other fossiliferous sections. The areas have yielded two main fossiliferous sections that show the possibility of finding important micro-vertebrates such as rodents.

Another section visited was the Basgo Formation. One of the sections here has yielded plant fossils (Fig. 101). Well- preserved plant leaf impressions are the most significant find that holds promising research prospects including paleoecological reconstructions. The well-preserved dicotyledon leaf (Fig. 101B) will open a new window to understand the topography of the Ladakh that prevailed at the time.

SPONSORED RESEARCH PROJECTS

Fig. 100: A, B. Field photographs of fossiliferous sctions exposed near the Taruche and Saspochey villages.

Fig. 101: A) Plant fossil locality exposed at Basgo village, B) Dicotyledon leaf fossil preserved in shale.

Fig. 102: (A) Locality exposed along the Wakka Chu river of Kargil, (B) locality exposed near the Pashkyum village of Kargil.

The next part of the field was carried out in the Kargil area. The three main formations of the Ladakh Molasse were visited i.e. The Kargil Formation, Tharumsa Formation and the Pashkyum Formation (Fig. 102). Field works along all three were carried out. The Kargil Formation was traversed along the Wakka Chu river section which hosts the best outcrop. This Formation proved to be the most fossiliferous and as many as seven layers were delineated. At the outcrop, fossils of gastropods and fish bones were readily visible which showed positive possibility of other micro-vertebrate fossils as well. Fieldwork in Pashkyum

Formation near the Pashkyum village has also yielded many fossiliferous layers. The silty to clayey sediments hosted gastropods and occasional fish-tooth fossils. Hence, this section also showed the positive potential of more important micro-vertebrate finds.

In conclusion, the fieldwork was a success as we were able to delineate many fossiliferous layers which hold a positive prospect of yielding new and important fossils. To that end, around 600 kg of samples have been collected collectively from all the above-mentioned sections and their processing has already started. Preliminary maceration and sorting of samples from the Kargil Formation are already yielding charophytes and fish fossils in abundance. We expect the same and more from other samples. We are hopeful that the findings will ultimately contribute towards the fulfillment of the objectives of this field and make a beneficial contribution to the palaeontology and understanding of the Ladakh Molasse and Palaeontological records.

ANRF-DST Sponsored Project
Paleoclimate, paleoenvironmental and biostratigraphy reconstruction in light of India-Asia collision and global bio-events of Surma Group, Neogene sediments of the Naga Hills, Indo-Myanmar Range
(Kapesa Lokho and M. Prakasam)

A core research grant (CRG) was awarded from Anusandhan National Research Foundation (ANRF)-Department of Science and Technology (DST), India, to Dr. Kapesa Lokho (Principal Investigator) and Dr. M. Prakasam (Co-Principal Investigator). The project, titled "Paleoclimate, paleoenvironmental and biostratigraphy reconstruction in light of India-Asia collision and global bio-events of Surma Group, Neogene sediments of the Naga Hills, Indo-Myanmar Range," will investigate past environmental changes in the Naga Hills region. Calcareous nannofossils acts as crucial biostratigraphical tool in establishing and understanding the geological time scales and the history of the Earth's climate and oceans. These microscopic marine organisms, which are primarily small, calcium carbonate plates (coccoliths) are valuable in relative dating and correlating of marine sequences. In this study, calcareous black silty-shale samples are used for reconstruction and dating the biostratigraphy and palaeoenvironmental setting. This is the first record of nannofossils being reported from the Surma group of Naga Hills consisting of *Coccolithus pelagicus, Calcidiscus leptoporous, Coccolithus miopelagicus, Helicosphaera carteri, Helicosphaera euphratis,*

Fig. 103: A flaser bedding formation from the Surma Group, Naga Hills of Indo-Myanmar Range.

Reticulofenestra haqii, Reticulofenestra minuta, Reticulofenestra pseudoumbilicus. Total organic carbon (TOC), major and trace elemental analysis were performed on 27 samples. Data synthesis are in progress. Additionally, field work for 13 days from 28th March to 9th April, 2025 was carried out. The work was carried out for strengthening of the high resolution for the fossiliferous section. In the field, sedimentary features such as flaser (Fig. 103) and lenticular bedding, ripple cross lamination and lunate ripples were observed.

DST Sponsored WISE Post-Doctoral Fellowship
Holocene vegetation and climate dynamics in the cold-arid regions of Lahaul-Spiti, Northwest Himalaya
(Deepika Tripathi)

A comprehensive field study lasting 15 days was conducted from late September to mid-October 2024 in the cold arid region of Lahaul Spiti. The objective was to gather samples for the examination of climatic and vegetation dynamics during the Holocene epoch. Approximately 30 surface samples were collected, in addition to 130 modern plant specimens as illustrated in figure 104. Furthermore, 84 sediment samples were obtained from two cores (30 samples from the first site and 54 samples from the second site) in the Spiti valley for multi-proxy analysis, which includes both biotic and abiotic proxies, as well as Accelerator Mass Spectrometry (AMS) ^{14}C dating.

Out of the 130 modern plants collected, 50 have been taxonomically classified with the assistance of taxonomist Dr. DS Rawat from GBPUAT, Pant Nagar, Uttarakhand. Phytolith analysis has been completed for 20 modern plants, with additional work ongoing, which aims to establish the first phytolith reference collection for the Lahaul-Spiti region.

SPONSORED RESEARCH PROJECTS

Fig. 104: Collection of surface soil samples and modern plant during field work in Lahaul-Spiti.

The processing of surface and sediment samples is being conducted in accordance with the specified protocols for each proxy (biotic and abiotic). To date, the pre-preparation of 20+20 samples for biotic proxies and 20 samples for abiotic proxies has been finalized.

ANRF-DST Sponsored Project
Provenance, Burial, and Exhumation History of the Karakoram Tethys Sequence, NW India
(Vikas Adlakha, Mahesh Kapawar and Saurabh Singhal)

A new zircon and apatite fission-track (ZFT-AFT) thermochronological study has been carried out along the Karakoram Fault (KF) zone in the Nubra Valley, SE Karakoram, India. The ZFT ages range from 8.7±0.7 to 11.3±0.6 Ma, and the AFT ages range from 3.8±0.5 to 6.9±1.1 Ma, respectively. The calculated exhumation rates using ZFT ages vary from ~0.54±0.04 to 0.66±0.04 mm yr -1 since ~9.87 Ma and for AFT ages from ~0.58±0.1 to 0.68±0.11 mm yr -1 since ~4.8 Ma. The exhumation rates from the Nubra Valley are more than double those observed in the southern Ladakh Batholith (LB) and are similar to the Karakoram Transpression Zone (KTZ) and Karakoram Terrane (KT) to the north of the KF zone. The consistent decreasing pattern of AFT ages from the LB towards the KT indicates that local tectonic influences play a negligible role and the role of regional tectonics in this zone's exhumation history. No systematic ZFT age pattern was found from south to north. There is evidence of the southward thrusting of the KT over the northern LB during the middle Miocene (~12 Ma) in the Nubra region. We suggest that the south-directed thrusting of the KT along the Shyok Suture Zone (SSZ)/Main Karakoram Thrust (MKT) results from intense crustal shortening in the KT during the Miocene. We propose that during the early Miocene, the delamination-induced high uplift triggered the initial phase of exhumation of the KT, the evidence of which exists in the form of the presence of mantle-derived $3He/4He$ isotope ratios in geothermal springs along the KF from the Nubra Valley and Miocene K-rich lamprophyres from the central Karakoram. The exhumation in the last phase was facilitated by the underthrusting of the Indian Plate beneath the KT.

Sponsered project: (INSPIRE Faculty)
Evolution of atmosphere-hydrosphere in the Mesoproterozoic ("boring billion"): a geochemical study
(Subhojit Saha)

Bilara Limestone (Marwar Basin)

The ~300 m thick limestone-dolomite-chert succession of the Bilara Group, Marwar basin has been studied for

Table 2: Sections studied from Bilara limestones with lat-long data.

Ashop	26°52'48.36"	73°31'14.94"
Khejarla	26°18'15.54"	73°41'4.14"
Birla mine	26°35'31.54"	73°48'2.96"
Gopa	27 °09'55.7"	72°16'32.2"
Harash Mine	26 °9'14.64	73 °44'13.41"
Lordiya	27 °5'23.53"	72 °22'53.89"
Bari Bawari	27 °13'45.6"	72°15'43.89"
Barna mine section	26° 7'9.90"	73°44'39.19"
CDB	26 °7'41.263"	73 °43'35.04"
MNTP	26°35'26.8"	73 °45'56.1"
RSMS	26 °34'36.22"	73 °46'2.59"
Tucklian I	26 °38'46.91"	73 °45'16.52"
Birla mine section	26°35'31.54"	73°48'2.96"
Man singh	26 °20'37.3"	73 °47'55.7"
Tucklian II	26°37'52.50"	73°47'28.40

carbon and oxygen isotopic studies. The Bilara Group classified under three Formations viz. Dhanapa dolomite, Gotan limestone and Pondlu dolomite, in order of superposition. The Bilara litho-succession is studied from 15 sections (Table 2).

Carbon isotope study in the Bilara Group of rocks

Samples were collected from quarry sections including Man Singh, Birla, CDB, Harash, JP, RSME, Tucklian (I & II) and mound/hillock sections including Gopa and Bari Bawari. Samples collected from the basal part of the Bilara lithopackage (GirbakharBilara contact) at the Lordiya section could not be measured because of heavy chertification. Maximum and minimum values of $\delta^{13}C_{carb}$ at the Man Singh quarry section are 1.8 and -6.6, at the Birla quarry section are 2.4 and -10.4, at the CDB quarry section are 2.6 and -4.4, at the Harash section are -0.1 and -7.5, at the JP mine section are 0.3 and -3.2, at the RSME quarry section are 0.9 and -5.1, at the Tucklian I quarry section are 1.3 and -6.3, at Tucklian II quarry section are 1.6 and -7.2, at the Ashop quarry section are 0.1 and -6.8, at the Gopa hillock section are -4.1 and -4.7 and at the Bari Bawari mound section are -1.9 and -2.6. A preliminary look at the data reveals that through the Bilara lithopackage the $\delta^{13}C_{carb}$ value varies in a wide range between a maximum value of 1.3 and a minimum value of -10.4. Average mean value of $\delta^{13}Ccarb$ data of sections is -2.5 and range of mean values of different sections between -1.6 and -4.5. Likewise, $\delta^{18}O_{carb}$ values of samples also vary widely between 7.4 and -10.9 with most values ranging between 0 and -5; values less than -7 are considered unacceptably altered.

A variable covariation between $\delta^{13}C_{carb}$ and $\delta^{18}O_{carb}$ are recorded in section to section from the Bilara succession. Whereas some sections record strong correlation (R^2 values up to 0.91; Man Singh 0.88, Bilara 0.91, CDP 0.71, Harash 0.78, Tucklian 1 0.75), some record moderate correlation (R^2 values around 0.5; Ashop 0.59, Bari Bawari 0.45) and others record weak to very weak correlation (R^2 as low as 0.0008; JP 0.27, RSME 0.38, Tucklian II 0.26, Gopa 0.0008). A cross-plot of data from all sections together shows a correlation value (R^2) of 0.25. From observation of similar character that is variable correlation values (strong to weak) in individual sections and moderate to weak correlation from combining of all sections of Wonoka Formation, south Australia and Johnnie Formation in southwestern USA, identified this as a common and variable character of the SWE.

ANRF-DST Sponsored Project
Delineation of Subsurface Geological features Presiction of Missing logs and conditioning of Vintage sonic logs by machine learning perspective
(Bappa Mukherjee)

Accurate well log data is critical for subsurface characterisation and decision-making in the petroleum exploration. We explore and compare the effectiveness of three distinct deep leaning (DL) approaches namely Long Short-Term Memory, Bidirectional Long Short-Term Memory, and Convolutional Long Short-Term Memory networks in predicting missing well log data, a common challenge in the data acquired by Energy and Production (E&P) companies. An example of the missing logs in different geological formation with detailed depth interval is depicted in figure 105. Our analysis revealed the complex, nonlinear relationships present in geophysical logs through correlation matrix and determining the rank of predictor features through Minimum Redundancy Maximum Relevance (MRMR) analysis. To weigh these models, we used real-field wireline log datasets from the Bhogpara oil field of Upper Assam basin. The performance of each model is evaluated through root mean square error, correlation coefficients, mean absolute error and variance between actual and predicted values. The uncertainty of the models was facilitated by Monte Carlo simulation. Deep learning models accurately predicted neutron porosity logs from gamma-ray, resistivity, density, and photoelectric factor logs. The high correlation coefficients during the training (exceeding 0.90) and test (exceeding 0.97) phases illustrated the predictive precision of the DL models. Conv-LSTM consistently outperforms LSTM and Bi-LSTM, indicating the integration of convolutional layers in feature extraction offers a significant advantage in capturing intricate patterns in log data. For example, the predicted neutron
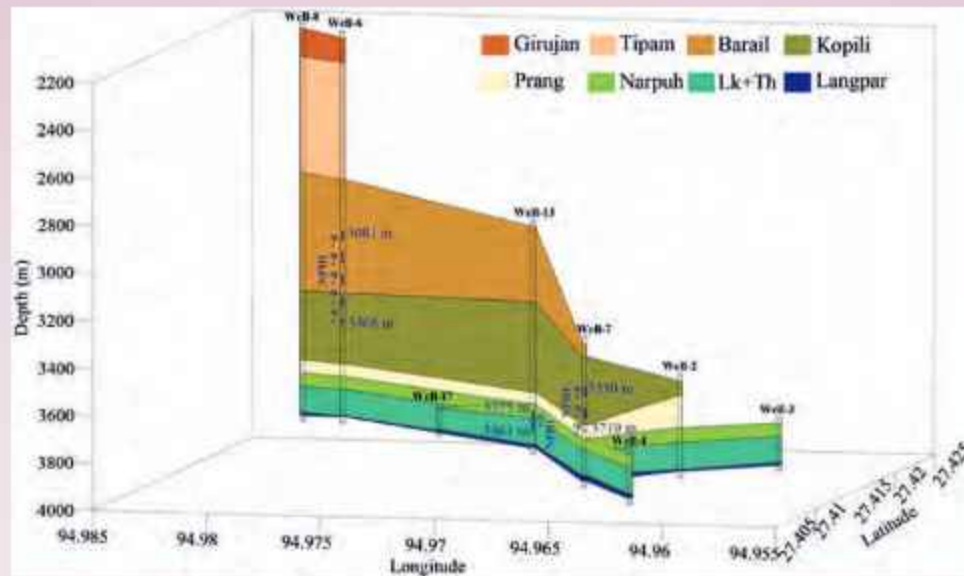
Fig. 105: Assume that the neutron porosity log is missing at wells 6 and 7 and 13, from the depth interval 3081 m to 3468 m (Barail to Kopili formation), 3550 m to 3719 m (Kopili to Prang formation), and 3775 m to 3861 m (Narpuh to Lk+Th formation), respectively. The absence of neutron porosity logs in the studied wells at distinct depth belongs to the mixed formations rather than single formation.
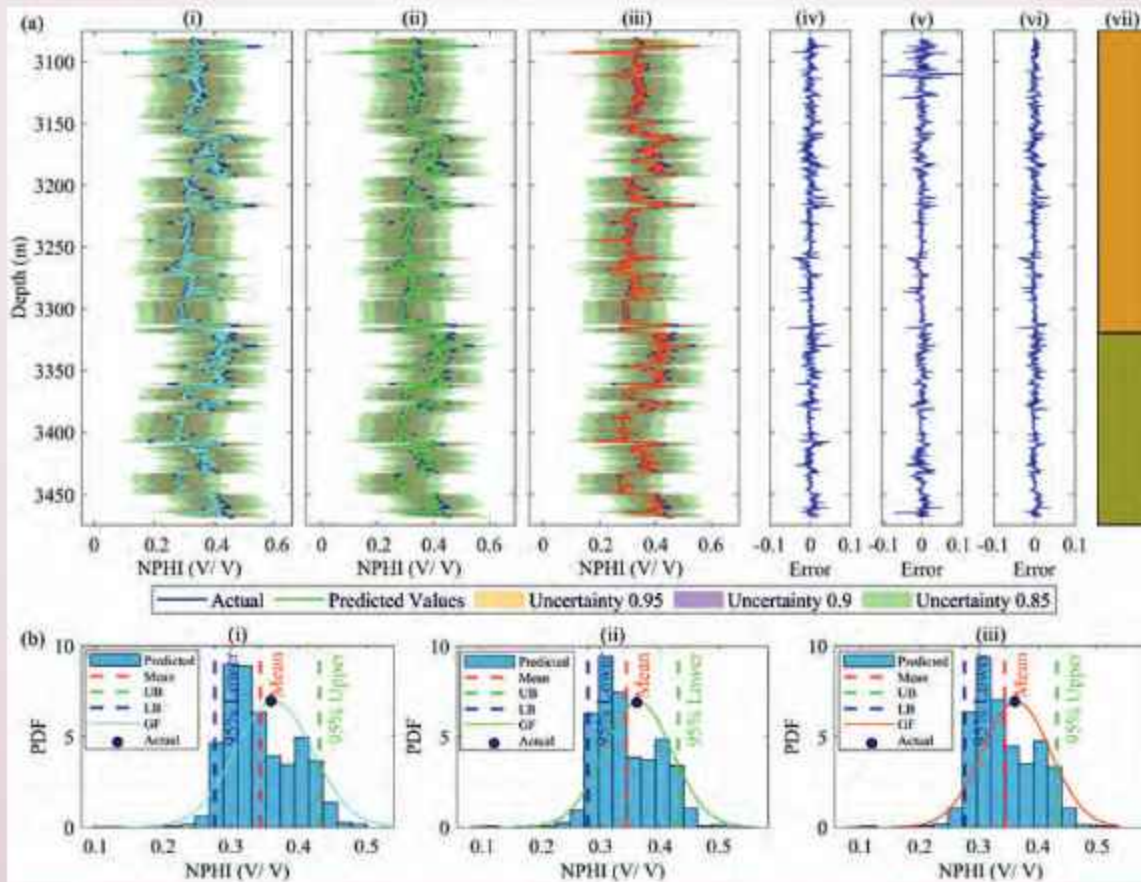
Fig. 106: Overlay of actual and predicted NPHI logs derived from DL models, and errors at the well-6: (a) LSTM (i), Bi-LSTM (ii), Conv-LSTM (iii), error in LSTM derived log (iv), error in Bi-LSTM derived log (v), error in Conv-LSTM derived log (vi), working depth interval partially belongs to Barail and Kopili formation(vii). (b) Monte Carlo simulation for the DL models (i) LSTM, (ii) Bi-LSTM and (iii) Conv-LSTM.

porosity log (NPHI) at well 2 is depicted in figure 106. The research showcases the effectiveness of deep learning architectures in predicting missing logs, a crucial aspect for E&P companies, as log data is vital for decision-making. The study presents a novel method for preserving data integrity and facilitating informed decision-making.

ANRF-DST Sponsored Project
Ore genesis, Fluid P-T Evolution and Physico-chemical characterization of Rangpo (Sikkim, India) base metal mineralization implication for the Himalayan metallogenic model
(Aditya Kharya)

Fifteen days of fieldwork were undertaken in the Rangpo area of Sikkim and in Gorubathan, West Bengal, with the primary objective of investigating the ore deposits and their associated host rocks. During the course of this work, representative ore and host rock samples were systematically collected from both study areas. Subsequent laboratory investigations focused in detail on the Rangpo deposit, where ore petrography, host rock petrography, and fluid inclusion studies were carried out to establish the paragenesis and the physicochemical conditions of mineralization.

Geothermometric and geobarometric analyses provided valuable insights into the temperature and pressure conditions of ore formation in the Rangpo area. FeS–ZnS geothermometry indicates that the mineralization occurred at temperatures ranging between 376 °C and 422 °C (Fig. 107). Complementary arsenic geothermometry using arsenopyrite compositions reveals a wider range of formation temperatures, from 322 °C to 477 °C (Fig. 108).
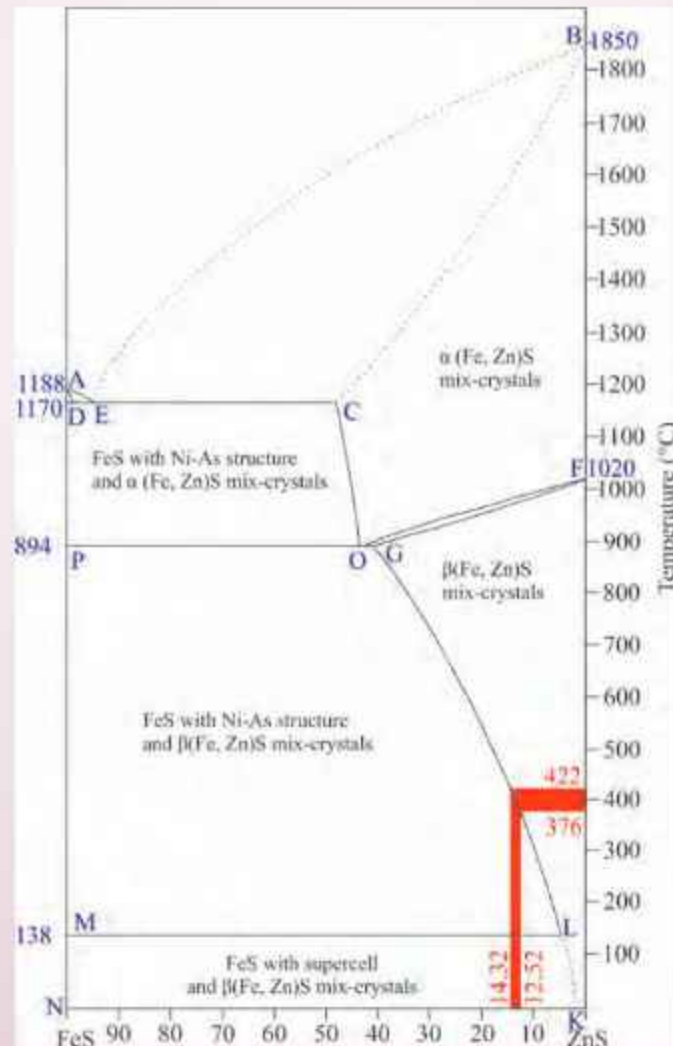
Fig. 107: FeS–ZnS phase equilibrium diagram (after Kullerud, 1953), illustrating the crystallization temperature of sphalerite.
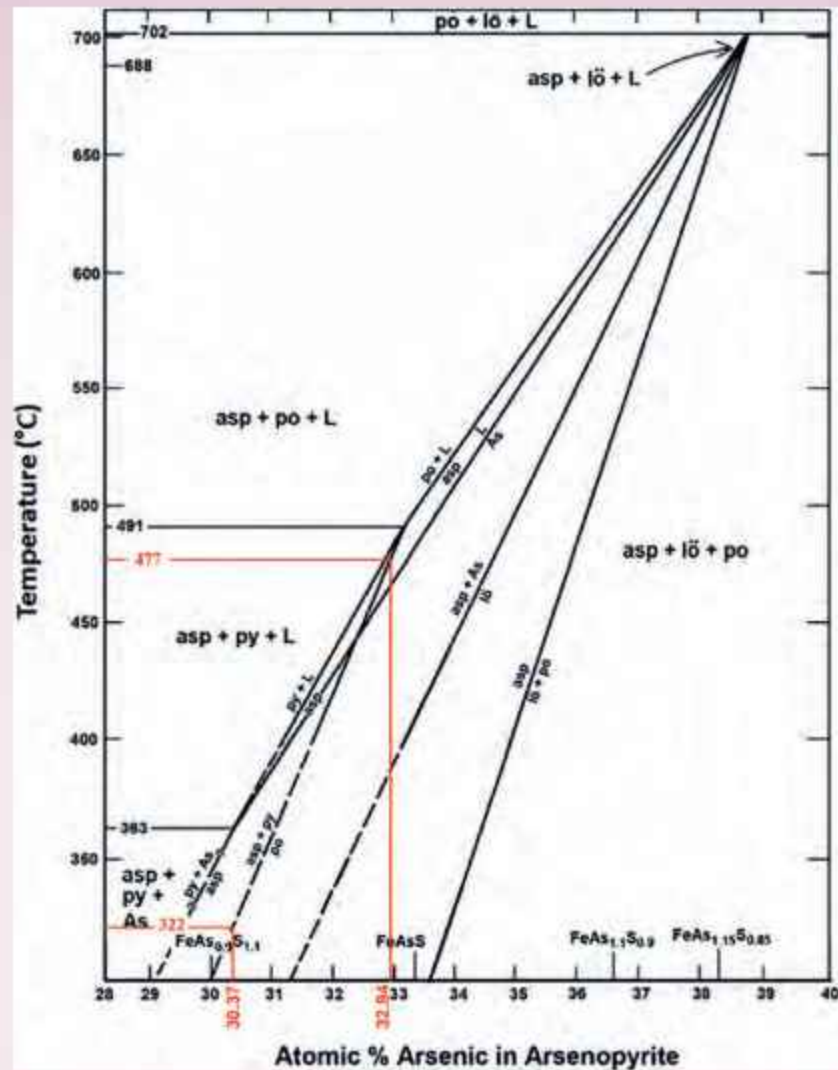
Fig. 108: Atomic % of As in arsenopyrite plotted on the phase equilibrium diagram of Kretschmar and Scott (1976), indicating the temperature regime of arsenopyrite crystallization.
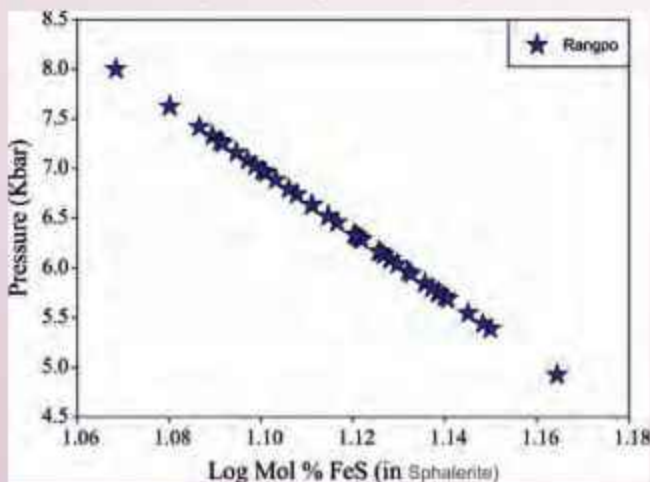
Fig. 109: Log mol% FeS diagram depicting the formation pressure conditions of sphalerite.

Sphalerite geobarometry further constrains the pressure conditions, yielding values between 5.19 and 7.06 kbar (Fig. 109). Integration of these results suggests that mineralization in the Rangpo area took place under pressure–temperature conditions between 322 °C at 5.16 kbar and 477 °C at 7.06 kbar.

These findings indicate that the Rangpo deposit formed under medium- to high-temperature hydrothermal conditions at mid-crustal depths. The combined approach of petrography, fluid inclusion studies, and geo-thermobarometry has provided robust constraints on the pressure–temperature regime of mineralization, offering new insights into the metallogenic evolution of the Sikkim–Darjeeling Himalaya.

ANRF-DST Sponsored Project

Crustal and upper mantle deformation and stress orientations through the shear wave splitting method beneath the Siang Valley, NE Himalaya
(Narendra Kumar)

This ANRF project has the main objective to explore a better understanding of the crustal and upper mantle deformation through the different seismological methods. We know that the Eastern Himalayan Syntaxis (EHS) is characterised by significant seismic activity, having produced the notable 1950 Assam earthquake (Ms 8.7, later revised to Mw 8.4, Ambraseys & Douglas 2004), which is the largest recorded in the Himalaya. This area is classified within zone V, indicating the highest level of vulnerability on India's seismic zoning map (BIS 2002). The EHS represents a complex triple junction where the Indian and Eurasian Plates converge with the northern extremity of the Burmese Plate (Curray 1989). At the eastern terminus of the Himalayan orogeny, a critical tectonic transition occurs, shifting from collisional dynamics to the north, which contributes to the uplift of the Tibetan Plateau, while also facilitating escape tectonics in Southeast Asia via strike-slip faults (Holt 1991; Molnar 1990; Beaumont et al. 2004; Misra 2009; Hazarika et al. 2013). The principal thrust sheets of the Himalaya, including the Main Boundary Thrust (MBT) and the Main Central Thrust (MCT), exhibit a pronounced bend as they connect with the Indo-Burma Ranges (IBR). Additionally, the Indus-Tsangpo Suture zone (ITSZ) also demonstrates a sharp deviation, locally referred to as the Tidding-Tuting suture zone within the Eastern Himalayan Syntaxis (EHS) (Figure. 1). The Siang antiform and the Mishmi Hills encompass a significant portion of the EHS, with the Mishmi Hills region emerging at the convergence of the Indian plate to the west, the Eurasian plate to the east and north, and the Burmese plate to the south. The Siang antiform, also referred to as the Siang window, serves as the focal point of the Syntaxis (Singh 1993; Acharyya 1998). The northeastern region of India has experienced two significant earthquakes, both exceeding a magnitude of 8.0: the Shillong earthquake on June 12, 1897 (Ms 8.7; Oldham 1899) and the Assam earthquake on August 15, 1950 (Tillotson 1951; Ben-Menahem et al. 1974). In addition to these major seismic events, the area has recorded over 20 substantial earthquakes (M>7.0) (Nandy 2001; Kayal 2008). The 1950 Assam earthquake (Ms 8.7) stands as the largest instrumentally documented event in the Himalaya, resulting in extensive destruction across upper Assam, the Mishmi Hills, and the Abor Hills (Podder 1950). This earthquake has been classified as a blind earthquake,

akin to the Gorkha earthquake of 2015. The 1950 event was attributed to right-lateral strike-slip faulting (Ben-Menahem et al. 1974), while the 1897 Shillong earthquake (M 8.7) is situated within the Assam seismic gap, as noted by Khattri & Wyss (1978). This region lies between the Eastern Himalaya and the northern segment of the Burmese arc.

Consequently, it is crucial to enhance our understanding and investigate the tectonic framework concerning the seismicity patterns and structural variations for effective seismic hazard assessment beneath the Siang window. Previous studies have primarily focused on the source parameters of earthquakes based on seismological data collected by various institutions; however, limited research has been conducted on the structural analysis beneath this region utilizing teleseismic data. Therefore, employing modern seismological techniques, such as shear wave splitting through S/SKS/SKKS and Ps phase analysis, alongside recorded seismological data from various seismic stations in the Siang Valley, will facilitate an investigation into the true nature of crustal and upper mantle deformation patterns, as well as the direction of Absolute Plate Motion (APM) beneath these seismic stations. A comprehensive understanding of the seismic structure and source parameters in this area will enable precise seismic hazard assessments, thereby mitigating risks and providing significant insights into the rupture zone.

ANRF-DST Sponsored Project

An Enhanced Landslide Risk Analysis and Prediction Model for the Kumaon Himalyan Region, India
(Naveen Chandra and RJ Perumal)

The project is currently in the initial stage. Compilation of landslide conditioning factors has been initiated, and thematic maps are under preparation. A field visit to the Kumaon Himalayan region is scheduled for the upcoming quarter, which will support data validation and ground-truthing.

ANRF-DST Sponsored Project

Decoding the Geodyanamic Evolution of Ladakh Batholith Dykes, North West Himalaya: Constraints from the Mineral Chemistry, Trace elements ratios, and Isotope Geochemistry
(Hrideya Chauhan)

Ladakh Himalaya is divided into four tectono-stratigraphic zones from north to south, i.e., Karakoram Zone, Shyok Suture Zone (SSZ), Indus Suture Zone (ISZ), Zanskar Zone (Searle et al., 1987). The Ladakh

SPONSORED RESEARCH PROJECTS

Batholith (LB) is a NW-SE trending longitudinal belt traceable throughout the ISZ and comprises diorite-granodiorite-granite rock assemblages. Although a significant amount of work has been carried out on the LB granitoids, however dykes intruding the LB have not been explored in details till date. The proposed project work will involve thorough studies on the dykes, mafic enclaves and associated host rocks which will include extensive field investigations, detailed petrography, geochemical analysis, mineral chemical analysis and radiogenic isotope analysis. Understanding the processes and relationships of formation of dykes with respect to the genesis of enclaves and associated host rocks, remains a major challenge of igneous petrology. In general, various discrepancies have been observed as follows: a) No ultra-potassic dykes have been found as reported by earlier worker b) Isotopic, structural and petrographic evidences suggest major differences in the formation and subsequent exhumation and retrogression histories in the LB. c) The dykes are geochemically diverse and exhibit various degrees of differentiation probably indicating heterogeneous sources, varying depths of generation, varying degrees of partial melting, fractionation of various mineral phases and possible role of crustal contamination and assimilation fractional crystallization. The results from this project will help in understanding the better picture of origin of dykes intruding the LB. As the formation of the LB is extremely important to understand and to construct the geodynamic model of the Ladakh Himalaya. Thus, gathering additional information from the dykes, mafic enclaves, and the associated host rocks will provide new insights into the present understanding of evolution of the Ladakh Himalaya as a whole. This will also throw light in better understanding of the range of geological records, history of collision of continents and disappearance of ocean basins as Ladakh is considered as a valuable geoheritage site of the world. Furthermore, such volcanic rocks have huge potential for Li, U, Th and rare earth mineral exploration.

RESEARCH PUBLICATIONS

Papers Published

1. Absar, A., Agnihotri, V., Ahmed, S., Alam, A., Azam, M.F., Bhat, M.S., Deshpande, R.D., Dimri, A.P., Jeelani, Gh., Jain, S., Juyal, N., Lone, S.A., Mal, S., Maharana, P., Maurya, A.S., Mukherjee, A., Muddu, S., Pottakkal, J., Romshoo, S.A., Sarin, M.M., Sain, K., Sharma, P. & Shrestha, A.B. 2024: Policy framework to combat the challenges of climate change in the Upper Indus Basin. Current Science, 127(6), 669-673. DOI: 10.18520/cs/v127/i6/669-673

2. Alam, M., Chauhan, P., Thakural, L.N., Malviya, D., Ahmad, R. & Sajid, M. 2025: Identification of groundwater recharge potential zone using geospatial approaches and multi criteria decision models in Udham Singh Nagar district, Uttarakhand, India. Advances in Space Research, 75(2), 1931-1944.

3. Babu, V.G., Kumar, N. & Pal, S.K. 2024: Stress regimes in the Himalaya-Karakoram-Tibet, the western part on India-Eurasia collision: stress field implications based on focal mechanism solution data. Geophysical Journal International, 239, 1380-1399.

4. Badhe, K., Ni, P., Wang, G.G., Liu, Z., Li, W., Ding, J. & Pan J. 2024: Fluid inclusion and pyrite geochemistry of the Jiapigou gold deposit, North China Craton: Implication for origin of orogenic gold deposit. Ore Geology Reviews, 174:106281. https://doi.org/10.1016/j.oregeorev.2024.106281

5. Banerjee, A., Mukherjee, B. & Sain, K. 2024: Machine learning assisted model based petrographic classification: A case study from Bokaro coal field. Acta Geodaetica et Geophysica, 59, 463-490.

6. Baruah, S., Dey, C., Chetia, T., Saikia, S., Gogoi, K., Hazarika, D., Phukan, M.K. & Kayal, J.R. 2024: The June 2022 Afghanistan earthquake M 6.0: Tectonic implications and Coulomb stress change. Himalayan Geology, 45(2), 252-259.

7. Bhambri, R. 2024: Contributions of Kenneth Mason to the physical geography of Himalaya and Karakoram. Progress in Physical Geography: Earth and Environment, 48(4), 637-645.

8. Bhargava, O.N., Singh, B.P., Shukla, U.K., Ganai, J., Singh, P., Thorie, A. & Mazumdar, P. 2024: Contributions to the Proterozoic–Phanerozoic successions in the Himalaya: Status report 2020-2024. Proceedings of the Indian National Science Academy, 90(2), 304-318. https://doi.org/10.1007/s43538-024-00275-0

9. Brice, A., Jayangondaperumal, R., Priyanka, R.S., Pandey, A., Mishra, R.L., Singh, I., Sati, M., Kumar, P. & Dash, S.P. 2024: Paleoseismological evidence for segmentation of the Main Himalayan Thrust in the Darjeeling-Sikkim Himalaya. Scientific Reports, 14:14537. https://doi.org/10.1038/s41598-024-63539-1

10. Brice, A., Pandey, A., Jayangondaperumal, R., Mohanta, A., Priyanka, R.S., Sati, M. & Sundriyal, Y. 2024: Damaging earthquakes of the Eastern Indian subcontinent and seismic hazard potential: insights from palaeoseismology. International Geology Review, 66(20), 3481-3503.

11. Chandra, N. & Vaidya, H. 2024: Automated detection of landslide events from multi-source remote sensing imagery: Performance evaluation and analysis of YOLO algorithms. Journal of Earth System Science, 133(3), 1-17.

12. Chandra, N. & Vaidya, H. 2024: Deep learning approaches for landslide information recognition: Current scenario and opportunities. Journal of Earth System Science, 133(2), 1-25.

13. Chandra, N., Vaidya, H., Satyam, N., Tang, X., Singh, S. & Meena, S.R. 2025: A Novel Multi-Layer Attention Boosted YOLOv10 Network for Landslide Mapping Using Remote Sensing Data. Transactions in GIS, 29:2, e70023. https://doi.org/10.1111/tgis.70023

14. Chandra, N., Vaidya, H., Sawant, S. & Meena, S.R. 2024: A Novel Attention-Based Generalized Efficient Layer Aggregation Network for Landslide Detection from Satellite Data in the Higher Himalayas, Nepal. Remote Sensing, 16(14):2598. https://doi.org/10.3390/rs16142598

15. Chatterjee, N., Gupta, A.K., Tiwari, S.K., Mohan, K. & Sharma, K. 2024: Quantification of Post-monsoon CO_2 Degassing Flux from the Headwaters of the Ganga River: Emphasis on Weathering Pattern of the Basin. Aquatic Geochemistry, 30(4), 287-315.

RESEARCH PUBLICATIONS

16. Chaubey, M., Singh, A.K., Imtisunep, S., Uysal I., Singh, B.P., Satyanarayanan, M., Longchar, B. & Khogenkumar, S. 2024: Formation of the associating high-Al and high-Cr chromitites in the Nagaland-Manipur Ophiolites in northeast India. International Geology Review, 67(2), 210-232. https://doi.org/10.1080/00206814.2024.2386565

17. Chauhan, M.M., Ali, S., Singh, B.P., Adlakha, V., Arif, M., Phartiyal, B., Venkateshwarlu, M. & Gahlaud, S.K.S. 2025: Reconstruction of the Late Miocene climate record in the Himalayan foreland Basin: The impact of Himalayan uplift and monsoon dynamics. Journal of Asian Earth Sciences, 280:106445. https://doi.org/10.1016/j.jseaes.2024.106445

18. Chauhan, M.M., Ali, S., Singh, B.P., Adlakha, V., Phartiyal, B., Kumar, K. & Sharma A. 2024: Silicate weathering linked with global climate change along the Mid-Pleistocene transition: A record from the Himalayan foreland Basin, India. Catena, 241:108047. https://doi.org/10.1016/j.catena.2024.108047

19. Chauhan, P., Akiner, M.E., Shaw, R. & Sain K. 2024: Forecast future disasters using hydro-meteorological datasets in the Yamuna river basin, Western Himalaya: Using Markov Chain and LSTM approaches, Artificial Intelligence in Geosciences, 5, 100069. https://doi.org/10.1016/j.aiig.2024.100069

20. Chaurasia, C., Thakur, S.S., Patel, S.C., Kumar, Samal, A., Kumar, S. & Gour, N. 2024: Tectonic evolution of the Higher Himalayan Crystalline Sequence, Dhauliganga valley, Garhwal Himalaya: Insights from P–T conditions of metamorphism and partial melting. Journal of Asian Earth Sciences, 265:106108. https://doi.org/10.1016/j.jseaes.2024.106108

21. Dahal, D.R., Mehta, M., Bhatt, C.M. & Luirei K. 2024. Flash floods and their cascading tumults: an example from Teesta River valley, Eastern Himalaya, Sikkim, India. Current Science, 126(10), 1280-1283.

22. Das, A., Hazarika, A., Neog, P., Kumar, N. & Yadav, D.K. 2025: Delineation of crustal structure and composition in the Northwest Himalaya and adjoining Indo-Gangetic Plain. Tectonophysics 904:230717. https://doi.org/10.1016/j.tecto.2025.230717

23. Das, S., Singh, S.K., Rai, S.K., Singhal, S., Rahaman, W., Rout, R.K. & Ali, S. 2025: Tectonics and climate controlled sedimentary provenance in the Teesta basin since Mid-Holocene. Geochemistry, 85:126224. https://doi.org/10.1016/j.chemer.2024.126224

24. Deshmukh, G.G., Jain, A.K., Mukherjee, P.K., Singhal, S., Dixit, R. & Srivastava, D.C. 2024: South Tibetan Detachment System (STDS), NW Himalaya: A possible Cambro–Ordovician tectonic terrane boundary, and its Cenozoic remobilization. Gondwana Research, 136, 142-168.

25. Devi, S., Pal, S.K., Sandeep, Kumar, P., Monika & Mittal, H. 2025: Source modelling of deep plate boundary 2021 Miyagi earthquake (Mw7.0) employing modified semi-empirical technique with site effects: A step forward towards hazard mitigation. Journal of Earthquake Engineering, 29(1), 55-74.

26. Diwate, P., Meena, N.K., Pandita, S., Luirei, K., Humane, S. & Bhushan, R. 2024: Diatoms from Indian Himalaya (Renuka Lake) Responses to 20th Century Global Warming and Climate Change. Geospatial Technology for Natural Resource Management, 303-320. https://doi.org/10.1002/9781394167494.ch12

27. Dutt, A., Shukla, A.D., Singh, A.K. & Narayanan A. 2024: A hydrous sub-arc mantle domain within the northeastern Neo-Tethyan ophiolites: Insights from cumulate hornblendites. Geochemistry, 84(3):126122 https://doi.org/10.1016/j.chemer.2024.126122

28. Dutt, S., Gupta, A.K., Jaiswal, J., Cheng, H. & Gupta, P. 2025: Linkage between global CO2 concentration and Indian summer monsoon between 309 and 260 kyr BP. Palaeogeography, Palaeoclimatology, Palaeoecology, 668:112906. https://doi.org/10.1016/j.palaeo.2025.112906

29. Gilbert, C.C., Ortiz, A., Pugh, K.D., Campisano. C.J., Patel, B.A., Singh, N.P., Fleagle, J.G. & Patnaik, R. 2025: Additional analyses of stem catarrhine and hominoid dental morphology support Kapi ramnagarensis as a stem hylobatid. Journal of Human Evolution, 103628. https://doi.org/10.1016/j.jhevol.2024.103628

30. Gogoi, B., Saikia, A., Chauhan, H., Taye, C.D. & Saikia, S. 2025: Geochemical characterization of a possible siderite deposit in the Abor volcano-

sedimentary sequence of the Eastern Himalayan Syntaxis. International Journal of Earth Sciences, 114, 407-423.

31. Gupta, A.K., Tiwari, A., Kumar, N., Paul, A., Sain, K., Yadav, D.K., Pal, A. & Baruah, D. 2025: Estimation of source parameters and scaling relationship of the local earthquakes in the Central Seismic gap NW Himalaya, India. Journal of Asian Earth Sciences, 280:106465, 1-18. https://doi.org/10.1016/j.jseaes.2024.106465

32. Haldar, C., Yadav, D.K., Sain, K. & Kumar, P. 2024: Crustal structure variation beneath the Indo-Gangetic Plain and Himalaya. Journal of Earth System Science, 133:191. https://doi.org/10.1007/s12040-024-02402-3

33. Hazarika, D., Shukla, N., Das, A., Hajra, S. & Mukhopadhyay, S. 2024: A shallow mantle seismic discontinuity beneath northeast India: Evidence from receiver function analyses. Journal of Asian Earth Sciences, 276:106375, https://doi.org/10.1016/j.jseaes.2024.106375,

34. Hazarika, G., Chauhan, H. & Gogoi, B. 2024: Fractal analysis and formation of biotite clots within double-layered mafic magmatic enclaves in the Bamuni Pluton, Mikir Massif, Northeast India. Periodico di Mineralogia, 93(2), 85-103.

35. Hifzurrahman & Sen, K. 2025: Pre-Himalayan metamorphism constrained from mineral chemistry and metamorphic modelling in a retrogressed garnet bearing micaschist from Himachal Lesser Himalaya. Himalayan Geology, 46(1), 61-76.

36. Hifzurrahman, Nasipuri, P., Ganaie, A.M., Balakrishnan, S. & Dash, J.K. 2024: Cambro-Ordovician metamorphism from Lesser Himachal Himalaya and its implication for Gondwana assembly. Mineralogy and Petrology, 118(2), 209-229. https://doi.org/10.1007/s00710-024-00855-4

37. Hussain, M.S., Phukon, P., Kalita, P., Singh, A.K., Kumar, D. & Saikia, H. 2024: Tectonic evolution of the Greater Himalayan Sequence and its associated fault systems in space and time: a monazite perspective. International Geology Review, 67(8), 1065-1097. https://doi.org/10.1080/00206814.2024.2425988

38. Iqbal, V., Parray, D.S., Islam, Z., Lone, S.A., Balaji, S., Saleem, M., Shah, R.A. & Bhat, G.R. 2024: Geoelectrical and Hydrochemical Insights in Tracing the Seawater Intrusion Along Coastal Aquifers of the East Coast of South Andaman Island, India. Earth Systems and Environment, 9, 653-675. https://doi.org/10.1007/s41748-024-00549-z

39. Kapawar, M., Kumar, V., Shankar, R. & Mamilla, V. 2024: Environmental Magnetic and Morphological Characteristics of Topsoils from the Coal Capital of India-Dhanbad. Water, Air, and Soil Pollution, 235:670. https://doi.org/10.1007/s11270-024-07483-w

40. Kapawar, M., Saha, S., Kumar, A. & Mamilla, V. 2024: Magnetic mineral characterization of the easternmost Indus Molasse sedimentary succession, Ladakh Himalaya: Implications for depositional environment and provenance. Journal of Earth System Science, 133:88. https://doi.org/10.1007/s12040-024-02302-6

41. Karakoti, I., Mehta, M. & Dobhal, D.P. 2024: Impact of climate change on Himalayan water resources: a predictive model for glacier surface melt assessment. Sustainable Water Resources Management, 10:150, 1-14. https://doi.org/10.1007/s40899-024-01110-6

42. Kaushik, S., Bagri, D.S., Sundriyal, Y., Kumar, S., Chauhan, N., Rana, N. 2024: Understanding the role of topography, climate, and sediment transport dynamics in flash flood hazards along the Dhauli Ganga River of northwest Himalaya, India. Journal of Earth System Science, 133:233. https://doi.org/10.1007/s12040-024-02444-7

43. Kothyari, G.C., Joshi, A., Dumka, R.K., Kotlia, B.S., Patidar, A.K., Joshi, M., Luirei, K., Naik, S.P., Taloor, A.K., Joshi, M. & Kothyari, H.C. 2024: Assessment of Active Deformation in the Surrounding Regions of the 7th to 12th AD Monuments in the Central Kumaon Himalayas: A Seismotectonic Approach using PSInSAR. Geoheritage, 16, 123.

44. Krishna, E.S., Venkateshwarlu, M., Kapawar, M.R., Sabale, P.D., Babu, N.R. & Shinde V.S. 2024: Rock magnetism and preliminary archaeointensity results from Harappa potsherds, India. Current Science, 126(10), 1236-1244. DOI:10.18520/cs/v126/i10/1236-1244

45. Kumar, A., Sain, K., Kumar, K., Patidar, P., Meenakshi, Reza, A., Verma, A. & Mishra, A. 2024: Anticipating the impact of glaciers, landslides and extreme weather events on vulnerable hydropower projects and the

RESEARCH PUBLICATIONS

development of an integrated multi-hazard warning system (IMWS). Sustainable Energy Technologies and Assessments, 65:103791. https://doi.org/10.1016/j.seta.2024.103791

46. Kumar, A., Singh, A.L., Rajak, P.K., Kumar, A. & Singh, P.K. 2024: Beneficiation of High Sulfur Tertiary Coal of Assam with Burkholderia sp. GR 8-02. An Eco-Friendly Approach Toward Clean Coal Production, Geomicrobiology Journal, 41(10), 996-1007. https://doi.org/10.1080/01490451.2024.2412005

47. Kumar, J., Mukherjee, B. & Sain, K. 2024. Porosity prediction using ensemble machine learning approaches: A case-study from Upper-Assam basin. Journal of Earth System Science, 133:99, 1-13. https://doi.org/10.1007/s12040-024-02310-6

48. Kumar, M., Singh, A.K., Bikramaditya R.K., Singh, N.S. & Imtisunep S. 2024: The Kerguelen mantle plume activity in Sylhet Trap mafic rocks of Southern Shillong Plateau, NE India: Implications for its role in magmatism of eastern India. Geological Journal, 59(8), 2243-2265. https://doi.org/10.1002/gj.5013

49. Kumar, P., Gahalaut, V.K. & Ghosh, A. 2025: Fault geometry control on earthquake segmentation and locking transition on mid-crustal ramp in Kumaun-Garhwal, Central Himalaya: Implications for regional tectonics and seismic hazard. Tectonics, 44:e2025TC008855. https://doi.org/10.1029/2025TC008855

50. Kumar, P., Matta, G. & Kumar, A. 2024: Harmonizing water quality: Integrating indices and chemo-metrics for sustainable management in the Ramganga river watershed. Analytical Chemistry Letters, 14(1), 29-47.

51. Kumar, P., Matta, G., Kumar, A. & Pant, G. 2024: Groundwater Quality and Potential Health Risk Assessment for Potable Use. World, 5(4), 2673-4060.

52. Kumar, P., Sahakian, V.J., Monika & Sandeep 2024: Frequency-dependent Layered Q Model and Attenuation Tomography of the Himachal North-West Himalaya, India: Insight to Explore Crustal Variation. Pure and Applied Geophysics, 181, 3539-3559.

53. Kumar, P.C., Bedle, H., Kumar, J. & Sain, K. 2024: Seismic aberrancy unraveling basement flexures: A study from northeast India. Interpretation, 12(4), T523-T536.

54. Kumar, P.C., Bedle, H., Kumar, J., Sain, K. & Konar, S. 2024: Unsupervised learning approach for revealing subsurface tectono-depositional environment: A study from NE India. Applied Geophysics, 229:105478. https://doi.org/10.1016/j.jappgeo.2024.105478

55. Kumar, P.C., Saikia, P.P., Bedle, H. & Sain, K. 2025: Unsupervised machine learning models applied to basement faults: An example from the Dibrugarh region, NE India. Journal of Asian Earth Sciences, 280: 106446. https://doi.org/10.1016/j.jseaes.2024.106446

56. Kumar, S., Ahmad, T. & Pundir, S. 2024: Petrotectonic evolution of Himalaya and Trans-Himalaya. Proceedings of the Indian National Science Academy, 90, 253-265. https://doi.org/10.1007/s43538-024-00276-z

57. Kumar, V., Rana, A.S., Mehta, M. & Rawat G. 2024: Manifestations of a glacier surge in central Himalaya using multi-temporal satellite data. Environmental Science and Pollution Research, 31, 66184-66202.

58. Kunmar, P., Mehta, M., Kumar, V., Rana, A.S. & Nainwal, H.C. 2025: Variations in meltwater discharge and morphological changes of Parkachik Glacier, Suru River Valley, Ladakh Himalaya. Himalayan Geology, 46(1), 77-90.

59. Kunmar, P., Rana, A.S., Kumar, V., Mehta, M. & Nainwal, H.C. 2025: Glacial landforms and geometric transformations: tracing the history of Pensilungpa and Durung-Drung glaciers in Suru and Doda River valleys, Western Himalaya, Ladakh. Environmental Monitoring and Assessment, 197, 272, 1-28.

60. Luirei, K., Kothyari, G.C., Gautam, P.K.R., Solanki, A., Patidar, A.K., Jamir, S., Datta, A. & Choudhury, T. 2024: Evolution of tectonic landscapes and deformation in the southeast Kumaun and western Nepal Himalaya. Journal of Mountain Science, 21(8), 2592-2617.

61. Meena, N.K., Khan, F., Sundriyal, Y., Wasson, R.J., Kumar, P. & Sharma, R. 2024: Holocene paleoclimatic records from Chakrata area, Northwest Himalaya. Quaternary International, 709, 43-54. https://doi.org/10.1016/j.quaint.2024.08.008

62. Mishra, A., Kumar, A., Sain, K., Verma, A. & Patidar, P. 2024: Glacier Changes and Fragmentation in Birahi Ganga Basin, Garhwal

Himalaya: Implications for Water Resources. Journal of the Geological Society of India, 100(8), 1075-1084.

63. Mishra, M.K., Alam, M., Kaulina, T.V., Ahmad, T. 2024: Geochemical characterization and zircon U–Pb geochronology of the Tirodi Gneissic Complex, Central Indian Tectonic Zone (CITZ): constraints on petrogenesis, Proterozoic crustal evolution and tectonic setting. Mineralogy and Petrology, 118, 159-183. https://doi.org/10.1007/s00710-024-00853-6

64. Mishra, R.L. 2024: An Appraisal of Geoheritage Potential: From The Delhi-Aravalli Fold- and The Himalayan Fold-Thrust Belts to the Coastal Plains of India. Geoheritage, 16:50, 1-16. https://doi.org/10.1007/s12371-024-00962-w

65. Mishra, S.R., Chakraborty, P.P., Das, K., Saha, S., Shibata, T., Mohanty, S.P. & Tripathi, S.C. 2024: Tracking provenance shift in the Cretaceous-Paleogene sedimentary succession of the Garhwal foreland basin, NW Himalaya using sediment geochemistry and U-Pb detrital zircon geochronology. Journal of Asian Earth Sciences, 264:106067. https://doi.org/10.1016/j.jseaes.2024.106067

66. Monika, Kumar, P., Sandeep, Joshi, A. & Pal, S.K. 2024: 3D Attenuation Tomography of the Uttarakhand, NW Himalaya: Linkage to fluid or partial melt Zones - seismic hazard. Soil Dynamics and Earthquake Engineering, 182:108699, 1-14. https://doi.org/10.1016/j.soildyn.2024.108699

67. Mukherjee, B., Kar, S. & Sain, K. 2024: Machine learning assisted state-of-the-art-of petrographic classification from geophysical logs. Pure and Applied Geophysics, 181, 2839-2871. https://doi.org/10.1007/s00024-024-03563-4

68. Mukherjee, B., Konar, S. & Sain, K. 2024: Characterisation of gas hydrate-hosted media using fractal analysis of geophysical logs: a case study from Krishna-Godavari basin. Carbonates Evaporites, 39:73. https://doi.org/10.1007/s13146-024-00982-1

69. Mukherjee, B., Sain, K. & Wu, X. 2024: Missing log prediction using machine learning perspectives: A case study from upper Assam basin. Earth Science Informatics, 17, 3071-3093. https://doi.org/10.1007/s12145-024-01323-5

70. Mukherjee, B., Sain, K., Ghosh, R. & Konar, S. 2024: Translation of machine learning approaches into gas hydrate saturation proxy: a case study from Krishna-Godavari (KG) offshore basin. Marine Geophysical Research, 45:12. https://doi.org/10.1007/s11001-024-09546-3

71. Mukherjee, B., Sain, K., Kar, S. & Srivardhan, V. 2024: Deep learning-aided simultaneous missing well log prediction in multiple stratigraphic units: a case study from the Bhogpara oil field, Upper Assam, Northeast India. Earth Science Informatics, 17, 4901-4929. https://doi.org/10.1007/s12145-024-01425-0

72. Mukherjee, B., Srivardhan, V., Sain, K. & Gupta, A. 2024: Chaotic behavior of geophysical logs for stratigraphic hiatuses: A case study from Upper Assam Shelf, India. Journal of Asian Earth Sciences, 271: 106233. https://doi.org/10.1016/j.jseaes.2024.106233

73. Mukherjee, B.K. & Saha, T. 2024: Tracing a remnant of subducted Indian felsic crust: insights from zircon studies. Journal of the Geological Society, 181(4), 116. https://doi.org/10.1144/jgs2023-116

74. Mukherjee, P.K., Kumar, P., Singhal, S., Singh, P., Upadhyay, D., Rahman, W., Thomson, J.K., Das, S., Jain, A.K. & Chopra, S. 2024: Geochronological and metal isotopic studies in India: an overview of new and existing geoanalytical facilities in India. Proceedings of the Indian National Science Academy, 90(2), 494-505.

75. Narayan, S., Kumar, V., Mukherjee, B., Shaoo, S.D. & Pal, S.K. 2024: Machine learning assisted appraisal of CO_2 sequestration in clastic reservoirs: A case study from Penobscot field, Canada Offshore. Marine and Petroleum Geology, 169:107054. https://doi.org/10.1016/j.marpetgeo.2024.107054

76. Pal, A., Yadav, D.K., Gupta, A.K. & Nainwal, H.C. 2024: Seismotectonics of Siang Valley and Adjoining Region Inferred from Focal Mechanism Solutions Using Waveform Inversion. Pure and Applied Geophysics, 182(3), 1217-1236.

77. Pal, A., Yadav, D.K., Kumar, N., Gupta, A.K., Paul, A. & Nainwal, H.C. 2024: Modelling of source parameters of local earthquakes and seismotectonic implications in Siang Valley, NE India. Journal of Earth System Science, 133, 63-76.

RESEARCH PUBLICATIONS

78. Pal, S.K., Sandeep, Gangajal, S., Kumar, P. & Mittal, H. 2024: Development of region-specific earthquake early warning scaling relations for the Garhwal region using observed and simulated datasets: A step forward to disaster mitigation. Bulletin of Earthquake Engineering, 22, 3875-3904.

79. Pappachen, J.P., Hamdan, H.A., Rajesh, S., Masoud Darya, A. & Shanableh, A. 2024: Possible seismo-ionospheric anomalies of Mw 6.0 and 6.4 south Iran twin earthquakes on 14 November 2021 from GPS and ionosonde observations. Arabian Journal of Geosciences, 17:201, https://doi.org/10.1007/s12517-024-12005-3

80. Pirasteh, S., Samad, A., Ahmad, R., Thakural, L.N., Khan, H.H., Chauhan, P., Khan, A. & Qamar, M.Z. 2025: Geospatial and AHP based identification of potential zones for groundwater recharge in Haridwar District of India. Frontiers in Environmental Science, 13. https://doi.org/10.3389/fenvs.2025.1421918

81. Pradhan, P., Pundir, S., Adlakha, V., Mukherjee, K., Patel, R.K. 2025: Exhumation history of the Karakoram Fault zone, NW India: New constraints from Zircon and Apatite Fission Track Thermochronology. Himalayan Geology, 46(1), 48-60.

82. Prajapati, R., Mukherjee, B., Singh, U.K. & Sain, K. 2024: Machine learning assisted lithology prediction using geophysical logs: A case study from Cambay basin. Journal of Earth System Science, 133:108. https://doi.org/10.1007/s12040-024-02326-y

83. Prakash, D., Pandey, R.K., Singh, S., Singh, C.K., Kumar, M., Mahanta, B., Kharya, A., Sachan, H.K. & Sharma, K. 2025: Phase equilibria modelling, fluid inclusion study, and U-Pb zircon dating of ultra-high temperature mafic granulites from Rampur domain, Eastern Ghats province: implications for the Indo-Antarctic correlation. Contributions to Mineralogy and Petrology, 180 (3).

84. Pundir, S. & Adlakha, V. 2024: Geological Evolution of the Karakoram Terrane since Neoproterozoic. Earth-Science Reviews, 257:104890. https://doi.org/10.1016/j.earscirev.2024.104890

85. Rajak, P.K., Gopinathan, P., Kumar, A. Kumar, O.P. Rahi, I.C., Sharma, A, Singh, P.K. & Karmakar, A. 2024: Geochemical and mineralogical assessment of environmentally sensitive elements in Neyveli lignite deposits, Cauvery Basin, India, Environmental Geochemistry and Health, 46:431. https://doi.org/10.1007/s10653-024-02193-y

86. Ram, B.K., Shawez, M., Gupta, V. & Rawat, G. 2024: Ground subsidence in Dar village (Darma valley), Pithoragarh district, Kumaun Himalaya, India: A Himalayan disaster in waiting. Journal of Earth System Science, 133:34. https://doi.org/10.1007/s12040-023-02244-5

87. Rana, S., Choudhary, S., Tiwari, S. K., Yadav, J. S. & Sharma, R. 2025: Source identification and geochemical characteristics of surface and groundwater from Larji-Rampur window, Himachal Himalaya: Implications for socio-environmental perspectives. Results in Earth Sciences, 3:100074. https://doi.org/10.1016/j.rines.2025.100074

88. Rathore, D., Gopinathan, P., Rajak, P.K., Kumar, A., Prakash, O., Karmakar, A., Singh, K.N. & Subramani, T. 2025: Elemental Composition and Petrographic Analysis of Coal in the Sohagpur Coalfield, India with Implications for Environmental Management. Geological Journal, 1-22. https://doi.org/10.1002/gj.5185

89. Ravindra, R., Kulkarni, A.V., Dimri, A.P., Sain, K., Sharma, M.C., Banerjee, A., Sharma, P., Meloth, T., Rashid, I. & Pant, N.C. 2024: Recent Indian studies in Himalayan cryosphere. Proceedings of the Indian National Science Academy, 90, 415-425. https://doi.org/10.1007/s43538-024-00237-6

90. Rawat, G. 2024: Natural Hazards are rooted in Himalayan topography. Science India, 19(100), 21-24.

91. Sagwal, S., Panda, S., Sengupta, D., Shahrukh, M., Kumar, S., Kumar, A. & Dutt, S. 2024: Flash flood dynamics in the foothills of the NW Himalayas: insights into hydrological and morphological controls. Environmental Monitoring and Assessment, 197:81. https://doi.org/10.1007/s10661-024-13541-x

92. Saha, S. 2024: Pre-Vegetation Mixed (Wave-Tide) Energy Trangressive Nearshore Sedimentation: Evidence from the Proterozoic Passive Margin Sequence of NW Himalaya, India. Geological Journal, 60, 359-386. https://doi.org/10.1002/gj.5078

93. Saha, S. 2025: Pre-Vegetation Mixed (Wave-Tide) Energy Trangressive Nearshore Sedimentation: Evidence from the Proterozoic Passive Margin Sequence of NW Himalaya, India. Geological Journal, 60(2), 359-386.

94. Sain, K. 2024: Georesources and geohazards in the Himalaya: a way forward for economy and ecology. Current Science, 126, 10, 1191-1192.

95. Sain, K. 2024: Glacial hazards and forest fires in Uttarakhand Himalaya and their plausible mitigation. Current Science, 127, 4, 383-384.

96. Sain, K., Chauhan, P., Bisht, P. & Vaideswaran, S.C. 2025: Cloudburst-induced debris flows and flash floods at Lasko valley in Pithoragarh district, India-Nepal border. Journal of Himalayan Geology, 46(1), 91-100.

97. Sain, K., Hazarika, D., Sen, K. & Jayangonda-perumal, R. 2024: Status of geo-scientific research at Wadia Institute of Himalayan Geology, Dehradun during 2020–2023. Proceedings of the Indian National Science Academy, 90, 530–551.

98. Sajwan, R.S., Joshi, V., Ahamad, T., Kumar, N., Parmar, P. & Jindal, M.K. 2024: Assessment of radon transportation and uranium content in the tectonically active zone of Himalaya, India. Science of the Total Environment, 926:171823. DOI: 10.1016/j.scitotenv.2024.171823

99. Sajwan, R.S., Joshi, V., Kumar, N., Ahmad, T., Dutt, S. & Lavanya, B.S.K. 2024: A study of 222Rn/220Rn exhalation rate and indoor 222Rn/220Rn levels in the higher Himalayan terrain. Radiation Protection Dosimetry, 200(11-12), 1018-1026.

100. Sarkar, S., Das, S., Choudhury, S. & Sinha, R.K. 2024: Land Subsidence Phenomena in Joshimath Town, Garhwal Himalaya, India: Field Observations and Possible Causes. Journal of the Geological Society of India, 100(4), 467-472. https://doi.org/10.17491/jgsi/2024/173863

101. Sengupta, D., Dutt, S., Warken, S. F., Singam, A., Frank, N., Sagwal, S. & Maurya, S. 2025: Climate-change induced human migration and socio-political changes in eastern India during the Meghalayan age. Palaeogeography, Palaeoclimatology, Palaeoecology, 667:112873. https://doi.org/10.1016/j.palaeo.2025.112873

102. Sharma, V., Bora, D.K., Hazarika, D. & Biswas, R. 2024: Characterization of seismic b value around Kopili fault and its neighboring region prior to 28th April 2021 earthquake. Journal of Seismology, 28, 1001-1025, https://doi.org/10.1007/s10950-024-10232-5.

103. Shawez, M., Gupta, V., Gupta, A.K. & Rawat, G. 2025: Spatial distribution of landslides in response to the geomorphometric constraints in Darma Valley, Kumaun Himalaya. Journal of Mountgain Science, 22, 48-70. https://doi.org/10.1007/s11629-024-8983-3

104. Shchepetkina, A., Moal-Darrigade, P., Pekar, S., Williams, T., Prakasam, M. et al. 2024: Estimating CaCO$_3$ Content Based on Natural Gamma Ray (NGR) in Deep-Ocean Sediment Cores. Stratigraphy, 21(3), 225-242.

105. Shrivas, A. & Pandey, C.P. 2024: Optical and Physico-chemical Characteristics of Ambient Aerosols Along Gangotri Glacier Valley in Western Himalaya, India. Aerosol Science and Engineering, 1-13.

106. Singh, M.R., Singh, P., Sethy, P.C. & Singh, A.K. 2024: Geochemistry of mafic rocks from the nagrota-kathindi section, himachal pradesh, northwestern himalaya: a probable example of plume-lithosphere interaction. Geological Journal, 59(12), 3175-3202.

107. Singh, N.A., Singh, N.P., Sharma, K.M., Patnaik, R. & Tiwari, R.P. 2024: Miocene cartilaginous fishes (Chondrichthyes, Elasmobranchii) from India: A review on global palaeobiogeography. Indian Journal of Geosciences, 78(3), 311-330.

108. Singh, S., Joshi, A., Singhal, S., Pandey, M. & Kushwaha, A. 2024: Southernmost limit of felsic magmatism along North Almora Thrust in the Himalayan domain. Geological Journal, 59(10), 2803-2818.

109. Singh, Y.P., Kingson, O., Sharma, K.M., Tiwari, R.P., Patnaik, R., Ghosh, P., Sharma, A., Pattanaik, J.K., Kumar, P., Thomas, H., Singh, N.P., Kisku, P.C. & Singh, N.A. 2025: Geochemistry of the siliciclastic sediments from the Raniganj Gondwana basin, West Bengal, India, and its geological implications. Acta Geochimica. https://doi.org/10.1007/s11631-025-00756-z

110. Singhal, S., Singh, S. & Singh, D. 2025: Minimizing Variable Downhole Fractionation in U-Pb Zircon Geochronology by LA-MC-ICP-MS at Smaller Spot Size. Journal of Mass Spectrometry. 60:e5115. https://doi.org/10.1002/jms.5115

111. Sonawane, D., Halder, S., Kumar, U., Satyapragyan, S. & Bhambri, R. 2025: Glacier Lake Changes in Uttarakhand, India from 2013 to

2023 using High Resolution Satellite Images. Journal of Geological Society of India, 101(5), 1-9.

112. Srivardhan, V. & Mukherjee, B. 2024: Estimating Reservoir Properties of 2D CT Scan Core Images using Machine Learning. Journal of Asian Earth Sciences, 133:200. https://doi.org/10.1007/s12040-024-02379-z

113. Tiwari, A., Sain, K., Tiwari, J., Kumar, A., Kumar, N., Paul, A. & Shukla, V. 2024: Seismic and radon signatures: A multiparametric approach to monitor surface dynamics of a hazardous 2021 rock-ice avalanche, Chamoli Himalaya. Earth Surface Processes and Landforms, 49(10), 2965-2979.

114. Tiwari, S.K., Yadav, J.S., Sain, K., Rai, S.K., Kharya, A., Kumar, V. & Sethy, P.C. 2024: Water quality assessment of Upper Ganga and Yamuna river systems during COVID-19 pandemic-induced lockdown: imprints of river rejuvenation. Geochemical Transactions, 25(8), 1-22.

115. Vandana & Kumar, N. 2025: Assimilation of seismic attenuation model of NW Himalaya and its surrounding region. Geosystems and Geoenvironment, 4:100378, 1-14. https://doi.org/10.1016/j.geogeo.2025.100378

116. Yadav, J., Parkash, R., Khyalia, B., Chauhan, R.P., Singh, P.P., Singh, P. & Dalal, R. 2024: Investigation of radon and thoron exhalation rates in soils: Manali-Leh Highway region of Himalayas. Journal of Environmental Radioactivity, 280, 107552. https://doi.org/10.1016/j.jenvrad.2024.107552

117. Yadav, J.S., Tiwari, S.K., Bhambri, R., Sain, K., Patidar, P. & Baiswar, A. 2024: Inter-Intraseasonality of Meteorological Drivers of Chorabari Glacier, Central Himalaya: Implications for Mass Fluctuations and Associated Hazards. Journal of Hydrometeorology, 2(10), 1541-1560. https://doi.org/10.1175/JHM-D-22-0231.1

Non SCI / Book Chapter

1. Choudhury, S., Bose, Shubham, Singh, Riya 2024: Silkyara –The Background and Layout of the Land: Observation of the Geology, pp. 17-24. In: Pant, Durgesh (ed), The Triumph of Silkyara: A Saga of Resilience and Leadership. Book World, Dehradun, 150p.

2. Mehta, M. 2025: Existing and Potential Changes in Himalayan Glaciers: In Climate Change Perspective, pp. 149-172. In: Rastogi, B.K., Kothyari, G.C., Luirei, K. (eds), Natural Hazards and Risk Mitigation: Natural Hazards in Himalayan and Risk Mitigation. Springer Transactions in Civil and Environmental Engineering.

3. Pandey, A. & Jayangondaperumal, R. 2024: Great Earthquakes of the Central Seismic Gap Through Paleoseismological Perspective, pp. 245-260. In: Rastogi, B.K., Kothyari, G.C., Luirei, K. (eds), Natural Hazards and Risk Mitigation: Natural Hazards in Himalayan and Risk Mitigation. Springer Transactions in Civil and Environmental Engineering.

4. Pandey, M. & Bisht, P. 2024: Stream Channel Dynamics over Alluvial Fan Systems: An Overview, 30p. In: Pandey, P.C., Srivastava, P.K. & Srivastava, S.K. (eds), Aquatic Ecosystems Monitoring: Conventional Assessment to Advanced Remote Sensing. CRC Press, 340p. https://doi.org/10.1201/9781003354000

5. Singh, V.B., Madhav, S., Gupta, R.K., Diwan, P. & Kumar, A. (Eds). 2025: Water Resources Management in Mountain Regions. John Wiley & Sons, 410p. DOI:10.1002/9781394249619

Excursion Guide

1. Jayangondaperumal, R. & Mishra, R.L. 2024: Excursion Guide to the Jammu Sub-Himalayan Belt, India. 8th NGRM, SMVDU, 22 to 25-11-2024, Katra, 34p, Wadia Institute of Himalayan Geology Special Publications, Special Publication No. 6 (ISSN No. 718966).

Technical Report

1. Jayangondaperumal, R. & Mehta M. 2024. Interim Report on the geological investigation for the construction of via duct on the bypass road project at Marwari, Joshimath. Submitted to KCC Buildcon Pvt. Ltd.

2. Mukherjee, B.K. 2024. 1st Report on the Pernote land sinking in Ramban, Jammu & Kashmir for the National Green Tribunal (NGT).

3. Mukherjee, B.K. 2024. Report on the Hill extinction assessment in the Banda Granite Mining area, UP, for the National Green Tribunal (NGT).

4. Sekar, K.C., Padalia, H., Sen, S., Kumar, A., Mondal, K., Kaistha, M.L., Singh, S. & Gupta, V. 2024. Joint Committee report in the matter of original application No. 720/2023 article published in Current Science, dated 25.10.2023 entitled "Need to declare the Higher Himalaya an eco-sensitive zone" submitted before Hon'ble National Green Tribunal (Principal Bench).

RESEARCH PUBLICATIONS

SEMINAR/SYMPOSIA/WORKSHOP/IMMERSION PROGRAMME

Himalaya Diwas

Himalaya Diwas was celebrated by Wadia Institute of Himalayan Geology (WIHG), Dehradun on 9th September 2024, with the over-arching theme as "Climate Change, Natural Disasters, and Eco-system of Himalaya". The one-day workshop mainly focused on (i) Ecology and Natural Resources (ii) Glaciers and its Hazards (iii) Landslide Mitigation and (iv) Earthquake-resilient Structure. Delegates include Uttarakhand, Himachal and across India with experts from different research disciplines. Over 200 participants from different research/academic institutes, state disaster management departments, universities/colleges of Dehradun, army personals, engineers, research scholars and students.

Recommendation by the panel discussion

Three plenary sessions covered by experts from across India expressed and demonstrated the status of the Himalaya highlighting natural disasters resulting from climate changes and anthropogenic activities. After plenary sessions covering disaster scenario in the Himachal Himalaya, Uttarakhand Himalaya and on the status of work carried out done by WIHG, Dehradun, a panel discussion was held at the end of the day with the theme "Natural Disasters in Himalaya: Challenges and Measures".

The panelists included Dr. V.C. Thakur, Dr. N.S. Virdi, Dr. B. R. Arora, Dr. Harish Bahuguna, Prof. Rajiv Sinha, Prof. A.K. Mahajan, Dr. Shantanu Sarkar, Dr. R.J. Perumal, Dr. Naresh Kumar and Dr. Rakesh Bhamdri. The panelist invited comments from Dr. Rakesh Bhamri (Scientist, WIHG), Shri Shiv K. Rai (Geologist, PWD), Shri D.D. Jat (Town Planning & Housing), Dr. Ch. Debojit. Singh (DDG, GSI), Dr. Naresh Kumar (Scientist, WIHG), and Dr. Alok Pandey (Central University Himachal Pradesh).

Prof. Rajiv Sinha, Indian Institute of Technology Kanpur briefed the day's talks and commented that huge data sets exist related to disasters and mitigation. However, he emphasized that the fundamental problem to be addressed is how to assimilate these datasets. He also said that we need to align different departments for implementation of plans. Dr. Rakesh Bhamri pointed out that there is no proper integration between scientific and government agencies and institutes are mostly working in isolation. This is the root cause which is required to be solved before attempting to mitigate the hazards.

Dr. Shantanu Sarkar (Director, ULMMC) said that good awareness program in localities of disaster is essential. He also said that in places of large scale mitigation, installation of instruments to monitor in future to be installed. Dr. Ch. Debojit Singh (DDG, GSI Dehradun) said that the sufficient work is already done and we should not forget the main motto "Maintaining the Ecosystem". He also said that involving the administrators in scientific forums is most important. Prof A.K. Mahajan (CUHP), highlighted how the Himachal Pradesh state Govt. has implemented recommendations by Geoscientists. He emphasized on the site microzonation for reducing the seismic hazard. He also highlighted the work being done for the safeguard due to landslides. Dr. Naresh Kumar (Scientist, WIHG) emphasized on implementation of earthquake resistant structures and also disaster related awareness among common the local communities.

Dr. V.C. Thakur (former Director, WIHG) appreciated Dr. S.S. Randhawa (SDMA, Himachal Pradesh) for very specific region-wise data presentations. He also recommended vulnerability checking before approval for construction in any locality and emphasized on the need to do multi-parametric studies on landslides. Dr. Harish Bahuguna (DDG, GSI) stressed on the Bhuskhalan portal developed by GSI that everyone needs to utilize the data and the reports to the maximum and give critical feedback to GSI. Dr. Alok Pandey (Central University Himachal Pradesh) emphasized that introduction of the subject Geology in schools & colleges should be strictly implemented. Dr. N.S. Virdi (Former Director, WIHG) emphasized that the govt. takes time but definitely rises to the need of the hour, like after the 1991 Uttarkashi Earthquake, the beam structures of houses were implemented as norms.

Summarizing the deliberation on the Himalayan Diwas, Prof B.R. Arora applauded the spectrum of presentations justifying the importance of the identified theme "Climate Change, Natural Disasters, and the Eco-system of Himalaya". Each presentation while highlighting the current-status of studies on landslides, glacier health, mud-impounding, earthquake hazard, etc deliberated upon the knowledge gaps. From the wide-ranging proceedings, a few key recommendations to bring better coordination and linkage between scientists and management authorities are:

i)   Number of presentations tracking the mechanisms,

SEMINAR/SYMPOSIA/WORKSHOP/IMMERSION PROGRAMME

severity and consequences of natural disasters resulting from climate changes emphasized upon the multi-parametric approach in collaborative mode. State Disaster Management Authority of Himachal Pradesh has already drawn and is implementing well-coordinated region-specific monitoring, allowing demarcation of most vulnerable locations for landslides. Taking stock of landslides over the 19 states of Himalaya, Geological Survey of India (GSI) has developed a Landslides Early Warning System, an excellent tool to forecast landslide occurrence on regional scale. There were several frontline presentations related to landslide risk reduction, glaciers retreat, water-discharge, need for earthquake resistant structures etc. Recognizing the importance of these scientific

Inaugural ceremony of the Himalaya Diwas

Group photograph of participants of the Himalaya Diwas

advances, it is recommended that WIHG may consider publication of a special volume of the Himalayan Geology so as unified approach can be adopted by monitoring agencies and the outcome can be shared with state disaster management authorizes for drawing mitigation strategies.

ii) Another major break-through of the proceedings was the great enthusiasm shown by the Himachal and Uttarakhand State Disaster Management Authorities to implement the risk reduction measures of natural hazards at root levels in the vulnerable zones. This lead is highly promising as several science institutions as time and again, the need to bridge the gap between institutions dealing modalities of natural hazard reduction and state and disasters authorities responsible for ground level implementation. To achieve these targets of great social importance, it is proposed to constitute high level working committees of including from both groups with well-defined roles of each group.

iii) Consistent with the hypothesis of the global warming, glaciers in central and northeast Himalaya show retreating trend. Partial increase of glaciers in the Karakoram (NW Himalaya) can be reconciled as they are nourished by the mid-latitude westerlies and hence represent winter-accumulation-summer ablation-summer. In contrast elsewhere in the Himalaya, glaciers are fed by southwest Monsoon and thus represent summer accumulation and summer ablations glaciers. This is in contrast to the glaciers elsewhere in the Himalaya are fed by SW Monsoon, which are summer accumulation summer ablations Similarly, inter- and intra-basin spatial variation can be explained in terms of the orientation, width, debris cover as well as ratio of the accumulation/ablation volume with respect to the snow line. Despite these advances, it remains to be established what fractions of water discharge in major rivers originating from the Himalaya is contributed by melt water from massive glaciers. It is proposed water discharge at several points along the extended track of rivers, right from the snout, be measured to quantify the relative contributions from the melt water and rain fall respectively. Such monitoring would benefit from collaborations from multi-institutions. To start, WIHG and National Institute of Hydrology should sign an agreement of collaboration.

iv) It was heartening to know that with continuous upgradation seismic network, there is great understanding of the spatial depth distributions of earthquakes. Integration with parallel programs of imaging the crustal structures has given new insight on the seismogenesis and well as nucleation of large earthquakes on the top of the down-going Indian plate and small earthquake on the ramp of this detachment. While the well planned multi-parametric monitoring is in progress, the prediction of the earthquakes is distant goal. Given the improved understanding of the physical parameters affecting the measured multi-parameters, the isolations of the week earthquake precursors require continuation of monitoring. To overcome the limitations in predictions, microdonations studies giving the estimate of peak ground accelerations at any given sight and several other physical parameters, helpful to construct earthquake resistant infra-structures are in place. Here, the disaster management has a major role to ensure permission for any new constructions be given after ensuring that the safe-guards issued by earthquake engineers are implements at design level itself. Parallel attempts on public awareness on what to do and what not to do during the occurrence of earthquakes should be encouraged, particularly to students in schools, by organizing popular lectures on the 'Science Day' or the anniversary of past earthquake in the region.

In the end, Prof. Arora reiterated the success of such programs where college/university students participate, should be judged that every student return home with sound message on how to cope with natural disasters.

Industry Immersion Programme

Under the Capacity Building Commission of the Government of India, an Industry Immersion Programme was conducted at Wadia Institute of Himalayan Geology, Dehradun, from September 17-18, 2024, to provide exposure to WIHG schemes, workings, and laboratories to officers of the Department of Science & Technology (DST). The objectives were (a) to provide exposure to how the WIHG operate for providing cutting-edge research & development, challenges, and how the institute is adapting to evolving trends in the industry; (b) to broaden DST officers' perspectives about on ground issues, and (c) to enable DST officers to better understand and appreciate the

SEMINAR/SYMPOSIA/WORKSHOP/IMMERSION PROGRAMME

Inaugural ceremony and Moments of Industry Immersion Programme

impact and implications of government's policies, programmes and schemes.

The programme was focused on deliberations through in-house talks and display of posters covering the sub-themes of Glacial Hazards and Plausible Remedial Measures, Landslide Management for Sustainable Development, Earthquake Indicators and Warning, Fluvial Extremes and Risk-Management, Green Energy for Climate Change Mitigation, AI/ML for Geo-resource Exploration and Mountain Building Processes

Shri Vinod Kumar Sharma, Coordinator and scientists of the DST, Dr. Karthik Dandhapani, Sh. Kunal Sharma, Sh. Udit Raj Singh, Sh. Ankur Mehta, Ms. Maloth Priya participated in the Program. Apart from academia, eminent persons from Industries, Dr. Sumit Dabral, Senior Manager (Geology), NHPC Ltd., Sh. Yogesh Sharma Ji M.D. Almora Magnesite Ltd. Sh. P. K. Bhatt Senior Manager (R&D) & Sh. Bubai Ghosh, Tehri Hydro Development Corporation Ltd, attended the event. In total, 11 talks were delivered by the scientists of the WIHG on the above-said themes, and three talks were delivered by respective industrial personals. The discussions were held to bring together the industry and academia on a common platform to work for the Viksit Bharat-2047. Dr. Vikas Adlakha coordinated the Programme from WIHG.

The 8th National Geo-Research Scholar's Meet (NGRSM)-2024

The 8th National Geo-Research Scholar's Meet was conducted by WIHG at Shree Mata Vaishno Devi University (SMVDU) in Katra, Jammu & Kashmir, from November 22-25, 2024. The event commenced with an inauguration ceremony followed by four technical sessions featuring nine eminent speakers from the geoscientific community across the country, who shared their insights to educate and inspire young researchers. In addition to the sessions, the conference included two days of geological fieldwork in and around Nodda Khad near Jyotipuram, Reasi, and the Reasi & Akhnoor transect. The field excursion was arranged to provide participants with first-hand experiences of the region's fascinating geological formations and landscapes. This two-day field trip aimed to foster insightful discussions, inspire innovative research, and strengthen collaborative networks among the attendees.

A total of 60 research scholars from Pan India participated in the program, showcasing their work through poster and oral presentations. The Chief Guest, Honorable Prof. S. K. Tandon, known for his work on river systems, and Quaternary geology, is a recipient of the Shanti Swarup Bhatnagar Prize and a former Chairman of the Governing Body of the Wadia Institute of Himalayan Geology (WIHG). He was joined by distinguished guests at the inaugural ceremony, including Prof. Talat Ahmed (Chairman of the Governing Body, WIHG), Prof. M. G. Thakkar (Director-Incharge, WIHG, Director-BSIP), Prof. (Dr.) Pragati Kumar (Vice-Chancellor, SMVDU), Prof. Naveen Juyal, Prof. R. Jayangonda Perumal, and Dr. Gopi Krishna (DST), all of whom emphasized the significance of geoscientific studies in understanding the Himalaya and surrounding regions.

On Day 1, during the various technical sessions, Prof. Talat Ahmed underscored the importance of the geodynamics of the Himalaya and the associated mountain-building processes. Prof. R. Jayangonda

Perumal delivered a detailed presentation on "Jammu Sub-Himalaya: Geology and Tectonics," which explored the structural framework, stratigraphic evolution, and tectonic processes of the region. He discussed the lithological characteristics, deformation patterns, and active fault systems, highlighting their implications for the Himalayan orogenic processes. His presentation also covered the role of foreland basin development, neotectonic activity, and seismicity in understanding the geodynamic evolution of the Jammu Sub-Himalaya. Prof. S.K. Tandon's insightful presentation focused on the Himalaya foreland, emphasizing its geological evolution, stratigraphic framework, and tectonic significance. He provided an overview of the foreland basin system, integrating field observations, sedimentological data, and structural analyses. Prof. M.G. Thakkar presented on "Introduction to Paleoseismology," discussing its fundamental principles, analytical methodologies, and key applications in reconstructing past seismic events, particularly in relation to long-term earthquake recurrence and active tectonic processes. Prof. Naveen Juyal delivered a lecture titled "A Brief Overview of Insights Derived from Fluvial, Lacustrine, and Glacial Deposits during My Research on the Indian Quaternary," emphasizing the significance of geomorphic, sedimentological, and chronological data from various depositional environments in reconstructing past climatic variability and tectonic processes across the Indian Quaternary.

Dr. Gopi Krishna (DST) spoke on "R&D Landscape: Opportunities and Challenges – Science, Technology, and Innovation through Experiential Learning and Technology Transfer," providing a comprehensive assessment of the current research and development ecosystem while highlighting the importance of interdisciplinary collaboration and innovation-driven approaches. Dr. Prahlad Ram discussed "Funding Opportunities and Project Management" under the aegis of ANRF, New Delhi, detailing various research funding schemes and strategies for effective project management to enhance the impact of scientific research. Dr. Sameer Tiwari and Dr. Pankaj Chauhan, conveners of the 8th NGRSM, addressed the participants by highlighting recent advancements in geothermal energy exploration and emphasizing the emerging role of artificial intelligence in glaciological research.

A mid-conference geological field excursion was conducted around Nodda Khad near Jyotipuram, of Reasi regions of Jammu Sub-Himalaya led by Prof. R. Jayangonda Perumal, Prof. Naveen Juyal, Prof. M. G. Thakkar, and Dr. R.L. Mishra. The Reasi area is part of the Outer Himalaya (Sub-Himalaya) and is characterized by rich geological diversity. The fieldwork focused on examining the stratigraphy, structural features, and geomorphic expressions of the active faults of the region, providing participants with firsthand insights into the tectono-sedimentary evolution of the Reasi regions of Jammu Sub-Himalaya. This exercise served as a practical platform for integrating stratigraphic, structural, and geomorphic perspectives, enhancing the scientific understanding of the dynamics of the Himalayan foreland basin and active tectonics in the Reasi region. Mr. Pankaj Kumar Verma, Registrar of the Wadia Institute of Himalayan Geology (WIHG), efficiently coordinated and oversaw all logistical arrangements and institutional support, which played a pivotal role in ensuring the smooth execution and overall success of the event.

SEMINAR/SYMPOSIA/WORKSHOP/IMMERSION PROGRAMME

Inaugural ceremony of the NGRSM-2024

Dignitaries releasing the abstract volume of NGRSM-2024

Group photo of the participants

Field photo of participants along with the eminent experts

AWARDS AND HONOURS

- Dr. Som Dutt received the Dr. J.G. Negi Young Scientist Award 2024 at I.G.U.

- Dr. Pankaj Chauhan jointly awarded (Coalition for Disaster Resilient Infrastructure) CDRI Fellowship for the year 2024-25, funded by national governments, UN agencies.

- Dr. Kapesa Lokho was awarded the best presentation at the International Conference on applied Research in Education (2025) during January 9-10, 2025 in Nay Pyi Taw, Myanmar.

- Dr. N. Premjit Singh received best poster award in the 29th Indian Colloquium on Micropalaeontology and Stratigraphy held on October 17-19, 2024 at Delhi University.

- Dr. Sameer Tiwari was selected as a LEAD Fellow for 2024 by INSA, New Delhi.

- Drs. Kalachand Sain and others was awarded with the Best Research Paper Award for the year 2023 by WIHG, in recognition of outstanding scholarly contribution and excellence in scientific research.

VISITS ABROAD

- Drs. Pinkey Bisht and Hiredya Chauhan visited the 36th Himalaya-Karakorum-Tibet workshop at the AGH University of Krakow, Poland (17-24 June 2024).

- Dr. Pankaj Chauhan visited the Singapore from 28 to 30 August 2024 to attend the International Conference on Resilience Systems (ICRS-2024), held at the National University of Singapore.

- Dr. Kapesa Lokho attended the International Conference on applied Research in Education (2025) during January 9-10, 2025 in Nay Pyi Taw, Myanmar.

- Dr. Pankaj Chauhan attended a meeting in Taiwan during October 2-4, 2024 on collaboration among India, Japan, and Taiwan regarding an advancement on the Early Warning System.

AWARDS AND HONOURS /VISITS ABROAD

PH.D. THESES

Sl. No.	Name of Student	Supervisor	Title of the Theses	University	Awarded/ Submitted
1	Sanjay K. Verma	Dr. Naresh Kumar Prof. Sanjit K. Pal Prof. P.N.S. Roy	Earth structure from free oscillations and seismic tomography: Spatial-Temporal anomalies of seismic wave speeds	IIT (ISM) Dhanbad	Awarded April, 2024
2	Abhishek Pratap Singh	Dr. R.K. Sehgal Dr. N. Premjit Singh	Reconstruction of biostratigraphy and palaeoecology of the Siwalik succession exposed around Nurpur (District Kangra, Himachal Pradesh) and Dunera (District Pathankot, Punjab), India	CSIR-AcSIR, WIHG, Dehradun	Awarded August, 2024
3	Shardha Jagtap	Dr. R. Jayangondaperumal Dr. A.K. Sharma	Pattern of Strain release and active tectonics of Surin Mastgarh Anticline (SMA) NW Sub Himalaya, Jammu & Kashmir: Implications for Seismic Hazard	Kumaun Univ., Nainital	Awarded August, 2024
4	Vikas Kumar	Dr. Aditya Kharya Dr. H.K. Sachan	P-T Fluid Evolution of The Karakorum Migmatite, Trans Himalaya, India	CSIR-AcSIR, WIHG, Dehradeun	Awarded August, 2024
5	Sumit	Dr. Anil Kumar	Sedimentological and Geomorphological evolution of Pangong Tso, Ladakh vis a vis climatic variability	CSIR-AcSIR, WIHG, Dehradun	Awarded August, 2024
6	Dipanwita Sengupta	Dr. Somdutt	Holocene climate variability in the Indian sub-continent: teleconnections and socio-economic consequences	CSIR-AcSIR, WIHG, Dehradun	Awarded Nov., 2024
7	Alosree Dey	Dr. Koushik Sen	Evaluating metamorphism and strain regime during continental subduction and exhumation of the Tso Morari Crystalline Complex, NW Himalaya	CSIR-AcSIR, WIHG, Dehradeun	Awarded May, 2024
8	Madhab Biswas	Dr. Kalachand Sain	A Seismic study of the Surin-Mastgarh Anticline, NW Himalaya: Implications on Geo-tectonics and Geo-resources	CSIR-AcSIR, WIHG, Dehradeun	Awarded May, 2024
9	Chandni Chaurasia	Dr. A.K. Samal Dr. S.S. Thakur	Metamorphic Evolution and Partial Melting Mechanism of the Higher Himalayan Crystalline Sequence (HHCS), Alaknanda-Dhauliganga Valley, Garhwal Himalaya	BHU, Varanasi	Awarded Dec., 2024
10	Kunal Mukherjee	Dr. Vikas Dr. Sayandeep Banerjee	Tectonic and Exhumation History of the Easternmost Arunachal Himalaya, NE India	BHU, Varanasi	Awarded March, 2025
11	Ashis Pal	Dr. Dilip K. Yadav Prof. H.C. Nainwal	Earthquake Source Characterisation and Stress Regime Investigation in North-East India with Special emphasis on Siang Valley, Arunachal Pradesh, India	HNB Garhwal University, Srinagar	Submitted Feb., 2025

PH.D. THESES

Sl. No.	Name of Student	Supervisor	Title of the Theses	University	Awarded/ Submitted
12	Pankaj Kumar	Dr. Manish Mehta	Dynamics of glacier changes and impacts of regional climate variability in the Suru River valley, Ladakh Himalaya, India	HNB Garhwal University, Srinagar	Submitted Feb., 2025
13	Vivek G. Babu	Dr. Naresh Kumar Prof. Sanjit K. Pal Dr. Dilip K Yadav	Quantification of seismic regimes of the Northwest Himalaya: Seismic hazard implication and characterization of earthquake source parameters	IIT (ISM), Dhanbad	Submitted Jan., 2025
14	Neeharika Shukla	Dr. Devajit Hazarika Prof. Sagarika Mukhopadhyay	Crust And Upper Mantle Structure In Northeast India	IIT, Roorkee	Submitted Feb., .2025

PH.D. THESES

PARTICIPATIONS IN SEMINAR/ SYMPOSIA/ MEETINGS/ TRAINING

- "Prabodh and Praveen" Hindi training course conducted by the Central Hindi Training Institute in New Delhi, May 1, 2024, to July 4, 2024)

  Participants: Rouf Ahmad Shah, N. Premjit Singh and M. Rajanikanta Singh

- National Geoscience Data Repository (NDGR) GSI-Dehradun, for Geochemical Mapping of Uttarakhand May 1, 2024, Pearl Avenue, Dehradun

  Participant: Barun Mukherjee

- Regional variability of the Indian summer monsoon in the last two millennia' in the 2nd Indian Quaternary Congress held at IISER Mohali, June 2-4, 2024

  Participant: Som Dutt

- 2nd Indian Quaternary Congress (IQC) -2024 on Quaternary Sciences for a Sustainable Future Earth (Q-SAFE) held at Indian Institute of Science and Education Research (IISER), Mohali, June 3-5, 2024

  Participant: Anil Kumar

- 2nd International Conference on Computer, Electronics, Electrical Engineering and their applications (IC2E3 2024), June 6-7, 2024

  Participant: Naveen Chandra

- 36th Himalaya-Karakorum-Tibet workshop at the AGH University of Krakow, Poland, June 17-24, 2024

  Participants: Talat Ahmed, Pinkey Bisht and Hiredya Chauhan

- The Gangotri and Dharali Traditional and Environmental Eventat Gangotri & Dharali in Uttarakhand, India, June 19-21, 2024

  Participant: Chhavi Pant Pandey

- The board of studies meeting of the Dept. of Geology, Univ. of Ladakh at UoL, Leh, Ref: Invitation email from the Dept. of Geology, Univ. of Ladakh, July 4-5, 2024

  Participant: R. Jayangondaperumal

- Energizing missing log imputation with deep learning: A case study from Bhogpara oil field, Assam-Arakan basin, UrjaVarta 2024, Bharat Mandapam, New Delhi, India, July 11-12, 2024

  Participant: Bappa Mukherjee

- International conference on 5th Asia-Pacific Science Technology Conference on Disasters Risk Reduction at Indian Institute of Roorkee, July 11-13, 2024

  Participant: Pankaj Chauhan

- Online Interview/Viva voce for Public Service Commission, July 19, 2024

  Participant: Kapesa Lokho

- Online meeting of the Executive Council of the Palaeontological Society of India, July 24 and September 23, 2024

  Participant: Kapesa Lokho

- Three-days training program on Administrative vigilance at INSA, New Delhi, July 31 to August 2, 2024

  Participant: R. Jayangondaperumal

- International Conference on Resilience System (ICRS-2024), held at National University, Singapore and paper presented on titled "Development in Low Cost Powerless Smart Early Warning System using IoT technology, for disaster risk reduction and resilience in the Himalayan region", August 28-30, 2024

  Participant: Pankaj Chauhan

- CITE-2024 Conference, IISER Pune, September 1-2, 2024

  Participant: Saurabh Singhal

- One-day workshop on 15th Himalaya Diwas on Climate Change, Natural Disasters and Eco-System of Himalaya at the Wadia Institute of Himalayan Geology, September 9, 2024

  Participants: WIHG Scientists and Research Scholars

- Chaired a technical session in *"International Conference on" Navigating global Energy transition for sustainable future ICNETS 2024"* organised by UPES, Dehradun, September 18-20, 2024.

  Participant: Bappa Mukherjee

- Advisory Committee (PAC)-Earth & Atmospheric Sciences (E&AS), DST at Department of Environmental Sciences, Babasaheb Bhimrao Ambedkar University, Lucknow, UP, October 6-8, 2024

  Participant: Kapesa Lokho

- 29th Indian Colloquium on Micropaleontology and Stratigraphy at Delhi University on the topic 'Orbital scale changes in the Indian summer monsoon conditions', October 17-19, 2024

  Participant: Som Dutt

- International Day for Disaster Risk Reduction on the theme of "Empowering the Next Generation for a Resilient Future on October 23, 2024 at new Delhi

  Participant: Naresh Kumar

- National conference on 'Recent Advancements in Earth Sciences' Geological Institute Conference (GIC), 2024, Presidency University, Kolkata (India), November 12, 2024.

  Participant: Subham Bose

- DST-SEC meeting at Amrita Vishwa Vidyapeetham, Coimbatore, November 13, 2024

  Participant: Kapesa Lokho

- Three-days Indo Swiss workshop on "Modelling Rock Ice Avalanches, Rockfalls, and Debris Flows" organised by CSIR-CBRI, November 20-22, 2024.

  Participant: Naveen Chandra

- 8th National Geo-Research Scholar Meet -2024, held at Shri Mata Vaishno Devi University, (SMVDU), Katra Campus, Jammu and Kashmir, November 22-25, 2024

  Participants: Scientists and research scholars of WIHG

- International seminar on Plate Tectonics, Sedimentation and Metallogeny through time Annual convention of Geological Society of India, Dharwad, November 26-28, 2024

  Participant: Kunda Badhe

- One-day Brainstorming Session was organized at NIH, Roorkee and presented work on Glaciological Studies in the Indian Himalayan Region (IHR) by WIHG as per the suggestion made during the second meeting of the Steering Committee (Monitoring of Glaciers), November 28, 2024

  Participant: Manish Mehta

- 19th Uttarakhand State Science and Technology Conference held at Doon University, Dehradun: November 28, 2024

  Participant: Pinkey Bisht

- 3rd Meeting of the Subject Expert Committee (SEC) on Earth and Atmospheric Sciences under WISE-PhD Programme of DST is scheduled to be held at INSA, New Delhi, November 28-29, 2024

  Participant: R. Jayangondaperumal

- Participated in the 10th India International Science Festival (IISF) held at IIT-Guwahati, November 30 to December 3, 2024

  Participants: R. Jayangondaperumal, Praveen Kumar, Pinkey Bisht, Amit Kumar, N. Premjit Singh, Bappa Mukherjee and Mahesh Kapawar

- IEEE 2024 India Geoscience and Remote Sensing Symposium (GARSS), Goa, India, December 2-5, 2024

  Participant: Naveen Chandra

- 61st Annual Convention of Indian Geophysical Union, held at Banaras Hindu University (BHU) in Varanasi, December 3-5, 2024

  Participants: Naresh Kumar, Som Dutt, C. Haldar and Jitender Kumar

- A training program on "Climate Risk Management Policy and Governance, Scientists & Technologists" working in the Government Sector at LBSNAA, Mussoorie, December 9-13, 2024.

  Participants: Jayendra Singh and Manish Mehta

- 40th Convention of the Indian Association of Sedimentologists 2024 held at Birbal Sahani Institute of Palaeosciences, Lucknow, on Transient fluvial activities and topographic irregularities in the Satluj River valley, NW Himalaya, December 11-13, 2024

  Participant: Anil Kumar

PARTICIPATIONS IN SEMINAR/ SYMPOSIA/ MEETINGS/ TRAINING

- 10th World Ayurveda Congress (WAC) was organised by Ministry of Ayush, Government of India, Vijnana Bharati and the World Ayurveda Foundation are the main organizers in support of the Government of Uttarakhand at Paradeground Dehradun, Uttarakhand, December 12-15, 2024

  Participants: Paramjeet Singh and Saurabh Singhal

- Group Monitoring meeting of Programme DST Training Program on "Policy for Science and Science for Policies" at Bengaluru National Institute of Advanced Studies (NIAS), Bengaluru, December 16-20, 2024

  Participant: Kapesa Lokho

- 7th Regional Science and Technology Congress, 2024-25, Midnapore College (Autonomous), Midnapore-721101, West Bengal, January, 3-4, 2025

  Participant: Bappa Mukherjee

- Five-days Drone Pilot license training at Droneacharya training Inst., Noida, January 6-10, 2025

  Participant: R. Jayangondaperumal

- A training on "Advanced Training on Glaciers and Glacial Lakes Observations for Sustainable Water Resource Management" at NIH Roorkee, February 24 to March 1, 2025.

  Participant: Jairam Singh Yadav

- Post budget webinar 2025 on "Investing in Innovation", organized by the department of science & technology, Govt. of India, March 5, 2025

  Participant: Pankaj Chauhan

- National Seminar on Dynamic Processes of the Earth: From Deep Interior to Surface (DPE 2025), UGC- Centre for Advanced Studies Department of Geology, Presidency University, Kolkata, March 21-22, 2025

  Participants: Bappa Mukherjee and C. Haldar

PARTICIPATIONS IN SEMINAR/ SYMPOSIA/ MEETINGS/ TRAINING

DISTINGUISHED LECTURES DELIVERED IN THE INSTITUTE

Sl. No.	Date	Speaker	Event & Topic
1	April 23, 2024	Prof. Talat Ahmad, GB Chairman, WIHG	Earth Day
2	May 20, 2024	Prof. Harsh K. Gupta, Former Secretary, Dept. of Ocean Development (MoES), Govt. of India	S.P. Nautiyal Memorial Lecture
3	June 13, 2024	Prof. S.S. Rai, IISER Pune	Seismic Anatomy of Deccan Traps: Volcanism and Earthquakes
4	June 29, 2024	Dr. O.P. Mishra, Scientist-G, MoES, New Delhi	56th Foundation Day
5	Aug. 23, 2024	Dr. R.S. Chatterjee, Group Director and Head & Scientist/ Engineer-G, IIRS Dehradun	National Space Day "Space Exploration in India with Emphasis on Earth Observation for Groundwater Depletion and Land Subsidence Studies"
6	Sept. 9, 2024	Prof. T.N. Singh, Director, IIT, Patna	Himalaya Diwas "Climate Change, Natural Disasters and Eco-system of Himalaya"
7	Sept. 17, 2024	Prof. L.S. Chamyal, Former HOD, Dept. of Geology, MSU, Baroda	Inversion tectonic and geomorphic development in the Cambay and Kachchh sedimentary basins during Qyuaternary
8	Oct. 4, 2024	Prof. R.G.S. Sastry, Adjunct Professor, School of Earth, Atmospheric and Ocean Sciences, IIT Bhubaneswar	ERI's limited role for groundwater exploration in hard rock region with underground utilities and Micro-gravity's role - A Case Study
9	Oct. 23, 2024	Mr. Deepak Kumar, Superintending Surveyor at Geodetic and Research Branch, Survey of India	Founder's Day "Introduction to Continuously Operated Reference Stations"
10	Nov. 12, 2024	Dr. R.P. Singh, Director, IIRS, Dehradun	10th IISF 24-Curtain Raiser "Journey of Space Research in India"
11	Feb. 28, 2025	Ms. Nebula Bagchi, Executive Director, GEOPIC	National Science Day "The Himalaya: Perspective from India`s National E & P Company"
12	March 10, 2025	Prof. Vinod Gaur, Former Secretary, Dept. of Ocean Development (MoES)	S. P. Nautiyal Memorial Lecture "5 Deep Questions about the Workings of Planet Earth, that may be learnt from its Grandest Scale Laboratory - the Himalaya"
13	March 18, 2025	Prof. Kusala Rajendran, Centre for Earth Sciences(Retired) and Member of the Governing Body WIHG	Special Lecture "On being a geophysicist: A journey of four decades"

LECTURES DELIVERED/ INVITED TALKS BY INSTITUTE SCIENTISTS

Name of Institute Scientist	Programe Organizer/Venue/ Institute	Date	Topic/ Title of lecture
Santosh K. Rai	Hindi workshop organized by WIHG, Dehradun	May 31, 2025	हिमालयी क्षेत्रों में वायुमंडलीय CO_2 की प्राकृतिक गतिशीलता
Kapesa Lokho	3rd Indian Analytical Congress IAC-2024 at CSIR-IIP, Dehradun	June 5-7, 2024	Enhancing microfossil analysis through coated and uncoated FE-SEM methods: Insights from Neo-Tethys of NE Himalaya
Pankaj Chauhan	Government Inter College Cantt. Chakrata, District-Dehradun	June 6-7, 2024	Science, education, disasters awareness and climate resilience of Chakrata under the VIKSIT BHARAT Programme
Pinkey Bisht	36th Himalaya-Karakorum-Tibet workshop, Kraków, Poland	June 17-24, 2024	Late Quaternary Glacial history of the Panchachuli glacier, Darma Valley, Central Himalaya
Rajeeb Lochan Mishra	For the requirement of Beam Time Request (BTR) for project proposal at The Inter University Accelerator Centre, New Delhi	June 24, 2024	Quaternary landform evolution, tectonics and structural analyses across four different transects of the Indian Himalaya, extending from the Beas to the Ganga Rivers in the western Himalaya, and from the Tista to the Dikrong Rivers in the eastern Himalaya
Bappa Mukherjee	UrjaVarta-2024, Bharat Mandapam, New Delhi	July 11-12, 2024	Missing log prediction in multiple stratigraphic unit
Parveen Kumar	FRI Deemed Univ., Dehradun	Aug. 07, 2024	Natural Hazard and Disaster
		Aug. 08, 2024	Earthquake Preparedness and Hazard Mitigation
		Aug. 09, 2024	Earthquake forecasting management
		Aug. 14, 2024	Disaster types and their effects
		Aug. 21, 2024	Characteristics of various Disasters
		Aug. 27, 2024	Earthquake Mock Drill Performance
Pankaj Chauhan	National University, Singapore	Aug. 11-13, 2024	Development in Low-cost Powerless Smart Early Warning System using IoT technology, for disaster risk reduction and resilience in the Himalayan region
Swapnamita Choudhury	In the 17th edition of The Doon School Model United Nations Conference, in the Science and Media Series of Talks in The Doon School, Dehradun	Aug. 16-17, 2024	Geology, Past and Present
R. Jayangondaperumal	WIHG, Dehradun	Aug. 17, 2024	An Overview of WIHG is presented to the experts of the DST members who have visited the Institute under the DST Immersion program
Naveen Chandra	Department of Civil Engineering, IIT Indore	Aug. 27, 2024	Deep Learning and Landslides: Data, Models, and Significance
Saurabh Singhal	CITE-2024 Conference, IISER, Pune	Sept. 1-2, 2024	High spatial resolution measurement of in-situ Hafnium isotope of zircon mineral using LA MC-ICPMS

Hiredya Chauhan	National Centre for Earth Science Studies (NCESS), Ministry of Earth sciences, Thiruvananthapuram	Sept. 2-4, 2024	Women in Geosciences: Opportunities, Challenges and Accomplishments
Rakesh Bhambri	Three-Week Capacity Building Program in Glaciology organized by the University of Kashmir, Srinagar	Sept. 4, 2024	Surge Glaciers and Associated Hazards in the Karakoram
Santosh K. Rai	DST Immersion Programme organized by WIHG, Dehradun	Sept. 17, 2024	Weathering and Erosion in Ganga Brahmaputra Fluvial System
Manish Mehta	DST Immersion Programme organized by WIHG, Dehradun	Sept. 17, 2024	Himalayan Glaciers
Devajit Hazarika	DST Immersion Programme organized by WIHG, Dehradun	Sept. 17-18, 2024	Earthquakes in the Himalaya and Earthquake Precursory Study
Anil Kumar	Industrial Immersion Program held at WIHG	Sept. 17-18, 2024	Climatic variability in Himalaya
Rakesh Bhambri	National Seminar on Disaster Risk Reduction in the Himalaya: Recent Advancements, organized by Jawaharlal Nehru University, New Delhi	Sept. 20, 2024	Impact of Climate Warming on Himalayan Glaciers and Associated Hazards
Kapesa Lokho	29th Indian Colloquium on Micropalaeontology and Stratigraphy (ICMS) held at Dept. of Geology, University of Delhi	Oct. 17-19, 2024	Larger Foraminiferal Biostratigraphy, Paleoenvironment and Paleogeography of the Early Eocene Kong Formation of the Zanskar, Tethyan Himalaya
		Oct. 17-19, 2024	Biostratigraphy and Environmental changes during the Middle Miocene: A nannofossil approach from the Surma Group of Naga Hills
N. Premjit Singh	29th Indian Colloquium on Micropalaeontology and Stratigraphy (ICMS) held at Dept. of Geology, University of Delhi	Oct. 17-19, 2024	Rodent fossils from the Siwaliks of Mohand, Saharanpur district, and biostratigraphic implication
Som Dutt	Aryabhatta Research Institute of Observational Sciences, Nainital	Nov. 20 -21, 2024	द्वितीय अखिल भारतीय वैज्ञानिक एवं तकनीकी राजभाषा संगोष्ठी में 'जलवायु परिवर्तन और भारत का इतिहास
Swapnamita Choudhury	ISRO sponsored workshop program on Landslide, held between November 25-30, 2024 at Department of Civil Engineering, Graphic Era (Deemed to be University, Dehradun	Nov. 25, 2024	Shallow and Deep seated landslides: Case Studies of two sites LiDAR technology in landslide management: the Joshimath experience
N. Premjit Singh	India International Science Festival 2024 organised at IIT Guwahati	Nov. 30 - Dec. 4, 2024	New Cenozoic Vertebrate Fossils from NW Himalaya
Bappa Mukherjee	India International Science Festival in 2024 held at IIT Guwahati	Nov. 30 - Dec. 4, 2024	Application of AI/ ML in geosciences in the Pragya Bharat Event

LECTURES DELIVERED/ INVITED TALK BY INSTITUTE SCIENTISTS

Naresh Kumar	61ˢᵗ Annual convention of IGU, BHU, Varanasi, UP	Dec. 3-5, 2024	Geo-hazard investigation in Uttarakhand: characterization based on local seismic signals
C. Haldar	61ˢᵗ Annual convention of IGU, BHU, Varanasi, UP	Dec. 3-5, 2024	Crust beneath the IGP and Himalaya
Swapnamita Choudhury	Faculty Development Programme (FDP) approved by AICTE under the ATAL Basic FDP organized at Tula's Institute, Dehradun	Dec. 19, 2024	Advancing Sustainable Development: Integrating Remote Sensing and GIS Technologies
Kapesa Lokho	International Conference on applied Research in Education (2025) in Nay Pyi Taw, Myanmar	Jan. 9-10, 2025	Geodynamic evolution of the Indo-Myanmar Range from the Mesozoic to the Cenozoic: inferences from the fossil records
Som Dutt	Department of Geophysics, Kurukshetra University	Jan. 11, 2025	J.G. Negi Award lecture
Rouf Ahmad Shah	Indian Forest Services (IFS) Probationers at Shastradhara, Dehradun	Jan. 11, 2025	Karst hydrosystems and their societal importance
Swapnamita Choudhury	The Oasis School, Dehradun	Jan. 29, 2025	Rocks and Fossils
Santosh K. Rai	Online 2-Week Refresher Course organised by the UGC-HRDC at Dept. of Environmental Studies, Jamia Millia Islamia University New Delhi	Feb. 09, 2025.	Environmental Geochemistry in Ganga -Brahmaputra Fluvial System
V.K. Gahalaut	Doon University, Dehradun	Feb. 22, 2025	Strain (Stress) map of the Indian subcontinent
Anil Kumar	WIHG, Dehradun	March 27, 2025	Student Orientation Program on 'Basics of Instrumentation: XRD, XRF and LPSA'
Rakesh Bhambri	Advanced Training of Trainers (ToT) Program on "Glaciers and Glacial Lakes Observations for Sustainable Water Resource Management", organized by the National Institute of Hydrology, Roorkee	Feb. 25, 2025	Glacier Surface Velocity Estimation Using Optical Images
Rakesh Bhambri	National Seminar on Natural Hazards in the Anthropocene: Mitigation, Resilience and Sustainability, organized by Kirori Mal College, University of Delhi	Feb. 28, 2025	Monitoring of Himalayan Glaciers and Associated Hazards Using Ground and Space Observations
Saurabh Singhal	Student Orientation Program at WIHG on the occasion of National Science Day 2025 as a resource person	Feb. 28, 2025	XRD, XRF, Raman Spectroscopy, OSL, MCICPMS
Santosh K. Rai	Student Orientation Program at WIHG on the occasion of National Science Day 2025 as a resource person	Feb. 28, 2025.	Stable Isotope, ICPMS, Ion Chromatograph, Water Chemistry

Rajesh S.	WIHG, National Science Day Celebrations 2025	Feb. 28, 2025	Lecture on the basics of Seismometer, GNSS and Gravity instruments
C. Perumalsamy	International Analytical Science Congress - 2025, Department of Chemistry, M.S. University, Baroda, Vadodara (Gujarat)	March 06-08, 2025	Accurate and precise determination of rare earth elements in the geological materials by Inductively Coupled Plasma Tandem Mass Specrometrometry
Pramod K. Rajak	1ˢᵗ International Conference on Advances in Sciences (ICAS 2025), Cluster University of Jammu, Jammu, J&K	March 19-20, 2025	Assessment of environmentally sensitive elements in Jammu coal deposits, Jammu & Kashmir, India
C. Haldar	National Seminar on Dynamic Processes of the Earth: From Deep Interior to Surface (DPE 2025) UGC- Centre for Advanced Studies Department of Geology, Presidency University, Kolkata	March 21-22, 2025	Crust and upper mantle beneath North-West Himalaya
V.K. Gahalaut	WIHG, Dehradun	March 28, 2025	Earthquakes and their occurrence processes in the Himalaya
Manish Mehta	The Institute of Town Planners of India (North Zone conference) Shimla, H.P.	March 29, 2025	Fragile Ecosystem of Himalaya
Gautam Rawat	ITPI-North Zone Conference 2025	March 29, 2025	Impact of Development in Himalaya

LECTURES DELIVERED/ INVITED TALK BY INSTITUTE SCIENTISTS

MEMBERSHIP OF ACADEMIC SOCIETIES

Kapesa Lokho	Member:	Executive Council Member of the Palaeontological Society of India (2024-2026)
Santosh K. Rai	Member:	Member of the Geochemical Society, (168259) America
Som Dutt	Member: Member:	Life Member of Association of Quaternary Researchers, India Life Member of Indian Geophysical Union
Anil Kumar	Member:	Life Member of Indian Geophysical Union
N. Premjit Singh	Member:	Life Member of the Journal of the Palaeontological Society of India
Kunda Badhe	Member:	Life member of Geological society of India

PUBLICATION AND DOCUMENTATION

The Publication & Documentation section brought out the (i) 'Himalayan Geology' volumes 45(2) 2024 and 46(1) 2025; (ii) Annual Report of the Institute for the year 2023-24 (bi-lingual); (iii) Hindi magazine 'Ashmika' volume 30 (2024); and (iv) Field Excursion Guide for NGRSM-2024 etc.

The section was also involved in the dissemination of the publications to individuals, institutions, lifetime subscribers, book agencies, national libraries, indexing agencies, under exchange program, and maintaining the sale & accounts of publications. Apart from this, works pertaining to the printing of publicity brochures and folders (bi-lingual) etc., are also taken up.

Himalayan Geology (journal) website http://www.himgeology.com is functioning along with an online manuscript submission facility under this section. All information regarding the journal including contents and abstracts is updated from time to time on the website. Online access of current published volume to the online subscribers and life time members (those who have given the choice to obtain the volumes in soft copy through online access/email) also has been provided. At present, 185 life time subscribers receive the journal through online access/email. The journal is indexing in UGC CARE, Scopus, Web of Science (SCIE), Thomson Reuters/Clarivate Analytics (US), Elsevier (Netherlands), and Indian Citation Index (India) regularly etc. The current impact factor of the journal is 1.1 (Source: Clarivate Analytics).

The section also provides the facility & technical support services of A0 size scanning and printing to the scientists, research scholars, and other staff of the Institute. During this period, more than 120 maps and posters printed for display in laboratories, workshop/seminars and exhibitions etc. and 113 maps/sheets scanned.

PUBLICATION AND DOCUMENTATION

LIBRARY

The Wadia Institute of Himalayan Geology library holds an extensive collection of books, monographs, periodicals, e-books, and other materials on mountain construction, as well as geological and geophysical features of the Himalaya. It occupies a distinct location with its collection. In addition, the collection and services available make it one of the country's most excellent earth science libraries. Scientists, researchers, project workers, and students use the Library entirely when publishing their research findings in reputable peer-reviewed publications. Our library also welcomes specialists and professionals from around the country to consult its themed and unusual collections. Key features are:

Specialised Collection: The library houses an extensive collection of books, journals, theses, and technical reports related to geology, geophysics, seismology, geomorphology, and related earth science disciplines.

E-Resources: Offers access to digital resources, including online journals, databases, and e-books through institutional subscriptions and national knowledge networks.

Archival Materials: Includes rare geological maps, Himalayan research archives, and reports from early geological expeditions.

One Nation One Subscription (ONOS): The library has One Nation One Subscription (ONOS) plans to get national licenses for e-journal/database subscriptions from the most notable journal publishers. ONOS includes 30 major international journal publishers. These publishers will make all journals available to scientists, students, and researchers at the collaborating institutions.

The library has a rich collection of e-books from various publishers and learned societies on the Institute's research focus areas.

Acquisition of Documents: The library acquired subscriptions to national and international journals and magazines this year. There are 30 reference books subscribed. Furthermore, 75 books have been acquired for the Hindi collections.

National Knowledge Resource Consortium (NKRC): The library is a member of the NKRC and continues to receive assistance from Consortia for online access to e-resources. In addition, WIHG Library has access to articles from Web of Science, Elsevier-Scopus, Grammarly, MAPMyAccess, databases and iThenticate (Plagiarism Detection Software).

Reprography Facility: The library serves as a central repository for the institute's demand. This facility is being extended to the scientific and administrative sections of the institute. About 76121 photocopies have been done this year.

Computer Facility: The library has a computer lab for users to access e-books, e-journals, and other e-resources, either subscribed to by the WIHG library or available through NKRC or ONOS. This facility was also extended to the students and summer trainees. The lab is also being used to conduct several tests to recruit the administrative and technical staff of the institute.

The WIHG library provides the following services to support Scientific, Technical and Administrative work:

- Circulation Service
- CAS and SDI
- Printing of Article
- Scanning of Document
- Plagiarism Check
- Reprographic Services
- Reference and Consultation Service
- Electronic information resource access
- Document Delivery Services
- CD-ROM Database, etc.

S.P. NAUTIYAL MUSEUM

The S.P. Nautiyal Museum continued to serve as a vibrant centre for geoscience education and public outreach throughout the year. With a recorded footfall of over 15,000 visitors, the museum remained a major attraction for students, educators, researchers, and tourists from across the country and abroad.

Showcasing an extensive collection of rocks, minerals, fossils, and thematic exhibits-covering topics such as continental drift, Earth's internal structure, geological time scales, glaciers, and the origin and evolution of life-the museum offered an enriching and immersive learning experience to all age groups.

Life-sized models of extinct mammals and interactive displays were especially appreciated for their educational value and visual appeal. Guided tours conducted by experts facilitated deeper engagement, helping visitors grasp complex geological concepts with clarity. Local schoolchildren also continued to benefit from academic project support and hands-on learning opportunities provided by the museum.

The regular dissemination of educational brochures and outreach materials further strengthened the museum's role as a bridge between the Institute and the broader public. By engaging with a diverse audience—including school and university students, professionals, and international guests-the S.P. Nautiyal Museum continues to play a pivotal role in fostering scientific curiosity and promoting awareness of Himalayan geosciences.

Major Outreach and Exhibition Activities: The S.P. Nautiyal Museum participated in several national-level exhibitions and outreach programs, showcasing the Institute's scientific work to a wider audience. These efforts enhanced WIHG's visibility and promoted geoscience awareness among students, academic institutions, and the general public.

State Level Youth Festival, Parade Ground, Dehradun (November 10–14, 2024)

The Institute showcased a wide array of geological exhibits and educational materials at the State Level Youth Festival in Dehradun. The museum's interactive models and engaging visuals attracted hundreds of young visitors, sparking curiosity about Earth sciences. The event served as an effective platform to inspire students and introduce them to Himalayan geology in an accessible and engaging manner.

India International Science Festival (IISF), IIT Guwahati, Assam (November 30–December 3, 2024)

At the prestigious IISF 2024, the S.P. Nautiyal Museum represented WIHG on a national platform, drawing attention to the Institute's research in Himalayan tectonics, seismology, and paleoclimate studies. The museum's thematic displays and informative brochures received strong appreciation from students, scientists, and policy makers, significantly raising awareness about Himalayan geoscience challenges and opportunities.

Visit of delegates and students in the Museum

'Viksit Bharat–Viksit Uttarakhand' Mega Exhibition, Nehru Stadium, Roorkee (March 4-6, 2025)

This exhibition focused on India's developmental journey, where WIHG highlighted the critical role of geosciences in sustainable development, disaster preparedness, and environmental conservation. The museum's participation drew interest from a wide audience, including school groups, local officials, and NGOs, helping to contextualize scientific research within real-world applications in the region.

Vasant Utsav, Raj Bhavan, Dehradun (March 7-9, 2025)

During the annual Vasant Utsav held at the Governor's residence, the museum curated an attractive exhibit that blended science with cultural celebration. The display of rocks, fossils, and glacier models resonated with families and dignitaries alike. The event provided an opportunity to engage with the general public in a relaxed setting, promoting geoscience appreciation beyond traditional academic spaces.

S.P. NAUTIYAL MUSEUM

TECHNICAL SERVICES

Analytical Services

The number of samples analyzed by various instruments is listed below:

Laboratory/Instruments	Number of samples analyzed		
	WIHG Users	**Outside Users**	**Total**
Inductively Coupled Plasma Mass Spectrometer (ICP-MS) Lab	1066	825	1891
Laser Ablation Inductively Coupled Plasma Mass Spectrometer (LA- MC-ICP-MS) Lab	-	-	-
Stable Isotope Lab	869	50	919
Luminescence Dating (TL/OSL) Lab	85	48	133
Fission Track Lab Apatite Fission Track Dates Zircon Fission Track Dates	27 54	- -	27 54
Mineral Separation Lab	11	4	15
Sample Preparation Lab EPMA Slides prepared Ordinary slides prepared Powdering	300 102 843	16 31 278	316 133 1121
XRD Lab.	108	27	135
X-Ray Fluorescene Spectrometer (XRF) Lab	869	362	1231
Laser Micro Raman Spectrometer (LMRS) & Fluid Inclusion Lab.	48	9	57
Rock magnetic & Palaeomagnetism Lab	175	60	235
Dendrochronology Lab	44	0	44
Laser Particle Size Analyzer (LPSA) Lab Sedimentology Lab Vibratory Sieve Shaker Clay Slide Preparation	449 64 0	53 1 0	502 65 0
Palynology Lab	54	0	54
Laser Water Isotope Analyzer (LWIA) Lab	50	0	50
Water Chemistry Lab (Ion-Chromatograph)	500	100	600
Total Organic Carbon Lab	715	10	725

TECHNICAL SERVICES

Sample Preparation Laboratory

The Sample Preparation Lab of WIHG, Dehradun, prepares samples for high-end geochemical, structural, sedimentological, and geotechnical investigations, at par with international standards. Presently, ordinary and EPMA thin-section slides are being prepared in this facility. Mineral Separation and slide preparation work for the geochronological and thermochronological investigation is an integrated component of this facility. The lab also performs the powdering of rock samples for XRF, ICPMS, and OSL investigations. The Lab is equipped with Buehler, Struers rock-cutting and polishing machines. In addition, the lab also has Frantz Magnetic Barrier Separation, Fritsch Jaw Crusher and Disk Mill, Holman Wilfley Table, and an Automatic Polishing machine. This high-end facility is being used by researchers of various R&D institutes and universities across India.

Fission Track Dating Laboratory

Fission Track Dating Facility has been successfully established at the Wadia Institute of Himalayan Geology, Dehradun, to facilitate basic research in Earth System Sciences (Thermochronology) and to develop a trained scientific workforce for national needs. The facility includes the mineral separation lab, slide separation lab, polishing lab, Fission-track counting system of international standards. This facility has its applications for the reconstruction of low-temperature (<300°C) thermal histories in upper crustal rocks. It is a powerful method for constraining the time-temperature history of rocks and provides constraints on millennial-scale denudation rates, landscape evolution, and tectonic history of different geological terrains such as orogenic belts, rifted margins, and more stable areas. It provides a means of assessing the timing and volume of sediment being delivered to sedimentary basins, and also serves as an estimator of the hydrocarbon maturity potential of the sedimentary basin. At present, the research work at the facility is ongoing to constrain the millennial-scale erosion and tectonic evolution history of the Karakoram, Zanskar, Kumaun-Garhwal, and Arunachal Himalayan regions of India.

Computer and Networking Section

The WIHG Computer and Network Section plays a pivotal role in ensuring seamless digital operations across the institute. It is responsible for managing, maintaining, and upgrading all IT infrastructure including computing resources, networking systems, and communication platforms. This section is committed to providing efficient, secure, and highly available services that support the academic, research, and administrative activities of the organization.

Core Services

Computer and Workstation Management

The section manages a diverse range of desktops, workstations, and laptops used by faculty, staff, and researchers. This includes installation, configuration, troubleshooting, regular maintenance, and timely upgrades. Systems are equipped with essential software packages tailored to individual or departmental needs.

Server and Storage Infrastructure

The section manages various servers which have been installed and configured in-house. All the servers are working on secure Linux environment and using latest Open Source Technology. The different types of servers being used are DNS, Mail, Web, Application, etc. The section has not only maintained a virus and spyware free environment by adopting centralized anti-virus and anti-spyware solution but has also been adopting the latest preventive security measures in this regard.

Virtualization is employed for scalability and better resource utilization.

Networking Services

- The section oversees a robust, secure, and high-speed network infrastructure. This includes:

- Uses the latest networking technologies for excellent speed and reliability of all the network related services which are the need of the hour.

- Maintains and upgrade the network as per the requirement. The network is not limited to the office but the same has been extended to the WIHG residential colony, Guest House, WIHG Students transit hostel so that all employees and students can have 24x7 connectivity.

- Provides VPN facility to facilitate the access of Institute resources securely over public network.

- Maintains the different web portals hosted by the Institute viz., Institute website, Institute publication portal, WAICS (Wadia Analytical Laboratory Instrument Facility and Consultancy Advisory Services) portal.

- Firewall and intrusion prevention systems for network security

- Bandwidth management and monitoring

Internet and External Connectivity

The Institute is connected with the National Knowledge Network through a high speed 1 Gbps link. For uninterrupted internet connectivity, redundant link and failover mechanisms are in place to ensure near 100% uptime.

Hardware and Software Support

- Preventive Maintenance: Regular checks of computing systems to prevent failures.

- Repairs and Replacements: For the hardware related issues, AMC services have been employed so that any hardware issue can be taken up immediately and resolved without any delay. Also, coordination with vendors/OEMs is done for warranty-based services.

- User Support Helpdesk: A responsive support helpdesk is available via phone to address user issues.

Online/Offline Meetings, Conferences, Webinars

Online Meetings, Conferences, Webinars: The section facilitates virtual meetings, webinars, and workshops using platforms like Zoom, Microsoft Teams, Google Meet, and other licensed tools. Facilities include:

- Meeting scheduling and setup support

- Recording and archival of sessions

Offline Meetings and Conferencing: Wadia Institute has been organizing Distinguished Lectures by Eminent Scientists/Professors around the year. Many of these lectures have been conducted online (or in hybrid mode) and WIHG Computer Section has been instrumental in the successful conducting of these lectures by providing all round support for the same.

During all other offline events, requisite arrangements as per the requirement are made for the success of the events.

High Availability and Reliability

The Computer and Network Section emphasizes high availability for all critical systems. The Computer and Network Section is committed to maintaining near 100% uptime across all services.

As per the instructions from the S&T Ministry, the Cyber Jagrookta Diwas (CJD) is being organized on the first Wednesday of every month to create the awareness about the latest cyber threats and cyber hygiene for the prevention of cyber crimes. Lectures and presentations are arranged for the Institute employees, research scholars and anciliary staff.

The Computer Section has been playing a very important role in all the fields, where IT services are utilized and that means nearly everywhere. It maintains and manages the high speed fiber connectivity of the various blocks/buildings; connectivity of the sophisticated scientific instruments installed in the Institute to carry out the research work; connectivity and operation of the different high-end workstations; installation and configuration of the scientific and general softwares; the CCTVs installed in the Institute for the overall security, etc., the services are being provided by the WIHG Computer Section. The section remains a backbone for institutional operations in a digitally connected world.

Drawing Section

The Drawing section provides the cartographic needs of the scientists of the Institute for in-house as well as sponsored project works. During the Year, the section has provided fifteen geological maps/structural maps/geomorphological maps/seismicity diagrams for the scientists and research scholars of the Institute. Besides, the tracing of three topographic sheets/aerial photo maps was carried out along with the preparation of the six geological columns. The section has also provided name labels and thematic captions during different activities and functions of the Institute.

TECHNICAL SERVICES

CELEBRATIONS

National Technology Day

National Technology Day (13 May 2024) WIHG celebrated National Technology Day under the theme "From Schools to Startups: Igniting Young Minds to Innovate". An Open Day was organized for school and college students, as well as the general public, offering guided tours of the museum and laboratories. The initiative provided participants with hands-on exposure to research in Earth sciences, fostering curiosity and scientific temperament among young learners.

Moments of the National Technology Day celebration

International Day for Biological Diversity

International Day for Biological Diversity (22 May 2024): To mark this occasion, Dr. Kalachand Sain, Director, WIHG, addressed staff and interns, emphasizing the critical role of biodiversity in sustaining ecosystems, particularly within the vulnerable Himalayan region.

International Yoga Day

10th International Day of Yoga (21 June 2024), WIHG observed the 10th International Day of Yoga with the theme "Yoga for Self and Society." A guided session led by a professional instructor saw active participation from all staff and scholars. Dr. Kalachand Sain highlighted yoga's role in promoting holistic well-being and scientific productivity. Scientists also shared personal reflections on the benefits of yoga in enhancing focus and mental clarity.

Employees and research scholars of the Institute practicing Yoga on the International Yoga Day

Foundation Day

56th Foundation Day (26 June 2024) To celebrate its 56th Foundation Day, WIHG hosted a keynote lecture by Dr. O.P. Mishra, Director, National Centre for Seismology. His talk, "Earthquake Risk Management vis-à-vis Technological Development," underscored advances in seismic resilience. The event also featured the Best Research Paper Award 2023, recognizing excellence in geoscience research.

Felicitation of the Dr. O.P. Mishra, Director, National Centre for Seismology during the Foundation Day celebration

Independence Day

On Independence Day 2024, the Wadia Institute of Himalayan Geology, Dehradun, joined the nation in celebrating the 78th anniversary of India's freedom with great pomp and purpose. The event was a noted milestone on the institute's annual calendar. The

Moments of the Independent Day celebration

CELEBRATIONS

institute's Director, accompanied by senior scientists, staff, and research scholars, hoisted the tricolour flag on the main lawn, followed by the national anthem. Following the official ceremonies, several sports, fun competitions, and a cultural Program were organised for the Institute employees and their family members. The prizes were distributed to the winners.

National Space Day

National Space Day (23 August 2024) : To commemorate National Space Day, WIHG organized an Open Day and slogan-writing competition, encouraging scientific awareness among students and staff. A special lecture by Dr. R.S. Chatterjee, Scientist-G, IIRS, highlighted India's advancements in Earth observation and its applications in monitoring groundwater depletion and land subsidence.

Moments of the National Space Day celebration

Swachhta Abhiyan (Swachhata Hi Seva)

The Institute launched a comprehensive cleanliness campaign themed "Swabhav Swachhata - Sanskar Swachhata." Activities included a Swachhta pledge, cleanliness drives, awareness rallies, film screenings, and a plantation drive near the research hostel. The campaign concluded with an award ceremony recognizing winners of various competitions.

Under the Swachhata Hi Seva (SHS) campaign from 14th Sept to 1st October 2024 (Ist Phase). This year the theme of Swachhta Abhiyan- 2024 was "Swabhav Swachhata – Sanskar Swachhata". In this direction we have taken the following activities at the Wadia Institute of Himalayan Geology (WIHG), Dehradun, Uttarakhand.

- Mass SWACHHATA PLEDGE was taken by all the employees of WIHG on September 17, 2024.

- Invited Lecture: A lecture has been organized at WIHG, which is delivered by the Invited Speaker Mr. Ashish Garg, President Eco-Group Society, Dehradun, the Topic of his Talk was "Cleanliness through Waste Management" on 21-09-2024.

- In-house Lectures: A lecture was delivered by the institute scientist Dr. Santosh Rai, on the topic "Tracing the Anthropogenic forcing of the Ganga River System" on 21-09-2024.

- Visited/Inspection by the DST team: A team of DST delegates, visited WIHG during 21-09-2024 and 22-09-2024. They visited different sections/ buildings/Labs of the WIHG institute to assess/evaluate the activities undertaken by WIHG. Discussion has been made with DST Inspection Team in WIHG committee room, regarding Swachhata in WIHG Campus.

CELEBRATIONS

Moments of the National Space Day celebration

Moments on the Occasion of Swachhata Special Campaign

CELEBRATIONS

In 2ⁿᵈ Phase (2ⁿᵈ OCT – 31ˢᵗ Oct. 2025), Special Campaign 4.0 for swachhta was observed/Celebrated at WIHG.

Moments on the Occasion of Swachhata Special Campaign

Plantation on the Occasion of Swachhata Special Campaign 4.0 in front of Research Scholars Hostel, WIHG

The event under "Swachhata Special Campaign 4.0" is for the construction of Waste Management pit for "Bio-degradable" and "Vermi-composting" in our Institute premises.

Bio-degradable Pit was constructed at WIHG, Near Store Building

The participation of the WIHG's employees and students in "Swachhata Selfie" program

When individuals click and share selfies while participating in clean-up activities, it fosters a sense of personal involvement, making them stakeholders in the larger cleanliness mission. For the wide dissemination of this program (SWACHHTA AWARENESS USING SELFIE), it was promoted through the internet, WIHG's website, and Facebook page.

CELEBRATIONS

Founder's Day

Founder's Day (23 October 2024) : WIHG commemorated the 141" birth anniversary of Prof. D.N. Wadia with floral tributes and a memorial lecture by Mr. Deepak Kumar, Superintending Surveyor, Survey of India. His talk on "Continuously Operated Reference Stations (CORS)" highlighted innovations in geodetic science.

Felicitation of the Mr. Deepak Kumar, Superintending Surveyor, Survey of India during the Founder's Day celebration

IISF 2024 Curtain Raiser (12 November 2024)

As a prelude to the 10" India International Science Festival, WIHG hosted a special lecture by Dr. R.P. Singh, Director, IIRS. His talk, "Journey of Space Research in India," traced the evolution of India's space capabilities, inspiring students and researchers.

Moments of the Founder's Day celebration

Vigilance Week

Vigilance Awareness Week-2024 was observed at WIHG Dehradun from October 28 to November 03, 2024. In this connection, an Integrity pledge has been taken by the employees of the Institute, followed by a lecture by Under Secretary Vigilance, DST, Ms. Anurag Devgan, "Preventive Vigilance" on November 13, 2024. During the Wadia Institute of Himalayan Geology vigilance week, Dehradun conducted a series of programs in conjunction with Vigilance Awareness Week (2024). Scientists from WIHG delivered talks on Vigilance Awareness and took pledges with the faculty and staff of different schools and colleges.

Moments of the Vigilance Awareness Week

Republic Day

The 76th Republic Day was celebrated in the Institute on 26 January 2025. On this occasion, Dr. Vineet K. Gahalaut, Director, unfurled the National Flag and delivered a formal address to the Institute employees and research scholars. To mark the occasion, various sports activities, craft exhibition, and competitions were organized for the employees and their children. Prize were distributed to the winner of various events.

Moments of the Republic Day celebration

National Science Day

National Science Day Celebration (28 February 2025) celebrated under the national theme "Empowering Indian Youth for Global Leadership in Science and Innovation for Viksit Bharat," the event featured a keynote lecture by Ms. Nebula Bagchi, Executive Director, GEOPIC, titled "The Himalaya: Perspective from India's National E&P Company." A wide array of activities engaged students, faculty, and the public, including an Open Day with guided museum and laboratory tours, orientation on geoscience instrumentation for students, lecture and quiz competitions, and poster and slogan contests on the theme "Viksit Bharat." The celebration concluded with a Popular Science Talk, fostering scientific awareness and innovation.

CELEBRATIONS

CELEBRATIONS

Moments of the National Science Day celebration

International Women's Day

The Wadia Institute of Himalayan Geology, Dehradun celebrated International Women's Day on March 7, 2025. The event was organized to promote gender equality and inclusion across all spheres of society with various programs and motivational lectures centred on the theme of women empowerment. The occasion was graced by an eminent author, educationalist and translator Ms. Bijoya Sawain and Dr NSK Harsh, Retired Scientist & Dean (Research) FRI, Dehradun as chief guests. The formal proceedings began with the lighting of the ceremonial lamp and Saraswati Vandana by research scholars followed by a speech from the Director highlighting the active role of women at workplace and their importance in the uplift-ment of the society followed by releasing of Institute's yearly Hindi Magazine "Ashmika" with a special guest Dr B.R. Arora, Former Director WIHG. During the keynote addresses, Ms. Bijoya Savian highlighted the role of women in literature and addressed patriarchal structures that have persisted across generations. She also shared contemporary examples of the social, economic, and mental empowerment of women in India. Dr N.S.K.

Harsh spoke about various legal provisions and acts that support women's rights and safety at the workplaces. He also emphasized the importance of cooperative work environments and personal hygiene awareness. After the keynote addresses, an interactive session was held where institute personnel shared their experiences and queries. The Chief Guest and the Director provided insightful responses with encouragement and a thought-provoking discussion. A melodious songs were sung by scientists and students that captivated the audience, and the senior-most woman employee shared her thoughts on women's progress and challenges in the workplace. A theatrical play emphasizing the importance of education for women was presented by students which was warmly applauded by the audience. Dr. Gautam Rawat, Rajbhasha Adhikari recited a self-written Hindi poem and delivered a speech advocating for women's inclusion and an equal opportunities. During the entire event a compilation of verses from the holy books were presented depicting on the importance and role of women. A heartfelt vote of thanks was delivered by a Senior Technical Officer expressing gratitude to all participants, organizers and attendees who made the celebration a success. The event concluded with the

distribution of gifts to all women personnel and a delicious lunch for all employees in honour of women's contribution in all sphere in the Institute and society. The International Women's Day 2025 celebration at the WIHG successfully promoted gender equality, inclusivity, and women's empowerment through thoughtful discussions, cultural events, plays and motivational lectures. The event was a resounding success, leaving the audience inspired and motivated to continue striving for a more equitable society.

Moments of the International Women's Day

CELEBRATIONS

DISTINGUISHED VISITORS TO THE INSTITUTE

- Dr. Shailesh Nayak, Chairman, Governing Body, WIHG and Director, NIAS, Bengaluru
- Prof. Vinod K. Gaur, Former Secretary, Dept. of Ocean Development (MoES), Govt. of India
- Prof. Harsh K. Gupta, Former Secretary, Dept. of Ocean Development (MoES), Govt. of India
- Prof. T.N. Singh, Director, IIT, Patna
- Shri Anant Swaroop, Additional Secretary, SDMA, Govt. of Uttarakhand
- Dr. R.P. Singh, Director, IIRS, Dehradun
- Prof. Rajiv Sinha, Professor, Indian Institute of Technology, Kanpur
- Dr. Harish Bahuguna, DDG, Geological Survey of India, Kolkata
- Dr. O.P. Mishra, Scientific-G, MoES, New Delhi
- Dr. Shantanu Sarkar, Director, ULMMC, Uttarakhand
- Prof. Kusala Rajendran, Professor (Retired), IISc, Banglore
- Prof. L.S. Chamyal, Former HOD, Dept. of Geology, MSU, Baroda
- Prof. R.G.S. Sastry, Adjunct Professor, School of Earth, Atmospheric and Ocean Sciences, IIT Bhubaneswar
- Dr. R.S. Chatterjee, Group Director & Head and Scientist/Engineer-G, IIRS Dehradun
- Ms. Nebula Bagchi, Executive Director, GEOPIC, Dehradun
- Mr. Deepak Kumar, Superintending Surveyor, Geodetic and Research Branch, Survey of India
- Prof. S.S. Rai, Visiting Faculty, IISER, Pune
- Dr. S.S. Randhawa, Consultant with SDMA, Govt. of Himachal Pradesh

Moments of distinguished visitors in the Institute

STATUS OF IMPLEMENTATION OF HINDI

The WIHG strictly adheres & complies with the policy and guidelines as formulated by the Rajbhasha Vibhag, Home Ministry, GoI and regularly submits it's quarterly, half-yearly & annual progress reports to Rajbhasha Vibhag and DST. Institute also submits its half-yearly and annual progress reports to NARAKAS, Dehradun in the desired formats. The Official Language Implementation Committee (OLIC) under the chairmanship of Director, WIHG is monitoring the implementation of Hindi in the Institute & it also reviews the draft of various Hindi reports before their submission to the aforementioned ministries. The committee monitors & formulates plans for progressive use of Official Language in the office. The committee takes cognizance of the progress in the Hindi implementation through its regular quarterly meetings.

The OLIC, WIHG regularly organizes quarterly workshops to promote the use of Official Language through the organization of interactive lecture series of prominent Speakers/Scientists & also through various Hindi typing workshops.

The Institute under the banner of OLIC organized Hindi Pakhwara from 14 Sep to 30 September 2024 in the Institute. This year an All India inaugural opening ceremony of the Hindi Pakhwara was organized at Bharat Mandapam, New Delhi by Rajbhasa Vibhag, Ministry of Home Affairs on 14 September 2024 which was duly attended by the Institute representatives.

Thereafter, various competitions/events were organized in WIHG from 15 September 2024 onwards, namely Photography, Diverse Language Knowledge & Noting-Drafting Competitions in various categories was held on 18 September 2024; Hindi essay & debate competitions for schools students were held on 20 & 23 September 2024; the invited Hindi lecture of prominent personalities of Dehradun were held on 19th & 24th September, wherein the Professor Saraswati Kala, School of Yogic Science & Naturopathy, SGRR University, Dehradun delivered her lecture on "Importance of Naturopathy and Acupressure therapy in present times" and Dr. Nand Lal Bharti, an Internationally acclaimed Artist delivered his lecture on "Jaunsari Tribe in Uttarakhand" respectively.

In the closing ceremony of the Pakhwara, a grand Kavi Sammelan was organized in the Institute's Auditorium. This magnificent event was warmly applauded by the audience & the prize distribution ceremony was held after the Kavi Sammelan. Sr. Scientists of WIHG Dr. RK Sehagal & Dr Gautam Rawat felicitated all the prize winners of various competitions held during the Pakhwara.

This year WIHG published the 30th issue of the Annual Hindi Magazine "Ashmika". Authors from various organizations, scholars and employees of the Institute contributed their articles pertaining to various disciplines of science, literature, poetry, stories & philosophy in the magazine. The articles published in the magazines are very informative and well appreciated by the readers.

STATUS OF IMPLEMENTATION OF HINDI

MISCELLANEOUS ITEMS

MISCELLANEOUS ITEMS

1. Reservation/Concessions for SC/ST employees

The government's orders on reservations for SC/ST/ OBCs are followed in recruitment to posts in various categories

2. Monitoring of personnel matters

Monitoring of personnel matters relating to employees of the Institute is done through various Committees appointed by the Director/Governing Body from time to time.

3. Mechanism for redressal of grievances

· Grievance Redressal Committee Regarding Dr. Paramjeet Singh's promotion from Scientist 'C' to Scientist 'D': The grievance committee verified the relevant documents being questioned in the grievance, raised by the applicant. The committee does not found any flaws in the proceeding of the interview, hence the case was disposed off.

· Regarding the report of the Grievance Redressal Committee (GRC) of Mr. Devi Singh for his request to refund the Application fees of the cancelled Advertised Post of MTS (Multi-Tasking Staff) via. Application no.3001/01/General Recruitment/ 2022-23/Estt./ dated 09.05.2024. The committee does not found any discrepancies in Institute part regarding the fee claim of the applicant for the cancelled post, and hence the case is disposed.

4. Welfare measures

The Institute has various welfare measures for the benefit of its employees. Various advances like House Building Advance, Conveyance Advance, Festival Advance, etc. are given to the employees. There is a salary Earner's Cooperative Society run by the Institute employees that provides loans to its members as and when required. The Institute also runs a canteen for the welfare of the employees and students. As a welfare measure, the Institute is providing recreational facilities to its employees.

5. Mechanism for redressal of complaints of sexual harassment of women employees at workplaces

An Internal Complaints Committee (ICC) was constituted to safeguard the women employees and to enquire into the complaints of sexual harassment of women employees at workplaces in the Institute. The Committee consists of one presiding officer from outside the Institute and four member from the Institute. As far as ICC is concerned, one case is subjudice and another is continuing.

6. Status of Vigilance Cases

No vigilance case is pending in the year 2024-2025.

7. Information on the RTI cases

The details of information on the RTI cases during the year 2024-25 are as under:

Details	Opening balance as on 01.04. 2024	Received during the year 2024-2025	Number of cases transferred to other public authorities	Decisions where requests/ appeals were rejected	Decisions where requests/ appeals were accepted
Requests for information	0	20	0	0	0
First appeals	0	0	0	0	0

8. Sanctioned Staff strength (category wise)

Group/ Category	Scientific	Technical	Administ-rative	Ancillary	Total
A	60	-	1	-	61
B	-	3	14	-	17
C	-	51	22	35	108
Total	60	54	37	35	186

9. Sanctioned and released budget grant for the year 2024-2025

Plan	:	Rs. 4865.00 Lakhs
Non- Plan	:	NIL
Total	:	Rs. 4865.00 Lakhs

STAFF OF THE INSTITUTE

Scientific Staff

1. Dr. Vineet Kumar Gahalaut — Director (Joined w.e.f. 23.01.2025)
2. Prof. Mahesh G. Thakkar — Director (Additional Charge: 9.8.2024 to 22.1.2025)
3. Dr. Kalachand Sain — Director (Relived on 08.08.2024)
4. Dr. R. Jayangondaperumal — Scientist 'F'
5. Dr. K.S. Luirei — Scientist 'F'
6. Dr. Kapesa Lokho — Scientist 'F'
7. Dr. R.K.Sehgal — Scientist 'F'
8. Dr. Santosh Kumar Rai — Scientist 'E'
9. Dr. Jayendra Singh — Scientist 'E'
10. Dr. B.K. Mukherjee — Scientist 'E'
11. Dr. Naresh Kumar — Scientist 'E'
12. Dr. Gautam Rawat — Scientist 'E'
13. Dr. Devajit Hazarika — Scientist 'E'
14. Dr. Kaushik Sen — Scientist 'E'
15. Dr. Satyajeet Singh Thakur — Scientist 'E'
16. Dr. Narendra Kumar Meena — Scientist 'E' (On Lien)
17. Dr. Param Kirti Rao Gautam — Scientist 'E'
18. Dr. Dilip Kumar Yadav — Scientist 'E'
19. Dr. Manish Mehta — Scientist 'E'
20. Dr. Rajesh S. — Scientist 'D'
21. Dr. Swapnamita C. Vaideswaran — Scientist 'D'
22. Dr. Vikas — Scientist 'D'
23. Dr. Som Dutt — Scientist 'D'
24. Dr. Anil Kumar — Scientist 'D'
25. Sh. Saurabh Singhal — Scientist 'D'
26. Dr. Narendra Kumar — Scientist 'D'
27. Dr. Parveen Kumar — Scientist 'D'
28. Dr. Vinit Kumar — Scientist 'D' (On Lien)
29. Dr. Aditya Kharya — Scientist 'D'
30. Dr. Suman Lata Srivastava — Scientist 'D'
31. Dr. Chhavi Pant Pandey — Scientist 'D'
32. Dr. Sameer Kumar Tiwari — Scientist 'D'
33. Dr. Paramjeet Singh — Scientist 'C'
34. Dr. Sudipta Sarkar — Scientist 'C'
35. Dr. Pinkey Bisht — Scientist 'C'
36. Dr. Rakesh Bhambri — Scientist 'C'
37. Dr. Amit Kumar — Scientist 'C'
38. Dr. C. Perumalsamy — Scientist 'C'
39. Dr. Pratap Chandra Sethy — Scientist 'C'
40. Dr. Hiredya Chauhan — Scientist 'C'
41. Dr. Vandana — Scientist 'C'
42. Dr. Rouf Ahmad Shah — Scientist 'C'
43. Dr. Pankaj Chauhan — Scientist 'C'
44. Dr. Priyadarshi Chinmoy Kumar — Scientist 'C'
45. Dr. Mutum Rajanikanta Singh — Scientist 'C'
46. Dr. Chinmay Haldar — Scientist 'C'
47. Dr. Subhojit Saha — Scientist 'C'
48. Dr. M. Prakasam — Scientist 'B'
49. Dr. Jairam Singh Yadav — Scientist 'B'
50. Dr. Subham Bose — Scientist 'B'
51. Dr. Naveen Chandra — Scientist 'B'
52. Dr. N. Premjit Singh — Scientist 'B'
53. Dr. Tariq Anwar Ansari — Scientist 'B'
54. Dr. Bappa Mukherjee — Scientist 'B'
55. Dr. Rajeeb Lochan Mishra — Scientist 'B'
56. Dr. Mahesh Ramrao Kapawar — Scientist 'B'
57. Dr. Kunda Badhe — Scientist 'B'
58. Dr. Jitender Kumar — Scientist 'B'
59. Dr. Pramod Kumar Rajak — Scientist 'B'

Technical Staff

1. Shri Sanjeev Kumar Dabral — Sr. Tech. Officer (Superannuated on31.11.2024)
2. Shri Rakesh Kumar — Sr. Tech. Officer
3. Shri N.K. Juyal — Sr. Tech. Officer (Superannuated on30.06.2024)
4. Shri C.B. Sharma — Executive Engineer
5. Shri T.K. Ahuja — Technical Officer
6. Shri S.S. Bhandari — Technical Officer
7. Shri Rambir Kaushik — Technical Officer
8. Shri Bharat Singh Rana — Technical Officer
9. Shri Gyan Prakash — Asstt. Pub. & Doc. Officer
10. Dr. Balram — Librarian
11. Shri R.M. Sharma — Sr. Laboratory Technician
12. Mrs. Sarita — Sr. Technical Assistant
13. Shri Rakesh Kumar — Sr. Technical Assistant
14. Mrs. Sakshi Maurya Chaudhary — Sr. Technical Assistant
15. Mrs. Disha Vishnoi — Sr. Technical Assistant
16. Dr. Gaurav Jain — Sr. Technical Assistant (Supernumerary Post) Joined on 23.08.2024 (Redeployed from Vigyan Prasar, New Delhi)
17. Shri Rahul Lodh — Laboratory Assistant
18. Shri Prateek Negi — Artist cum Modeller
19. Shri Vipin Chauhan — Technical Assistant
20. Shri Deepak Kumar — Technical Assistant
21. Shri Pramod Kumar — Technical Assistant

STAFF OF THE INSTITUTE

STAFF OF THE INSTITUTE

22. Shri Akash Khati — Technical Assistant
23. Shri Nand Ram — Elect.cumPump.Optr.
    (Superannuated on30.06.2024)
24. Shri Tarun Jain — Draftsman
25. Shri Pankaj Semwal — Draftsman
    (Died on 17.12.2024)
26. Shri Anil Singh — Draftsman
27. Shri Santu Das — Section Cutter
    (Superannuated on31.08.2024)
28. Shri Puneet Kumar — Section Cutter
29. Shri Amit Bhandari — Jr. Photographer
30. Shri Hari Singh Chauhan — F.C.L.A.
    (Superannuated on30.04.2024)
31. Shri Preetam Singh — F.C.L.A.
32. Shri Sanjeev Kumar — F.C.L.A.
33. Shri Deepak Tiwari — F.C.L.A.
34. Shri Ajay Kumar Upadhaya — F.C.L.A.
35. Ms. Sangeeta Bora — F.C.L.A.
36. Mrs. Anjali — F.C.L.A.
37. Shri Ajay Kumar — F.C.L.A.
38. Shri Vipin Kumar Aditya — F.C.L.A.
39. Shri Nitesh Kumar — F.C.L.A.
40. Shri Abhishek Kumar — F.C.L.A.
41. Shri Sandeep Singh — F.C.L.A.
42. Shri Ajit Kumar — F.C.L.A.
43. Shri Narender Manral — Field Attendant
44. Shri Aakash Sharma — Field Attendant
45. Shri Ashish Singh — Field Attendant
46. Shri Aakash Saini — Field Attendant

Administrative Staff

1. Shri Pankaj Kumar Verma — Registrar
2. Shri S.K.Srivastava — Administrative Officer
3. Shri Manas Kumar Biswas — Store & Purchase Officer
4. Shri Rahul Sharma — Asstt. Fin. & A/c Officer
5. Shri Ankit Rawat — Sr. Personal Assistant
6. Mrs. Shalini Rawat — Stenographer, Gr. II
7. Mrs. Neelam Chabak — Assistant
8. Mrs. Seema Juyal — Assistant
   (Superannuated on31.08.2024)
9. Shri Yashpal Singh Bisht — Jr. Translation Officer
10. Mrs. Suman Nanda — Assistant
11. Shri Kulwant Singh Manral — Assistant
12. Mrs. Richa Kukreja — Stenographer, Gr. III
13. Shri Vijai Ram Bhatt — Upper Division Clerk
14. Shri Girish Chander Singh — Upper Division Clerk
15. Shri Rajeev Yadav — Upper Division Clerk
16. Shri Amardeep Kumar — Upper Division Clerk
17. Shri Dhanveer Singh — Upper Division Clerk

18. Mrs. Megha Khugshal — Upper Division Clerk
19. Mrs. Surbhi — Upper Division Clerk
20. Shri Deepak Jakhmola — Upper Division Clerk
21. Shri Dinesh Kumar Singh — Upper Division Clerk
22. Mrs. Rachna — Upper Division Clerk
23. Mrs. Pushpa Barthwal — Lower Division Clerk
    (Superannuated on31.01.2025)
24. Shri Amit Kumar — Lower Division Clerk
25. Shri Pintu Kumar — Lower Division Clerk
26. Shri Naved Khan — Lower Division Clerk
27. Shri Vishesh Kumar Gautam — Lower Division Clerk
28. Ms. Saba — Lower Division Clerk
29. Shri Manjeet Rana — Lower Division Clerk

Ancillary Staff

1. Shri Manmohan — Driver
2. Shri Vikkee Tomar — Driver
3. Shri Bhupendra Kumar — Driver
4. Shri Rajesh Yadav — Driver
5. Shri Pradeep Shah — Driver
6. Shri S.K. Gupta — M.T.S.
   (Superannuated on 31.05.2024)
7. Shri Surendra Singh — M.T.S.
8. Shri Satya Narayan — M.T.S.
9. Shri Rohlu Ram — M.T.S.
10. Shri H.S. Manral — M.T.S.
11. Shri G.D. Sharma — M.T.S.
12. Shri Dinesh Parsad Saklani — M.T.S.
13. Shri Pritam — M.T.S.
14. Shri Ashish Rana — M.T.S.
15. Shri Sunil Kumar — M.T.S.
16. Shri Harish Kumar Verma — M.T.S.
17. Shri Kamlesh Singh — M.T.S.
18. Shri Rajkiran Singh — M.T.S.
19. Shri Abdul Basit — M.T.S.
20. Shri Yogender Saklani — M.T.S.
21. Ms. Deepti Pandey — M.T.S.
22. Mrs. Sakshi Chauhan — M.T.S.
23. Shri Chandrapal — M.T.S.
    (Joined on 02.09.2024)
    (Redeployed from Vigyan Prasar, New Delhi)

Contracutal Staff

1. Shri Rezaw Uddin Chaudhary — Driver
2. Sh. Vijay Singh — Driver
3. Shri Rudra Chettri — M.T.S.
4. Shri Laxman Singh Bhandari — M.T.S.
5. Shri Kalidas — M.T.S.
6. Shri Ummed Singh — M.T.S.

MEMBERS OF THE GOVERNING BODY/RESEARCH ADVISORY COMMITTEE/FINANCE COMMITTEE/BUILDING COMMITTEE

Governing Body
(upto Feb. 17, 2025)

Sl.	Name	Address	Status
1.	Prof. Talat Ahmad	Vice-Chancellor, University of Kashmir, Hazratbal, Srinagar-190006 (J&K)	Chairman
2.	Secretary, DST or his/her nominee	Department of Science and Technology, Technology Bhawan, New Mehrauli Road, New Delhi- 110016	Member
3.	Financial Adviser, DST or his/her nominee	Department of Science and Technology, Technology Bhawan, New Mehrauli Road, New Delhi- 110016	Member
4.	Dr. O.P. Mishra	Scientist-G, Ministry of Earth Sciences, Govt. of India Prithvi Bhawan, Lodhi Road, New Delhi- 110003	Member
5.	Prof. M. Jayananda	Head, Centre for Earth and Space Sciences, University of Hyderabad, P.O. Central University, Gachibowli, Hyderabad-500046 (Telangana)	Member
6.	Prof. Pulak Sengupta	Professor, Department of Geological Sciences, Jadavpur University, 188, Raja Subodh Chandra Mallick Road, Poddar Nagar, Jadavpur, Kolkata-700032 (WB)	Member
7.	Dr. N.V. Chalapathi Rao	Professor, Department of Geology, Banaras Hindu University Ajagara, Varanasi-221005 (UP)	Member
8.	Prof. Anupam Chattopadhyay	Department of Geology, University of Delhi (North Campus), 34 Chhatra Marg, Delhi-110007	Member
9.	Prof. Saibal Gupta	Professor & Head, Department of Geology & Geophysics, Indian Institute of Technology-Kharagpur, Kharagpur -721302 (WB)	Member
10.	Prof. S.C. Patel	Professor, Department of Earth Sciences Indian Institute of Technology-Bombay Powai, Mumbai-400076 (Maharashtra)	Member
11.	Prof. Shakil Romshoo	Vice-Chancellor Islamic University of Science & Technology, 1-University Avenue, Awantipora, Pulwama-192122 (J&K)	Member
12	Director, WIHG	Wadia Institute of Himalayan Geology, 33, G.M.S. Road, Dehradun- 248001	Member Secretary
13.	Registrar, WIHG	Wadia Institute of Himalayan Geology, 33, G.M.S. Road, Dehradun- 248001	Non-Member-Asstt. Secretary

MEMBERS OF THE GOVERNING BODY/RESEARCH ADVISORY COMMITTEE/FINANCE COMMITTEE/BUILDING COMMITTEE

Governing Body
(w.e.f. Feb. 18, 2025

Sl.	Name	Address	Status
1.	Dr. Shailesh Nayak	Director, National Institute of Advanced Studies, Indian Institute of Science campus, Bengaluru- 560012	Chairman
2.	Secretary, DST or his/her nominee	Department of Science and Technology, Technology Bhawan, New Mehrauli Road, New Delhi- 110016	Member
3.	Financial Adviser, DST or his/her nominee	Department of Science and Technology, Technology Bhawan, New Mehrauli Road, New Delhi- 110016	Member
4.	Prof. Talat Ahmad	Ex-VC, KU and JMI, New Delhi Lane No. 6, House No. 8, Ashirwad Enclave, Dehradun-248001	Member
5.	Prof. A.P. Dimri	Director, Indian Institute of Geomagnetism, Plot No. 5, Sector 18, Near Kalamboli Highway, New Panvel, Navi Mumbai, 410218	Member
6.	Dr. Sunil Kumar Singh	Director, National Institute of Oceanography, Dona Paula- 403004, Goa	Member
7.	Dr. O.P. Mishra	Scientist-G, Ministry of Earth Sciences, Govt. of India, Prithvi Bhawan, Lodhi Road, New Delhi- 110003	Member
8.	Dr. Prakash Chauhan	Director, National Remote Sensing Centre, Indian Space Research Organisation, Dept. of Space, Govt. of India, Balanagar, Hyderabad-500037	Member
9.	Dr. N.V. Chalapathi Rao	Director, National Centre of Earth Science Studies, Post Box No. 7250, Akkulam Road, Thiruvananthapuram-695011 (Kerala)	Member
10.	Prof. Kusala Rajendran	Retd. from Indian Institute of Science, Bangalore-560012	Member
11.	Dr. Prakash Kumar	Director, CSIR-National Geophysical Research Institute, Uppal Road, Hyderabad-500007	Member
12	Director, WIHG	Wadia Institute of Himalayan Geology, 33, G.M.S. Road, Dehradun- 248001	Member
13.	Registrar, WIHG	Wadia Institute of Himalayan Geology, 33, G.M.S. Road, Dehradun- 248001	Non-Member- Asstt. Secretary

Research Advisory Committee

Sl.	Name	Address	Status
1.	Dr. Shailesh Nayak	Director, National Institute of Advanced Studies, Indian Institute of Science campus, Bengaluru -560012	Chairman
2.	Prof. T.N. Singh	Director, Indian Institute of Technology-Patna, Bihta, Patna-801106 (Bihar)	Member
3.	Prof. D.C. Srivastava	Emeritus Professor, Department of Earth Sciences, Indian Institute of Technology-Roorkee, Roorkee-247667	Member
4.	Shri Rajesh Kumar Srivastava	Director, Oil and Natural Gas Corporation Limited, 5, Nelson Mendela Road, Vasant Kunj, New Delhi-110070	Member
5.	Dr. Rasik Ravindra	608, Lalleshwari Apart Sector 21 D, Faridabad-121001	Member
6.	Prof. Rajesh K. Srivastava	Professor & Former Head, Dept. of Geology, Banaras Hindu University, Varanasi- 221005 (UP)	Member
7.	Dr. Binita Phartiyal	Scientist 'E', Birbal Sahni Institute of Palaeoscience, 53, University Road, Lucknow- 226007 (UP)	Member
8.	Dr. Prakash Chauhan	Director, Indian Institute of Remote Sensing, 4, Kalidas Road, Dehradun- 248001	Member
9.	Dr. O.P. Mishra	Scientist 'G' and Head, NCS, Ministry of Earth Sciences, Govt. of India, Prithvi Bhavan, Lodhi Road, New Delhi-110003	Member
10.	Dr. Prasun Jana	Deputy Director General, Geological Survey of India, Dehradun-248001	Member
11.	Prof. Kusala Rajendran	Centre of Earth Sciences, Indian Institute of Science, Bengalore-560012	Member
12.	Prof. L.S. Chamyal	Head, Dept. of Geology, Faculty of Science, The M.S. University of Baroda, Vadodara-390002 (Gujarat)	Member
13.	Prof. Santanu Banerjee	Department of Earth Sciences, Indian Institute of Technology-Bombay, Powai, Mumbai-400076 (Maharashtra)	Member
14.	Dr. V. Balaram	Scientist 'G' (Retd.), SCIR-NGRI, Hyderabad, Consultant IUAC, Delhi	Member
15.	Prof. Devesh K. Sinha	Oceanography and Marine Geology, Dept. of Geology, Delhi University, Delhi- 110007	Member
16.	Prof. Saibal Gupta	Professor & Head, Department of Geology & Geophysics, Indian Institute of Technology-Kharagpur Kharagpur-721302 (WB)	Member
17.	Director, WIHG	Wadia Institute of Himalayan Geology, 33, G.M.S. Road, Dehradun- 248001	Member
18.	Dr. R.J. Perumal	Scientist 'F', Wadia Institute of Himalayan Geology, 33, G.M.S. Road, Dehradun- 248001	Member Secretary

MEMBERS OF THE GOVERNING BODY/RESEARCH ADVISORY COMMITTEE/FINANCE COMMITTEE/BUILDING COMMITTEE

Finance Committee

Sl.	Name	Address	Status
1.	Financial Adviser, DST or his/her nominee	Department of Science and Technology, Technology Bhawan, New Mehrauli Road, New Delhi- 110016	Chairman
2.	Prof. Anupam Chattopadhyay	Department of Geology, University of Delhi (North Campus), 34 Chhatra Marg, Delhi- 110007	Member
3.	Director, WIHG	Wadia Institute of Himalayan Geology, 33, G.M.S. Road, Dehradun- 248001	Member
4.	Registrar, WIHG	Wadia Institute of Himalayan Geology, 33, G.M.S. Road, Dehradun- 248001	Member
5.	AF&AO, WIHG	Wadia Institute of Himalayan Geology, 33, G.M.S. Road, Dehradun- 248001	Member Secretary

Building Committee

Sl.	Name	Address	Status
1.	Director, WIHG	Wadia Institute of Himalayan Geology, 33, G.M.S. Road, Dehradun- 248001	Chairman
2.	Financial Adviser, DST or his/her nominee	Department of Science and Technology, Technology Bhawan, New Mehrauli Road, New Delhi- 110016	Member
3.	Representative of Survey of India	Hathibarkala, Dehradun	Member
4.	Chief Engineer, CPWD or his/her nominee	CPWD, Dehradun- 248001	Member
5.	Shri Ashish Kumar Singh (Representative of ONGC, Dehradun)	SE (Civil), Tel Bhawan, Oil & Natural Gas Corporation, Dehradun-248001	Member
6.	Dr. R.J. Perumal	Scientist-F, Wadia Institute of Himalayan Geology, 33, G.M.S. Road, Dehradun- 248001	Member
7.	Shri Rajesh Kumar (Representative of Director, IIP, Dehradun)	Sr. Principal Scientist, Head ASD, CSIR- Indian Institute of Petroleum Haridwar Road, Dehradun-248005	Member
8.	Registrar, WIHG	Wadia Institute of Himalayan Geology, 33, G.M.S. Road, Dehradun- 248001	Member
9.	Executive Engineer, WIHG	Wadia Institute of Himalayan Geology, 33, G.M.S. Road, Dehradun- 248001	Member Secretary

STATEMENT OF ACCOUNTS

STATEMENT OF ACCOUNTS

KRA & CO.
Chartered Accountant

CA INDIA

HO: 1st floor, 01, Shri Raj Complex, Opp Nagri Bus Stand, Kathua, Jammu and Kashmir, 184101
Ph. 9419158267
e-mail : ajay.kraindia@gmail.com

AUDITOR'S REPORT ON CONSOLIDATED FINANCIAL STATEMENTS

The Members of Governing Body,
Wadia Institute of Himalayan Geology,
33, GMS Road, Dehradun
Uttarakhand

We have audited the accompanying Consolidated Financial Statements of **WADIA INSTITUTE OF HIMALAYAN GEOLOGY, 33, GMS Road, Dehradun** for the year ended March 31st, 2025 which comprises Balance Sheet ,Income and Expenditure Account, Receipt and Payment Account and summary of significant accounting policies.

Society's management is responsible for the preparation of these Financial Statements in accordance with law. This responsibility includes the design, implementation and maintenance of internal control relevant to the preparation and presentation of the financial statements that give a true and fair view and are free from material misstatement, whether due to fraud or error.

Our responsibility is to express an opinion on these financial statements based on our audit. We conducted our audit in accordance with the Standards on Auditing issued by the Institute of Chartered Accountants of India. Those Standards require that we comply with ethical requirements and plan and perform the audit to obtain reasonable assurance about whether the financial statements are free from material misstatement.

An audit involves performing procedures to obtain audit evidence about the amounts and disclosures in the financial statements. The procedures selected depend on the auditor's judgment, including the assessment of the risks of material misstatement of the financial statements, whether due to fraud or error. In making those risk assessments, the auditor considers internal control relevant to the Society's preparation and fair presentation of the financial statements in order to design audit procedures that are appropriate in the circumstances. An audit also includes evaluating the appropriateness of accounting policies used and the reasonableness of the accounting estimates made by management, as well as evaluating the overall presentation of the financial statements.
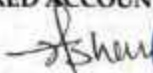
We believe that the audit evidence we have obtained is sufficient and appropriate to provide a basis for our audit opinion.

In our opinion and to the best of our information and according to the explanations given to us, the financial statements give the information required by the Act in all material respects and give a true and fair view in conformity with the accounting principles generally accepted in India subject to our comments given in Annexure-"1":

a) in the case of the Balance Sheet, of the state of affairs of the Society as at March 31st, 2025;

b) in the case of the Income and Expenditure Account of the Deficit for the year ended on that date; and

c) in the case of the Receipt and Payment Account, of the cash flows for the year ended on that date.

FOR KRA & CO
CHARTERED ACCOUNTANTS

CA AJAY KUMAR
FCA
FRN: 020266N
M.NO: 503015
UDIN :- 25503015BMGLLV6106

Date: 06th June, 2025
Place: Dehradun

STATEMENT OF ACCOUNTS

Annexure-1 to the Consolidated Financial Statement of Audit Report (F.Y. 2024-25)

The following observations were noticed during the course of audit for the Financial Year 2024-25. The same have been discussed with the management and comments/explanations of the management thereon have also been observed.

Sl. No.	Comments/Observations by Chartered Accountants
1	It was observed that the institute has not opened bank account with State Bank of India as required by the provisions of FCRA account. Hence, all the transactions and returns pertaining to FCRA are pending.
2	The physical verification of Fixed Assets and Library for the financial year 2024-25 has not been undertaken. The reason for not complying with the rule laid down in GFR regarding physical verification of Assets may be specified.

FOR KRA & CO
CHARTERED ACCOUNTANTS

CA AJAY KUMAR
FCA
FRN: 020266N
M.NO: 503015
UDIN :- 25503015BMGLLV6106

Date: 6ᵗʰ June, 2025
Place: Dehradun

Action Taken Report on observations of the Chartered Accountant- Annexure-1 to the Consolidated Financial Statement of Audit Report (F.Y. 2024-25)

Sl. No.	Comments/Observations by Chartered Accountants	Replies and Action taken by the Institute
1	It was observed that the institute has not opened bank account with State Bank of India as required by the provisions of FCRA account. Hence, all the transactions and returns pertaining to FCRA are pending.	Noted for strict compliance. It is to be intimated that there has been no foreign transaction during the period under Audit.
2	The physical verification of Fixed Assets and Library for the financial year 2024-25 has not been undertaken. The reason for not complying with the rule laid down in GFR regarding physical verification of Assets may be specified.	Physical verification for the year 2023-24 has already been completed. Action with regard to the physical verification for the year 2024-2025 is in progress and report will be submitted to the next audit.

FOR K R A & CO
CHARTERED ACCOUNTANTS

CA AJAY KUMAR
FCA

(Rahul Sharma)
AE & AO

(Pankaj Kumar Verma)
Registrar

(Dr. V. K. Gahalaut)
Director

STATEMENT OF ACCOUNTS

WADIA INSTITUTE OF HIMALAYAN GEOLOGY, DEHRADUN

BALANCE SHEET
(AS AT 31st MARCH 2025)

(Amt in Rs...)

PARTICULARS	SCHEDULE	CURRENT YEAR	PREVIOUS YEAR
LIABILITIES			
Corpus/ Capital Fund	1	78,31,57,158	80,28,25,623
Reserves and Surplus	2	-	-
Earmaked/ Endowment Fund	3	17,29,623	33,96,395
Secured Loans & Borrowings	4	-	-
Unsecured Loans & Borrowings	5	-	-
Deferred Credit Liabilities	6	-	-
Current Liabilities & Provisions	7	75,86,391	76,53,632
TOTAL		**79,24,73,172**	**81,38,75,650**
ASSETS			
Fixed Assets	8	41,76,24,409	37,96,98,636
Investments from Earmaked/ Endowment Funds	9	1,23,850	1,16,089
Investment- Others	10	-	-
Current Assets, Loans & Advances	11	37,47,24,913	43,40,60,926
TOTAL		**79,24,73,171**	**81,38,75,650**
Significant Accounting Policies	37		
Contingent Liabilities and Notes on Accounts	38		

AUDITOR'S REPORT

"As per our separate report of even date"

FOR KRA & CO.
CHARTERED ACCOUNTANTS

CA AJAY KUMAR
(F.C.A)

(RAHUL SHARMA)
A E & A.O

(PANKAJ KUMAR VERMA)
Registrar

(DR. V.K. GAHALAUT)
Director

Date : 6th June,2025
Place : Dehradun

WADIA INSTITUTE OF HIMALAYAN GEOLOGY, DEHRADUN

INCOME & EXPENDITURE ACCOUNT
FOR THE PERIOD ENDED 31st MARCH 2025

(Amt in Rs...)

S.NO.	PARTICULARS	SCH.	CURRENT YEAR	PREVIOUS YEAR
A	**INCOME**			
	Income from sales/ services	12	-	-
	Grants/ Subsidies	13	44,89,63,568	45,95,28,063
	Fees/Subscription	14	-	-
	Income from Investments	15	10,78,187	11,31,316
	Income from Royalty, Publication etc.	16	1,17,690	1,45,430
	Interest earned	17	1,23,81,939	1,27,78,059
	Other Income	18	1,33,45,342	1,05,47,054
	Increase/ Decrease in Stock (Goods & WIP)	19	-	-
	TOTAL (A)		47,58,86,726	48,41,29,922
B	**EXPENDITURE**			
	Establishment Expenses	20	37,35,67,025	23,22,66,228
	Other Research & Administrative Expenses	21	10,33,19,965	8,25,63,317
	Grant Refunded	22	10,39,476	22,55,347
	Interest/ Bank Charges	23	39,99,275	43,39,776
	Depreciation Account	8	6,92,86,740	6,63,30,606
	Increase/ Decrease in stock of Finished goods, WIP& Stock of Publication	A-2	21,588	- 33,757
	(Profit)/ Loss on sale of Assets	36	- 92,565	-
	TOTAL (B)		55,11,41,504	38,77,21,517
	Surplus/ (Deficit) being excess of Income over Expenditure (A - B)		- 7,52,54,778	9,64,08,405
	Transfer to Special Reserve (Specify each)		-	-
	Transfer to / from General Reserve		-	-
	SURPLUS /(DEFICIT) CARRIED TO CAPITAL FUND		- 7,52,54,778	9,64,08,405

AUDITOR'S REPORT
"As per our separate report of even date"

FOR KRA & CO.
CHARTERED ACCOUNTANTS

CA AJAY KUMAR
(F.C.A)

(RAHUL SHARMA) (PANKAJ KUMAR VERMA) (DR. V.K.GAHALAUT)
AF & A.O Registrar Director

Date : 6th June,2025
Place: Dehradun

STATEMENT OF ACCOUNTS

STATEMENT OF ACCOUNTS

WADIA INSTITUTE OF HIMALAYAN GEOLOGY, DEHRA DUN

RECEIPTS & PAYMENTS ACCOUNT
(FOR THE YEAR ENDED 31st MARCH 2025)

(Amt in Rs...)

PARTICULARS	SCH.	CURRENT YEAR	PREVIOUS YEAR
RECEIPTS			
Opening Balance	24	22,60,44,479	21,79,83,393
Grants - in - Aids	26	50,84,63,568	51,51,28,063
Grants - in - Aids/Other Receipts (Ear Marked)	27	26,67,170	1,11,91,761
Loan & Advances	28	26,53,18,055	22,12,38,342
Loan & Advances (Ear Marked)	31	73,166	-
Fees/Subscription	14	-	-
Income from Investments	15	10,78,187	11,31,316
Income from Royalty, Publication etc.	16	1,17,690	1,45,430
Interest earned	17	1,23,81,939	1,27,78,059
Other Income	18	1,33,45,342	1,05,47,054
Investment (L/C Margin Money)	34	6,68,78,485	-
TOTAL		**1,09,63,68,081**	**99,01,43,419**
PAYMENTS			
Establishment Expenses	20	37,35,67,025	23,22,66,228
Other Administrative Expenses	21	10,33,19,965	8,25,63,317
Grant Refunded	22	10,46,707	1,60,83,800
Interest/ Bank Charges	23	39,99,275	43,39,776
Loans & Advances	29	27,00,18,579	36,67,19,661
Loans & Advances (Ear Marked)	32	7,761	6,383
Investment (L/C Margin Money)	35	2,04,52,092	-
Fixed Assets	36	10,72,27,468	5,11,16,530
Ear Marked Fund Expenses	33	25,76,213	1,10,03,246
Grant - in - Aid (Ear Marked) Refunded	30	17,57,729	-
Closing Balance	25	21,23,95,267	22,60,44,479
TOTAL		**1,09,63,68,081**	**99,01,43,419**

AUDITOR'S REPORT
"As per our separate report of even date"

FOR KRA & CO.
CHARTERED ACCOUNTANTS

CA AJAY KUMAR
(F.C.A)

(RAHUL SHARMA)
A F & A.O

(PANKAJ KUMAR VERMA)
Registrar

(DR. V.K.GAHALAUT)
Director

Date : 6th June 2025
Place: Dehradun

WADIA INSTITUTE OF HIMALAYAN GEOLOGY,
33, GMS ROAD DEHRADUN

SCHEDULE FORMING PART OF ACCOUNTS FOR THE YEAR ENDED 31ST MARCH, 2025

SCHEDULE – 37: SIGNIFICANT ACCOUNTING POLICIES

1. **ACOUNTING CONVENTION**

   The financial statements are prepared on the basis of historical cost convention, unless otherwise stated and on the cash method of accounting except interest accrued on fixed deposit.

2. **INVESTMENTS**

   Investments classifieds as "long term investments" are carried at cost.

3. **FIXED ASSETS**

   a) Fixed Assets are stated at net book value as recommended in the "Uniform Accounting Format" of financial statements for the Central Autonomous Bodies as made compulsory by the Ministry of Finance w.e.f. 01.04.2001.
   b) Additions to fixed assets are taken at cost of acquisition, inclusive of freight, duties and taxes, incidental and direct expenses related to acquisition.

4. **DEPRECIATION**

   a) Depreciation is provided on Written down Value method as per rates specified in the Income Tax Act, 1961.

   b) When an asset is discarded or sold or deleted, the original cost is deducted from the gross block, the W.D.V. is deducted from the W.D.V. block and accumulated depreciation on the asset upto the date of deletion is deducted from accumulated depreciation of the respective block.

   c) In respect of addition to/ deduction from fixed assets during the year, depreciation is considered on full yearly basis.

WADIA INSTITUTE OF HIMALAYAN GEOLOGY, 33, GMS ROAD DEHRADUN

5. **MISCELLANEOUS EXPENDITURE**

   Deferred revenue expenditure, if any, will be written off over a period of 5 years from the year it is incurred.

6. **ACCOUNTING FOR SALES & SERVICES**

   The consultancy services provided by the institute is accounted for on net service basis.

7. **GOVERNMENT GRANTS / SUBSIDIES**

   a) Government grants of the nature of contribution towards Capital Cost are directly credited to Corpus Fund and Other Revenue cost are transferred to Income & Expenditure account and the surplus or deficit after deducting all the expenses is transferred to Capital / Corpus fund.

   b) Grants towards Earmarked / Endowment Funds are directly transferred to the respective fund account.

   c) Government grants / subsidy are accounted on realization basis.

(Rahul Sharma)
A.F. & A.O

(Pankaj Kumar Verma)
Registrar

(Dr V.K.Gahalaut)
Director

Date : 6th June, 2025
Place: Dehradun

WADIA INSTITUTE OF HIMALAYAN GEOLOGY,
33 GMS ROAD, DEHRADUN

SCHEDULE FORMING PART OF ACCOUNTS FOR THE YEAR ENDED 31ST MARCH, 2025

SCHEDULE – 38: CONTINGENT LIABILITIES AND NOTES ON ACCOUNTS

1. **CONTINGENT LIABILITIES**

(Amount in Rs.)

a)	Claims against the Entity not acknowledged as debts		- Nil -
b)	In respect of		
	i)	Bank Guarantees given by /on behalf of the Entity	- Nil -
	ii)	Letter of credit opened by Bank on behalf of the entity	-Nil-
	iii)	Bills discounted with banks	- Nil -
c)	Disputed demands in respect of		
	i)	Income –tax (TDS)	- Nil -
	ii)	Sales tax	- Nil -
	iii)	Municipal Taxes	- Nil -
d)	In respect of claims from parties for non-execution of orders, but contested by the Entity		- Nil -

2. **CAPITAL COMMITMENTS**

Estimated Value of contracts remaining to be executed on capital account and not provided for (net of advances)		
a)	Construction of Building	- Nil -
b)	Other Assets	-Nil -

3. **LEASE OBLIGATIONS**

Future obligations for rentals under finance lease arrangements for plant and machinery amount to Rs. Nil	- Nil -

4. **CURRENTS ASSETS, LOANS AND ADVANCES**

In the opinion of the Institute, the current assets, loans and advances have a value on realization in the ordinary course of business, equal at least to the aggregate amount shown in the Balance Sheet.

5. **TAXATION**

In view of there being no taxable income of the Institute under income tax Act, 1961, no provision for Income Tax has been considered necessary

WADIA INSTITUTE OF HIMALAYAN GEOLOGY,
33 GMS ROAD, DEHRADUN

6. FOREIGN CURRENCY TRANSACTIONS

a)	Value of Imports Calculated on C.I.F basis:	
	i)	Purchase of finished goods	- Nil -
	ii)	Raw Materials & Components (including in transit)	- Nil -
	iii)	Capital goods	- Nil -
	iv)	Stores, Spares and Consumables	- Nil -
b)	Expenditure in foreign currency	
	i)	Travel (for attending Seminar/Conference abroad)	- Nil -
	ii)	Remittances and Interest payment to Financial Institutions / Banks in Foreign Currency	- Nil -
	iii)	Other expenditure	
		Commission on Sales	- Nil -
		Legal and Professional Expenses	- Nil -
		Miscellaneous Expenses	- Nil -
c)	Earnings	
	i)	Value of Exports on FOB basis	- Nil -
	ii)	Grants for Projects	- Nil -

7. The payments to auditors during the F.Y. 2024 -25 is as follows:

	Remuneration to auditors	
i)	As Auditors	1,75,112/-
	Taxation matters	- Nil -
	For Management Services	- Nil -
	For Certification	- Nil -
ii)	Others	- Nil -

8. Separate Financial Statements have been prepared for:

a) Wadia Institute of Himalayan Geology.
b) Contributory/ General Provident Fund.
c) Pension Fund.
d) Consolidated financial statement of projects sponsored by other Agencies.
e) Individual financial statements of Projects sponsored by other agencies.

9. Corresponding figures for the previous year have been regrouped / rearranged, wherever necessary.

10. Annexed Schedules & Annexures are an integral part of the Balance Sheet as on 31st March, 2025, Income and Expenditure Account and Receipt & Payment for the year ended on 31st March, 2025.

(Rahul Sharma)
A.F. & A.O

(Pankaj Kumar Verma)
Registrar

(Dr. V.K.Gahalaut)
Director

Date : 6th June, 2025
Place: Dehradun

वाडिया हिमालय भूविज्ञान संस्थान
WADIA INSTITUTE OF HIMALAYAN GEOLOGY

सदस्यता/Membership No.

LTSS-.......................

हिमालयन जियोलॉजी
HIMALAYAN GEOLOGY

आजीवन ग्राहक सदस्यता हेतु पंजीकरण प्रपत्र
Registration form for Life Time Subscriber membership

केवल व्यक्तिगत उपयोग हेतु/for individuals use only

1. मैं "हिमालयन जियोलॉजी" का आजीवन ग्राहक बनना चाहता हूँ।
   I would like to become a Life Time Subscriber for "Himalayan Geology".

2. आजीवन सब्सक्रिप्शन शुल्क की राशि निदेशक, वाडिया हिमालय भूविज्ञान संस्थान के पक्ष में ऑनलाइन भुगतान विवरण/ड्राफ्ट/चैक के साथ निम्नलिखित के लिए संलग्न है।

   The Life Time subscription fee with online payment details/Draft/Cheque in favour of Director, Wadia Institute of Himalayan Geology is enclosed herewith for the following:

   Type of subscription (Tick [✓] which is applicable): ☐ Print copy ☐ Soft copy by online access/email

   ☐ Fee for Print copy : Rs. 7500.00 (India) US$ 750.00 (Foreign)
   ☐ Fee for Soft copy : Rs. 4000.00 (India) US$ 250.00 (Foreign)

   नाम/Name: ....

   पता/Address:..

   ....

   ....

   ईमेल/Email: ....

   मोबाइल/Mobile: ....

   मैं प्रमाणित करता हूँ कि यह सदस्यता केवल मेरे निजी प्रयोग के लिए है तथा यह प्रिंट/साफ्ट-सदस्य प्रति, प्रकाशन होने से कम से कम दो वर्ष की अवधि तक किसी पुस्तकालय या वाचनालय को उपलब्ध नहीं करवाई जाएगी।

   I certify that the subscription is for my personal use only and that print/soft subscriptions will not be released to libraries or reading rooms for at least 2 years after publication.

   हस्ताक्षर / Signature

आफॅर (सीमित अवधि के लिए): नये पंजीकृत आजीवन ग्राहकों को "हिमालयन जियोलॉजी" के पुराने प्रिंट वोल्यूमों का एक मुफ्त सैट (1971 से 2012 तक, उपलब्धता के आधार पर) उपलब्ध कराया जाएगा (डाक शुल्क ग्राहक द्वारा वहन किया जाएगा)।

Offer (for a limited period) : A free set of old print volumes (1971 to 2012, subject to availability) of "Himalayan Geology" will be provided to the newly registered Life Time Subscribers (Postage to be borne by the Subscriber).
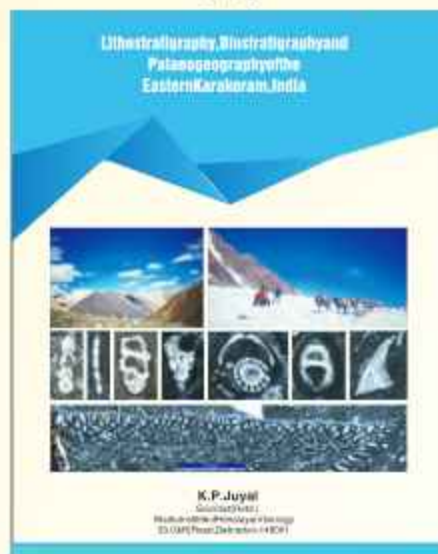
कार्यालय उपयोग हेतु /*For office use*

रसीद सं./Receipt No.:.......................दिनांक/Dated:...................................राशि/Amt. Rs.........................

जारी मौजूदा वोल्यूम /Issue Current Vol. No.:...

Latest Publications

2018   2015

Lithostratigraphy,Biostratigraphyand
Palaeogeographyofthe
EasternKarakoram,India

SIWALIK MAMMALIAN FAUNAS OF THE HIMALAYAN FOOTHILLS

With reference to biochronology, linkages and migration

GLACIER LAKE INVENTORY OF UTTARAKHAND

K.P.Juyal

Wadia Institute of Himalayan Geology

Wadia Institute of Himalayan Geology
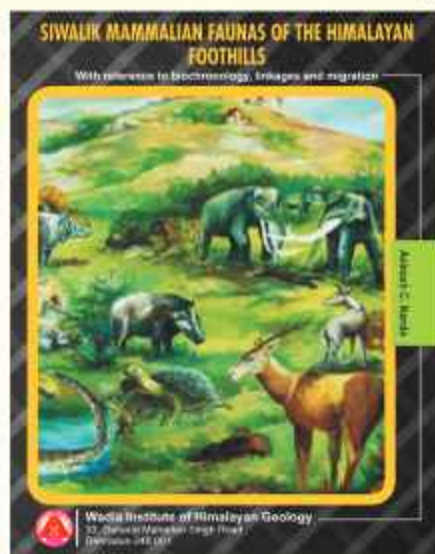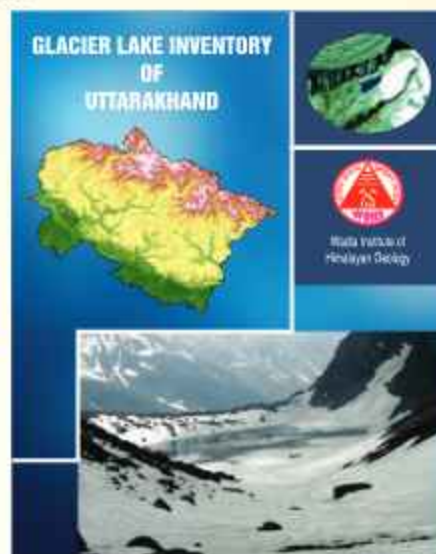
Rs.600/- (India), US$ 50/- (Abroad)   Rs.1200/- (India), US$ 100/- (Abroad)   Price: Rs. 500/- (India), US$ 50/- (Abroad)

Previous Publications

GEOLOGY OF KUMAUN LESSER HIMALAYA

GEOLOGY OF INDUS SUTURE ZONE OF LADAKH
Wadia Institute of Himalayan Geology   Dehra Dun

EXCURSION GUIDE ON THE HIMALAYAN FORELAND BASIN
(JAMMU-KALAKOT-UDHAMPUR SECTOR)

EXCURSION GUIDE
THE SIWALIK FORELAND BASIN
(DEHRA DUN-NAHAN SECTOR)

WADIA INSTITUTE OF HIMALAYAN GEOLOGY
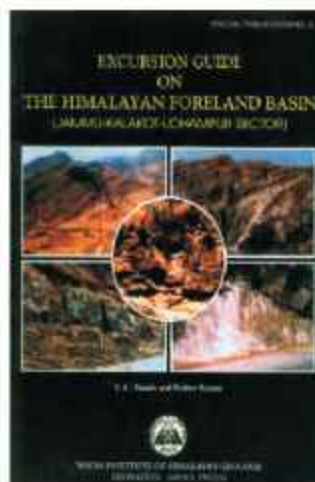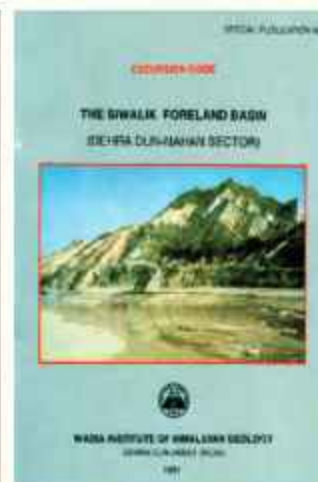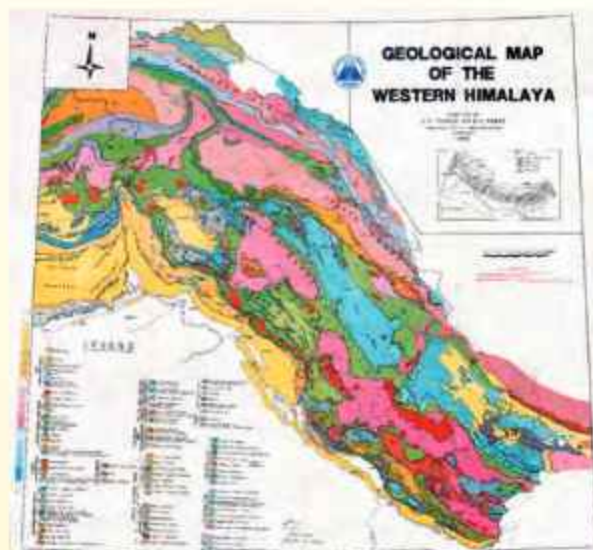
Rs.180/- (India), US$ 50/- (Abroad)   Rs.205/- (India), US$ 40/- (Abroad)   Rs.180/- (India), US$ 15/- (Abroad)   Rs.45/- (India), US$ 8/- (Abroad)

GEOLOGICAL MAP OF THE WESTERN HIMALAYA

Rs.200/- (India), US$ 15/- (Abroad)

WADIA INSTITUTE OF HIMALAYAN GEOLOGY, DEHRA DUN
PUBLICATIONS AVAILABLE FOR SALE

HIMALAYAN GEOLOGY

(These volumes are the Proceedings of the Annual Seminars on Himalayan Geology organizsed by the Institute)

		(in Rs)	(in US $)
Volume 1	(1971)	130.00	26.00
Volume 2*	(1972)	50.00	
Volume 3*	(1973)	70.00	
Volume 4*	(1974)	115.00	50.00
Volume 5	(1975)	90.00	50.00
Volume 6	(1976)	110.00	50.00
Volume 7	(1977)	110.00	50.00
Volume 8(1)	(1978)	180.00	50.00
Volume 8(2)	(1978)	150.00	45.00
Volume 9(1)	(1979)	125.00	35.00
Volume 9(2)	(1979)	140.00	45.00
Volume 10	(1980)	160.00	35.00
Volume 11	(1981)	300.00	60.00
Volume 12	(1982)	235.00	47.00
Volume 13*	(1989)	1000.00	100.00
Volume 14* (in Hindi)	(1993)	600.00	-
Volume 15*	(1994)	750.00	

(Available from M/s Oxford & IBH Publishing Co. Pvt. Ltd., New Delhi, Bombay, Kolkata)

Volume 16*	(1999)	1000.00	100.00

Journal of Himalayan Geology
(A bi-annual Journal : published from 1990 to 1995)

Annual Subscription	(in Rs)	(in US $)
Institutional	500.00	50.00
Individual	100.00	25.00

Volume 1 (1990) to Volume 6 (1995)*

HIMALAYAN GEOLOGY
(A bi-annual Journal incorporating Journal of Himalayan Geology)

Annual Subscription:	(in Rs)	(in US $)
Institutional	500.00	50.00
Individual	100.00	25.00

Volume 17 (1996)*

HIMALAYAN GEOLOGY

Revised Annual Subscription (w.e.f. 1997):	(in Rs)	(in US$)
Institutional	750.00	50.00
Individual (incl. postage)	100.00	25.00

Volume 18 (1997) to Volume 26 (2005)*

Volume 27 (2006) to Volume 32 (2011)*

Volume 33 (2012)

Volume 34 (2013) to Volume 36 (2016)*

Volume 37 (2015) to Volume 38 (2017)

Revised Annual Subscription (w.e.f. 2018):	(in Rs)	(in US$)
Institutional	2000.00	150.00
Individual (incl. postage)	600.00	50.00

Volume 39 (2018) to Volume 43 (2022)

Revised Annual Subscription (w.e.f. 2023):	(in Rs)	(in US$)
Institutional	3000.00	225.00
Individual (incl. postage)	1000.00	100.00

Volume 44 (2023) to Volume 46 (2025)

OTHER PUBLICATIONS

Geology of Kumaun Lesser Himalaya, 1980 (by K.S. Valdiya)	Rs. 180.00 US $ 50.00
Geology of Indus Suture Zone of Ladakh, 1983 (by V.C.Thakur & K.K. Sharma)	Rs. 205.00 US $ 40.00
Bibliography on Himalayan Geology, 1975-85	Rs. 100.00 US $ 30.00
Geological Map of Western Himalaya, 1992 (by V.C. Thakur & B.S. Rawat)	Rs. 200.00 US $ 15.00
Excursion Guide :The Siwalik Foreland Basin (Dehra Dun-Nahan Sector), (WIHG Spl. Publ. 1,1991) (by Rohtash Kumar and Others)	Rs. 45.00 US $ 8.00
Excursion Guide : The Himalayan Foreland Basin (Jammu-Kalakot-Udhampur Sector) (WIHG Spl Publ. 2, 1999) (by A.C. Nanda & Kishor Kumar)	Rs. 180.00 US $ 15.00
Glacier Lake Inventory of Uttarakhand (by Rakesh Bhambri et al. 2015)	Rs. 500.00 US $ 50.00
Siwalik Mammalian Faunas of the Himalayan Foothills With reference to biochronology, linkages and migration (by Avinash C. Nanda, 2015)	Rs. 1200.00 US $ 100.00
Lithostratigraphy, Biostratigraphy and Palaeogeography of the Eastern Karakoram, India (by K.P. Juyal, 2018)	Rs. 600.00 US $ 50.00

Note: 'Journal of Himalayan Geology' & 'Himalayan Geology' have been merged and are being published as Himalayan Geology' after 1996.

 * **Out of Stock**

Life Time Subscription of Himalayan Geology (Individuals only)
Fee for Print copy : India: 7500.00   Abroad: US$ 750.00
Fee for Soft copy : India: 4000.00   Abroad: US$ 250.00

Trade Discount (In India only)
1-10 copies: 10%, 11-15 copies: 15% and >15 copies: 20%

Offer (for a limited period): A free set of old print volumes (1971 to 2012, subject to availability) of 'Himalayan Geology' will be provided to the new registered Life Time Subscribers (Postage to be borne by the subscriber).

Publications: *may be purchased from Publication & Documentation Section and Draft/Cheque may be drawn in the name of The Director, Wadia Institute of Himalayan Geology, 33- General Mahadeo Singh Road, Dehra Dun – 248 001*

Wadia Institute of Himalayan Geology
(An Autonomous Institute of Dept. of Science & Technology, Govt. of India)
33, General Mahadeo Singh Road, Dehradun-248001 (INDIA)